

# Sheffield Hallam University

*Synand characterisation of silicone based mesophase forming materials.*

COCKETT, Sean.

Available from the Sheffield Hallam University Research Archive (SHURA) at:

<http://shura.shu.ac.uk/19486/>

## A Sheffield Hallam University thesis

This thesis is protected by copyright which belongs to the author.

The content must not be changed in any way or sold commercially in any format or medium without the formal permission of the author.

When referring to this work, full bibliographic details including the author, title, awarding institution and date of the thesis must be given.

Please visit <http://shura.shu.ac.uk/19486/> and <http://shura.shu.ac.uk/information.html> for further details about copyright and re-use permissions.

101 381 001 5



BRN 265561

10001

ProQuest Number: 10694367

All rights reserved

INFORMATION TO ALL USERS

The quality of this reproduction is dependent upon the quality of the copy submitted.

In the unlikely event that the author did not send a complete manuscript and there are missing pages, these will be noted. Also, if material had to be removed, a note will indicate the deletion.



ProQuest 10694367

Published by ProQuest LLC (2017). Copyright of the Dissertation is held by the Author.

All rights reserved.

This work is protected against unauthorized copying under Title 17, United States Code  
Microform Edition © ProQuest LLC.

ProQuest LLC.  
789 East Eisenhower Parkway  
P.O. Box 1346  
Ann Arbor, MI 48106 – 1346



## TABLE OF CONTENTS

	<u>PAGE</u>
Acknowledgements	
Abstract	
<u>CHAPTER 1. INTRODUCTION</u>	1
1.1 Mesomorphism and Liquid Crystallinity	1
1.2 Molecular Structures of Conventional Mesomorphic Materials	3
1.3 Mesophases	5
1.3.1 Amphiphilic Mesophases	5
1.3.2 Non-Amphiphilic Mesophases	13
1.4 Properties and Applications	16
1.4.1 Amphiphilic Mesophases	16
1.4.2 Non-Amphiphilic Mesophases	18
1.5 Mesomorphic Polymers	19
1.6 Molecular Structures and Classification of Mesomorphic Polymers	20
1.6.1 Amphiphilic Polymers	21
1.6.2 Non-Amphiphilic Polymers	22
1.6.2.1 Main-Chain Polymers	22
1.6.2.2 Side-Chain Polymers	24
1.7 Aims and Outline of Present Research Project	27

<u>CHAPTER 2. PHASE BEHAVIOUR OF THE ALKALI AND ALKALINE</u>		
	<u>EARTH METAL SOAPS AND AMPHIPHILIC POLYMERS</u>	31
2.1	Introduction	31
2.2	Alkali and Alkaline-Earth Metal Soaps	31
2.2.1	Thermotropic Behaviour of the Alkali Metal Soaps	31
2.2.2	Thermotropic Behaviour of the Alkaline-Earth Metal Soaps	36
2.2.3	Thermotropic Behaviour of Branched Chain Soaps	37
2.2.4	Aqueous Lyotropic Behaviour of the Alkali Metal Soaps	38
2.2.5	Aqueous Lyotropic Behaviour of the Alkaline-Earth Metal Soaps	42
2.2.6	Aqueous Lyotropic Behaviour of Branch Chain Soaps	42
2.2.7	Lyotropic Behaviour of the Alkali and Alkaline-Earth Metal Soaps in Non-Polar Solvents	43
2.3	Polymeric Amphiphiles	45
 <u>CHAPTER 3. SYNTHETIC STRATEGY</u>		57
3.1	Introduction	57
3.2	Synthesis of Reactive Siloxane Precursors	60
3.2.1	Introduction	60
3.2.2	Cyclic Hydrogenmethylsiloxane Oligomers	63
3.2.3	Linear End-Functionalised Dimethylsiloxanes	64
3.2.3.1	$\alpha,\omega$ -Si-H Functionalised Siloxanes	64
3.2.3.2	$\alpha$ -Si-H Functionalised Siloxanes	67
3.3	Synthesis of Mesogens	69
3.3.1	Non-Amphiphilic Mesogens	69
3.3.2	Protected Amphiphilic Mesogens	71
3.4	Coupling of Mesogen and Siloxane	73
3.5	Purification of Mesogen Functionalised Siloxanes	75

<u>CHAPTER 4. SYNTHESIS</u>	78
4.1 Introduction	78
4.2 Experimental	78
4.2.1 Materials	78
4.2.2 Analytical Techniques	79
4.2.3 Preparation of Si-H Functionalised Siloxanes	81
4.2.3.1 Cyclic Hydrogenmethylsiloxane Oligomers	81
4.2.3.2 $\alpha,\omega$ -Si-H Functionalised Dimethylsiloxanes. General Procedure	86
4.2.3.3 $\alpha$ -Si-H Functionalised Siloxanes. General Procedure	89
4.2.4 Synthesis of Vinyl Terminated Mesogens	92
4.2.4.1 Non-Amphiphilic Mesogens	92
4.2.4.2 Protection of the Carboxyl Group of Undecenoic Acid. Synthesis of Trimethylsilyl 10-Undecenoate	95
4.2.5 Coupling of Mesogens and Siloxanes. General Procedure	95
4.2.6 Isolation of Products	99
4.2.6.1 Cyclic Non-Amphiphilic Oligomers	99
4.2.6.2 Cyclic Amphiphilic Oligomers	101
4.2.6.3 Linear Amphiphilic Polymers	102
4.2.7 Salts of the Amphiphilic Siloxanes. General Procedure	104
4.2.7.1 Sodium Salts	104
4.2.7.2 Calcium Salts	109
Appendix 4.1 - Gas Chromatography/Mass Spectrometry Data for the Commercial Sample of Cyclic Hydrogenmethylsiloxane Oligomers	110

<u>CHAPTER 5. CHARACTERISATION OF PHASE BEHAVIOUR</u>	117
5.1 Introduction	117
5.2. Polarising Microscopy	118
5.2.1 Introduction	118
5.2.2 Principles	118
5.2.3 Experimental	119
5.3 Differential Scanning Calorimetry	121
5.3.1 Introduction	121
5.3.2 Principles	121
5.3.3 Experimental	122
5.4 X-ray Diffraction	124
5.4.1 Introduction	124
5.4.2 Principles	125
5.4.3 Assignment of Structure and Calculation of Lattice Parameters	126
5.4.3.1 Phases with One-Dimensional Periodicity	126
5.4.3.2 Phases with Two-Dimensional Periodicity	128
5.4.3.3 Phases with Three-Dimensional Periodicity	129
5.4.3.4 Estimates of the Volumes of Polar and Non-polar Moieties	129
5.4.3 Experimental	130
 <u>CHAPTER 6. PHASE BEHAVIOUR OF THE CYCLIC AMPHIPHILIC SILOXANES</u>	 132
6.1 Introduction	132
6.2 Thermotropic Phase Behaviour	135
6.2.1 The Sodium Salts	135
6.2.1.1 Results	135
6.2.1.1.1 Polarising Optical Microscopy	135

6.2.1.1.2	Differential Scanning Calorimetry	137
6.2.1.1.3	Thermo-Gravimetric Analysis	145
6.2.1.1.4	X-Ray Diffraction	146
6.2.1.2	Discussion	147
6.2.1.3	Conclusions	171
6.2.2	The Calcium Salt	173
6.2.2.1	Results	173
6.2.2.1.1	Polarising Optical Microscopy	173
6.2.2.1.2	Differential Scanning Calorimetry	175
6.2.2.1.3	Thermo-Gravimetric Analysis	179
6.2.2.1.4	X-Ray Diffraction	180
6.2.2.2	Discussion	181
6.2.2.3	Conclusions	193
6.3	Lyotropic Phase Behaviour	195
6.3.1	The Sodium Salts	195
6.3.1.1	Results	195
6.3.1.1.1	Polarising Optical Microscopy	195
6.3.1.2	Discussion	198
6.3.1.3	Conclusions	206
6.3.2	The Calcium Salt	207
6.3.2.1	Polarising Optical Microscopy	207
6.3.2.2	Discussion	207
6.3.2.3	Conclusions	208

## CHAPTER 7. PHASE BEHAVIOUR OF THE LINEAR AMPHIPHILIC

	<u>SILOXANES</u>	209
7.1	Introduction	209
7.2	Thermotropic Phase Behaviour	211

7.2.1	The Sodium Salts	211
7.2.1.1	Results	211
7.2.1.1.1	Polarising Optical Microscopy	211
7.2.1.1.2	Differential Scanning Calorimetry	215
7.2.1.1.3	X-Ray Diffraction	219
7.2.1.1.4	Thermo-Gravimetric Analysis	223
7.2.1.2	Discussion	224
7.2.1.3	Conclusions	242
7.2.2	The Calcium Salt	245
7.2.2.1	Results	245
7.2.2.1.1	Polarising Optical Microscopy	245
7.2.2.1.2	Differential Scanning Calorimetry	246
7.2.2.2	Discussion	247
7.2.2.3	Conclusions	251
7.3	Lyotropic Phase Behaviour	254
7.3.1	The Sodium Salt	254
7.3.1.1	Results	254
7.3.1.1.1	Polarising Optical Microscopy	254
7.3.1.2	Discussion	254
7.3.1.2.1	The Aqueous Phase Behaviour	254
7.3.1.2.1	The Non-Aqueous Phase Behaviour	255
7.3.2	The Calcium Salt	256
7.3.2.1	Results	256
7.3.2.1.1	Polarising Optical Microscopy	256
7.3.2.2	Discussion	257

<u>CHAPTER 8. PHASE BEHAVIOUR OF THE CYCLIC NON-AMPHIPHILIC</u>		
	<u>SILOXANES</u>	258
8.1	Introduction	258
8.2	Results	259
8.2.1	Polarising Optical Microscopy	259
8.2.2	Differential Scanning Calorimetry	264
8.3	Discussion	269
8.4	Conclusions	279
<u>CHAPTER 9. FUTURE WORK</u>		280
9.1	Validation of Key Areas	280
9.2	Extension of this Work	281
<u>REFERENCES</u>		284

## **ACKNOWLEDGEMENTS**

I would like to take this opportunity to thank Dr. K. Dodgson and Dr. D. Simmonds for their advice and guidance throughout the course of this work.

I am also grateful to all the members of the Department of Chemistry, Sheffield City Polytechnic for their help and encouragement throughout the project. In particular, I would like to thank Mrs J. Hague and Dr. M. Rose for their assistance with GCMS, and W. Harrison, R. Broughton, S. Marsden, M. Northern and I. Walker for their technical assistance and general good humour in the laboratory.

I would also like to thank Unilever Research for their support and the generous access to their facilities at Port Sunlight. I would particularly like to express my gratitude to Prof. G. J. T. Tiddy for his invaluable friendship, advice and support. I also wish to thank Peter and Claire for their friendship and comfortable lodgings, and all the staff at Unilever for making the visits to Port Sunlight so enjoyable.

Last but not least, I would like to thank Louise for her assistance in preparing this thesis.

## ABSTRACT

The aim of this project was to synthesise and characterise a range of novel cyclic and linear mesogenic siloxanes. A synthetic strategy based upon the synthesis of linear side-chain siloxanes was adopted. End-functionalised linear siloxane precursors were synthesised via ring opening polymerisation reactions. The coupling of mesogen and siloxane was carried out via a hydrosilylation reaction in solution. Products were isolated by phase-separation and gel permeation chromatography (GPC).

Thermotropic behaviour was studied using optical microscopy, differential scanning calorimetry (DSC) and, in some cases, X-ray diffraction. An overview of the lyotropic behaviour of the amphiphiles was obtained using the penetration technique.

The principles explaining the thermotropic behaviour of conventional amphiphiles appear to be generally applicable to these amphiphilic siloxanes. Thus, the amphiphiles aggregate in the neat state. The shape of these aggregates is determined primarily by packing constraints. The amphiphiles undergo a step-wise melting process, with the non-polar and the polar moieties dominating the low and the high temperature transitions, respectively. The behaviour of different molecules can be explained by reference to the nature of the respective polar and non-polar moieties.

The aqueous lyotropic phase behaviour of  $\text{NaD}_4$  appears to be similar to that of sodium myristate. Thus, the effect of attaching amphiphiles to a siloxane chain is to extend the non-polar chain of the amphiphile by approximately three methylene units. The linear amphiphiles did not form any aqueous lyotropic mesophases. This was explained in terms of the reversed micelle structure, which was dictated by packing constraints. There was no mesophase behaviour in non-polar solvents due to the strong forces of attraction between polar groups.

The model considerations applied to non-amphiphilic side-chain polymers appear to be applicable to the non-amphiphilic cyclics studied here. Thus, suitable flexible spacer groups will decouple the motions of mesogenic side-chains from those of an oligomeric cyclic backbone such that the mesogens may align. However, more efficient spacers are required to decouple the motions and steric effects of the cyclic backbone than is the case with the equivalent linear backbones.

## CHAPTER 1. INTRODUCTION

### 1.1 Mesomorphism and Liquid Crystallinity

Conventionally, three phases of matter have been recognised: crystalline solids, isotropic liquids and gases. Each of these phases may be characterised according to their molecular order<sup>1</sup>. For instance, within a crystalline solid the molecules are positioned on a three dimensional crystal lattice with orientational and positional ordering, and with very little molecular mobility; within a liquid there is no long range structure and little short range order, but rapid molecular motions and rapid molecular mobility; and, within a gas there is no order and very rapid molecular motions. The characteristic physical properties of each of these phases can, therefore, be related to their molecular organisation; highly ordered crystalline solids having a constant volume and a constant shape; highly disordered gases having neither a constant volume nor a constant shape; and, liquids—which possess an order intermediate between that of the crystalline solids and gases—having a constant volume, but not retaining a constant shape.

Although not recognised as such, the first observations of a mesophase (i.e. a phase whose molecular order and, hence, whose properties are intermediate between that of crystalline solids and isotropic liquids<sup>2</sup>) were made in 1853 by Virchow during his studies on Myelin<sup>3</sup>. Later, in 1888, whilst attempting to isolate a pure sample of Cholesteryl benzoate, Reinitzer<sup>4</sup> observed a phase region between 145.5°C and 178.5°C which possessed low rigidity, a liquid-like property, and also optical-anisotropy, a crystal-like property. Lehmann<sup>5</sup> subsequently termed this mesophase a 'liquid crystal', because of this unusual combination of properties.

As mesophases are states of matter with structural orders which are intermediate between that of the crystalline solids and the isotropic liquids, and as three basic types of structural ordering exist—positional, orientational and conformational—Wunderlich and Grebowicz<sup>6</sup> proposed that three types of mesophases are possible:

- liquid crystals; characterised by orientational order but varying degrees of positional disorder.
- plastic crystals; with positional order but orientational disorder.
- condis crystals; defined, by them for the first time, as conformationally disordered but with positional and orientational order.

The transition from a crystalline solid, through one or more of these mesophases, to the isotropic liquid, may be brought about by thermal processes or by the influence of a solvent (i.e. thermotropic and lyotropic mesomorphism, respectively)<sup>7</sup>. However, it is important to note that thermotropic mesophases can, on occasion, incorporate a considerable amount of a solvent into their structures with the resulting modification of their properties, and that the results of thermal processes in lyotropic mesophases can have an equally significant effect. Hence, lyotropic and thermotropic behaviour may, to some degree, be characteristic of all mesophases.

As the molecular order encountered in mesophases is intermediate between that of crystalline solids and isotropic liquids, mesophases exhibit properties which are common to both these conventional phases, as well as properties which are peculiar to themselves<sup>2</sup>. Examples of the unique

features of this state of matter include:

- the long range orientational ordering of the molecules in some mesophases can be controlled by external fields<sup>8,9</sup> (i.e electrical and magnetic).
- some mesophases exhibit optical activity up to a thousand times greater than conventional optically active materials<sup>10,11</sup>.
- some mesophases change colour as a result of the effect of temperature on their structure<sup>11</sup>.

These are amongst the properties that give rise to the increasing interest in this 'relatively new' state of matter.

## 1.2 Molecular Structures of Conventional Mesomorphic Materials

Molecules that form mesophases are termed mesogens. The structural characteristics which are necessary to produce small molecule mesogens have been reviewed by Gray and Winsor<sup>7</sup>, and by Brown and Shaw<sup>12</sup>.

Mesogens, and also the mesophases they form, can be divided into two main chemical classes<sup>7</sup>: amphiphilic and non-amphiphilic.

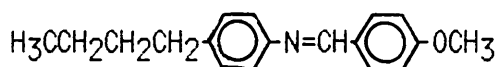
Amphiphilic molecules contain localised lipophilic (oil-liking) and hydrophilic (water-liking) moieties in their structures<sup>13</sup>. Typical examples of amphiphiles are shown in Table 1.1.

Sodium dodecyl sulphate	$n\text{-C}_{12}\text{H}_{25}\text{OSO}_3\text{Na}$
Hexadecyl trimethylammonium bromide	$n\text{-C}_{16}\text{H}_{33}\text{NMe}_3\text{Br}$
Sodium perfluorooctanoate	$n\text{-C}_7\text{F}_{15}\text{CO}_2\text{Na}$
Tetraethylene glycol dodecyl ether	$n\text{-C}_{12}\text{H}_{25}(\text{OCH}_2\text{CH}_2)_4\text{OH}$

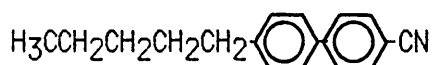
Table 1.1 Typical amphiphiles (the hydrophilic moieties are represented in bold text)

A large variety of molecular structures can provide the hydrophilic segment (the polar head group), including ionic and nonionic groups. The lipophilic segment (the non-polar tail group) has generally been limited to hydrocarbon or fluorocarbon chains. Although most amphiphiles contain one head group and one tail group, the number, chemical nature, and structure of both these groups can vary greatly.

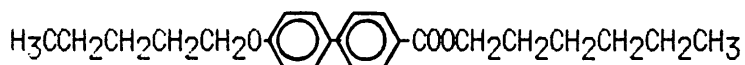
Non-amphiphilic mesogens are generally organic molecules with a fairly rigid rod-like or disc-like structure, which often possess a significant dipole moment<sup>7,14</sup>. Typical examples of non-amphiphilic mesogens are given in table 1.2, with their non-systematic, industrial ciphers shown in brackets.



N-p-methoxybenzylidene-p-n-butylaniline (MBBA)

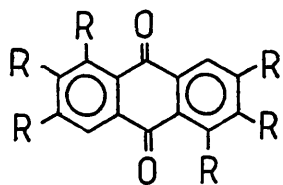


4-Cyano-4'-n-pentylbiphenyl (5CB)



n-Hexyl 4'-n-pentyloxybiphenyl-4-carboxylate (650BC)

Rod-like



Disc-like

Rufigallol-hexa-n-octanoate (were  $\text{R}=\text{O}_2\text{C}(\text{CH}_2)_6\text{CH}_3$ )

Table 1.2. Typical non-amphiphilic mesogens

These rod- and disc-like mesogens are highly geometrically anisotropic (i.e. the rod-like mesogens are characterised by a high length to diameter ratio, and the disc-like mesogens possess a high diameter to thickness ratio). The core of these molecules is such that the rigidity/linearity is preserved.

### 1.3 Mesophases

#### 1.3.1 Amphiphilic Mesophases

The lyotropic and thermotropic mesophases formed by typical amphiphiles may be regarded as structural arrangements of aggregates of these molecules (termed micelles), in which most aspects of the three dimensional periodicity of crystalline solids have been lost, and in which the molecular mobility is relatively high, being not much slower than that of isotropic liquids<sup>13</sup>.

Amphiphile aggregates may be divided into three main shapes<sup>13</sup>; cylinders, discs, and spheres. For each of these geometries, the amphiphile can be arranged so that the polar group forms the aggregate surface and the non-polar group forms the interior, or visa versa (hereafter, referred to as normal and reversed micelles, respectively; see figure 1.1).

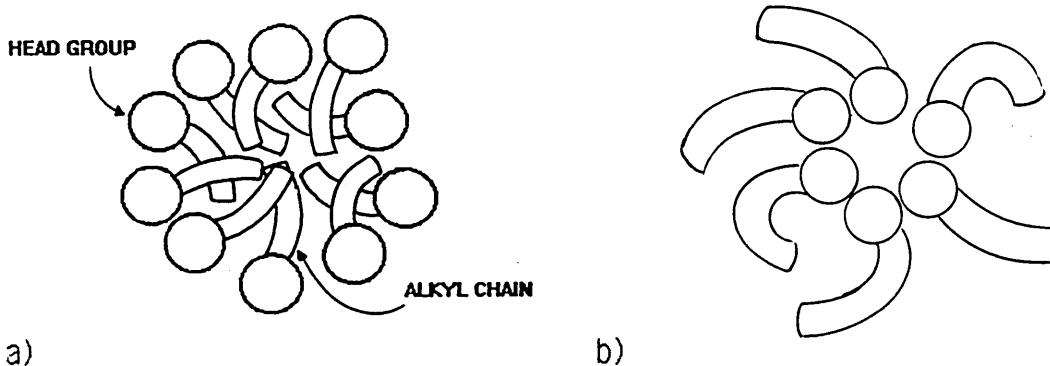


Figure 1.1 Schematic representation of a) normal and b) reversed spherical micelles

The preferred geometry of an amphiphile aggregate and the number of molecules that constitute an individual aggregate (i.e. the aggregation number) depend upon the molecular structure of the mesogen (i.e. molecular packing constraints and inter-molecular forces) and, in lyotropic systems, upon the nature and concentration of the solvent<sup>13,15,16</sup>. As the growth of the rod aggregates is essentially unlimited in at least one dimension, the aggregation numbers range from several hundred to around 30000. For discs, the growth of the aggregate is limited by the unfavourable free energy of the "edge" molecules. Hence, disc micelles rarely have aggregation numbers greater than 1000. In spheres the size of the aggregate is effectively governed by the length of the amphiphile and the aggregation numbers are around 50-100.

Whilst the geometric structures of the aggregates formed in thermotropic and lyotropic systems are similar, the forces responsible for the occurrence of these aggregates may be very different<sup>13</sup>. The presence of the solvent in lyotropic systems may fundamentally affect the nature of the interactions responsible for mesophase formation, especially if that solvent is water.

In aqueous lyotropic systems the properties of amphiphiles arise from the 'hydrophobic effect'<sup>17</sup>. As water/water hydrogen bonds are stronger than the van der Waals interactions occurring between non-polar and polar molecules, non-polar molecules such as alkanes have a limited solubility in water. On the other hand, polar groups are soluble in water because of their ability to form strong polar bonds with this solvent. Hence, compared to the parent non-polar species, amphiphiles have an increased aqueous solubility due to the presence of a polar group.

Although the aggregation of amphiphiles to form micelles, reduces the enthalpically 'less favourable' contact of the non-polar chains with water, whilst allowing the polar groups to remain hydrated, the forces driving this micellisation are essentially entropic in nature<sup>17</sup>. Water is a highly structured liquid, with hydrogen bonds linking the individual molecules together; the precise arrangement about each molecule is not fully established. The water molecules which are in closest contact with the non-polar moiety of an amphiphile are thought to rearrange themselves so as to regenerate hydrogen bonds which have been broken due to the presence of this non-polar moiety. In doing so, there is a restriction on the range of conformations available to the water molecules relative to that of pure water, thereby producing a decrease in the entropy of the system. It is the minimisation of this effect which is the driving force behind micellization in aqueous systems.

Micellization occurs at a critical concentration for a particular system<sup>13,17</sup>. This critical concentration is termed the critical micelle concentration (c.m.c.). Since micelle formation in aqueous systems occurs as a consequence of less favourable contact between non-polar groups and water, it is not surprising that c.m.c. values decrease with an increase in the chain length of the non-polar moiety of an amphiphile. The process of micellisation in aqueous systems has been quantitatively described using thermodynamic treatments<sup>18,19</sup>.

In dilute aqueous solutions, micelles do not interact to any significant degree, and these solutions are isotropic. The main effect of increasing amphiphile concentration above the c.m.c. is to increase the number of micelles<sup>13,16</sup>. This leads to increasing interactions between the micelles

that arise from excluded volume, solvation (hydration), steric and electrostatic effects. All of these are repulsive forces which act to increase micelle size and eventually to produce a disorder/order transition in the relative arrangement of the micelles. This results in the formation of an ordered lyotropic mesophase from an isotropic micellar solution<sup>13,16</sup>. Further increase in amphiphile concentration may lead to the formation of a sequence of different mesophases arising from changes in the shape and the mutual arrangement of the micelles<sup>13,15,16</sup>.

Reversed micelles and reversed mesophases<sup>20,21</sup> can result with some amphiphiles in the neat state, and when some amphiphiles (with a little water) are dissolved in non-polar solvents. Their properties are similar to those of the micelles and mesophases encountered in aqueous systems, although the thermodynamics of formation are quite different<sup>16,20</sup>. In these systems, the forces driving the aggregation process are essentially enthalpic in nature; the strong forces of attraction between polar groups causing phase separation of these groups from the non-polar moieties of the amphiphile and any non-polar solvent which is present.

As with aqueous systems, the c.m.c. of lyotropic systems based on non-polar solvents will be characteristic of that system. Again, increasing amphiphile concentration above the c.m.c. increases the number of micelles, and eventually produces a disorder/order transition resulting in the formation of a lyotropic mesophase. Further increase in amphiphile concentration may lead to the formation of a sequence of different mesophases<sup>20,21</sup>.

The formation of all amphiphilic mesophases depends on the operation of two sets of interactions<sup>7,13,16</sup>; intermolecular forces (attractive and repulsive) which determine micelle size and shape, and intermicellar forces (repulsive) which determine the relative arrangement of the micelles and, therefore, the nature of the mesophase.

Five well established amphiphilic mesophase structures exist<sup>13</sup>. These are the lamellar phase, hexagonal phases, two cubic phases, and nematic phases. Only a brief account of these phases will be given here as they have been extensively described elsewhere<sup>13,16,22-25</sup>. Details of the structures of the more equivocal phases can be found in the literature<sup>13,16</sup>. Although a variety of alternative systems for the nomenclature of amphiphilic mesophases have been published<sup>23-25</sup>, in this thesis the one given by Tiddy will be employed<sup>25</sup>. Thus, each type of mesophase structure will be represented by a particular letter (e.g. hexagonal-H) while subscripts 1 or 2 will refer to normal and reversed structures, respectively.

The hexagonal mesophase consist of extended cylindrical micelles packed in a two dimensional hexagonal array (see figure 1.2). With normal micelles the normal hexagonal ( $H_1$ ) phase results. Up to date this phase has only been encountered in the presence of a solvent (usually water). With reversed micelles the reversed hexagonal ( $H_2$ ) phase results. This phase has been encountered with some amphiphiles in the pure state and in the presence of non-polar solvents (and a little water).

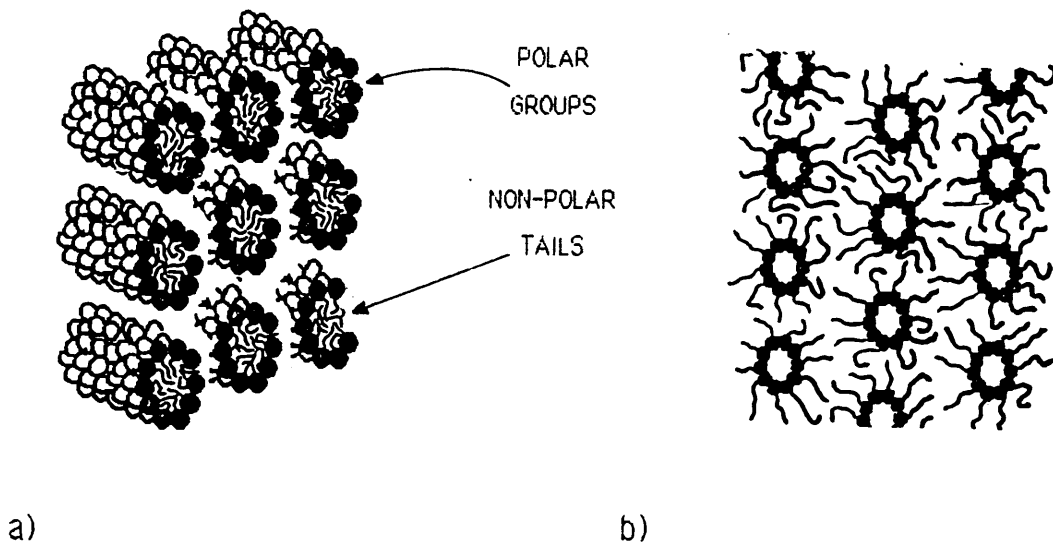


Figure 1.2 Schematic representation of a) normal and b) reversed hexagonal phase structures ( $H_1$  and  $H_2$ , respectively).

The lamellar mesophase ( $L_\alpha$ ) consists of parallel extended bilayer or disc micelles (see figure 1.3). Typically, the dimensions of these layers are of the order of microns or more. This phase occurs with some amphiphiles in the pure state and both oil and/or water can be incorporated into the structure. This is perhaps the most common mesophase structure encountered in amphiphilic systems.

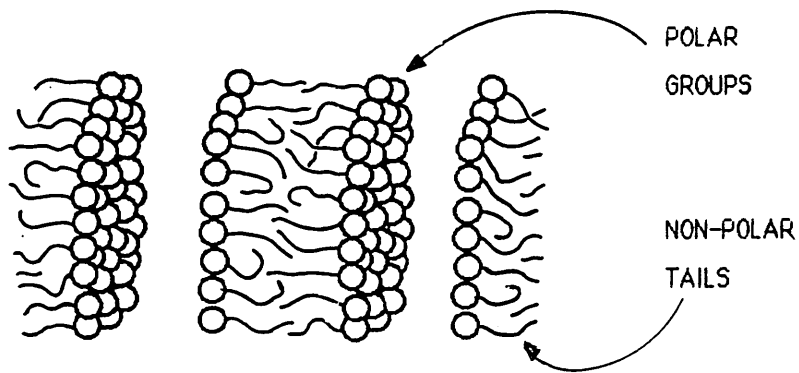


Figure 1.3 Schematic representation of the lamellar phase structure.

Various cubic mesophases are thought to exist. The most widely studied cubic phases,  $V_1$  and  $V_2$ , are thought to involve a regular three dimensional network of micelles (see figure 1.4a). In these phases both the polar and non-polar regions are thought to be bi-continuous, although the exact structure remains to be resolved.

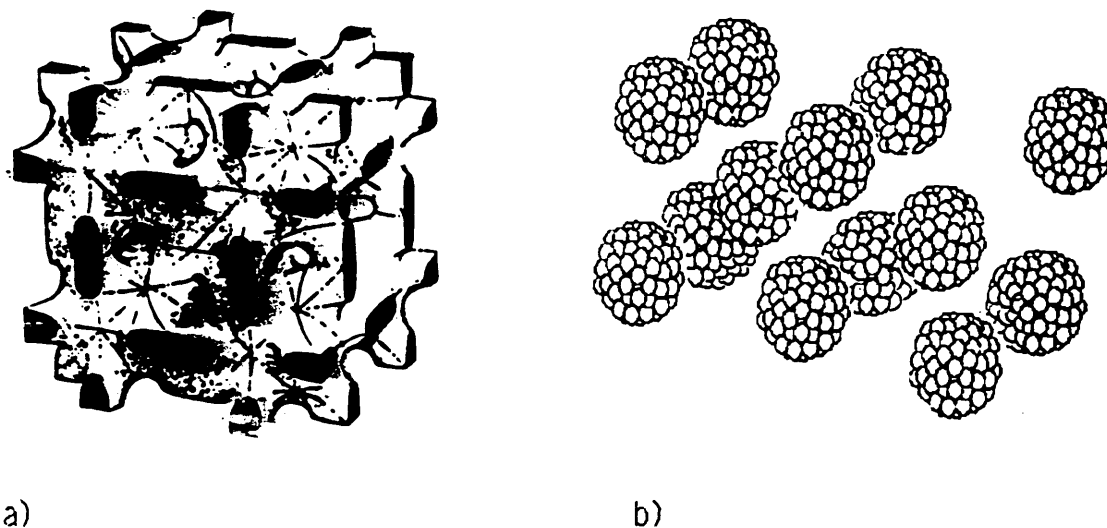


Figure 1.4 Schematic representation of the structure of a) the  $V_1$  and b) the  $I_1$  mesophases.

The  $I_1$  and  $I_2$  cubic phase are made up small micelles (spheres, cylinders, or discs whose geometric anisotropy approaches zero) packed in some form of cubic lattice (see figure 1.4b). Examples of both body-centred and face-centred normal structures appear in the literature<sup>26,27</sup>. It is interesting to note that, as the  $I_1$  and  $I_2$  mesophases are characterised by orientational disorder but with positional order, Wunderlich and Grebowicz<sup>6</sup> would classify these mesophases as plastic crystals.

Two types of nematic phase have been reported; uniaxial and biaxial. These phases have only been observed in surfactant/water systems and generally arise with short chain surfactants (i.e. chain length ( $C_n$ )  $< 14$ ). The viscosity of these phases is very low and they can be easily poured and may be aligned in strong magnetic fields. The uniaxial phases consist of ordered small cylindrical micelles ( $N_C$ ) or ordered small disc micelles ( $N_D$ ) with orientational ordering, but little or no positional ordering (see figure 1.5)<sup>28-31</sup>. The structure of the biaxial phases has yet to be fully established<sup>13,16,32</sup>.

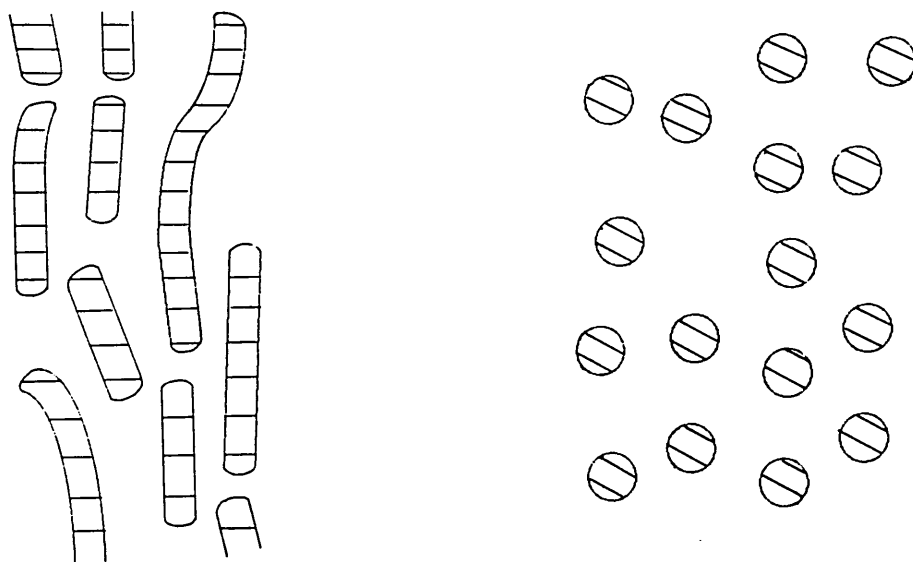


Figure 1.5 Schematic representation of the structure of the  $N_C$  and  $N_D$  phases.

Although amphiphilic mesophases consist of ordered aggregates and may have a very high viscosity, at the molecular level, micelles are transient species which form and break up very quickly; the molecular mobility being not much slower than that of isotropic liquids<sup>13</sup>.

### 1.3.2 Non-Amphiphilic Mesophases

The lyotropic and thermotropic mesophases formed by non-amphiphilic mesogens should be regarded as structural arrangements of individual molecules, and not the arrangement of aggregates of molecules, as is the case in amphiphilic systems. The formation of non-amphiphilic mesophases is essentially a consequence of mesogen asymmetry (mesogen geometry)<sup>33-35</sup> and anisotropy of intermolecular attractions and repulsions (i.e. excluded volume effects)<sup>36-41</sup>. As a consequence of these interactions there is a limit to the number of rod-like and disc-like units that can be accommodated in a random arrangement in solution and in the melt. When this limiting concentration is exceeded an ordered arrangement of the molecules—in which some aspect of the three dimensional periodicity of crystalline solids is absent—is preferred.

On the basis of molecular arrangement, the mesophases formed by non-amphiphilic mesogens can be divided into three main classes<sup>7,8</sup>; smectic, nematic and cholesteric.

The smectic group of phases has long range orientational ordering of the major molecular axis and has a layered structure (see figure 1.6). Varying degrees of positional order and molecular tilt within these layers give rise to various smectic modifications<sup>42</sup>. The direction of the local preferred alignment of the long axis of the molecules is called the director ( $n$ ). The local areas of preferred alignment are known as domains; the alignments in neighbouring domains being independent of each other unless some external force is applied (e.g. electric and magnetic fields, or a shearing force). The smectic phases are of relatively high order and high viscosity.

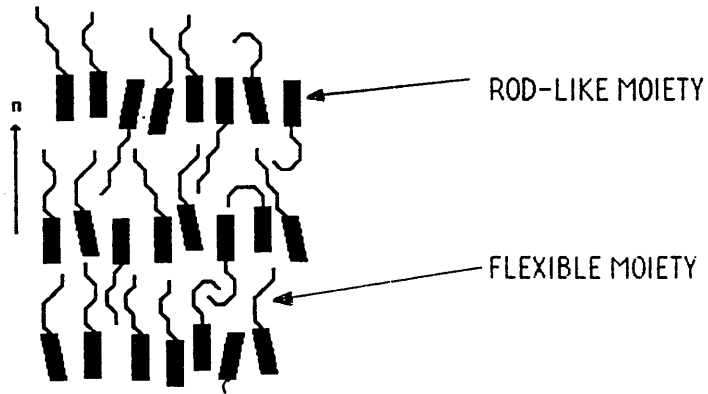


Figure 1.6 Schematic representation of a smectic phase

In the nematic phase there is orientational ordering, but little or no positional ordering of the molecules (see figure 1.7). Again, there is a local preferred alignment of the long axis of the molecules in domains, and the alignments of neighbouring domains is independent of each other, unless some external force is applied. Compared with the smectic modifications, the nematic phase is one of relatively low order and viscosity.

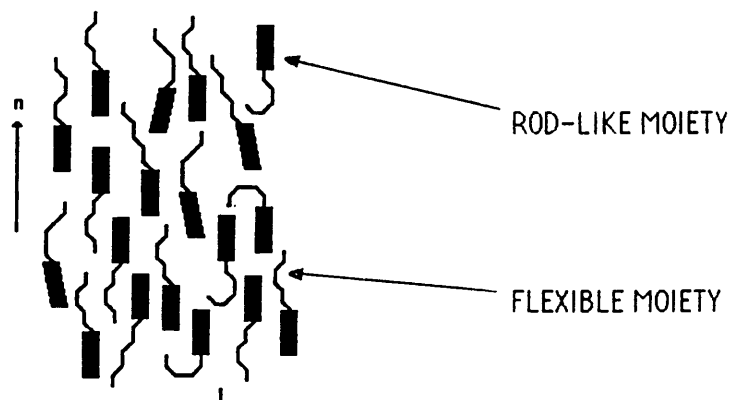


Figure 1.7 Schematic representation of a nematic phase.

A special type of nematic phase is the cholesteric phase. The cholesteric phase is formed by optically active compounds, where the mesogens are assembled in layers in which their molecular arrangement is like that of the nematic phase, but each layer is turned through a definite angle relative to the next, so that overall there is a helical type of structure (see figure 1.8). The successive turns are maintained in position by intermolecular forces (e.g. hydrogen bonds and dipole-dipole interactions).

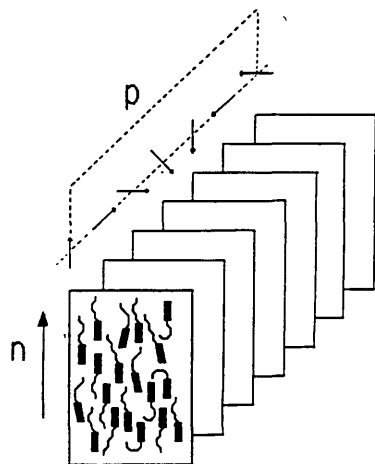


Figure 1.8 Schematic representation of a cholesteric phase (where  $p$  = the pitch of the helix).

The cholesteric phase is of low viscosity and possesses interesting optical properties<sup>10,11</sup>, which include: an optical activity up to a thousand times greater than conventional optically active materials, and a variation in their colour as a result of the effect of temperature on the helical pitch length.

At this point it is worth re-iterating that although amphiphilic and non-amphiphilic mesophases have historically been studied by separate groups, there is much common ground. For instance, the relative arrangements of the structural units in these two classes of mesophase (i.e. the amphiphilic micelles and the non-amphiphilic molecules) arise essentially due to intermolecular or interaggregate forces. It is, therefore,

not surprising that structural units of similar geometry give rise to mesophases with similar structures and, to some degree, similar properties. For example, the arrangement of rod micelles in the hexagonal mesophase<sup>13</sup> is analogous to the arrangement of rod-like molecules in the smectic 'G' mesophase<sup>42</sup>; the arrangement of the individual amphiphilic mesogens in the lamellar mesophase is analogous to the arrangement of the non-amphiphilic mesogens in a number of smectic modifications; and numerous non-amphiphilic molecules with a fairly globular structure (i.e. geometrically isotropic) such as cyclohexane, carbon tetrachloride, hexachloroethane and camphor exhibit a mesophase structure<sup>6</sup> which is very similar to the  $I_1$  and  $I_2$  cubic phase formed in some amphiphilic systems<sup>13</sup>.

#### 1.4 Properties and Applications

##### 1.4.1 Amphiphilic Mesophases

Although most people are unaware of the existence of mesophases, amphiphiles, and the lyotropic mesophases that result from their dispersion in water, have been used in cleaning products for centuries and are commonly encountered in every day life<sup>13</sup>. Lyotropic mesophases occur during the detergency of oily soils, they are fundamental to the stability of many emulsion products and even occur during cooking. In general, the usefulness of the amphiphiles in these applications, lies in their surface activity and their ability to act as molecular bridges between dissimilar polar and non-polar regions; both effects being facets of the chemical nature of an amphiphile. In addition, amphiphiles and their aggregates are also used to modify the rheological behaviour of some functional fluids (i.e. increase the viscosity of a shampoo to give an aesthetically pleasing 'richness')<sup>43</sup>.

Amphiphiles also occur widely in biological systems<sup>44,45</sup>. Biological membranes are composed primarily of lipids and proteins. The lipids vary in composition but are generally amphiphilic in nature consisting of a polar head and a non-polar tail. In aqueous environments, the lipids align in tail-to-tail continuous bilayers with the polar head group in contact with the aqueous phase, rather like a lamellar mesophase<sup>24,44</sup> (see figure 1.9). The proteins extend throughout the lipid bilayer. Water, gases, hydrophobic and hydrophilic molecules or ions are transported across membranes through both proteins and lipid bilayers. The motions and conformations of the proteins and lipids are interrelated and greatly affect the permeability of the membrane itself. Thus, phase transitions induced by temperature change or additives such as cholesterol—thermotropic and lyotropic effects, respectively—significantly alter the structure and properties of the membrane, which in turn profoundly influences the transport characteristics of the membrane.

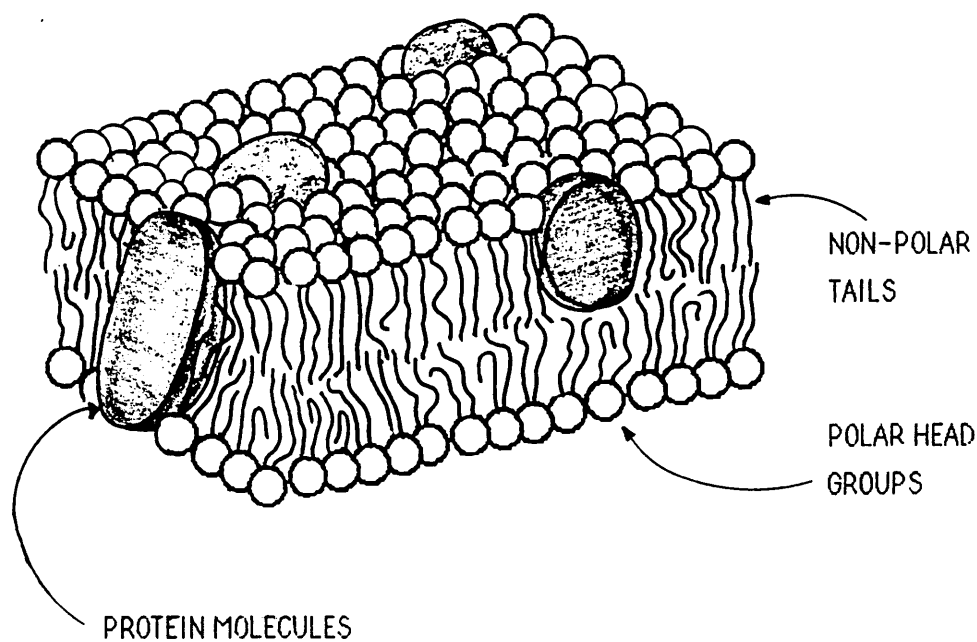


Figure 1.9 Schematic representation of a lipids bilayer.

Although no synthetic equivalents have achieved the versatility of biological membranes, Ringsdorf *et al.*<sup>46</sup> and Kunitake *et al.*<sup>47</sup> have recently synthesised polymerisable lipids which may be used to model biological membranes; the study of which, may be of interest to medicine and industry alike.

#### 1.4.2 Non-Amphiphilic Mesophases

Although the thermotropic mesophases of certain non-amphiphiles have been known since the late nineteenth century<sup>4,5</sup>, it is only in recent years that these materials have found widespread application. They have been used in the fabrication of electro-optical devices<sup>9,48-51</sup>, as highly selective stationary phases for Gas Chromatography (G.C)<sup>52-54</sup>, and as thermal mapping agents in thermography<sup>11,55</sup>.

The manufacturers of electro-optical devices (e.g. watches, calculators, television sets and large display devices) have made use of their ability to control the molecular order within a mesophase with the application of external fields, and the resultant different optical properties of macroscopically ordered and disordered mesophase regions.

The selectivity of certain non-amphiphilic mesogens as stationary phases for G.C. depends on the relative solubility of the analyte molecules in the mesophase matrix. The analyte molecule with a molecular geometry closest to that of the mesogen can be incorporated into this matrix with the least disruption to the structure. This molecule, all else being equal, is preferentially solubilised and, hence, a separation can be effected.

The use of mesophases in thermography arises from the unusual optical properties of the cholesteric phase and their variation with temperature<sup>11</sup>. The cholesteric phase has a helical structure, and when the pitch of this helix is comparable to the wavelength of visible light, interference occurs and the mesophase appears highly coloured. A variation in temperature alters the pitch of the helix, which alters the wavelength of visible light which undergoes interference. Thus, a colour change occurs in the mesophase. Consequently, as the observed colour is dependent on temperature, cholesteric mesophases can be used as visual temperature sensors.

### 1.5 Mesomorphic Polymers

As yet only 'small molecule' mesomorphism has been discussed. However, mesomorphic polymers have been known since the 1940's. The first polymers observed to form a mesophase were of biological origin, namely aqueous solutions of the rod-like Tobacco Mosaic Virus (T.M.V.) and Collagen, which form nematic mesophases at high polymer concentrations<sup>56</sup>. The first synthetic polymer to form a mesophase was discovered in the course of evaporating a chloroform solution of poly( $\alpha$ -benzyl-L-glutamate) (PBLG). PBLG forms a rod-like alpha helix structure as a result of intermolecular hydrogen bonding and association with the solvent, which in turn results in the formation of a nematic mesophase at high polymer concentrations<sup>57,58</sup>.

In 1949, Onsager predicted that rigid rod-like molecules would, under appropriate circumstances, also form stable mesophases<sup>33</sup>. Later, Flory extended Onsager's theory to concentrated solutions, utilising a lattice model, and proposed that above a critical concentration the macromolecules would form a lyotropic mesophase<sup>34</sup>. This theoretical prediction was

verified in 1965, when Kwolek discovered that certain wholly aromatic polyamides gave anisotropic solutions in alkylamide and alkylurea solvent<sup>59</sup>. Materials of this type were the first mesomorphic polymers to be commercialised when, in the 1970's, Du Pont<sup>60,61</sup> and Monsanto<sup>62</sup> produced high modulus fibres spun from lyotropic mesophases of aromatic polyamides (i.e. Kevlar and X-500, respectively). Unlike a coiled polymer such as polyethylene, which has a potential axial modulus of 300 Giga Pascals (GPa) and an actual tensile modulus of the order of only a few GPa, the spinning of fibres from ordered polymer melts (i.e. lyotropic mesophases of Kevlar or X-500), and the preservation of the aligned molecular order in the final fibre, results in polymeric materials which approach their theoretical axial tensile moduli, at least in the direction of alignment<sup>63</sup>.

Following the advent of these materials there has been an increase in interest in mesomorphic polymers.

### 1.6 Molecular structure and Classification of Mesomorphic Polymers

The empirical structure-property relationships in monomeric mesogens have been established for some time<sup>7,12</sup>. The theoretical treatment of the mesophases formed by these mesogens, and the attendant properties have been reviewed by de Gennes<sup>41</sup>. The recent interest in mesomorphic polymers led to the application of these relationships to polymers and, hence, to the systematic polymerisation and polymer fixation of many monomeric mesogens in an effort to produce polymeric equivalents<sup>64</sup>.

As with the monomeric mesogens, mesomorphic polymers may be classified according to their chemical nature (i.e. amphiphilic or non-amphiphilic), and/or depending on whether the mesophase is observed by variation of

solvent content or by variation of temperature (i.e. lyotropic and thermotropic behaviour, respectively)<sup>64</sup>. Subsequently, one can distinguish whether the mesogen forms part of the polymer main-chain or is attached as side-chains; these are known as liquid crystalline main-chain and liquid crystalline side-chain polymers, respectively. Within these two main structural categories there are also a number of further possible modifications. These include combinations of main-chain and side-chain polymers, and also elastomeric polymers which are produced by introducing a limited number of cross-links between polymer chains.

### 1.6.1 Amphiphilic Polymers

Despite the recent interest in mesomorphic polymers, studies of the mesophase behaviour of amphiphilic polymers, especially in the neat state, are relatively limited and, as yet, mesomorphic amphiphilic polymers have not achieved any significant commercial success.

The first report of an amphiphilic side-chain polymer exhibiting a lyotropic mesophase was published by Friberg *et al.*<sup>65</sup>, who synthesised a low molecular weight polymer of sodium-10-undecenoate, and reported the existence of a lamellar mesophase in a 1:1 mixture of this polymer with water at 20°C. Since then, the lyotropic phase behaviour of a number of amphiphilic side-chain polymers based on conventional monomeric ionic<sup>66</sup> and non-ionic<sup>66-72</sup> amphiphiles in combination with the polyacrylate<sup>69,72</sup>, polymethacrylate<sup>72</sup> and polysiloxane<sup>66-68,70-72</sup> backbones has been investigated.

From this work, it has been established that in general, it is the ability of individual amphiphilic units to pack into the various aggregate geometries

that tends to dominate the phase behaviour of polymeric amphiphiles as compared to their monomeric equivalents. As the study of amphiphilic polymers will form the major part of this work, the phase behaviour of these materials will be reviewed in greater detail in chapter 2.

## 1.6.2 Non-Amphiphilic Polymers

### 1.6.2.1 Main-Chain Polymers

In general, monomeric non-amphiphilic mesogens are characterised by their rigid, rod-like or disc-like structures<sup>7</sup>. If these monomers are joined to form the backbone of a polymer, the polymer itself becomes rigid and rod-like and would, on the basis of geometric anisotropy, be expected to form a mesophase in a manner analogous to the small molecule equivalent<sup>34,73</sup>.

With polymers such as aromatic polyamides (i.e. Kevlar), the strong hydrogen bonding between amide groups and the rigidity of the polymer backbone, mean that the crystalline melting point ( $T_m$ ) of the polymer is greater than the degradation temperature, and melt processing is not possible<sup>63</sup>. It is worth emphasising that non-amphiphilic molecules form mesophases essentially as a result of their geometry and, on this basis, the aromatic polyamides would form a thermotropic mesophase due to their extended rigid structure, were it not for the onset of thermal degradation below  $T_m$ . Such polymers may, however, form lyotropic mesophases in which the addition of the solvent lowers the melting point of the polymer<sup>63,73</sup> (i.e. similar to the depression of freezing point observed when solutes are added to solvents). These concentrated polymer solutions may then be processed below the  $T_m$  of the neat polymer.

In concentrated solutions and at a specific concentration, these rigid polymers undergo a disorder/order transition and approach a parallel alignment, giving rise to a nematic mesophase (as predicted by Onsager<sup>33</sup> and Flory<sup>34</sup>). Although this molecular alignment is present in domains, if the nematic solution is exposed to a shear gradient during processing (i.e. spun through a nozzle), a macroscopically almost singularly aligned lyotropic melt is produced (see figure 1.10). Removal of the solvent results in a macroscopically alignment fibre which, as we have seen, possess unusually high mechanical properties<sup>63</sup>.

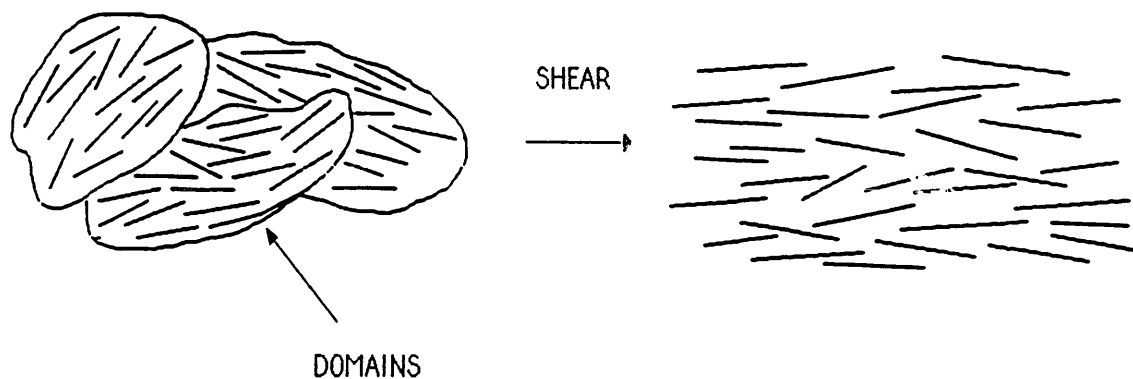


Figure 1.10 Schematic representation of the effect of shear on the orientation of neighbouring domains.

The difficulties with these lyotropic systems are that generally the solvents required are difficult to handle (e.g. concentrated acids), and the necessity for subsequent solvent removal limits their application to the preparation of products with small cross-sectional areas (i.e. fibres)<sup>63,73</sup>. These limitations stimulated the development of aromatic polyesters, which, because of their less rigid structure and the lack of hydrogen bonding, melt below their degradation temperature and form mesophases in the neat state<sup>73,74</sup>. These thermotropic polymers may, therefore, be

processed similarly to conventional thermoplastics and are not limited to the production of fibres.

In order to prepare thermotropic main-chain polymers from rigid non-amphiphilic monomers, it is necessary to disrupt the efficient packing of the macromolecules<sup>73</sup>. This may be achieved by introducing bulky groups onto the chain, disrupting the linearity of the chain, or inserting flexible segments between the mesogenic elements along the main-chain; all of which reduce the melting temperature of the polymer<sup>73,74</sup>. Examples of such main-chain mesogenic polymers include, aromatic polyesters<sup>74</sup>, polyazomethines<sup>75</sup>, polyisocyanates<sup>76</sup>, polydiacetylenes<sup>77</sup>, polycinnamates<sup>78, 79</sup> and polystilbene polyesters<sup>80</sup>.

It is worth noting, that for main-chain polymers it is not always necessary for the monomer units of the backbone to be inherently rigid<sup>75</sup>. Chain rigidity can be caused by the secondary structure of the polymer, i.e. the formation of a rigid helical structure held in place by strong intramolecular hydrogen bonding, as exemplified by the polyglutamates. However, mesomorphism in such polymers is generally not as common as the those prepared by the polymerisation of conventional mesogenic monomers.

#### 1.6.2.2 Side-Chain Polymers

If the rod- or disc-type mesogens are attached to a polymer back bone as side-chains, two extreme cases are possible; direct attachment of the mesogen to the backbone or attachment via a long 'spacer' group<sup>64,73</sup>. In the former case, the tendency of the polymer back bone to adopt a statistical distribution of possible chain conformations tends to result, except in a few cases<sup>81-84</sup>, in a disruption of the parallel alignment of the mesogens which

is necessary to produce a mesophase<sup>64</sup>. In the latter case, the presence of the spacer group decouples the motions of the mesogens and the backbone, allowing the mesogens to align themselves independently of the backbone and form a mesophase in a manner analogous to that of their small molecule equivalents (see figure 1.11)<sup>64,73</sup>.

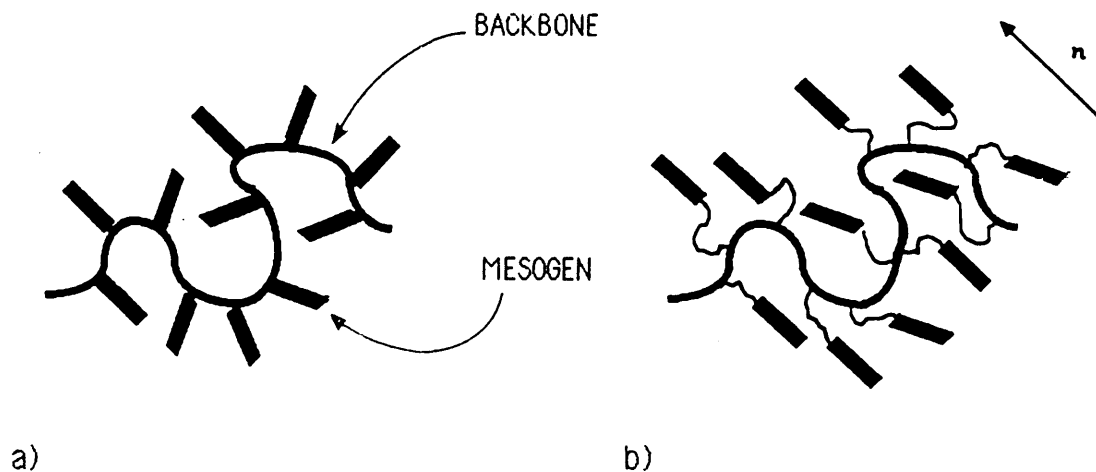


Figure 1.11 Schematic representation of a) direct attachment of mesogen to backbone and b) attachment via a spacer group

In mesogenic side-chain polymers it is the side-chains themselves that are essentially responsible for mesophase formation<sup>64,73</sup>. Hence, providing that the attachment to the polymer does not significantly restrict the motions of the mesogens, the position of this attachment may be on the longitudinal or the lateral axis of the mesogen. A variety of molecular configurations, each with different behaviour and properties, may therefore be envisaged (see figure 1.12 for an outline of side-chain structures)<sup>64,85</sup>.

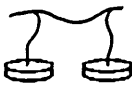
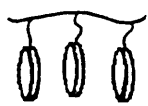
—		○	
LATERAL	LINEAR	LATERAL	LINEAR
			

Figure 1.12 Possible molecular configurations of mesogenic side-chain polymers incorporating rod- and disc-like mesogens, but not including elastomeric structures.

A feature of side-chain polymers is that the mesomorphic arrangement of the side-chains can, in most cases, be frozen in the glassy state of the polymer<sup>86</sup>. If the backbone is a hydrocarbon, the glass transition lies above ambient temperature. The ability to prepare orientationally ordered phases of mesogenic side-chain polymers at just above room temperature, and freeze the orientational order by cooling to room temperature, has practical applications in the field of high density data storage<sup>87</sup>. If the hydrocarbon backbone is replaced by a polysiloxane, which is characterised by highly flexible chain segments, polymers with glass transitions below ambient temperature are produced<sup>88,89</sup>. Mesogenic polymers such as these may be used in display devices, although their response time may be greater than those based on monomeric mesogens. Various non-amphiphilic side-chain polymers, based on polyacrylates<sup>90,91</sup>, polymethylacrylates<sup>90,91</sup> and polysiloxanes<sup>92-101</sup> have been synthesised and some have shown interesting electro-optical properties.

Interesting examples of non-amphiphilic side-chain polymers are the N-acryl derivatives of polymethacryloyl-L-lysine, which reportedly have glass transition temperatures,  $T_g$ , around 100–120°C, but their crystalline melting points,  $T_m$ , are 40–50°C<sup>102</sup>. These species are rare examples of

polymers in which  $T_g > T_m$ . Even when melted, they do not pass into an isotropic phase, as do conventional mesogenic side-chain polymers, but form a structure in which the mesophase domains seem to be placed within the glassy matrix of the polymer. Only above  $T_g$ , when the segmental mobility is high enough, does the mesomorphic order disappear and the isotropic phase appear.

### 1.7 Aims and Outline of Present Research Project

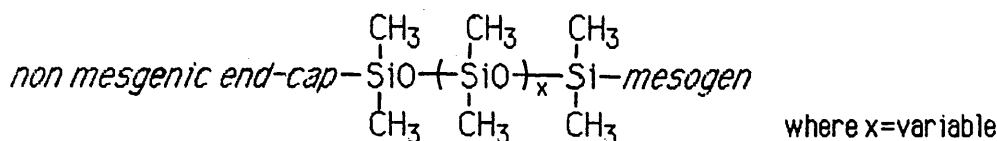
As we have seen, due to their particular combination of properties<sup>103,104</sup> (i.e. their very flexible backbone segments (low  $T_g$ ) and their 'hydrophobic' nature), polysiloxanes have been used as the polymeric moiety in a number of investigations of the thermotropic and lyotropic mesomorphism of amphiphilic and non-amphiphilic polymers. Generally these mesogenic siloxanes have been prepared via the coupling of a reactive siloxane backbone and a suitably functionalised mesogen<sup>64</sup>. The structure and number of the reactive sites on the siloxane precursor, along with the nature of the mesogen, therefore determine the structure and properties of the resultant mesogenic polymer. The starting point for this thesis—which describes the synthesis, and outlines the phase behaviour of a number of novel amphiphilic and non-amphiphilic mesogenic siloxanes—was therefore the potential to synthesise a variety of reactive siloxane moieties which, when coupled to conventional amphiphilic and non-amphiphilic mesogens, would give rise to some envisaged novel structures. The structures of interest were as follows:

- mesogenic side-chain oligomeric cyclic siloxanes, with mesogens attached via spacer groups to each siloxane repeat unit.
- linear dimethyl siloxanes of various chain lengths with mesogenic groups attached to one or both chain ends.

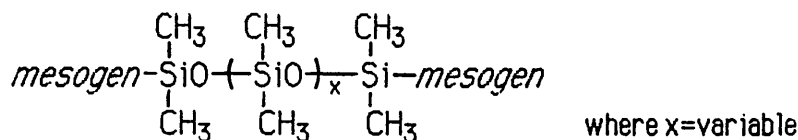
The structures of these target molecules is shown below in figure 1.13.



a) target cyclic side-chain mesogenic siloxanes



b) target linear monofunctional mesogenic siloxanes



c) target linear difunctional mesogenic siloxanes

Figure 1.13 The target cyclic and linear, amphiphilic and non-amphiphilic mesogenic siloxanes

Following the preparation and characterisation of these target molecules, it was planned to compare and contrast their phase behaviour with that of existing related monomeric and, where applicable, polymeric systems. Consequently, the mesogens employed during this study were chosen to allow comparisons with the existing literature relating to monomeric mesogens and linear side-chains mesogenic siloxanes. The amphiphilic

mesogens chosen for study were based on the salts of a C<sub>11</sub> fatty acid as studied by Hall<sup>66</sup>, while the non-amphiphilic mesogens were based on 4'-methoxyphenyl 4-( $\alpha$ -alkenyl)oxybenzoate as studied by Finkelmann *et al.*<sup>99</sup>.

Having begun the practical work, it soon became apparent that time constraints would not allow all the envisaged materials detailed in figure 1.13 to be prepared and studied. As the majority of published data on siloxane based mesogenic polymers refers to the thermotropic phase behaviour of non-amphiphilic polymers, it was decided to concentrate this thesis primarily, but not exclusively, on the phase behaviour of the novel amphiphilic systems. Nevertheless, synthetic routes were investigated and have been outlined for all the target structures given in figure 1.13 (see chapters 3 and 4). The materials whose phase behaviour have been studied are detailed in figure 1.14.

As amphiphilic materials form the major part of this thesis, a more detailed review of the phase behaviour of related monomeric and polymeric amphiphiles is given in chapter 2. In chapter 3 there is an outline of the development of a synthetic strategy for all the target materials, whilst details of the synthetic work actually carried out are given in chapter 4. The main experimental techniques encountered in the characterisation of materials are discussed in chapter 5. For convenience and clarity, the results and discussion related to the phase behaviour of the cyclic and linear amphiphilic polymers—which forms the majority of this thesis—and a brief discussion of the behaviour of the cyclic non-amphiphilic polymers, have been covered separately in chapters 6, 7 and 8, respectively. Recommendations for future work have also been outlined in chapter 9.



## CHAPTER 2. PHASE BEHAVIOUR OF ALKALI AND ALKALINE-EARTH METAL SOAPS AND AMPHIPHILIC POLYMERS

### 2.1 Introduction

The amphiphilic siloxanes which have been prepared and studied during this work represent variations of the established monomeric anionic amphiphiles (termed soaps) and, the more recently developed, amphiphilic polymers (see also chapter 1). Hence, prior to discussing the phase behaviour of the novel systems studied during this work, it is proposed to review the phase behaviour of the conventional alkali and alkaline-earth metal soaps and the recent work on amphiphilic polymers.

### 2.2 Alkali and Alkaline-Earth Metal Soaps

#### 2.2.1 Thermotropic Behaviour of the Alkali Metal Soaps

The alkali metal salts of many carboxylic ( $\text{RCO}_2\text{M}$ ) acids undergo a process of step-wise melting, involving one or more intermediate phases between the crystalline solid and the isotropic liquid<sup>105-107</sup>. The number and structure of these intermediate phases depend upon the cation and the length and the structure of the hydrocarbon chain. However, with the exception of lithium, the thermotropic behaviour of the majority of the alkali metal soaps (i.e. Na, K, Rb and Cs) is qualitatively very similar<sup>108</sup>.

For the straight chain soaps, it has been established that conventional melting occurs only when the number of carbon atoms in the hydrocarbon chain ( $n_c$ ) is less than or equal to three<sup>109,110</sup>. At greater chain lengths (Na and K,  $n_c=4$ ; Rb,  $n_c=5$ ; Cs,  $n_c=6$  and Li,  $n_c=12$ ), these soaps pass through one or more mesophases before the transition to the isotropic liquid<sup>111-115</sup>.

The only thermotropic mesophases formed by short-chain soaps (i.e.  $n_c < 12$ ) that have been studied in any depth are those of sodium<sup>116-129</sup>. Ubbelohde *et al.* carried out extensive studies of the properties and the phase behaviour of sodium n-butanoate and sodium 3-methylbutanoate<sup>116-123</sup>. They concluded that these soaps melted from the lamellar crystalline solid (see figure 2.1a), via a mesophase, to the isotropic liquid. Their X-ray diffraction studies suggested that this intermediate phase consisted of randomly oriented liquid crystal domains of 'sandwich-type' bilayers stabilised by electrostatic forces<sup>118</sup> (see figure 2.1 b).

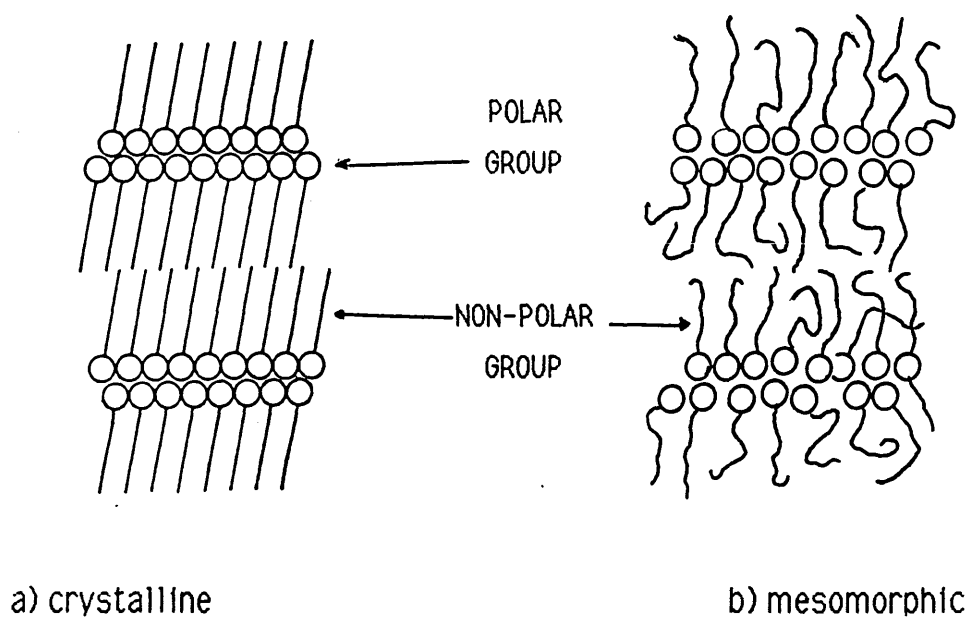


Figure 2.1 Schematic representation of the crystalline and mesomorphic lamellar phases

Polarised microscopy carried out by Bonekamp *et al.*<sup>129</sup> supported these findings, indicating that both sodium n-butanoate and sodium 3-methylbutanoate form a lamellar mesophase structure (smectic A or neat) prior to the formation of the isotropic melt.

Nuclear magnetic resonance (NMR) studies on a range of straight and branched short-chain sodium soaps<sup>124-128</sup>, along with data obtained from polarised microscopy<sup>129</sup>, have shown that the mesophase properties of these soaps may be very dependent on the structure of the the alkyl chain. For instance, soaps such as sodium 2-methylpropanoate do not form thermotropic mesophases<sup>109,130</sup>, whilst the unbranched equivalent, sodium butanoate, does. On the basis of these observations, a model for the arrangement of the polar groups in the lamellar mesophase was proposed for all short-chain sodium soaps<sup>128</sup>. This model proposed an ionic double layer with interdigitated polar groups, as opposed to the 'sandwich-type' bilayer structure originally proposed by Ubbelohde *et al.*<sup>118</sup>.

The thermotropic phase behaviour of straight long-chain soaps (where  $n_c \geq 12$ ) has been investigated for many years<sup>130-140</sup>. The structures of the phases occurring during the transition of these soaps from the crystalline solid to the isotropic liquid have been extensively studied by Skoulios *et al.* using X-ray diffraction<sup>108,115,141-147</sup>. Not all of the structures original proposed during this work have been corroborated by addition techniques<sup>148</sup>.

At room temperature, straight long-chain soaps form lamellar crystalline phases. In these structures, it is thought that the molecules are packed in a three-dimensional lattice in which the polar groups and the hydrocarbon chains form alternating double layers<sup>108</sup>. The hydrocarbon chains are fully extended and inclined with respect to the end-group planes (see figure 2.1a).

As the temperature is raised, the hydrocarbon chains begin to melt. This results in the formation of semi-crystalline phases (ribbon or disc) in which the polar groups are thought to be in a crystalline type of

organisation, dispersed in a liquid hydrocarbon matrix<sup>24,108,149</sup>. The number of these ribbon or disc phases (sometimes also termed the plastic<sup>150</sup>, or subwaxy, waxy, superwaxy and subneat phases<sup>151</sup>) depends on the length of the hydrocarbon chain and the cation<sup>149</sup>.

For the sodium soaps (even-numbered homologues from  $C_{12}$  to  $C_{18}$ ), these phases are thought to consist of groups of parallel ribbons of indefinite length, packed in a two dimensional rectangular lattice<sup>141-144</sup> (figure 2.2).

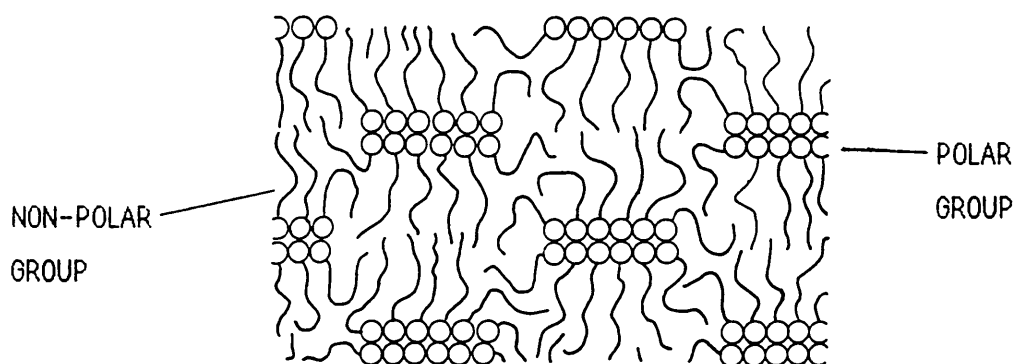


Figure 2.2 A cross-section of the structure of the two-dimensional rectangular lattice of the ribbon phase of the sodium soaps<sup>142</sup>.

The phases formed by the potassium soaps (even-numbered homologues from  $C_{16}$  to  $C_{22}$ ) are thought to consist of groups of parallel ribbons, of indefinite length, packed in a two dimensional oblique lattice<sup>144-146</sup>.

For the rubidium soaps (even-numbered homologues from  $C_{16}$  to  $C_{20}$ ) disc phases are thought to form<sup>147</sup>. These phases consist of groups of parallel discs packed on a face centred orthorhombic lattice, the discs representing the loci of the polar groups which are separated by the disordered non-polar chains. The caesium soaps ( $C_{18}$ ,  $C_{20}$  and  $C_{22}$ ) also form disc phases, in which the discs are located in parallel and equidistant planes but with loose lateral correlation between the discs themselves<sup>108</sup>.

In all these semi-crystalline phases, the breadth of the ribbons or the size of the discs is determined by the competition between the thermal agitation of the hydrocarbon chains and the strong forces of attraction between the head groups and the counter ions. Hence, the breadth of the ribbons or the size of the discs decreases discontinuously with rising temperature, with each decrease corresponding to a phase transition<sup>24</sup>. As the ribbons or discs decrease in breadth with rising temperature and become more symmetrical, the lattices of the successive phases tend towards a two-dimensional hexagonal arrangement. However, according to Skoulios *et al.*, the lamellar bilayer mesophase (smectic A or neat soap) is eventually formed by all these long-chain soaps as the phase immediately preceding the isotropic melt<sup>106</sup>. This transition from a semi-crystalline phase to the lamellar mesophase is thought to arise as a result of the complete melting of the polar groups.

For lithium soaps, it has been established that conventional melting occurs with less than 12 carbon atoms in the n-alkyl chain<sup>115</sup>. At greater chain lengths, intermediate semi-crystalline phases (possibly of a ribbon type) and mesophases are known to form between the crystalline solid and the isotropic liquid<sup>115,148,150</sup>. A review of the published data for the thermal behaviour of selected lithium soaps (i.e. the C<sub>14</sub>, C<sub>16</sub> and C<sub>18</sub> soaps) presented conflicting data from different laboratories and demonstrated that the phase behaviour of these soaps, despite being less complicated than the corresponding soaps of the majority of alkali-metals, has not been fully resolved<sup>148</sup>.

### 2.2.2 Thermotropic Behaviour of the Alkaline-Earth Metals Soaps

To date, the thermotropic phase behaviour of the short-chain alkaline-earth metal soaps has not been studied in depth. The straight long-chain soaps,  $(RCO.O)_2M$ , like the equivalent alkali metal soaps, undergo a process of step-wise melting involving one or more intermediate phases between the crystalline lamellar and the isotropic liquid<sup>152-163</sup>. As was the case with the alkali metal soaps, the number and structure of these intermediate phases depends upon both the cation and the length and structure of the hydrocarbon chain. On the basis of X-ray diffraction, Spegt and Skoulios proposed a number of structures for these intermediate phases, including various high temperature mesophases<sup>164-169</sup>. Some of the structures proposed for the low temperature polymorphs of these soaps have since been reinterpreted in terms of the arrangements of long rod structures<sup>170</sup>, rather than the disc structures originally proposed by Spegt and Skoulios<sup>166,167</sup>. Even these latterly proposed structures are not regarded as definite.

The soaps of calcium<sup>160</sup> and strontium<sup>167</sup> form an hexagonal mesophase made up of parallel rod micelles of indefinite length arranged in a two-dimensional hexagonal array (see figure 2.3).

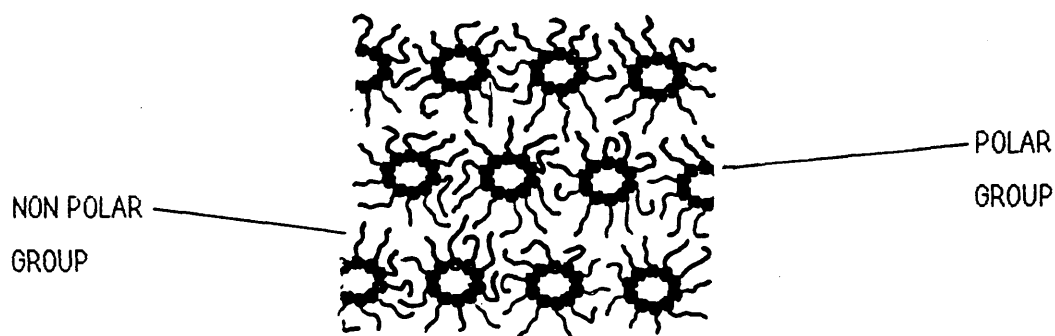


Figure 2.3 A cross-section of the structure of the two-dimensional reversed hexagonal structure.

In this structure, the polar groups form the central core of the rods whilst the hydrocarbon chains extend radially from them and form the continuous medium. Although X-ray diffraction measurements indicate that the hydrocarbon chains are fully disordered, the exact arrangement of the polar groups remains to be established<sup>167</sup>.

The soaps of magnesium and cadmium are thought to form two hexagonal mesophases preceding the transition to the isotropic melt<sup>164,168</sup>. In each case, the higher temperature structure is believed to possess a slightly less compact arrangement of the polar groups.

For the soaps of barium and strontium, it has been proposed that a body centred cubic mesophase is the phase immediately preceding the isotropic melt<sup>167,171</sup>. This mesophase is thought to be made up of rod micelles of finite length arranged in a body centred cubic lattice. The polar groups form the central core of the rods whilst the hydrocarbon chains extend radially from them, forming the continuous medium.

### 2.2.3 Thermotropic Behaviour of the Branched Chain Soaps

As we have seen, the thermotropic phase behaviour of the alkali and alkaline-earth metal soaps depends on the cation and also the length and the structure of the hydrocarbon chain. In amphiphiles in which the hydrocarbon chains are of a non-compact structure (i.e branched), the anhydrous soap may exist as a mesophase at room temperature, where the unbranched equivalent would be crystalline<sup>172-175</sup>. This is primarily due to steric effects, as the chain branching not only prevents the hydrocarbon chains themselves from crystallising, but also inhibits the close approach and crystallisation of the polar groups.

A well known amphiphile exhibiting such phase behaviour is Aerosol OT (sodium di-2-ethylhexylsulphosuccinate). This branched chain soap exists as a reversed hexagonal structure at room temperature, whilst the equivalent straight chain soap (sodium di-hexylsulphosuccinate) crystallises readily<sup>173</sup>.

#### 2.2.4 The Aqueous Lyotropic Phase Behaviour of the Alkali Metal Soaps

The phase behaviour of amphiphile/water systems has been studied for many years<sup>132-139</sup>. Phase diagrams of the long-chain sodium and potassium soaps/water systems were originally reported by McBain and co-workers, to elucidate the principles underlying the soap boiling process<sup>132,136-138</sup>. A representative composition phase diagram for these systems—in this case sodium laurate/water—is shown in Figure 2.4. In this phase diagram, the vertical axis at zero percent water, shows the phase behaviour of the neat soap as a function of increasing temperature. The horizontal axis demonstrates the variation in phase behaviour as a function of added water.

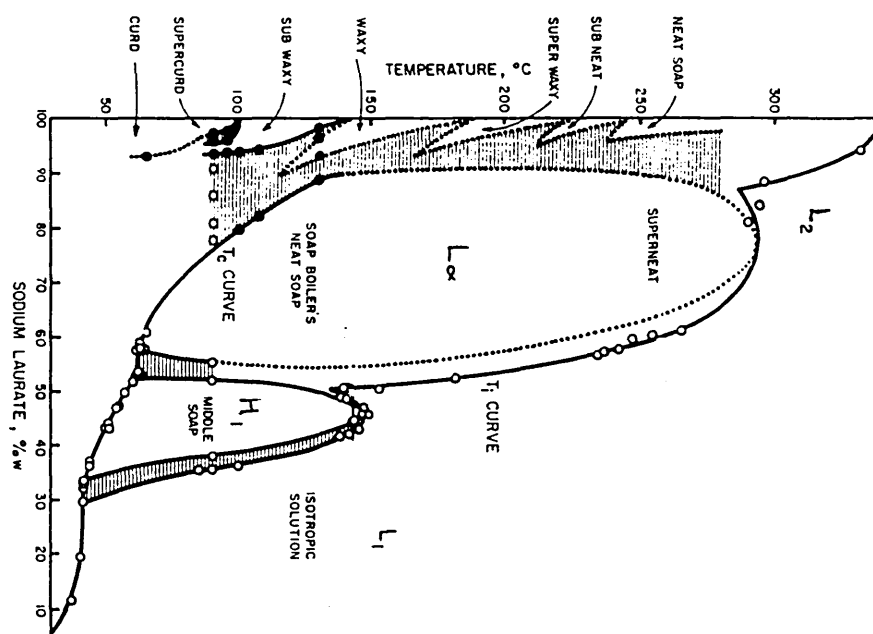


Figure 2.4 The phase diagram for sodium laurate/water (taken from reference 11).

Whilst each of the crystalline and semi-crystalline phases of the neat soap (see section 2.2.1) can incorporate only a very small amount of water, the high temperature lamellar mesophase can incorporate up to 40% by weight of water in its bilayer structure. The presence of this water greatly reduces the temperature stability of this phase and the temperature at which the phase forms.

At higher water concentrations, the hexagonal ( $H_1$  or middle) mesophase is formed. In this phase, the soap molecules are packed in parallel rod micelles of indefinite length which are arranged in a two dimensional hexagonal array. The core of the rods is made up of the liquid hydrocarbon chains, whilst the polar groups occupy the interface in contact with the aqueous continuous phase.

In these systems, it has been established that the sequence of phases occurring with increasing temperature and/or concentration is the lamellar ( $L_\infty$ ) and hexagonal ( $H_1$ )<sup>176</sup>. These phases were originally thought to coexist at intermediate soap concentrations<sup>138</sup>. Latterly, more detailed investigations of various sodium soap/water systems have demonstrated the existence of a variety of other birefringent and non-birefringent mesophases occurring over a narrow concentration around the lamellar to hexagonal transition region<sup>176-184</sup>.

On the basis of low-angle X-ray diffraction patterns, Luzzati *et al.*<sup>177,178</sup> proposed the deformed hexagonal and the complex hexagonal structures for the birefringent 'intermediate' phases formed by the  $C_{14}$ ,  $C_{16}$  and  $C_{18}$  sodium soaps. The deformed hexagonal structure ( $H_{1d}$ ) is composed of long rod

micelles on a rectangular lattice. In the complex hexagonal structure ( $H_c$ ), the amphiphile forms hollow, circular, long rod micelles with a water interior, which are hexagonally packed in a water continuum.

More recently, Tiddy *et al.*<sup>185</sup> used a range of techniques to systematically study the occurrence of these intermediate phases with several series of anionic amphiphiles as a function of chain length. Similar phase behaviour was demonstrated for the sodium and potassium soaps and the sodium alkyl sulphates. With the short hydrocarbon chain derivatives, a non-birefringent bicontinuous cubic phase ( $V_1$ ) occurs, while at higher chain lengths, the birefringent 'intermediate' phases predominate.

On the basis of optical microscopy, NMR and X-ray diffraction, Tiddy<sup>185</sup> agreed with the structure of the deformed hexagonal as proposed by Luzzati<sup>177,178</sup>. However, in view of the fact that the complex hexagonal structure proposed by Luzzati would necessitate widely differing surface areas per head group on the inner and outer surfaces of the micelle—which seemed unlikely—a thin bilayer structure with a hydrogen-bonded water network linking the bilayers, was the structure proposed for this phase.

On increasing the water concentration to approximately 70% by weight, an isotropic micellar solution is formed. A variety of techniques have been used to investigate the size and shape of these micelles. These include light scattering, neutron scattering, viscosity measurements and osmotic pressures. At higher soap concentrations (i.e. at soap concentrations just less than that required for the hexagonal phase to form), the isotropic micellar solution is thought to be made up of small rod micelles, whilst at soap concentrations approaching the c.m.c spherical micelles predominate<sup>13</sup>.

As the temperature is increased, a point is reached for each soap/water composition where the increased thermal agitation breaks down the long range order in the mesophase, resulting in the formation of the isotropic micellar solution<sup>13</sup>.

The same basic diagrams are characteristic of all the long chain soaps of sodium, potassium, rubidium and caesium<sup>139,146,176-178,185-187</sup>. Variations do occur due to differences in the thermotropic behaviour of the anhydrous soaps, changes in the cohesive forces in the polar regions with increasing atomic number of the cation, and the formation of low temperature 'gel' phases<sup>106,188-191</sup>.

The 'gel' phase is made up of single layers of parallel, interdigitated soap molecules. The hydrocarbon chains are stiff and fully extended whilst the polar regions (i.e the polar groups and water) are thought to be fluid.

As with thermotropic behaviour, the lyotropic behaviour of the lithium soaps is somewhat different from the majority of the alkali metal soaps. In fact, the straight chain lithium soaps are quite insoluble in water until well above 100°C and hence, few studies of lithium soap/water systems have been published<sup>192</sup>. Vold<sup>140</sup> used visual observations to construct a phase diagram for lithium palmitate/water system. In general, the phase diagram was very similar to that of the sodium palmitate/water system as determined by McBain *et al.*<sup>132</sup>. The most important difference was the greater temperature and composition stability of the mesophase region (H<sub>1</sub>) formed by the lithium soap.

### 2.2.5 The Aqueous Lyotropic Phase Behaviour of the Alkali-Earth Metal Soaps

The straight long-chain alkali-earth metal soaps, like those of lithium, are quite insoluble in water until well above 100°C. Hence, little work has been carried out on these soap/water systems.

### 2.2.6 The Aqueous Lyotropic Phase Behaviour of Branched Chain Soaps

As discussed in section 2.2.3, a number of branched chain soaps exist as a mesophase at room temperature, whereas the equivalent unbranched soaps are crystalline. At room temperature, the addition of water to these mesomorphic soaps results in the formation of the isotropic liquid phase or hydrated mesophases, depending on the amphiphile concentration<sup>193</sup>.

For instance, Aerosol OT which exists as a reversed hexagonal mesophase in the neat state<sup>173</sup>, can solubilise up to 16% by weight of water in this structure, with a corresponding increase in the dimensions of the rod micelles<sup>194</sup>. Further increase in the water content gives rise to a viscous isotropic phase ( $V_2$ ), followed by the lamellar mesophase. At approximately 90% by weight of water, a two phase region consisting of the lamellar mesophase and the isotropic micellar solution exists, whilst at greater than approximately 98.7% by weight of water, the isotropic micellar phase is formed<sup>195</sup>.

More recently, Khan *et al.*<sup>196</sup> studied the aqueous phase behaviour of calcium and magnesium di-2-ethylhexylsulphosuccinate and compared the behaviour of these soaps with the corresponding sodium soap (Aerosol OT). Whilst all three soaps exhibited the same sequence of phases with increasing amphiphile concentration (i.e the isotropic solution, and the lamellar, cubic and reversed hexagonal mesophases), the phase diagrams of the calcium and

magnesium soaps differed from that of the sodium soap in two respects. Firstly, the aqueous solubility of the calcium and magnesium systems was found to be much lower than that of the sodium system. Secondly, the lamellar phase of the divalent soaps was observed to swell to a lesser degree and to incorporate much less water than the sodium soap. This behaviour has been explained in terms of the different long range electrostatic interaction arising from the respective counter-ions<sup>197</sup>.

### 2.2.7 The Lyotropic Phase Behaviour of the Alkali and Alkaline-Earth Metal Soaps in Non-polar Solvents

Although most of the published literature on micelle formation concerns aqueous systems, work has been carried out in non-polar solvents<sup>20,131,198-200</sup>. The aggregation of amphiphiles into reversed micelles occurs when some amphiphiles, possibly with a little water, are dissolved in non-polar solvents (see section 1.3.1.). The properties of these reversed micelles are similar to those of normal micelles, although the micellisation in non-polar solvents is driven by attractions between polar head groups (and possibly a little water) which form the micelle interior, rather than the 'solvophobic' effect encountered in aqueous systems<sup>13,20</sup>.

At room temperature, the crystalline long-chain alkali and alkaline-earth metal soaps show very little solubility in hydrocarbons due to the very strong cohesive forces of the polar groups<sup>201-205</sup>. As we have seen, when heated these anhydrous soaps undergo a process of step-wise melting, in which first the hydrocarbon chains and then the polar groups undergo progressive disordering (see sections 2.2.1 and 2.2.2). During this progressive melting, hydrocarbon solvents can be dissolved in limited amounts in the disordered hydrocarbon regions of the amphiphile, while the

polar groups essentially retain their crystalline order<sup>167,206,207</sup>. In general, at the temperature at which a soap undergoes a thermotropic transition to a mesophase—which is accompanied by the melting of the polar regions—complete solubility of the soap in the non-polar solvent will occur. For example, the amphiphiles of branched soaps which are mesomorphic at room temperature, are also soluble in a range of non-polar solvents at this temperature. They are therefore known as the 'oil-soluble soaps'<sup>20</sup>.

Whilst the formation of lyotropic mesophases occurs in many concentrated amphiphile/water systems, and has been studied extensively and is relatively well understood, the formation of anhydrous mesophases in soap/non-polar solvent systems is relatively rare. Few fundamental studies<sup>173,201,202,206-211</sup> have been made and hence, these systems are less well understood than their aqueous counterparts.

Smith and McBain used visual observations to construct binary phase diagrams for the sodium stearate ( $\text{NaC}_{18}$ )-toluene and  $\text{NaC}_{18}$ -cyclohexane systems<sup>209</sup>. At room temperature there was little interaction between the soap and the non polar solvents, but at higher temperatures the existence of two liquid crystalline 'phase islands' was reported. The mesophase occurring at highest soap concentrations was termed the 'white, waxy, liquid crystalline phase', the other was termed the 'golden, liquid crystalline phase'. The structure of the mesophases observed in the  $\text{NaC}_{18}$ -cyclohexane system was subsequently investigated by Skoulios using X-ray diffraction techniques<sup>206</sup>. The 'white, waxy, liquid crystalline phase' was thought to be a solvent swollen, ribbon phase of the pure anhydrous soap. The 'golden phase' was thought to be a lamellar mesophase with a solvent swollen bilayer structure.

Two groups of researchers, Stross and Abram<sup>202,210</sup> and Doscher and Vold<sup>211</sup>, investigated the phase behaviour of the NaC<sub>18</sub>-cetane (n-hexadecane) system. Whilst both groups agree that the behaviour of this system was very different to that of the NaC<sub>18</sub>-hydrocarbon systems studied by Smith and McBain<sup>209</sup>, there were major differences in the reported phase behaviour of the NaC<sub>18</sub>-cetane system. Stross and Abrams suggested that the discrepancies between their findings and those of Doscher and Vold may have been due to the failure of the latter to maintain truly anhydrous conditions. These differences may, therefore, illustrate one of the major experimental difficulties encountered when working with non-aqueous systems; that of the ingress of atmospheric moisture. Hence, where possible, such studies should be carried out in an inert, dry atmosphere.

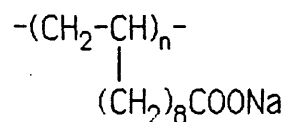
### 2.3 Polymeric Amphiphiles

The wide spread study of monomeric amphiphiles has established empirical relationships between the structure of an amphiphile and the structure of micelles and mesophases formed by that amphiphile<sup>13</sup>. The recent increasing interest in polymer liquid crystals has led to the application of these relationships to polymeric materials and hence, to the polymerisation or the polymer fixation of monomeric amphiphiles in an effort to investigate the properties of their polymeric equivalents<sup>64</sup>. Even so, studies of the mesophase behaviour of amphiphilic polymers, especially in the neat state, are relatively limited.

A class of amphiphilic polymer, the 'polysoaps'—defined as 'polymers to whose chain soap molecules have been attached'<sup>212</sup>—were first synthesised and studied in the early 1950's. Strauss and Jackson synthesised addition

compounds of poly-2-vinyl pyridine and n-dodecyl bromide, and investigated the properties of these materials in dilute aqueous and alcoholic solutions<sup>212</sup>. No investigation of mesophase formation was reported.

Several groups have synthesised low molecular weight polymers of sodium-10-undecenoate, all of which had the following basic structure:

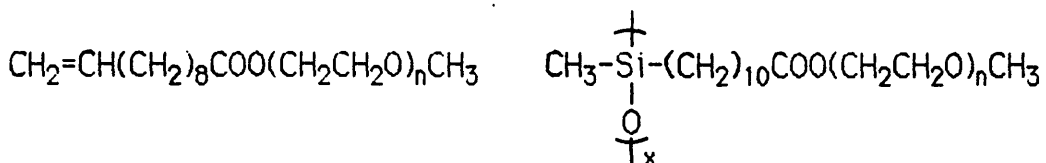


Paleos *et al.*<sup>213</sup> and Larrabee *et al.*<sup>214</sup> synthesised oligomers of sodium 10-undecenoate, carrying out the polymerisation in aqueous solution above the c.m.c. of the monomeric amphiphile. Again, no investigation of mesophase formation was reported, with the subsequent investigations concentrated on micellar behaviour in dilute aqueous solution.

Friberg *et al.*<sup>65</sup> also synthesised a low molecular weight polymer of sodium-10-undecenoate, initiating the polymerisation in the aqueous hexagonal mesophase (H<sub>1</sub>) (i.e. 50 weight % of the amphiphile). The polymeric amphiphile was found to exhibit a lamellar mesophase at 20°C, compared with the hexagonal mesophase of the corresponding monomer/water system. This change in phase behaviour was explained in terms of the rigid polyethylene backbone, resulting from the polymerisation reaction, restricting the free orientation of the amphiphilic side-chains.

The first report of an amphiphilic side-chain polysiloxane exhibiting lyotropic mesomorphism was published by Finkelmann *et al.*<sup>70</sup>, in which the lyotropic phase behaviour of aqueous solutions of a non-ionic monomeric

amphiphile and the corresponding polymeric amphiphile were compared (see figure 2.5).



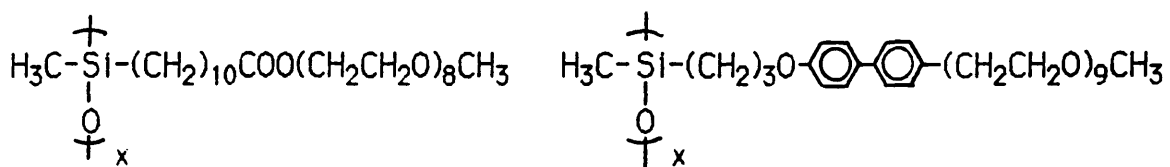
a) where  $n = 4, 6, 8$

b) where  $x = 95$  and  $n = 4, 6, 8$

**Figure 2.5** a) The non-ionic monomeric amphiphiles and b) the corresponding amphiphilic polysiloxanes studied by Finkelmann *et al.*<sup>70</sup>.

It was found that in the polymeric system, the mesophases were stable over a much broader range of temperatures and compositions. This was attributed to a restriction of the motions of the amphiphiles, due to the linkage to the polymer main chain. However, there was also a recognition that the effective lengthening of the hydrophobic moiety of the amphiphilic repeat unit due to polymer fixation may contribute to a similar effect.

Finkelmann *et al.*<sup>68</sup> subsequently contrasted the aqueous phase behaviour of two related non-ionic amphiphilic siloxanes in which the monomeric amphiphiles incorporated rigid and flexible hydrophobic groups (see figure 2.6 a) and b), respectively).



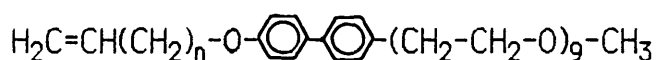
a)

b)

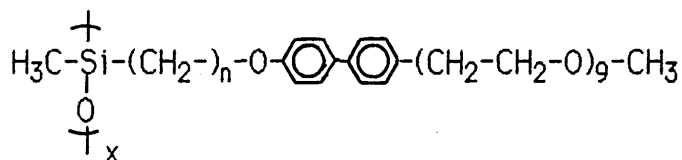
**Figure 2.6** Non-ionic polymeric amphiphiles incorporating b) rigid and a) flexible hydrophobic moieties.

In both these systems, the polymer fixation of the monomeric amphiphiles enhanced the temperature and concentration stability of the mesophases which were characteristic of the respective monomeric amphiphile. Again, this was primarily attributed to a restriction of the motions of the amphiphiles due to linkage to the polymer main chain, although the lengthening of the hydrophobic moiety of the amphiphilic repeat unit resulting from polymer fixation was also considered as an alternative explanation.

The study of the aqueous phase behaviour of non-ionic amphiphilic siloxanes in which the monomeric amphiphiles incorporated rigid hydrophobic groups was subsequently extended by Finkelmann *et al.*<sup>71</sup>. Again, polymer fixation of the monomeric amphiphiles enhanced the temperature and concentration stability of the mesophases which were characteristic of the respective monomers. During this work, the first observation of a lyotropic nematic mesophase exhibited by an amphiphilic polymer was reported. The monomeric amphiphiles and the repeat units of the corresponding amphiphilic polymers studied during this work are represented in figure 2.7:



a) where  $n = 1$  and  $4$



b) where  $n = 3$  and  $6$

**Figure 2.7** a) monomeric and b) polymeric amphiphiles incorporating rigid hydrophobic moieties.

It is interesting to note that the occurrence of the nematic phase was not noted in the initial study of the polymeric amphiphile in question (i.e. figure 2.7 b) where  $n = 3$ ). This may have been due to the narrow temperature and composition range over which the nematic phase occurred.

The aqueous phase behaviour of a monomeric monosaccharide and the polymeric equivalent has been investigated<sup>69</sup>. For the polymeric amphiphile no c.m.c. was observed. It was assumed that the first macromolecule in solution formed a micelle. When compared with the behaviour of the monomer, the temperature and composition stability of the lamellar mesophase formed by the polymeric monosaccharide was greatly enhanced. It was proposed that the polymerisation of this monomer did not significantly alter the lipophilic/hydrophilic balance of the amphiphilic repeat unit and hence, the modified phase behaviour of the polymer was primarily due to a change in micellar kinetics. It was suggested that individual amphiphilic side-chains could not easily escape from the micelle because they were fixed to the polymer backbone. Consequently, the micelle itself was stabilised and, as a mesophase is made up of micelles, the resulting lamellar phase was more stable.

Thus far, the few examples of amphiphilic side-chain polymers exhibiting mesomorphic behaviour have comprised of a non-polar polymer with polar groups attached as side-chains to this backbone via a hydrocarbon spacer (see figure 2.8 a). Jahns and Finkelmann<sup>215</sup> investigated the mesophase behaviour in aqueous solution of an amphiphilic side-chain polymer polymerised at the hydrophilic moiety of the amphiphile (see figure 2.8 b). This type of molecular configuration had been noted previously<sup>212</sup>.

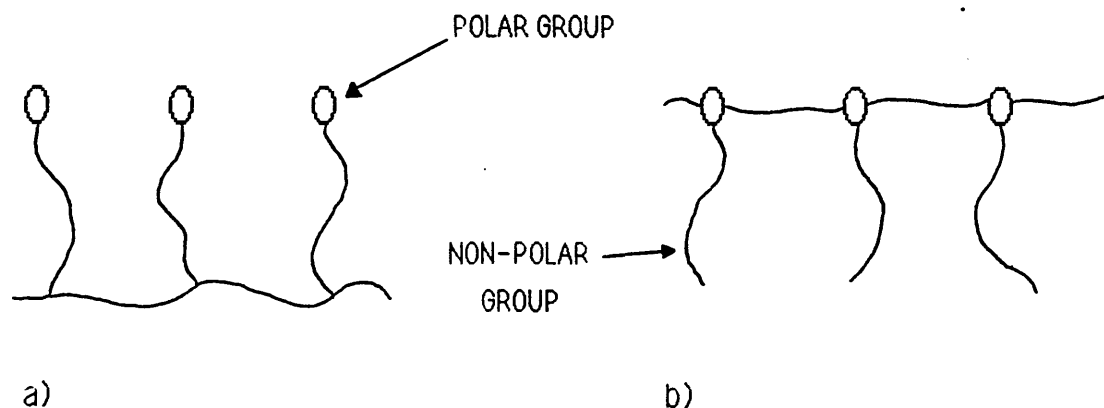
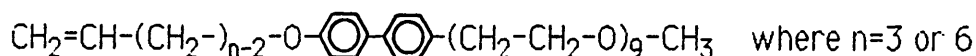


**Figure 2.8** Schematic representation of amphiphilic side-chain polymers polymerised at (a) the hydrophobic tail and (b) the polar head group.

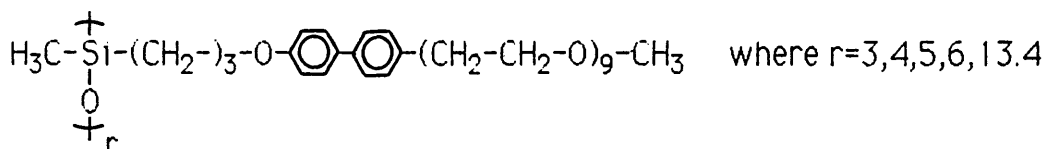
Jahns and Finkelmann<sup>215</sup> originally proposed that polymers of this general structure would, for steric reasons, preferentially form inversed micelles and therefore, reversed mesophases. This was not found to be the case, with the polymeric amphiphile exhibiting normal hexagonal, cubic and lamellar mesophases with increasing polymer concentrations in aqueous solution.

Tanaka and Nakaya<sup>216</sup> also prepared amphiphilic side-chain polymers polymerised at the hydrophilic moiety of the amphiphile. They prepared polyurethanes containing long alkyl chains in the side-chains and amino or quaternary ammonium groups in the main-chains. Optical microscopy and differential scanning calorimetry (DSC) were used to investigate the thermotropic behaviour of the neat materials. Some of the amphiphilic polyurethanes exhibited a thermotropic mesophase which was thought to be made up of alternating polar and non-polar regions; rather like a lamellar bilayer.

Recently, Luhmann and Finkelmann<sup>67</sup> considered the phase behaviour of aqueous solutions of a range of non-ionic amphiphilic monomers whose hydrophobic moiety incorporated a rod-like segment, and the polymeric and oligomeric side-chain amphiphiles synthesised by the fixation of one these monomers to various siloxanes backbones. The structures of the polymeric and oligomeric amphiphiles and the equivalent monomeric amphiphiles is given in figure 2.9.



(a)



(b)

**Figure 2.9** a) The monomeric amphiphiles (hereafter referred to as  $\text{MC}_n\text{BiE}_9$ ) and b) the polymeric/oligomeric amphiphiles (hereafter referred to as  $\text{P}_r\text{C}_3\text{BiE}_9$ ) studied in reference 67.

Although, the phase behaviour of the monomeric amphiphiles was generally consistent with that of common non-ionic amphiphiles<sup>25,217</sup>, the introduction of the biphenyl moiety resulted in a characteristic change in mesophase behaviour as the flexible hydrophobic moiety became shorter. With decreasing length of the flexible hydrophobic chain, there was a tendency of the amphiphiles towards crystallisation and an increase in krafft temperature. Hence,  $\text{MC}_3\text{BiE}_9$  did not form any mesophases. With increasing hydrophobic chain length (i.e  $\text{MC}_6\text{BiE}_9$ ) there was a decrease in the krafft temperature and an increase in water solubility at room

temperature. Hence,  $MC_6BiE_9$  was reported to exhibit two isotropic phases, and the hexagonal and lamellar mesophases.

In general, the aqueous phase behaviour of the polymeric and oligomeric amphiphilic siloxanes ( $P_rC_3BiE_9$ ) resembled that of  $MC_6BiE_9$ . From this it was concluded that:

- the effect of the attachment of the amphiphilic units to every monomer unit of a polysiloxane chain is equivalent to an increase of the hydrophobic chain by 3-4 methylene units
- the attachment of the amphiphilic units to a polysiloxane backbone does not significantly restrict the translational and rotational motions of the amphiphiles.

In addition, the comparison of the oligomeric and the polymeric amphiphiles ( $P_rC_3BiE_9$  where  $r=3, 4, 5, 6, 13.4$  and  $55$ ) indicated that increasing the degree of polymerisation had the following effects:

- increasing the temperature stability of the lamellar mesophase, possibly due to increased interactions between adjacent hydrophobic layers
- decreasing the temperature stability of the mesophases built up of isotropic micelles, due to changes in the packing constraint of these multi-amphiphile units
- the thermal stability of the hexagonal phase was found to be independent of the degree of polymerisation, as neither of the aforementioned effects was thought to play a significant role in a mesophase built up of long rod micelles.

The variation in phase behaviour with the degree of polymerisation of amphiphilic side-chain polymers was also investigated by Luhmann<sup>218</sup> in aqueous solutions of oligooxyethylene alkylethers and their polymeric equivalents. As above, with increasing degree of polymerisation, the clearing temperature of the lamellar phase increased, that of the hexagonal phase stayed constant, whilst that of the cubic phase decreased.

Hall<sup>66</sup> has also investigated the phase behaviour of aqueous solutions of a non-ionic side-chain polysiloxane. This material was of a similar structure to that studied by Finkelmann *et al.*<sup>70</sup> (see figure 2.5), the main difference being the degree of polymerisation of the siloxane backbones (i.e.  $\overline{DP} \approx 35$  and 95, respectively). In general, the lyotropic phase behaviour of the two polymers was very similar. The mesophases formed by the polymeric amphiphiles were stable over a greater range of temperature and composition than the corresponding monomer. The stabilisation of the mesophase regions was explained in terms of a lengthening of the hydrophobic part of the amphiphilic chain due to fixation to the siloxane backbone, rather than the restriction of the motions of the amphiphiles due to linkage to the main-chain, as originally emphasised by Finkelmann<sup>70</sup>.

This change in phase behaviour on lengthening the hydrophobic moiety of the amphiphile following polymer fixation, mimics the change in behaviour observed when comparing  $C_{12}EO_8$  and  $C_{16}EO_8$ <sup>217</sup>. Indeed, the phase diagrams of  $C_{16}EO_8$  and the polymeric non-ionic amphiphile were shown to be qualitatively very similar. Thus, Hall also concluded that, as an approximation, the effect of attaching amphiphilic units to every monomer unit of a polysiloxane chain is equivalent to an increase in length of the alkyl chain of the amphiphile by 3 methylene units.

During this research, Hall also examined the phase behaviour of the same linear siloxane ( $\overline{DP} \approx 35$ ) with an ionic sodium alkanoate side-chain attached to every silicon atom of the siloxane backbone (see figure 2.10). This material represented the first example of the attachment of ionic amphiphiles as side-chains to a siloxane polymer.

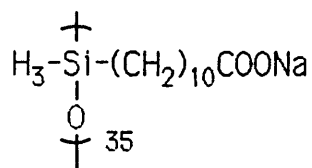


Figure 2.10 The first reported example of an ionic polysiloxanes exhibiting lyotropic mesomorphism<sup>66</sup>.

An overview of the properties of the polymer/water system was obtained using the penetration technique of Lawrence<sup>219</sup>. The polymeric amphiphile formed the hexagonal ( $H_1$ ) mesophase at room temperature, and at higher amphiphile concentrations and higher temperatures (70°C), the lamellar ( $L_\alpha$ ) mesophase. Contrasting the phase behaviour of the polymer with the that of the conventional sodium n-alkanoates<sup>185</sup>, and with reference to their previous experience with the non-ionic side-chain polysiloxane, it was concluded that:

- attachment of amphiphilic units to a polysiloxane backbone does not significantly restrict the translational motion and micelle packing of the amphiphiles
- there is little difference between the phase behaviour of the polymeric amphiphile and that of conventional sodium alkanoates
- the general behaviour of this ionic polysiloxane could be explained in terms of the increase in alkyl chain length of the amphiphile due to fixation to the siloxane backbone.



of the respective backbones. The polymethacrylate, which has the least flexible main-chain, exhibited the lamellar phase only in the presence of water. In contrast, the polyacrylate and the polysiloxane exhibited the lamellar phase in the neat state as well as in aqueous solution. The polysiloxane, which has the most flexible main-chain, showed the highest clearing temperature, and a lamellar mesophase that extended over the widest temperature and composition range. Therefore, in line with previous studies, it was concluded that polymer fixation stabilises the lamellar mesophase and, the more flexible the nature of the polymer backbone, the greater the effect of this stabilisation.

Recently Loffler and Finkelmann<sup>220</sup> prepared a non-ionic side-chain methacrylate copolymer containing 4 mole % of a difunctional comonomer (2-hydroxyethyl methacrylate). This linear polymer was then cross-linked via the reaction of the hydroxyl group of the comonomer with 4,4'-methylenediphenyl diisocyanate (MDI). The lyotropic phase behaviour of the linear and 'lightly' cross-linked polymers upon swelling in water was subsequently investigated. Both polymers formed lyotropic hexagonal phases over a similar range of polymer concentrations. However, the mesophase to isotropic phase transition temperatures were reduced for the cross-linked polymer. It was suggested that this was due to a distortion of the phase structure at, and in, the vicinity of the cross-link sites.

## CHAPTER 3. SYNTHETIC STRATEGY

### 3.1 Introduction

During the course of this work various amphiphilic and non-amphiphilic siloxanes which had been identified as of possible academic and practical interest, have been synthesised. The various target molecules could be thought of as consisting of two components; the mesogen, and the siloxane chain to which this mesogen was attached. The target molecules contained one or more mesogens, but in every case an individual mesogen was attached to the siloxane chain at only one point. Hence, the mesogen did not form part of the backbone itself, although in some molecules the mesogen did constitute a chain-end. In this respect and in terms of the development of a synthetic strategy, all the target materials were considered to be variants of side-chain polymers.

Amphiphilic and non-amphiphilic side-chain polymers have been prepared by one of two methods<sup>64</sup>. In the first method, a reactive group capable of undergoing a polymerisation reaction is attached to a mesogenic molecule. On polymerisation, this reactive groups forms the polymer backbone and the mesogens constitute the side-chains:

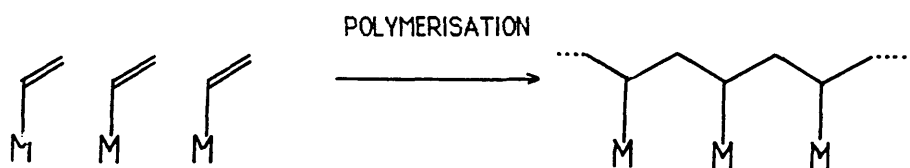


Figure 3.1 Schematic representation of the polymerisation of functionalised mesogens, where M= mesogen.

This method has been used extensively in the synthesis of mesogenic side-chain polymers based on a hydrocarbon back-bone, where the reactive group is a vinyl unit capable of undergoing addition polymerisation (i.e. acrylates<sup>221</sup>, methacrylates<sup>221</sup> and chloroacrylates<sup>222</sup>).

In the second method, reactive mesogenic groups are attached to a preformed reactive polymer (see figure 3.2). This method has been used extensively in the synthesis of mesogenic side-chain polysiloxanes<sup>89</sup>.

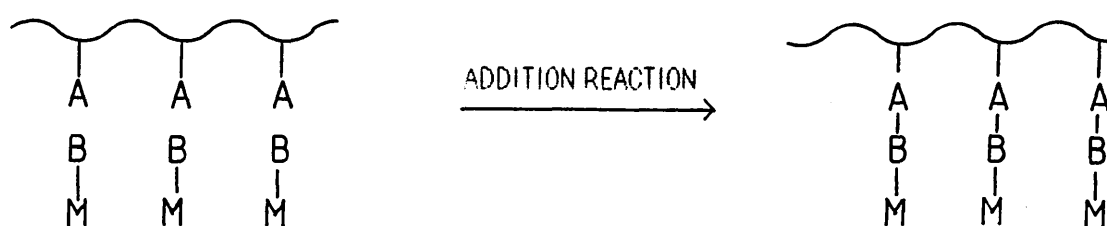


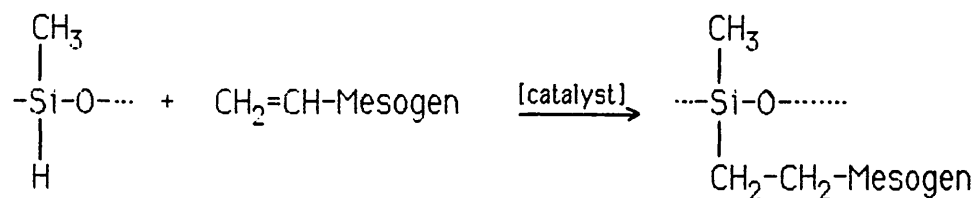
Figure 3.2 The addition of reactive mesogens to a reactive polymer.

The main factors that affect the phase properties of a given mesogenic side-chain polymer are<sup>223</sup>:

- the purity
- the average degree of polymerisation ( $\overline{DP}$ )
- the polydispersity

A potential advantage of the second method of synthesising mesogenic side-chain polymers is that by starting with a well characterised reactive polymer it is possible to have greater control over these factors. Hence, unambiguous results which relate mesogenic structure and the nature of the reactive polymer to the properties of the resulting side-chain polymer, can be obtained; providing that full occupancy of the reactive sites on the polymer can be ensured and detected, and that the product can be isolated<sup>223</sup>.

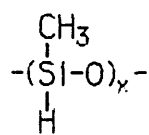
The catalysed hydrosilylation reaction, coupling Si-H functionalised siloxanes and vinyl functionalised mesogens, fulfils these requirements, being both quantitative and easily monitored by infra-red spectroscopy<sup>223</sup> (see reaction scheme 3.1). This method of attachment has the added advantage of coupling the siloxane and mesogenic moieties via the Si-C bond. This bond is less readily hydrolysed than the Si-O-C linkage sometimes employed in the preparation of siloxane containing block copolymers<sup>224-226</sup>. The catalysed hydrosilylation reaction, coupling Si-H functionalised siloxanes and vinyl functionalised mesogens has therefore, been adopted during this work.



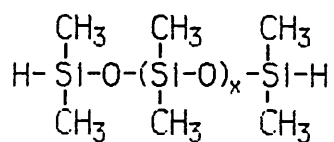
### Reaction scheme 3.1 The hydrosilylation reaction

The use of this approach led to a natural subdivision of the synthetic work into four main areas:

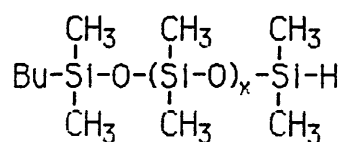
- (1) the synthesis of Si-H functionalised siloxanes, which when coupled to a mesogen(s) by the hydrosilylation reaction would lead directly to the envisaged structures; the structures of these siloxane precursors are given in figure 3.3.
- (2) the synthesis of vinyl terminated mesogens.
- (3) the coupling of the mesogen(s) to the siloxane.
- (4) the purification of the resulting products.



a)



b)



c)

**Figure 3.3** Functionalised precursors: a) cyclic hydrogenmethylsiloxanes, b)  $\alpha,\omega$ -functionalised linear dimethylsiloxanes and c)  $\alpha$ -functionalised linear dimethylsiloxanes.

The synthetic routes which have therefore been developed, the problems encountered, and the methods by which they have been overcome, will form the basis of this chapter.

## 3.2 Synthesis of Reactive Siloxane Precursors

### 3.2.1 Introduction

Polysiloxanes are a family of polymers with a silicone-oxygen backbone which has organic groups ( $R_1$  and/or  $R_2$ ) attached to a significant proportion of the silicon atoms by silicon-carbon bonds<sup>227</sup> (see figure 3.4). Generally,  $R_1$  and  $R_2$  are alkyl or aryl groups, with the most common polymer being polydimethylsiloxane, where  $R_1 = R_2 = \text{CH}_3$ .

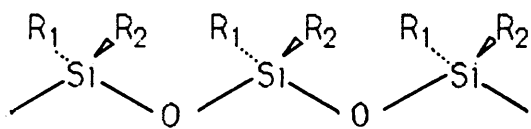
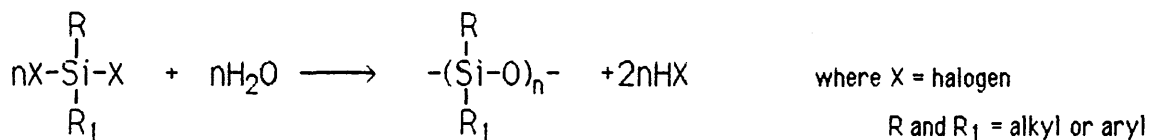


**Figure 3.4** Schematic diagram of a siloxane backbone

In general, siloxanes are synthesised by aqueous hydrolysis of organohalosilanes, in particular chlorosilanes<sup>227</sup>. In these reactions, halosilanes are rapidly hydrolysed in aqueous medium to give silanols. Most silanols are unstable and rapidly condense with a halosilane or another

silanol to form the Si-O-Si link with the elimination of HCl or water respectively. The complete hydrolysis of organo dihalosilanes results in the formation of unbranched cyclic and linear siloxanes:



### Reaction scheme 3.2 The hydrolysis of organo dihalosilanes

If R and R<sub>1</sub> are also hydrolysable, further hydrolysis may lead to cross-linking.

For a condensation reaction to occur, the two reactive groups must first be in close proximity. Hence, the polycondensation reaction is essentially controlled by statistical and steric processes<sup>227,229</sup>. The formation of a cyclic structure requires that the groups at opposite ends of a growing chain be in close proximity and that they condense together. Statistically, this is much more likely to occur with relatively short chains, the likelihood decreasing with increasing length of the growing chain. Thus, the polycondensation process favours the formation of cyclic material of a relatively low  $\overline{DP}$ . However, because of steric strain, no cyclic dimers have been reported and generally only a small amount of the cyclic trimer is formed. The cyclic tetramer and pentamer thus constitute by far the majority of the cyclic siloxanes, with gradually decreasing amounts of the higher homologues up to a  $\overline{DP}$  of several hundred. Due to steric effects, the exact composition of the cyclic fraction will vary with the nature of the organic substituents on the backbone.

The chains that do not undergo ring closure (i.e. the linear fraction), will continue to grow until termination occurs by some alternative mechanism or all the monomer has been consumed<sup>227</sup>. Hence, the linear chain length is a function of the reaction conditions and the amount of chain terminator added. In the absence of a considerable amount of a chain terminator (i.e. a monohalosilane), the  $\overline{DP}$  of the linear fraction of such a reaction would be much greater than that of the cyclic fraction. An important consequence of this difference in  $\overline{DP}$ , as well as the obvious structural differences, is that the cyclic and linear fractions can be isolated by fractional phase-separation. The relative ratio of the linear and cyclic fractions will depend on the solvent concentration; indeed, there is a critical solvent concentration above which only cyclic species will be formed<sup>228</sup>.

Although the various reactive siloxanes required during this study may have been synthesised by the hydrolysis of the appropriate halosilanes, this type of heterogeneous and highly exothermic reaction is difficult to control and results in a complex mixture of products with a broad distribution molecular masses<sup>227,229</sup>. The required products would therefore be produced in low yields and would be difficult to isolate. As we have seen that the phase behaviour of a given mesogenic side-chain polymer is dependent upon the purity, the  $\overline{DP}$ , and the polydispersity of the polymer, this is not the preferred method for the synthesis of the final side-chain polymers or the reactive siloxanes precursors. Only the oligomeric cyclics could, by distillation, be easily isolated from the resulting reaction mixture. Hence, where possible, it is these commercially available oligomers that have been the precursors used in the synthesis of the target reactive siloxanes.

### 3.2.2 Cyclic Hydrogenmethylsiloxane Oligomers

In the synthesis of molecules with mesogens attached to every unit of a cyclic siloxane, the cyclic hydrogenmethylsiloxane oligomers (see figure 3.3a.), were themselves the required reactive siloxanes. Initially, a commercially available mixture of these oligomers was obtained for further purification (see section 4.2.31). Gas Chromatography (GC) and Gas Chromatography/Mass Spectrometry (GCMS) indicated that this mixture also contained low molecular weight linear siloxane species (see appendix 4.1). These linear species had similar boiling points and GC retention times to those of the cyclic oligomers and, therefore, hindered the isolation of the cyclic species. In an effort to increase the molecular weight of the linear fraction so that the low molecular weight cyclic fraction could be isolated by distillation, an equilibration reaction using acid-activated Fuller's earth was carried out on this mixture<sup>229</sup>. Following the equilibration reaction, the cyclic fraction was easily isolated by distillation under reduced pressure. The yield of the cyclic fraction was about 15%. This mixture of low molecular weight cyclic siloxanes could then be used as the stock for the subsequent isolation of the individual cyclic siloxanes.

Considerable time and effort was spent renovating and commissioning a preparative gas chromatogram for the isolation of mono-disperse samples the cyclic siloxanes. Preparative scale columns were prepared and a method for the separation of the individual rings was developed. Whilst samples of the cyclic tetramer were successfully isolated by this means, this was an extremely time consuming technique and was abandoned in favour of spinning band distillation. Again, considerable effort was spent renovating the equipment and developing a method. Samples of the cyclic tetramer and pentamers were successfully isolated by this technique. This too was

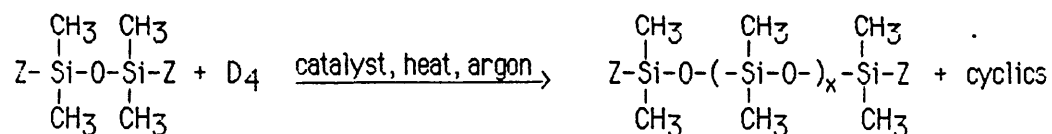
eventually abandoned in favour of obtaining the individual cyclic tetramer and pentamer directly from Petrach Systems (purity >99% and >95%, respectively). Nevertheless, methods of isolating mono-disperse oligomeric cyclic siloxanes with a  $\overline{DP}$  of 4 and 5 had been established (see section 4.2.3.1).

### 3.2.3 Linear End-Functionalised Dimethylsiloxanes

In the synthesis of the linear dimethylsiloxanes with mesogens at one or both ends of the chain, the commercially available cyclic dimethyl trimer and tetramer formed the respective monomers for the ring opening polymerisation reactions used in the synthesis of the target reactive siloxanes (see figure 3.3 b) and c), respectively). As these ring opening reactions are generally homogeneous, not exothermic, and mechanistically much less complex than the hydrolysis of halosilanes, they are easier to control and give higher yields of less disperse polymers. Hence, these reactions are the preferred methods of synthesising well characterised end-functionalised siloxanes and it is these reactions that will be detailed in the following section.

#### 3.2.3.1 $\alpha,\omega$ -Si-H Functionalised Siloxanes

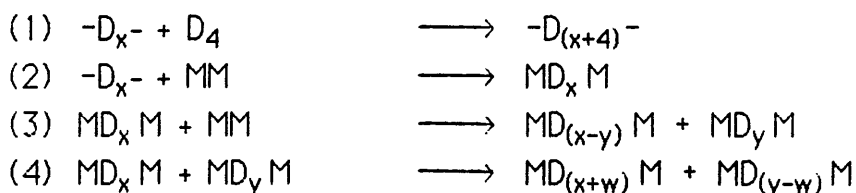
$\alpha,\omega$ -functionalised siloxanes have been used extensively as precursors in the synthesis of segmented copolymers<sup>230-233</sup> and, in the modification of network structures<sup>234,235</sup>. In general, these siloxanes have been synthesised via the ring opening polymerisation of cyclic non-functionalised oligomers and a functionalised disiloxane<sup>236</sup> (see reaction scheme 3.3). Following this reaction, essentially all of the linear chains are end-capped with the functional group 'Z' and all the cyclic species are non-functional.



### Reaction scheme 3.3 Preparation of $\alpha,\omega$ -functionalised siloxanes

Due to the partial ionic nature of the siloxane bond, it is susceptible to cleavage by nucleophilic or electrophilic reagents<sup>229</sup>. The polymerisation of cyclosiloxanes under the influence of these catalysts proceeds by an ionic mechanism. The general rules applicable to the ionic polymerisation process<sup>237</sup> are also characteristic of the polymerisation of cyclosiloxanes under these conditions.

During the polymerisation of unstrained cyclosiloxanes (i.e. not the cyclic trimer,  $\text{D}_3$ ), where the energy of the siloxane bond of the cyclic species is close to the energy of the bond in the linear polymer, the cleavage of any siloxane bond by the catalyst forms an active site that may subsequently cleave any other siloxane bond in the system<sup>229,236</sup>. Hence, a variety of interchange reactions take place and a ring-chain equilibrium is set up. Examples of the types of interchanges thought to be occurring in these 'equilibration' reactions are given in reaction scheme 3.4.



Note - with dimethylsiloxy units it is convention to use "D" to refer to a difunctional siloxane unit and "M" to refer to a monofunctional siloxane unit; the functionality being the number of siloxane bonds the silicone atom of a monomer unit is involved in.

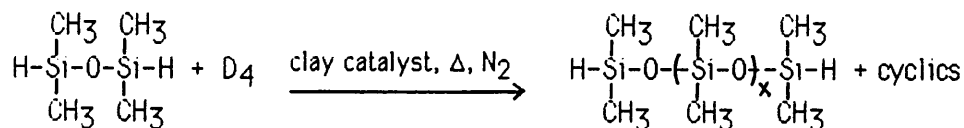
### Reaction scheme 3.4 The interchange reactions occurring in an equilibration.

The position of the ring-chain equilibrium in these equilibration reactions is obviously independent of the nature and concentration of catalyst, but may be influenced by the nature of the organic substituents on the siloxane backbone and the solvent concentration<sup>229</sup>. It should be noted that in the absence of the disiloxane, which acts as a chain terminator and thus controls the  $\overline{DP}$  of the linear chains as well as introducing reactive end-groups, a high molecular weight silicone gum may be formed.

There are a variety of catalysts that can be used to effect an equilibration reaction<sup>236</sup>. The choice of catalyst depends upon the type of functional disiloxane that is used. The anionic equilibration of siloxanes using basic catalysts, has been studied extensively<sup>229,236</sup>. This type of polymerisation is unsuitable for the preparation of Si-H functionalised siloxanes, because the Si-H bond is cleaved under these conditions<sup>229,236,238</sup>. The cationic equilibration of siloxanes, using acidic catalysts, completely retains the Si-H group at low temperatures<sup>236</sup>. It is also known that certain clay cation exchangers of the phyllo- and ino-silicate type (i.e. with a crystal lattice with a leaf-like or chord-like structure which are capable of undergoing sorption and exchange reactions in the interior of the crystal) catalyse the equilibration reaction and completely retain the Si-H group at temperatures between 0 and 150°C<sup>238</sup>. The use of such a clay has the added advantages of:

- maintaining a uniform dispersion of the catalyst throughout the reaction mixture and hence forming a uniform product
- the quantitative removal of the catalyst from the reaction mixture can be achieved by simple mechanical filtration.

Hence, acid-activated Fuller's earth has been employed as the catalyst for the cationic polymerisation of  $D_4$  with hexamethyldisiloxane:

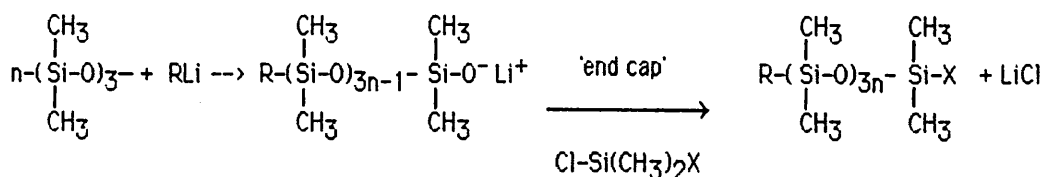


### Reaction scheme 3.5 The cationic polymerisation of $D_4$

The molecular weight of the resulting functionalised siloxane is a function of the ratio of  $D_4$  to disiloxane and the solvent concentration<sup>236,238</sup>. In the absence of solvent and at thermodynamic equilibrium, the amount of cyclic material is known and hence, the required ratio of  $D_4$  to disiloxane for a polymer of a particular  $\overline{DP}$  can be determined (see section 4.2.3.2).

#### 3.2.3.2 $\alpha$ -Si-H Functionalised Siloxane

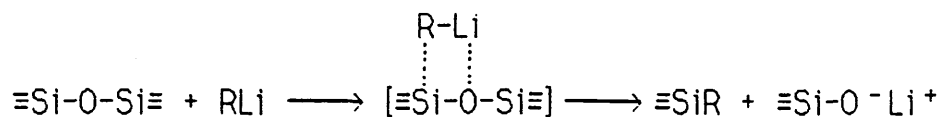
$\alpha$ -functionalised siloxanes have been used in the synthesis of graft copolymers<sup>239</sup>. Generally these siloxanes have been prepared by the anionic polymerisation of hexamethylcyclotrisiloxane ( $D_3$ ) with organolithium compounds, followed by end-capping with a functional chlorosilane<sup>240</sup>:



where X = a functional group

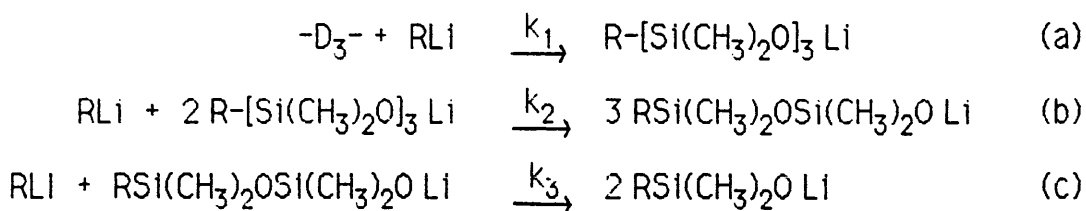
### Reaction scheme 3.6 Preparation of $\alpha$ -functionalised siloxanes by the anionic polymerisation of $D_3$ .

Although there is some doubt over the exact reaction mechanism, the cleavage of a siloxane bond by an organolithium reagent is thought to proceed via the formation of a four membered cyclic transition complex<sup>229</sup>:



Reaction scheme 3.7 The cleavage of the siloxane bond.

The lithium siloxanolate produced is much more readily cleaved by RLi than  $\text{D}_3$  and the reaction rapidly proceeds to reaction scheme 3.8(c)<sup>229</sup>:



$$k_1 \ll k_2 \text{ or } k_3$$

Reaction scheme 3.8 Further cleavage of the siloxane bond.

It is the polarised silanolate molecule that is thought to be the active polymerisation centre. In the case of lithium silanolates, due to the low degree of ionisation of this bond, the reaction is generally carried out in polar aprotic solvents<sup>236</sup>. The acceleration of the polymerisation of  $\text{D}_3$  in a polar aprotic solvent, such as tetrahydrofuran (THF), is thought to be associated with the breakdown of groups of ion pairs and the conversion of the contact ion pair to a more active form, specifically to a separate ion pair by solvation of the lithium cation by the electron donating solvent. Thus, the concentration of available active centres increases and more

effective active centres are formed. These active centres then cleave the siloxane bonds of the strained  $D_3$ , which is then added in a step-wise fashion until all the monomer has been consumed.

The large steric strain associated with the cyclic trimer that is absent in the larger rings and linears, results in a greater reactivity of a lithium silanolate towards  $D_3$ . Consequently, it is possible to selectively polymerise  $D_3$  under these conditions, with the exclusion of the redistribution processes outlined in reaction scheme 3.4, that occur in an equilibration reaction<sup>236</sup>. In the absence of these statistically and sterically controlled processes there is little or no chain transfer or chain termination and therefore, a linear polymer of relatively narrow  $\overline{DP}$  distribution and free from cyclic material is formed.

Once the reaction is complete, termination is achieved with the addition of a chlorosilane, in this case dimethylchlorosilane. The  $\overline{DP}$  of the resulting siloxane is a function of the ratio of  $D_3$  to initiator and can therefore, be calculated<sup>239,240</sup>(see section 4.2.3.3).

### 3.3. Synthesis of Mesogens

#### 3.3.1 Non-Amphiphilic Mesogens

The target non-amphiphilic mesogens consisted of a phenyl benzoate ester 'core', coupled via an ether linkage to vinyl terminated alkyl 'spacers' of varying length. A diagrammatic representation of these mesogens can be seen in figure 3.5.

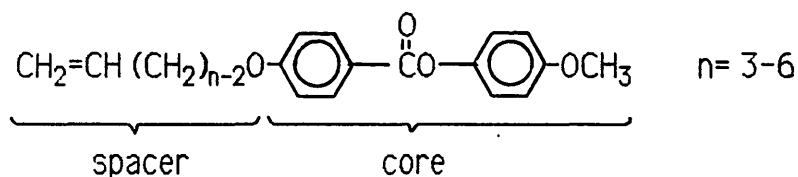
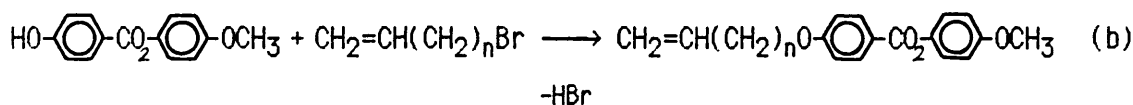
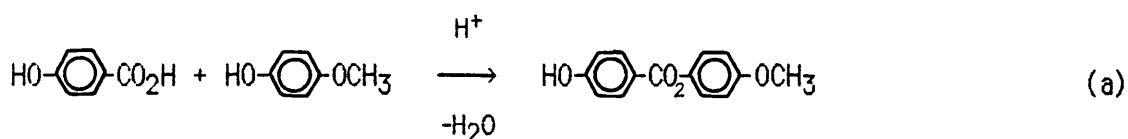


Figure 3.5 Diagrammatic representation of the non-amphiphilic mesogens.

Standard synthetic organic methods, which have been reviewed elsewhere<sup>241</sup>, have been used in the synthesis of these mesogens. Of the synthetic routes available, one was chosen in which the core of the mesogen was synthesised initially, and to which the various vinyl terminated spacers were subsequently coupled in a further reaction (see reaction scheme 3.9 a) and b), respectively).



Reaction scheme 3.9 The preparation of vinyl terminated non-amphiphilic mesogens.

The synthesis of a common core for all the non-amphiphilic mesogens minimised the amount of synthetic work required. The coupling of the spacer groups in the last reaction step, also maximises the use of these reagents, the longer chains examples of which are expensive.

It is worth noting that the synthesis of the core involves a condensation reaction between a benzoic acid and a phenol. There are, however, two phenol derivatives present (i.e. p-methoxyphenol and p-hydroxybenzoic acid) and there exists the potential for two competing reactions to occur. In practice, this was not the case. This may be explained by the increased nucleophilicity of the p-methoxyphenol relative to the p-hydroxybenzoic acid, due to the electron donating effect of the methoxy group of p-methoxyphenol and some resonance stabilisation of p-hydroxybenzoic acid.

### 3.3.2 Protected Amphiphilic Mesogens

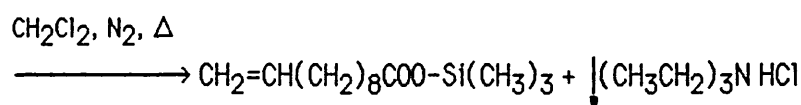
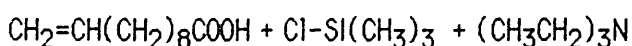
The target amphiphilic polymers consisted of a siloxane moiety with amphiphiles attached to one or more of the siloxane repeat units at the silicon atom. The amphiphiles of interest were the sodium and calcium salts of undecanoic acid ( $C_{11}$ ). The synthesis of the sodium and calcium salts of the commercially available 10-undecenoic acid, and the coupling of these salts to the reactive siloxane backbones via the hydrosilylation reaction would lead directly to the target structures. However, it is known that a solvent which is common to both the salts and the siloxane polymers and in which the coupling reaction could be carried out, is not easily found<sup>66</sup>. It was therefore necessary to form the salts after coupling the  $C_{11}$  side-chain(s) to the polymer.

The hexachloroplatinic acid to be used to catalyze the hydrosilylation reaction coupling the vinyl functional mesogen to the reactive siloxane, is also known to catalyze the reaction of a silyl group with a free carboxylic acid<sup>66</sup>. Hence, it was necessary to protect the carboxyl function group of the  $C_{11}$  amphiphile prior to coupling with the polymer. Whilst many such

protecting groups exist<sup>242,243</sup>, the appropriate choice required that:

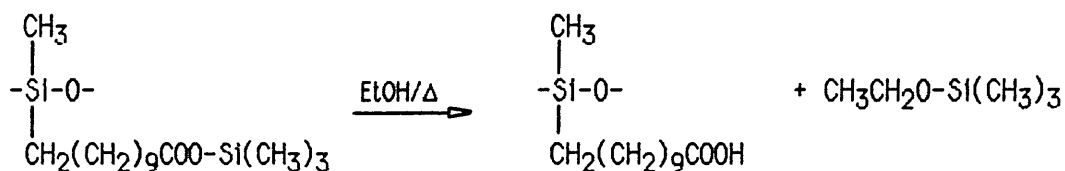
- the attachment of the protecting group be carried out in the absence of a strong acid catalyst, which could attack the terminal vinyl group of the amphiphile.
- both the protected amphiphile and the siloxane precursor be soluble in a common solvent.
- the removal of the protecting group be quantitative and carried out in the absence of strong acid or base conditions which may lead to the equilibration of a siloxane backbone<sup>229,236</sup>.

The protecting group thought best to meet these requirements was the trimethylsilyl ester<sup>244</sup>. The protection of the carboxyl moiety of the amphiphile was carried out according to reaction scheme 3.10.



Reaction scheme 3.10 Protection of the carboxyl moiety of the amphiphile.

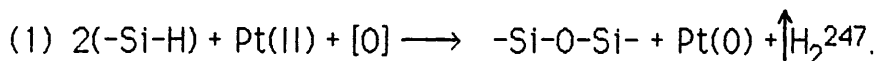
Subsequent to the coupling of the protected amphiphile to the siloxane backbone and the isolation of the resultant polymer (details of which will be given in section 3.4 and 3.5, respectively), the deprotection was achieved in a stirred solution of warm ethanol:



Reaction scheme 3.11 Deprotection of the carboxyl moiety of the amphiphilic polymers.



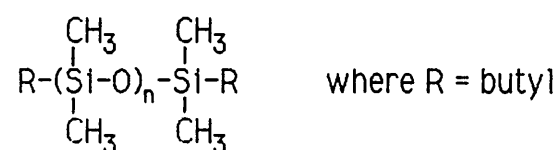
Gray *et al.*<sup>246</sup> have shown that the nature of the catalyst used to effect the hydrosilylation is crucial if the reaction is to be reproducible and controllable. Pt(IV), the catalytic species in the proposed reaction mechanism, is gradually reduced in solution to Pt(II) and Pt(0). Whilst both these species catalyse the hydrosilylation reaction they may also catalyse the following side reactions:



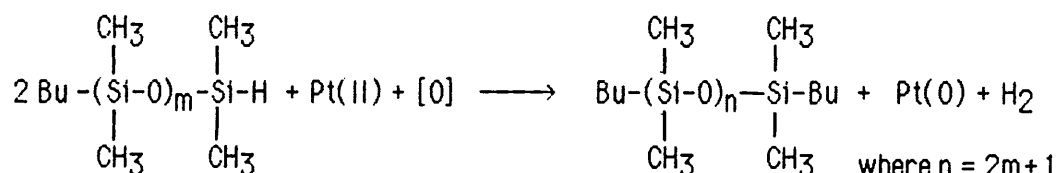
(2) Pt catalysed reactions leading to splitting of Si-C bonds<sup>248</sup>.

Gray *et al.*<sup>246</sup> demonstrated that a given series of mesogenic side-chain polysiloxanes prepared with aged and fresh solutions of  $\text{H}_2\text{PtCl}_6$  were different in appearance and phase behaviour. These differences were explained in terms of the above side reactions. The production of finely divided Pt(0) was thought to be responsible for the discolouration of the polymers produced with aged catalyst, whilst either of the possible side reactions may have contributed to a degree of cross-linking of the products.

During some of our early attempts to carry out the hydrosilylation reaction, similar observations were made with aged tetrahydrofuran (THF) solutions of the catalyst. Products were discoloured, and effervescence often occurred on mixing solutions of the catalyst and the siloxane. In addition, during the preparation of an amphiphilic  $\alpha$ -functionalised linear siloxane, an impurity was isolated that may have arisen from one of these side reactions. The IR and  $^1\text{H}$  NMR spectra of this impurity were consistent with the following structure:



This, along with the evolution of a gas when mixing solutions of catalyst and siloxane, leads to the suggestion that the impurity may have arisen from the reaction of the Si-H functionalised siloxane with the solution of aged catalyst in analogous fashion to side reaction (1), in the following way:



Reaction scheme 3.14 Proposed side reaction resulting in observed impurity.

It is, therefore, necessary to use fresh solutions of catalyst and to rigorously exclude moisture and light from the reaction, if clean products with reproducible phase behaviour are to be synthesised<sup>246</sup>.

A 10% molar excess of the alkene was employed to ensure full reaction of the Si-H sites of the reactive siloxane<sup>246,249</sup>. The extent of reaction was followed directly on an evaporated film of the reaction mixture by monitoring the decrease in intensity of the Si-H IR absorption at 2160 cm<sup>-1</sup>. As we have seen, aged solutions of catalyst can give rise to unwanted side-reactions and so once the reaction was complete, the purification of products was carried out immediately.

### 3.5 Purification of Mesogen Functionalised Siloxanes

Reported miscibility<sup>250,251</sup> and doping<sup>252</sup> studies have demonstrated that small amounts of low molar mass non-amphiphilic mesogens can have a profound effect upon the properties of the corresponding mesogenic polymer.

Consequently, it is important to ensure that the final mesogenic polymer is free from any excess of monomeric mesogen.

The isolation of mesogenic polymers may be achieved by various techniques, including GPC<sup>222,253</sup>, precipitation<sup>52,221,223,246,254-256</sup>, fractionation<sup>257,258</sup> and distillation. Precipitation is the most common method of isolation and has been the preferred method for the isolation of the various amphiphilic molecules synthesised during this study. In this respect, it is worth noting that Gray *et al.*<sup>223</sup> demonstrated that as many as ten reprecipitations are required to isolate non-amphiphilic polymers whose transitions were independent of the number of precipitations carried out.

However, Gray *et al.*<sup>223</sup> also noted that the use of many precipitation to isolate a non monodisperse polymer may give rise to fractionation of the product, and this may influence the properties of the resulting product. In a study of monodisperse non-amphiphilic siloxane oligomers, Stevens *et al.*<sup>259</sup> showed that there was a change in the phase transition temperatures in the  $\overline{DP}$  range 1-10, the change being much less pronounced in the  $\overline{DP}$  range 10-50. Thus, the fractionation of polydisperse mesogenic polymers during isolation should have a minimal effect on polymers of a high  $\overline{DP}$ , but may become increasingly important with mesogenic oligomers of the type studied here.

Due to the small quantities of the cyclic non-amphiphilic siloxanes prepared for study during this thesis, these materials were isolated by GPC using a Sephadex LH-20 gel and THF as the eluting solvent. In all cases, the purity of the products was monitored by a combination of TLC, <sup>1</sup>H nmr and IR.

The cyclic and linear amphiphilic siloxanes were isolated using phase-separation. The purity of the products was monitored by a combination of  $^1\text{H}$  nmr and IR.

## **CHAPTER 4. SYNTHESIS**

### 4.1 Introduction

The synthetic strategy and the reaction schemes employed for the synthesis of materials have been outlined in chapter 3. In accordance with this strategy, the synthetic work was divided into four main areas:

- (1) the synthesis of Si-H functionalised siloxanes
- (2) the synthesis of vinyl terminated amphiphilic and non-amphiphilic mesogens
- (3) the coupling of mesogen(s) to siloxanes
- (4) the purification of products.

The details of this synthetic work will form the basis of this chapter.

### 4.2 Experimental

#### 4.2.1 Materials

Unless otherwise specified all materials were used as supplied from Aldrich Chemicals.

All solvents were 'Analar' grade. Tetrahydrofuran (THF) was refluxed over potassium metal and distilled prior to use. The fraction boiling at 63-67°C was collected. All other solvents were dried using activated 4A molecular sieves and distilled prior to use.

n-Butyl lithium in hexane was prepared, in vacuo, from the reaction of n-chlorobutane and lithium, and was stored under dry nitrogen.

#### 4.2.2 Analytical Techniques

Infra red (IR) spectra were recorded using a Perkin Elmer 580B spectrophotometer. Liquids were analysed as films between sodium chloride plates and solids were analysed using potassium bromide discs.

$^1\text{H}$  nmr spectra were recorded at ambient temperature on either a Joel PMX60, or a Bruker WP80, or a Bruker 560 spectrometer, using  $\text{CDCl}_3$ ,  $(\text{CD}_3)_2\text{CO}$ ,  $(\text{CD}_3)_2\text{SO}$  and  $\text{D}_2\text{O}$  as solvents. The data given are for room temperature measurements. Chemical shifts are given in p.p.m. downfield from tetramethylsilane (TMS). For siloxane samples, TMS in  $\text{CDCl}_3$  was used as an external standard, prior to the sample itself. For non-siloxane samples, TMS was used as an internal standard.

Gas Liquid Chromatography (GLC) analyses were run on a Perkin Elmer chromatogram fitted with a Flame Ionisation Detector (FID), using a 3%OVI column. Analysis conditions were  $60^\circ\text{C}$  for 5 min., then ramped at  $10^\circ\text{C}\cdot\text{min}^{-1}$  to  $125^\circ\text{C}$ , with a  $\text{N}_2$  flow rate of  $15\text{ ml}\cdot\text{min}^{-1}$ .

Preparative Gas Liquid Chromatography was carried out on a Pye chromatogram fitted with a Flame Ionisation Detector (FID), using a 5%OVI column. Analysis conditions were  $60^\circ\text{C}$  for 5 min., then ramped at  $10^\circ\text{C}\cdot\text{min}^{-1}$  to  $150^\circ\text{C}$ , with a  $\text{N}_2$  flow rate of  $60\text{ ml}\cdot\text{min}^{-1}$ .

GPC curves of linear siloxane polymers were obtained using a Waters Associate instrument, fitted with microstyragel columns (Porasil 60A and Bondagel E500) and a Waters R401 refractometer. Toluene was used as the solvent with a flow rate of  $1\text{ ml}\cdot\text{min}^{-1}$ . A calibration curve was prepared

using previously characterised standard samples of linear poly(dimethylsiloxane) (PDMS) with a narrow distribution of molecular masses ( $M_w/M_n < 1.2$ )<sup>260</sup>. The calibration curve for the PDMS samples covered the number average molar mass ( $M_n$ ) range  $600 < M_n < 15000$ . The calibration curve is shown in figure 4.1. All analyses, including the preparation of the calibration curve, were carried out using octamethylcyclotetrasiloxane ( $D_4$ ) as the internal standard. All measurements were carried out at 23°C.

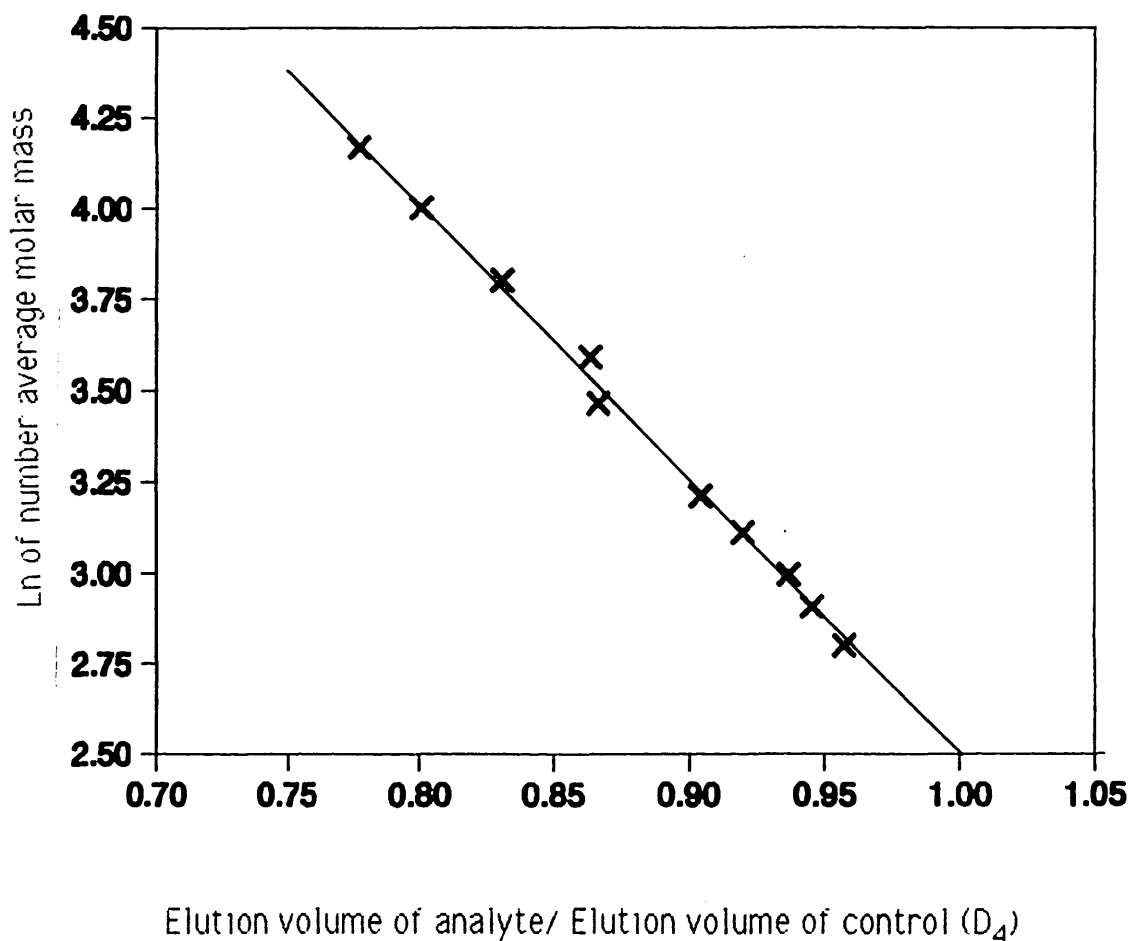


Figure 4.1 GPC calibration curve for linear PDMS.

### 4.2.3 Preparation of Si-H Functionalised Siloxanes.

#### 4.2.3.1 Cyclic Hydrogenmethylsiloxane Oligomers (see figure 3.3 a).

A mixture of cyclic hydrogenmethylsiloxane oligomers was obtained from Petrach Systems. Gas chromatography-mass spectrometry (GCMS) indicated that this mixture also contained small amounts of trimethylsilyl terminated, linear hydrogenmethylsiloxane oligomers (see appendix 4.1). This mixture was equilibrated over acid-activated Fuller's earth catalyst ( $N_2$ , 48 hours,  $60^\circ C$ )<sup>238,261</sup> (see section 4.2.3.2 for the preparation of the catalyst). The cyclic fraction was then isolated by distillation under reduced pressure ( $80^\circ C$ , 0.2 torr, 1 hour)(~15% yield).

A mono-dispersed sample of the cyclic hydrogenmethylsiloxane tetramer was isolated from this mixture of cyclic oligomers using preparative GC. Figure 4.2 shows the GC trace obtained during this procedure.

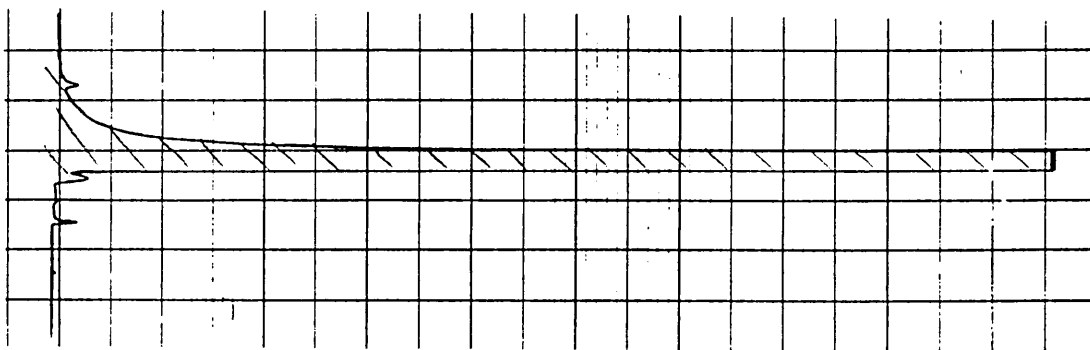


Figure 4.2 The GC trace obtained during the isolation of the cyclic hydrogenmethylsiloxane tetramer using preparative GC.

Mono-dispersed samples of the cyclic hydrogenmethylsiloxane tetramer and pentamer were also isolated from the mixture of cyclic oligomers using a spinning band fractionation column (see figure 4.3). The mixture, along with wooden splints to reduce bumping, was heated to 50 °C. The pressure in the column was then gradually reduced until the first sign of refluxing occurred at the base of the fractionating column. The spinning band of the column was switched on. Heat was then gradually applied to the column until the most volatile fraction reached the fractionating head, and was refluxing at a steady rate. At least 10 minutes were allowed for the system to reach equilibrium, and then 0.5cm<sup>3</sup> samples were taken from the fractionating head with a reflux ratio of 10:1. GLC analysis of these fractions was carried out and the pure fractions of the cyclic tetramer were retained. The fractions rich in the cyclic pentamer, but lacking the less volatile tetramer, were retained and recombined. This fraction was then redistilled, as above. Again, GC analysis of the various fractions obtained was carried out, and the pure fractions of the cyclic pentamer were retained. The IR and <sup>1</sup>H nmr spectra were consistent with the required structures (see figure 4.4 and 4.5).

These methods of obtaining these siloxane precursors were subsequently abandoned in favour of obtained these materials direct from Petrach Systems. The purity of the commercial tetramer and pentamer was >99% and >95%, respectively.

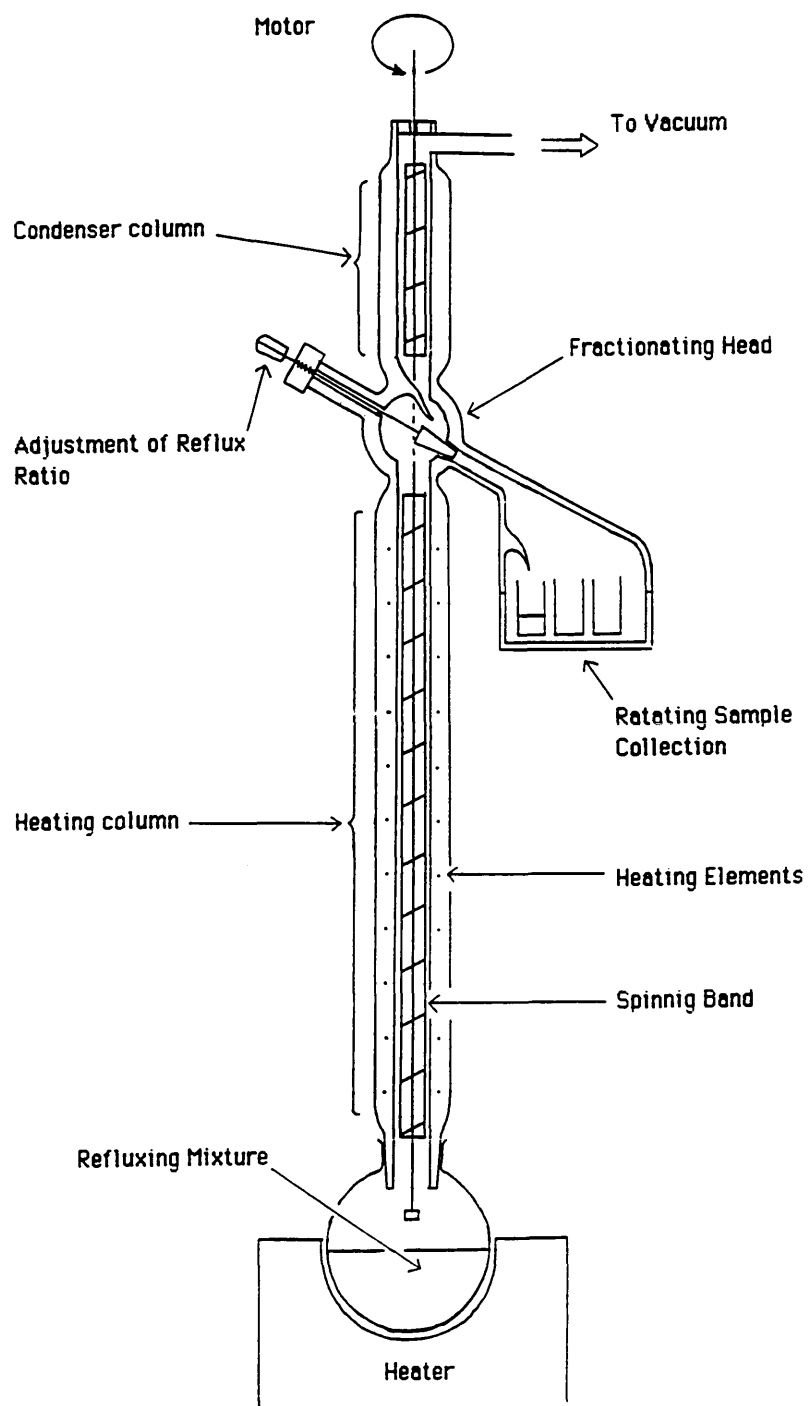


Figure 4.3 Spinning band fractionation column.

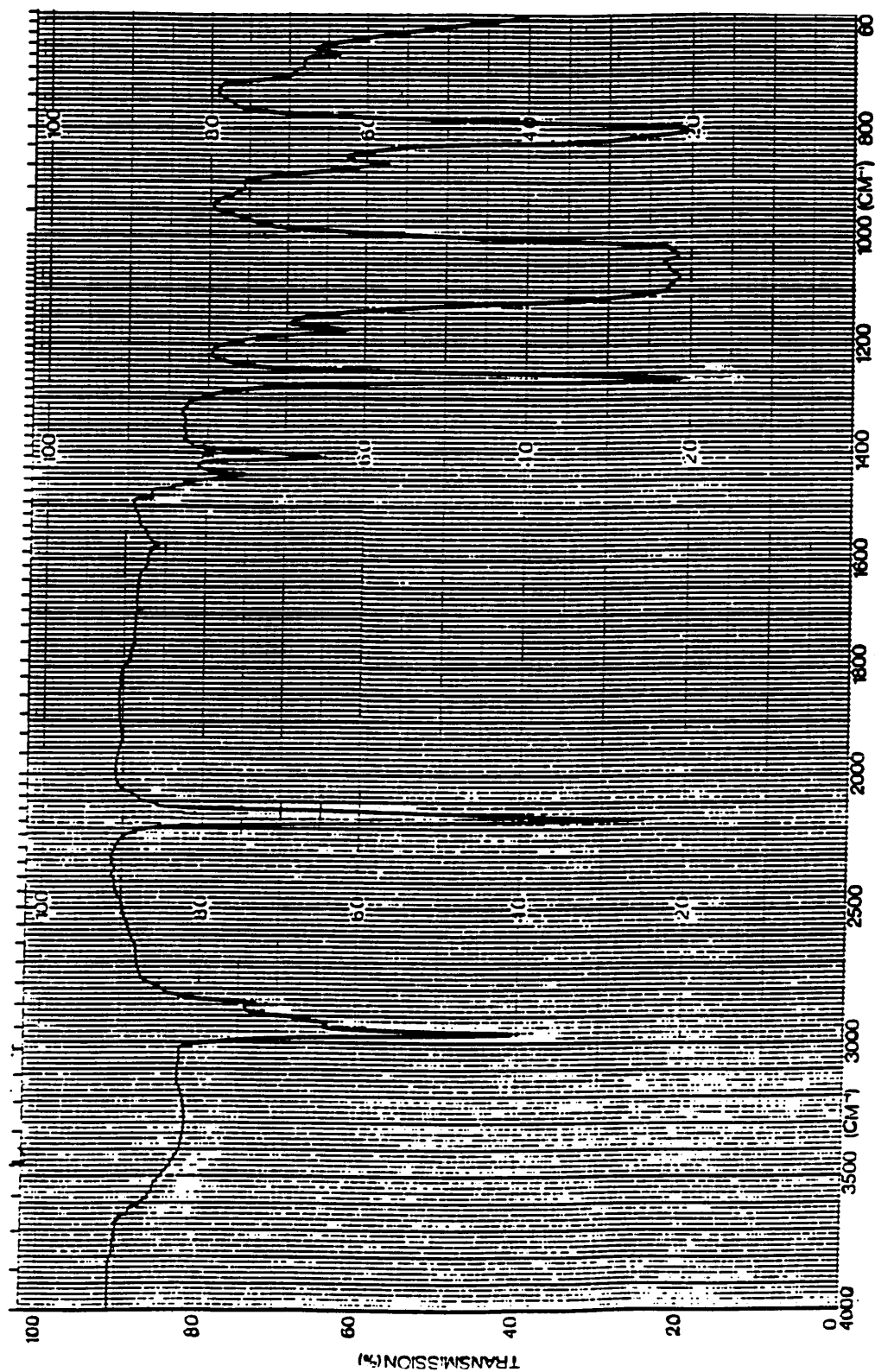


Figure 4.4 IR spectrum of cyclic hydrogenmethylsiloxane tetramer.  
 Signal (cm<sup>-1</sup>): 2160(Si-H), 1300-750 (Si-O-Si).

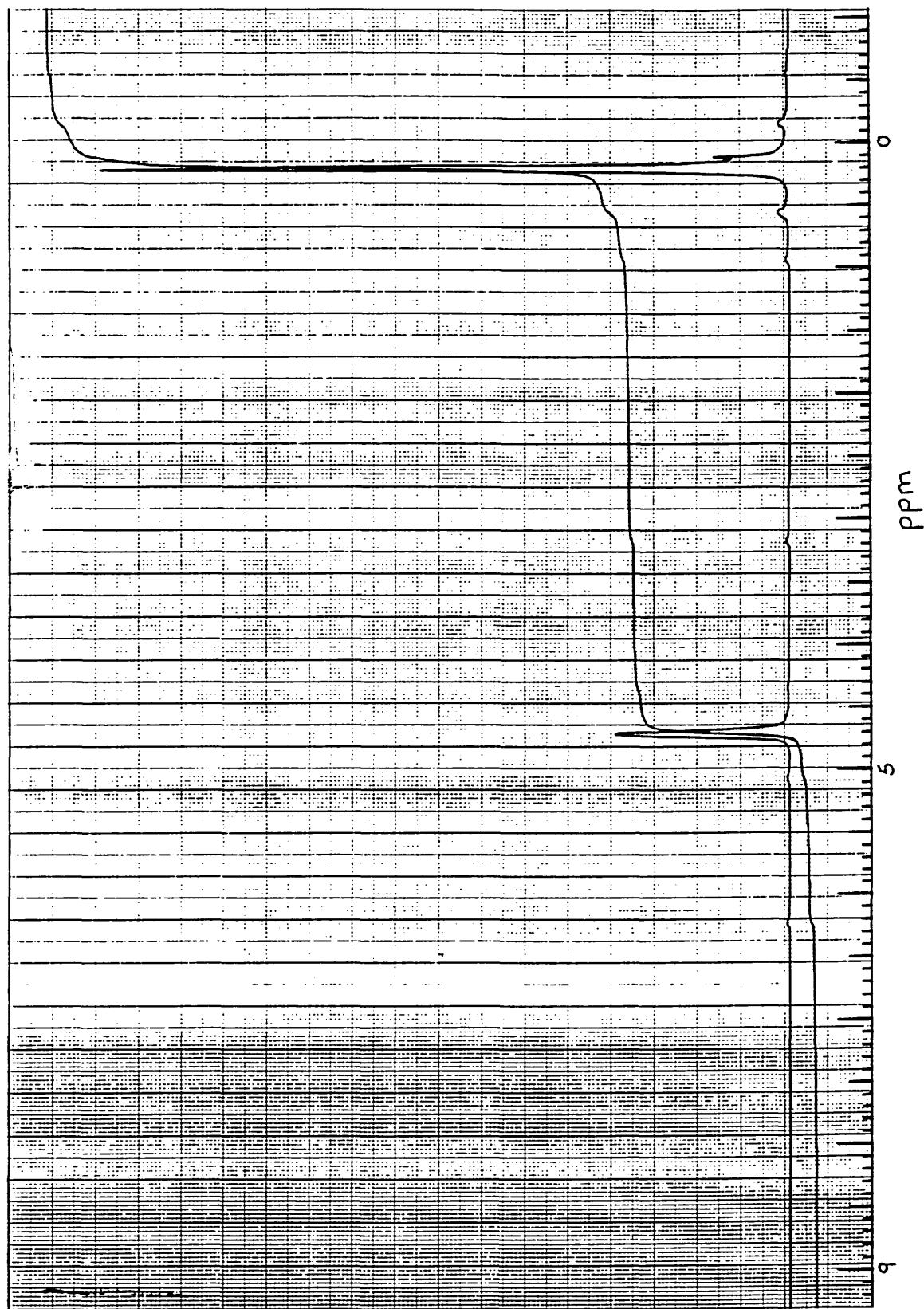


Figure 4.5  $^1\text{H}$  nmr spectrum of cyclic hydrogenmethylsiloxane tetramer.  
 $^1\text{H}$  nmr signal (ppm): 0.2 (3H, s,  $\text{CH}_3$ ), 4.75 (1H, s, Si-H).

#### 4.2.3.2. $\alpha,\omega$ -Si-H Functionalised Dimethylsiloxanes<sup>238,261</sup> (see figure 3.3 b)

##### a) Preparation of the Catalyst

Fuller's earth (10g) was stirred in dilute H<sub>2</sub>SO<sub>4</sub> (50ml) for 12 hours at ambient temperature, then filtered and washed with distilled water until the washings were neutral. The catalyst was then vacuum dried at 100°C.

##### b) $\alpha,\omega$ -Si-H Functionalised Dimethylsiloxanes. General Procedure

Octamethylcyclotetrasiloxane (D<sub>4</sub>), tetramethyldisiloxane (TMDS) and acid activated Fuller's earth (0.2g) were heated under N<sub>2</sub> with stirring for 72 hours at 60°C. The reaction mixture was then cooled and filtered to remove the catalyst. The filtrate was heated under vacuum for 6 hours (150°C, 0.1 torr) to remove low molecular mass cyclic contaminants. The residue was then phase-separated three times from an acetone/water mixture (80/20). The IR and <sup>1</sup>H nmr spectra were consistent with the required structures (see figure 4.6 and 4.7). The molecular weights were determined by GPC and <sup>1</sup>H nmr (see table 4.1).

nominal M <sub>n</sub>	D <sub>4</sub> (g, moles.10 <sup>-2</sup> )	TMDS (g, moles.10 <sup>-3</sup> )	M <sub>n</sub> (GPC)	M <sub>n</sub> ( <sup>1</sup> H nmr)
1000	20.0, 6.74	2.70, 20.10	1120	1080
2000	20.0, 6.74	1.17, 8.70	1950	2150
5000	20.0, 6.74	0.45, 3.35	4750	-----

Table 4.1. The polymerisation conditions employed in the preparation of  $\alpha,\omega$ -Si-H functionalised dimethylsiloxanes, and the M<sub>n</sub> data characterising the products obtained.

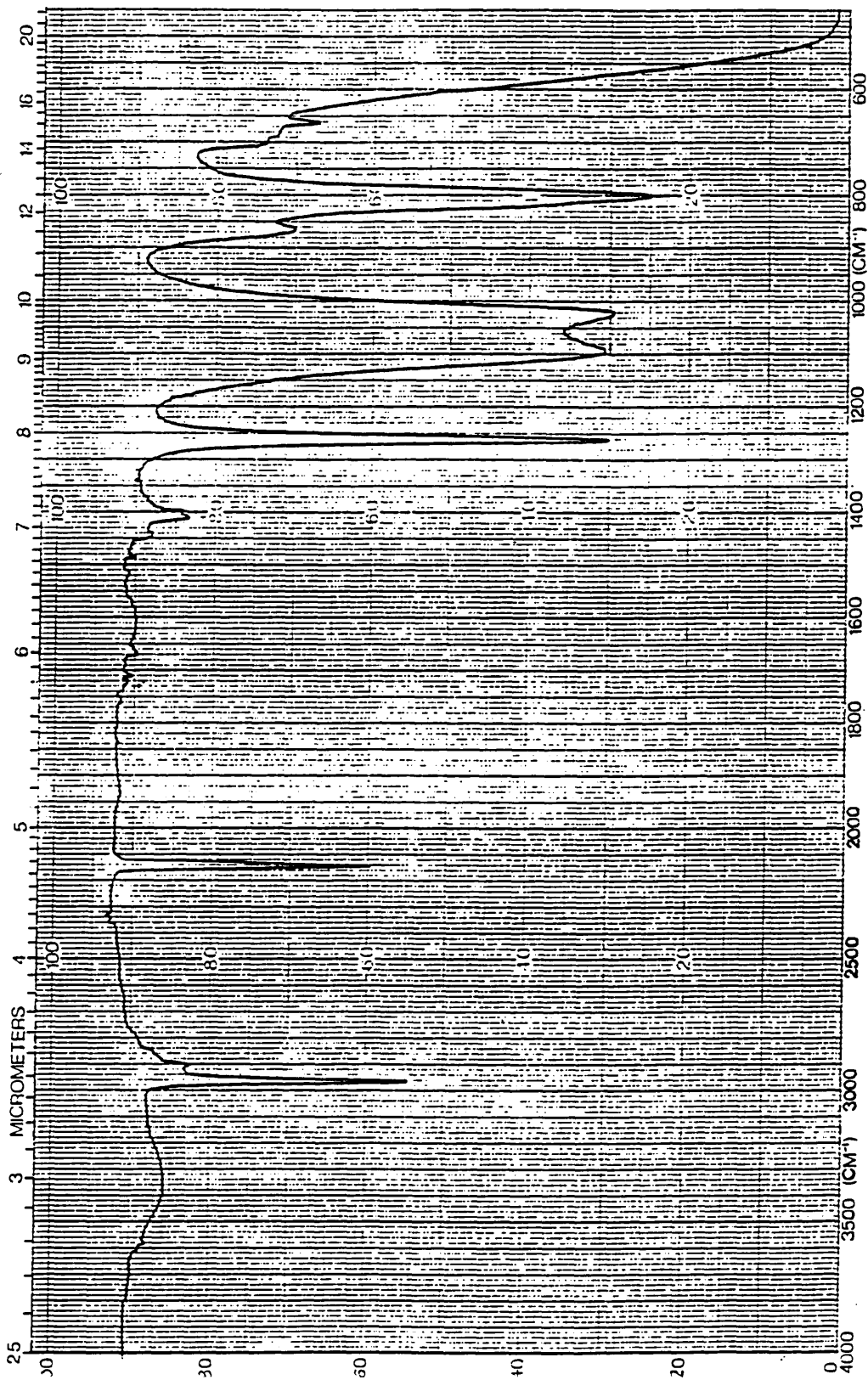


Figure 4.6 IR spectrum of  $\alpha,\omega$ Si-H functionalised dimethylsiloxane (nominal  $M_n=1000$ ).

IR signal ( $\text{cm}^{-1}$ ): 2160(Si-H), 1300-750 (Si-O-Si)

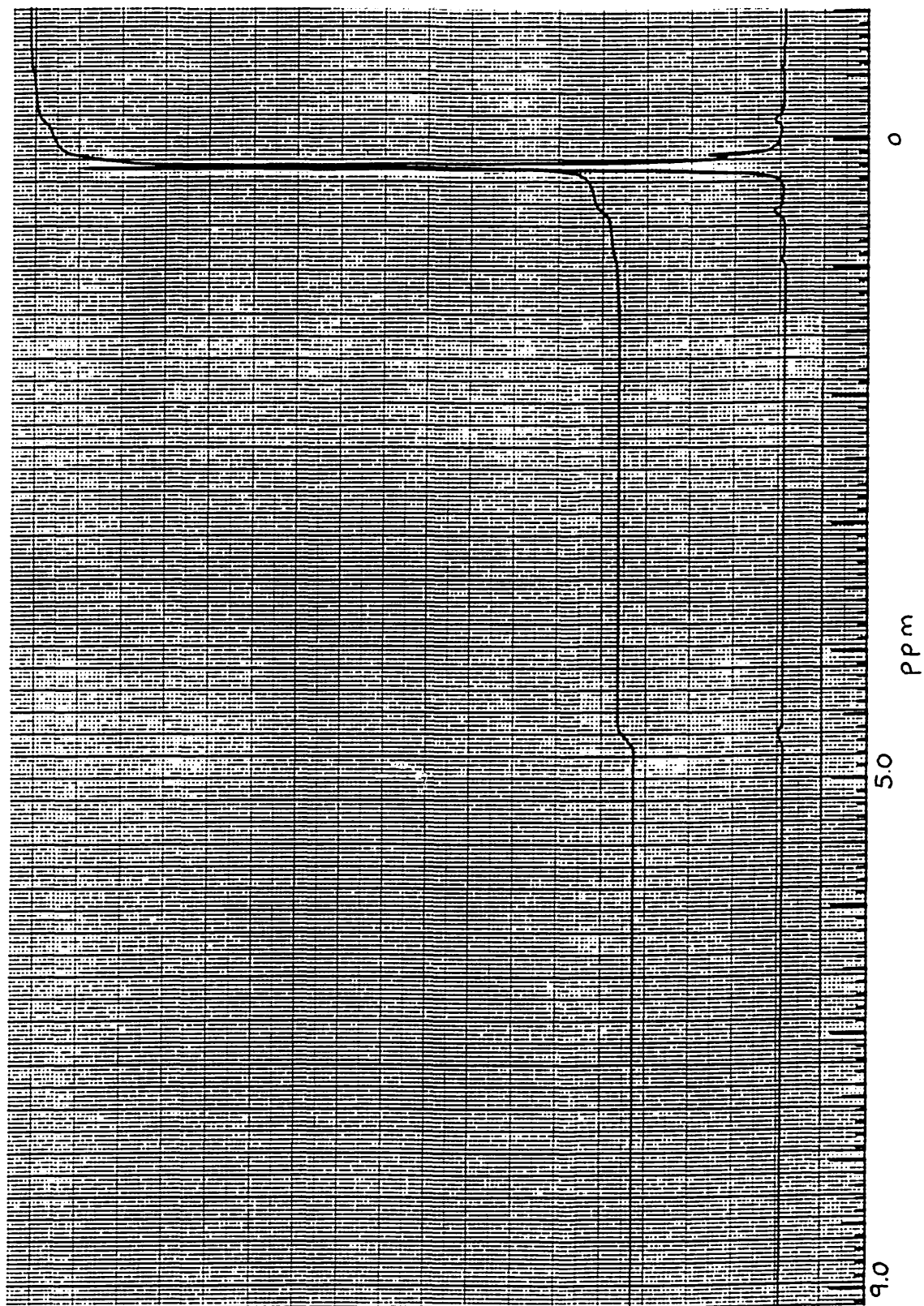


Figure 4.7 <sup>1</sup>H nmr spectrum of α,ω-Si-H functionalised dimethylsiloxane (nominal M<sub>n</sub>=1000).

<sup>1</sup>H nmr signal (ppm): 0.2 (15 3H, s, CH<sub>3</sub>), 4.75 (2 1H, s, Si-H).

#### 4.2.3.3 $\alpha$ -Si-H Functionalised Dimethylsiloxanes, General Procedure<sup>239</sup>

(see figure 3.3 c)

A 50% solution of hexamethylcyclotrisiloxane ( $D_3$ ) in THF was slowly added to a stirred solution of n-butyllithium in hexane ( $1.58\text{M}\cdot\text{dm}^{-3}$ ) at  $0^\circ\text{C}$ . After 20 hours the reaction was cooled to  $-78^\circ\text{C}$  and dimethylchlorosilane (DMCS, 10 mole % excess with respect to the moles of n-butyllithium used) was slowly added (see table 4.2). The mixture was allowed to heat to ambient temperature and was then added to water (150ml). The non-aqueous layer was separated and any hexane present was removed under reduced pressure. The product was phase-separated five times from an acetone/water mixture (80/20). The residue was then taken up in acetone, dried ( $\text{Mg}_2\text{SO}_4$ ) and filtered. The acetone was then removed under reduced pressure in order to provide the final product. The IR and  $^1\text{H}$  nmr spectra were consistent with the required structures (see figure 4.8 and 4.9). The molecular weights were determined by GPC and GLC. (see table 4.2)

nominal $M_n$	$D_3$ (g,moles $10^{-2}$ )	BuLi (g,moles $10^{-2}$ )	DMCS (g,moles $10^{-2}$ )	$M_n$ (GPC)	$M_n$ ( $^1\text{H}$ nmr)
500	20.0, 9.0	3.34, 5.21	5.42, 5.73	510	480
1000	20.0, 9.0	1.45, 2.26	2.35, 2.49	915	880
1500	20.0, 9.0	0.93, 1.45	1.51, 1.60	1560	1410
2000	20.0, 9.0	0.68, 1.06	1.11, 1.17	2175	2050
5000	20.0, 9.0	0.26, 0.41	0.43, 0.45	5200	4650

Note:  $^1\text{H}$  nmr spectra recorded on a Bruker WP80.  $M_n$  ( $^1\text{H}$  nmr) was calculated by comparison of the signal due to Si-H with the signal due to rest of the molecule.

Table 4.2 The polymerisation conditions employed in the preparation of  $\alpha$ -functionalised dimethylsiloxanes, and the  $M_n$  data characterising the products obtained.

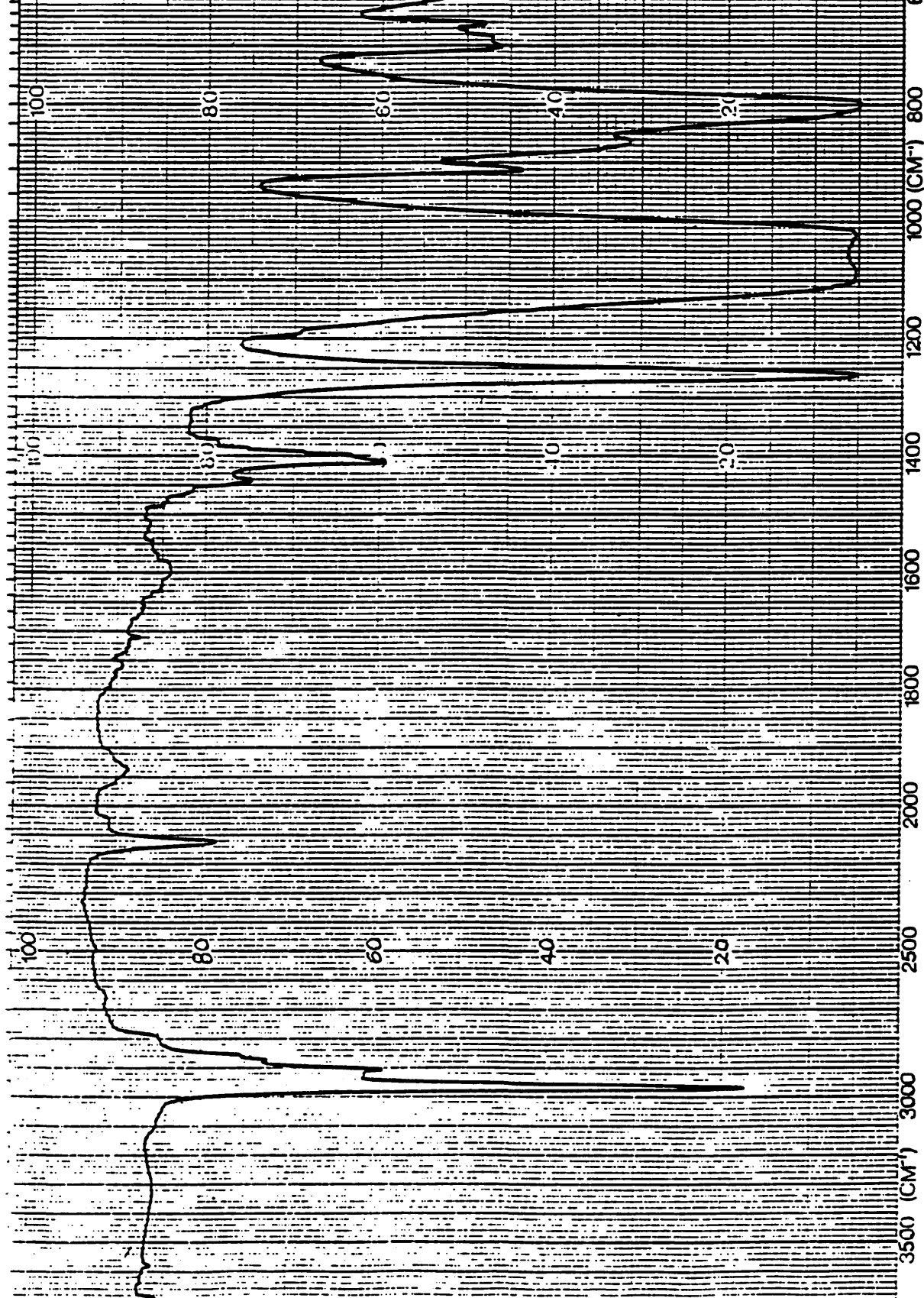


Figure 4.8 IR spectrum of  $\alpha$ -Si-H functionalised dimethylsiloxane (nominal  $M_n = 2000$ )  
IR signal ( $\text{cm}^{-1}$ ): 2160(Si-H), 1300-750 (Si-O-Si)

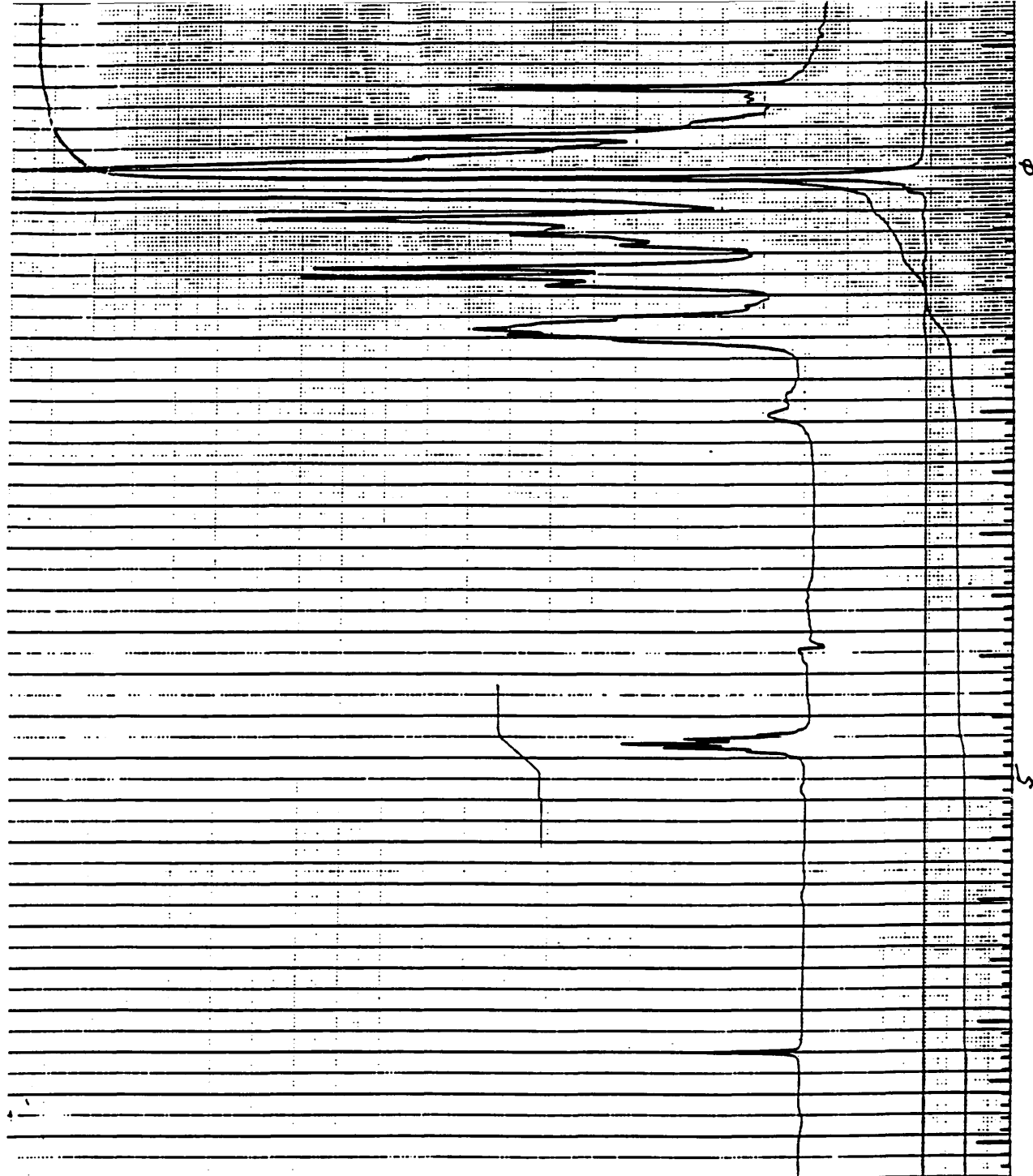


Figure 49  $^1\text{H}$  nmr spectrum of  $\alpha$ -Si-H functionalised dimethylsiloxane (nominal  $M_n=2000$ ).

$^1\text{H}$  nmr (ppm): 0.1 (27.5 3H, s, Si-CH<sub>3</sub>), 0.3-1.6 (9H, m, nBu), 4.75 (1H, s, Si-H)

Note: the respective  $^1\text{H}$  nmr and IR signal intensities vary with the molecular weight of the sample. Hence, these figures give only the signal positions and the species thereby indicated.

## 4.2.4 Synthesis of Vinyl Terminated Mesogens

### 4.2.4.1 Non-Amphiphilic Mesogens (see figure 3.5)

#### a) 4-Methoxyphenyl-4-hydroxybenzoate<sup>262</sup>

A mixture of 4-hydroxybenzoic acid (4.9g, 0.036M) and 4-methoxyphenol (4.96g, 0.04M) in benzene (20ml) containing sulphuric acid (10 drops) was refluxed for six days. Water was removed using a Dean Stark trap. The reaction was monitored by TLC (70% petroleum spirits/ 30% ethyl acetate). When the 4-hydroxybenzoic acid was consumed, the solid product was filtered off. This residue was dissolved in diethylether (250ml), washed with saturated aqueous sodium bicarbonate three times and dried ( $Mg_2SO_4$ ). The diethylether was reduced in volume to 100ml and hexane (100ml) was added. The crude product was filtered off, and was recrystallised from diethylether and hexane to give a white solid (6.80g, 79%), mp 192–194°C. The  $^1H$  nmr spectrum was consistent with the required structure (figure 4.10)

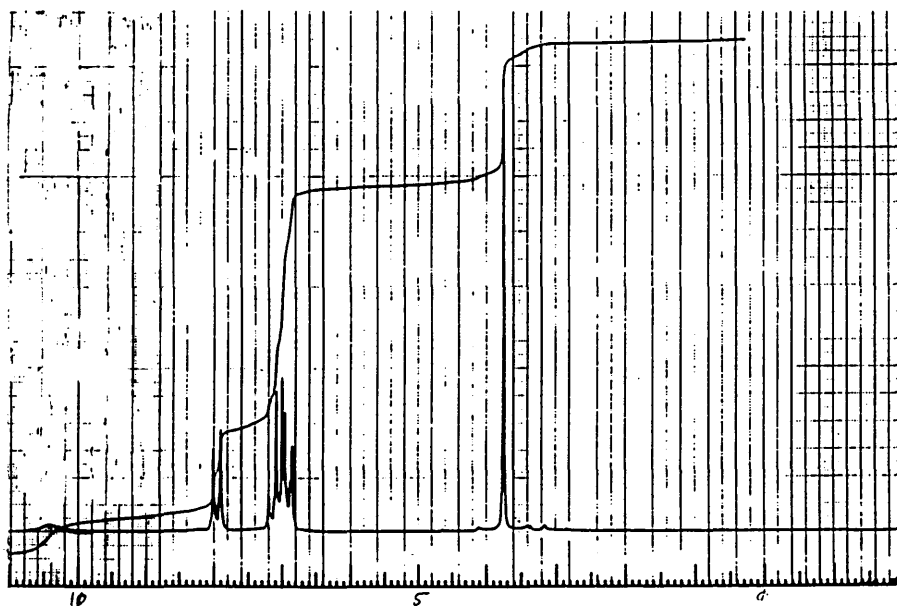


Figure 4.10  $^1H$  nmr spectrum of 4-methoxyphenyl-4-hydroxybenzoate.

$^1H$  nmr signal (d-DMSO); 3.75 (3H, s,  $OCH_3$ ), 7.5 (8H, m, aromatic H), 10.4 (1H, s, OH). Note: the signal position for ROH may vary with the solvent and the solution concentration.

b) Coupling Vinyl Terminated Spacer to 4-Methoxyphenyl-4-hydroxybenzoate.

General Procedure.

An alkyl bromide (0.028M) was added to a stirred solution of 4-methoxyphenyl-4-hydroxybenzoate (6.8g, 0.028M) and  $K_2CO_3$  (5.4g, 0.028M) in dry acetone, under  $N_2$  (see table 4.3). The mixture was refluxed for 48 hours. The reaction was monitored by TLC (90% petroleum spirits/10% ethyl acetate). The product was obtained by column chromatography (90% petroleum spirits/10% ethyl acetate). Yields of white solid were about 70%. The  $^1H$  nmr spectrum was consistent with the required structures (see figure 4.11 for example spectrum).

<u>Alkyl bromide</u>	<u>Value of x in figure 3.5</u>	<u><math>^1H</math> nmr data (CDCl<sub>3</sub>)</u>
allylbromide	3	7.6 (8H, m, aromatic H); 6.0 (1H, m, CH); 5.2 (2H, t, :CH <sub>2</sub> ) 4.5 (2H, t, OCH <sub>2</sub> ); 3.8 (3H, s, OCH <sub>3</sub> )
4-bromo-1-butene	4	7.5 (8H, m, aromatic H); 5.9 (1H, m, CH); 5.2 (2H, t, :CH <sub>2</sub> ) 4.2 (2H, t, OCH <sub>2</sub> ); 3.8 (3H, s, OCH <sub>3</sub> ); 2.25 (2H, m, CH <sub>2</sub> )
5-bromo-1-pentene	5	7.4 (8H, m, aromatic H); 5.7 (1H, m, CH); 5.0 (2H, t, :CH <sub>2</sub> ) 4.0 (2H, t, OCH <sub>2</sub> ); 3.8 (3H, s, OCH <sub>3</sub> ); 2.0 (4H, m, 2 CH <sub>2</sub> )
6-bromo-1-hexene	6	7.6 (8H, m, aromatic H); 5.8 (1H, m, CH); 5.0 (2H, t, :CH <sub>2</sub> ) 4.0 (2H, t, OCH <sub>2</sub> ); 3.8 (3H, s, OCH <sub>3</sub> ); 1.8 (6H, m, 3 CH <sub>2</sub> )

Table 4.3 The alkyl bromide used in the preparation of non-amphiphilic mesogens (see figure 3.5), and the  $^1H$  nmr data characterising these mesogens.

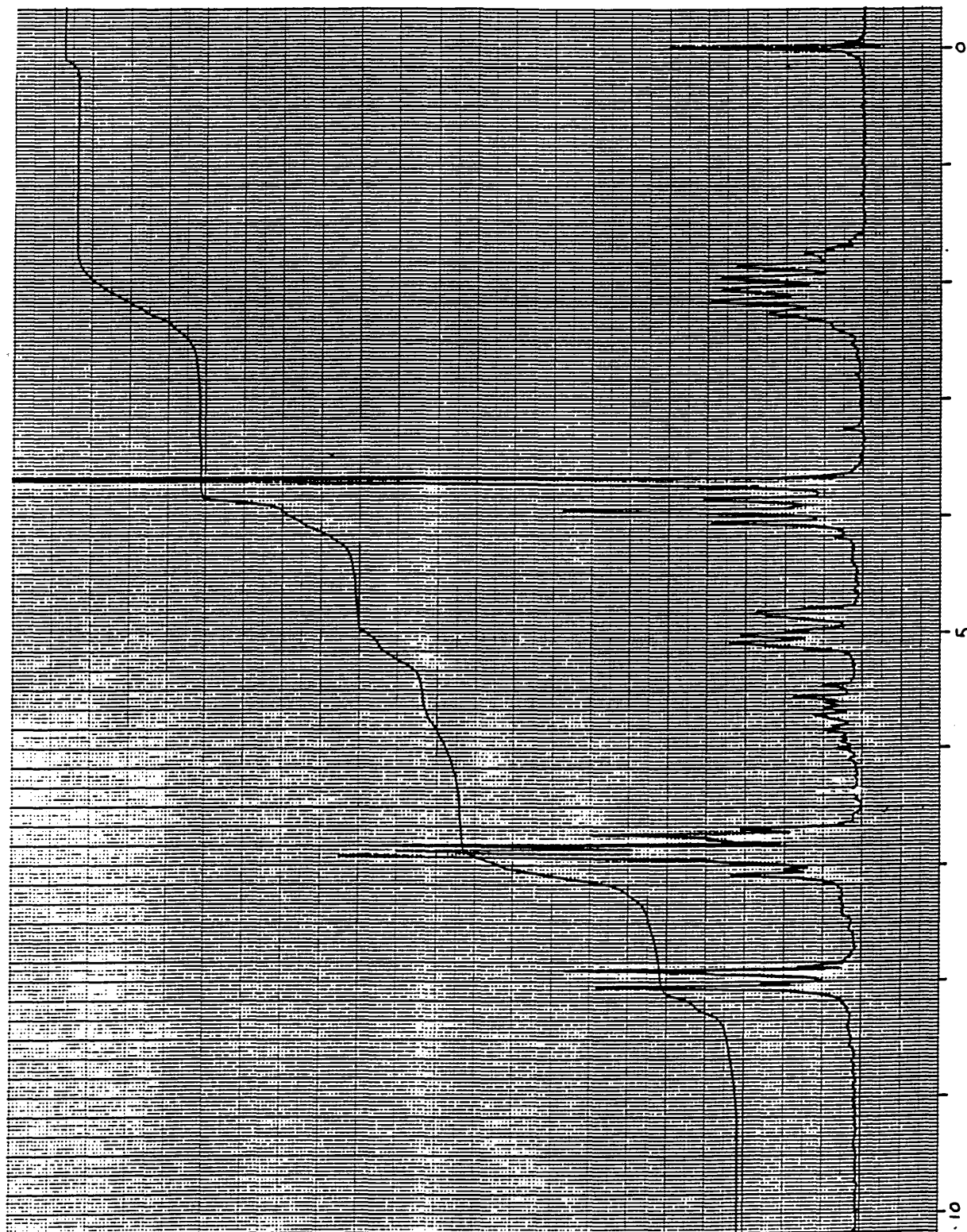


Figure 4.11 <sup>1</sup>H nmr spectrum of 4'-methoxyphenyl-4-pent-1-enoxybenzoate (i.e. the non-amphiphilic mesogen incorporating a pentyl spacer group).

<sup>1</sup>H nmr signal (ppm); 2.0 (2 2H, m, 2 CH<sub>2</sub>), 3.6 (3H, s, OCH<sub>3</sub>), 3.95 (2H, t, OCH<sub>2</sub>), 5.0 (2H, t, CH<sub>2</sub>), 5.75 (1H, m, CH), 7.5 (8H, m, aromatic H).

#### 4.2.4.2 Protection of the Carboxyl Group of 10-Undecenoic acid. Synthesis of Trimethylsilyl 10-Undecenoate<sup>244</sup>

Trimethylchlorosilane (54.47g, 0.5M, 10% mole excess with respect to moles of acid) in dichloromethane (40ml) was added to a stirred solution of 10-undecenoic acid (84g, 0.456M, freshly distilled at 110°C, 0.2 mmHg) in dichloromethane (30ml). After refluxing under N<sub>2</sub> for 4 hours, the reaction mixture was cooled to -78°C and a solution of triethylamine (50.6g, 0.5M) in dichloromethane, was slowly added. The mixture was refluxed for a further 16 hours. The extent of reaction was followed by monitoring the disappearance of the -COOH IR stretching band (2900-3500 cm<sup>-1</sup>). When reaction was complete the mixture was cooled, and filtered under N<sub>2</sub> to remove the solid triethylamine hydrochloride. The filtrate was evaporated under reduced pressure to remove the solvent. The residue was dissolved in petroleum spirits and a second fraction of triethylamine hydrochloride removed by filtration under N<sub>2</sub>. The solvent was removed under reduced pressure and the ester (a colourless liquid) obtained by vacuum distillation (72°C, 0.3 mm Hg) (yield 85.4g, 73%). The IR and <sup>1</sup>H nmr spectra were consistent with the required structure (see figures 4.12 and 4.13).

#### 4.2.5 Coupling of Mesogens and Siloxanes. General Procedure<sup>246,249</sup>

Catalyst solutions of hexachloroplatinic acid in dry THF were prepared in a dry box under N<sub>2</sub> and used immediately. All apparatus was flame dried under N<sub>2</sub> and wrapped in foil. The appropriate Si-H functionalised siloxane and alkene terminated mesogen (10% molar excess with respect to the Si-H content of the siloxane) were dissolved in THF (50% solution). An aliquot of catalyst solution was added, such that the alkene/catalyst molar ratio was 1:10<sup>-4</sup>. The mixture was stirred at 50°C for up to 5 days. The extent of

reaction was followed by IR, the disappearance of an adsorption band at 2060-2080  $\text{cm}^{-1}$  (Si-H stretching) indicated complete reaction (see figure 4.14)

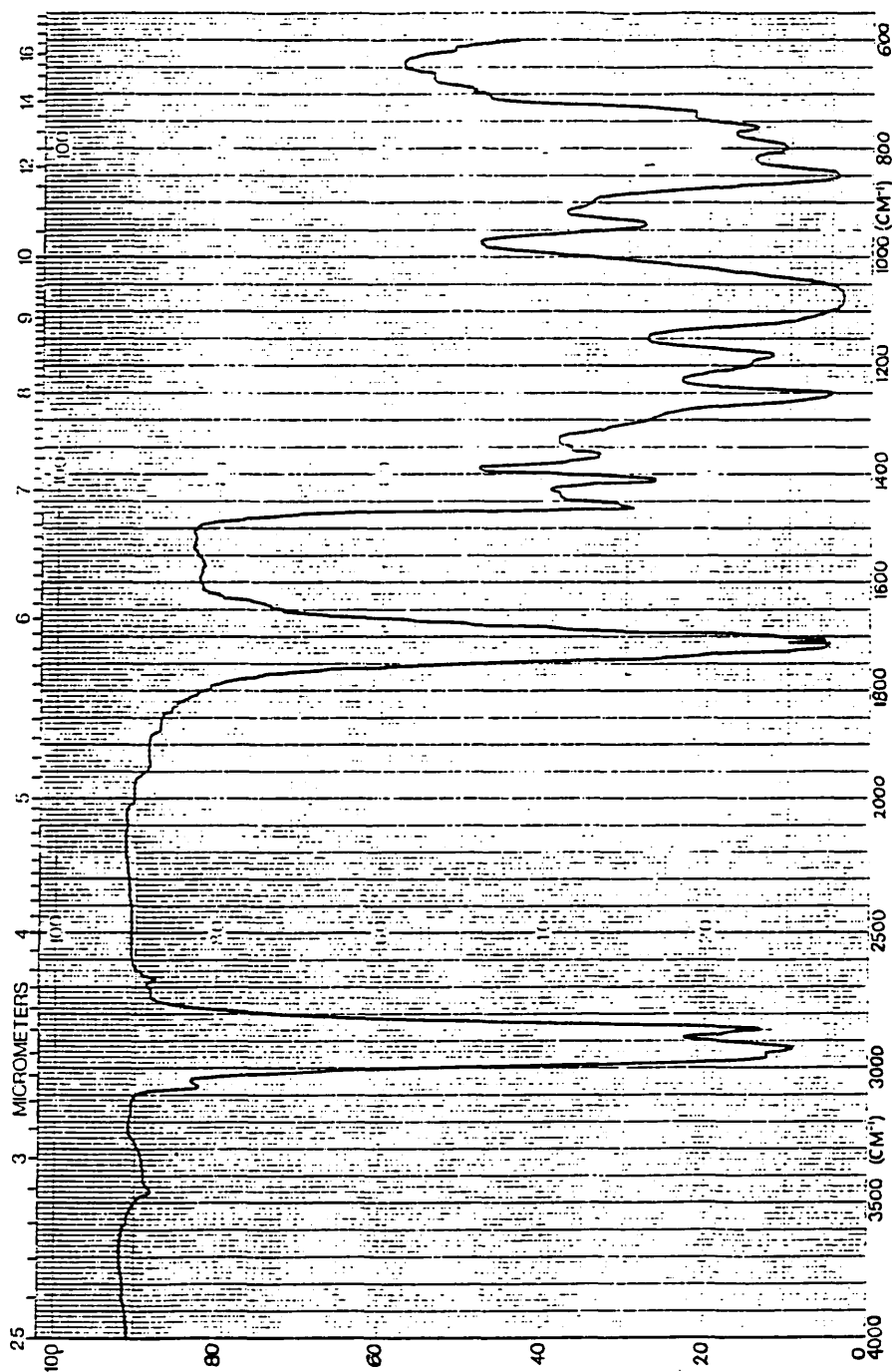


Figure 4.12 IR spectrum of trimethylsilyl 10-undecenoate.

IR signal ( $\text{cm}^{-1}$ ): 2900 ( $\text{CH}_2$ ), 1720 (C=O), 1300-750 (Si-O-Si).  
Note the absence of OH at 3000-3500  $\text{cm}^{-1}$ .

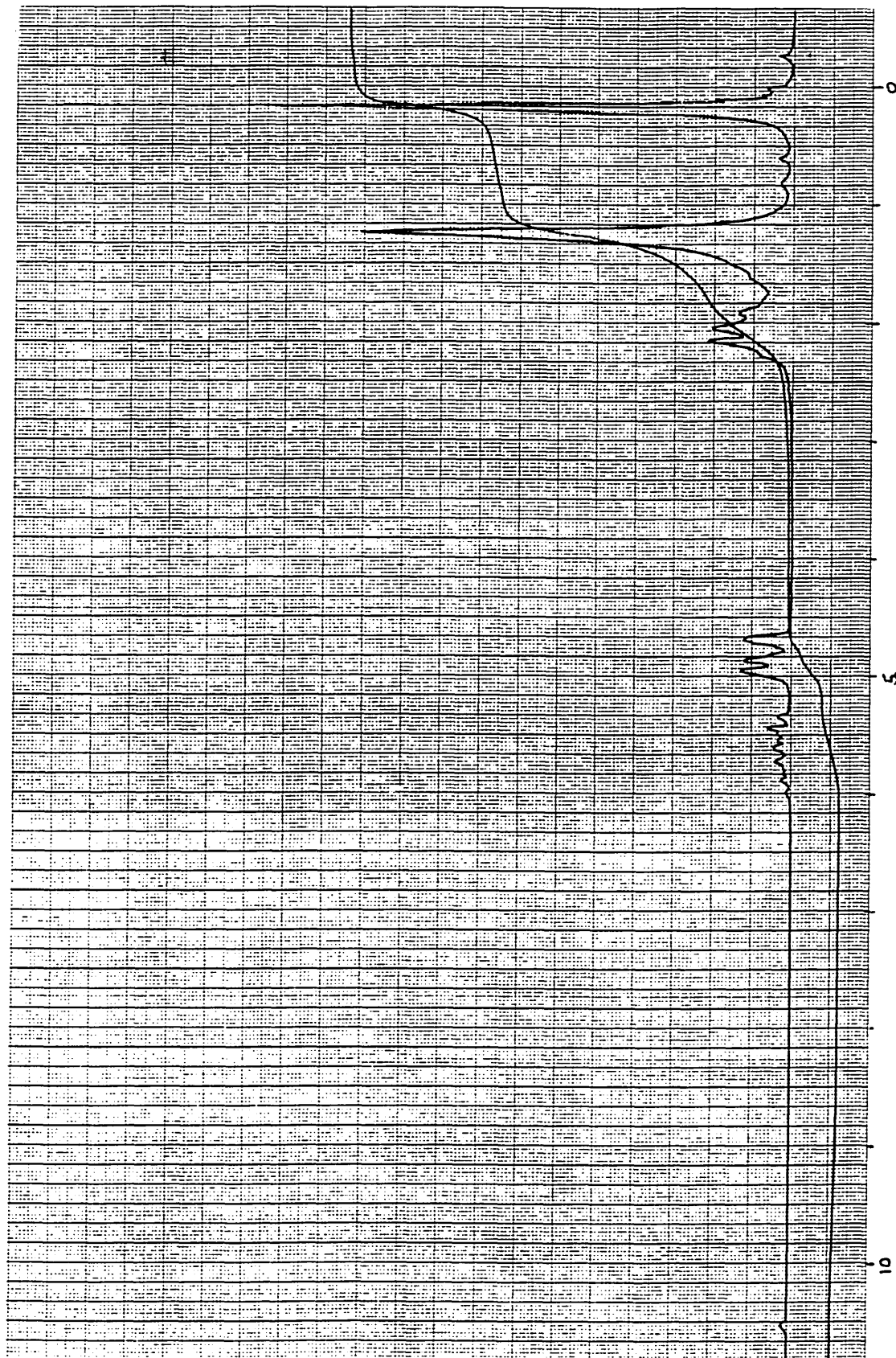


Figure 4.13 <sup>1</sup>H nmr spectrum of trimethylsilyl undecenoate.

<sup>1</sup>H nmr signal (ppm); 0.2 (9H, s, Si-CH<sub>3</sub>), 1.0-2.3 (16H, m, CH<sub>2</sub>),  
4.8 (2H, t, CH<sub>2</sub>), 5.6 (1H, m, CH)

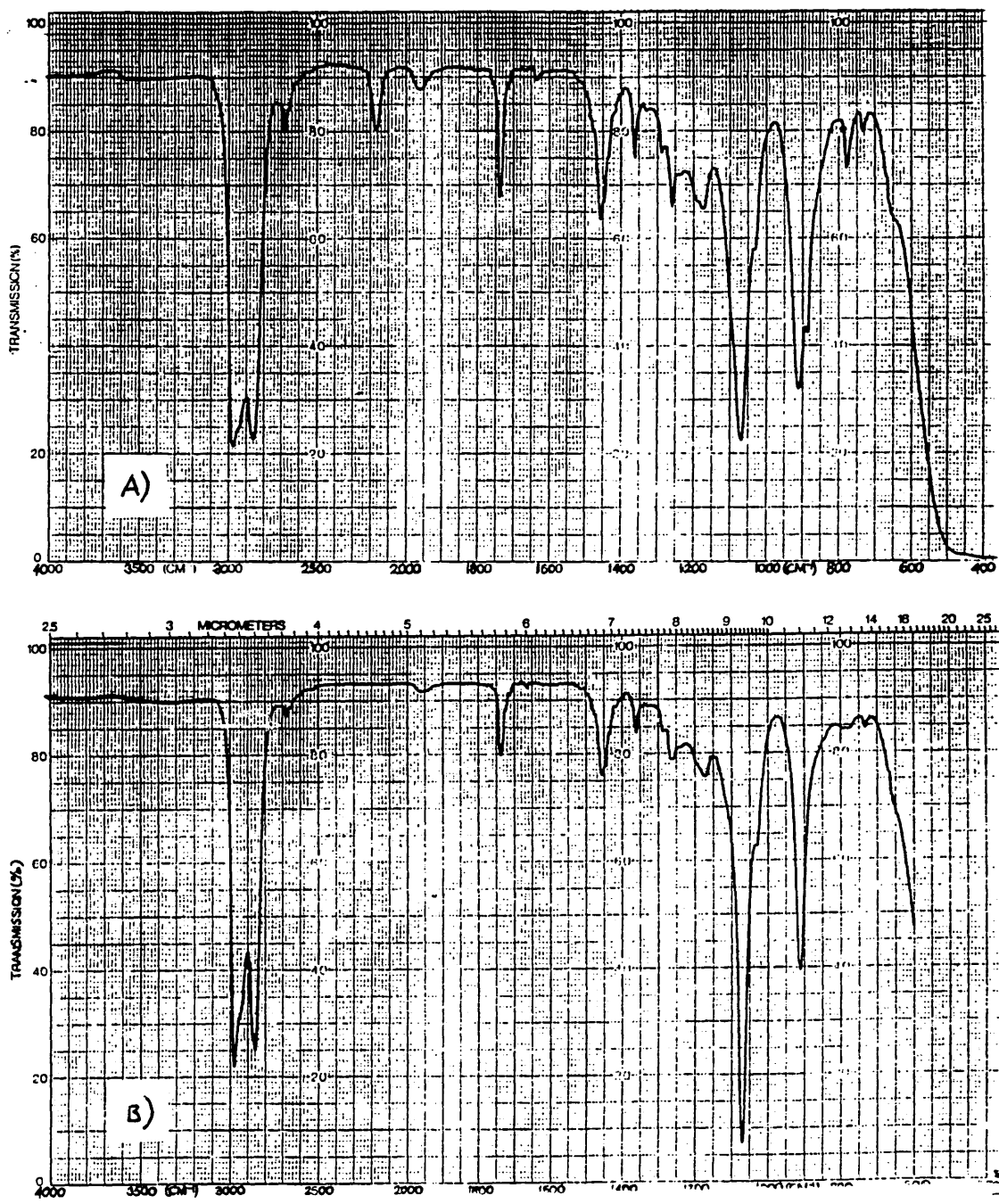


Figure 4.14 IR spectra of coupling reaction of methyl undecenoate and 1,3,5,7 tetrahydrocyclotetrasiloxane (hydrogenmethyl D<sub>4</sub>), after A) 30 minutes and B) 48 hours.  
 Note: absence of Si-H at 2160 cm<sup>-1</sup> in B) indicating complete reaction.

## 4.2.6 Isolation of Products

The work up and isolation of products varied according to the nature of the backbone and the mesogen.

### 4.2.6.1 Cyclic Non-Amphiphilic Oligomers

The cyclic non-amphiphilic oligomers were isolated by GPC using a Shephadex LH-20 gel and THF as the eluting solvent. The column was monitored by TLC (90% petroleum spirits/10% ethyl acetate). The solvent was removed under reduced pressure, and the polymer dried under vacuum as the isotropic liquid. The IR and  $^1\text{H}$  nmr spectra were consistent with the required structures (see figures 4.15 and 4.16).

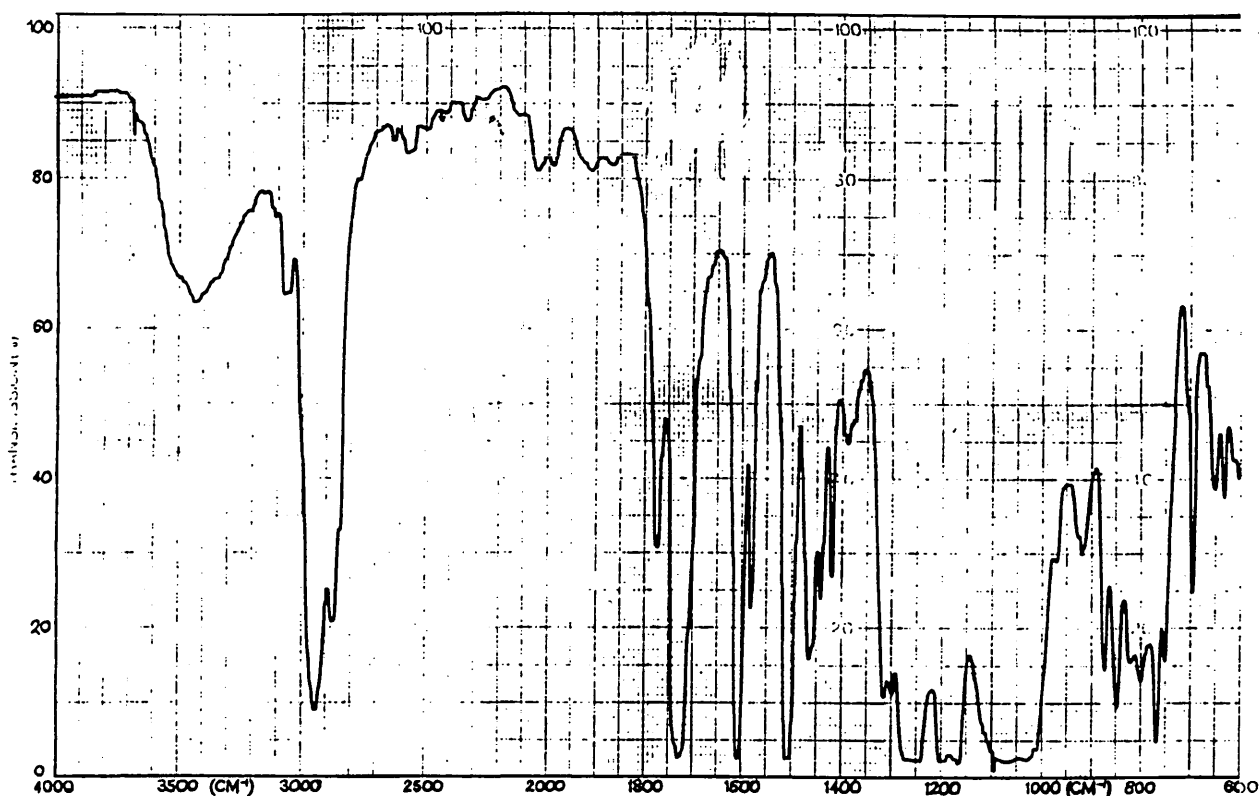


Figure 4.15 IR spectrum of  $\text{D}_4\text{C}_6$  (see figure 8.1 for key to nomenclature).

IR signal ( $\text{cm}^{-1}$ ): 2950 (CH), 1725 (C=O), 1600 (C=C), 1300-750 (Si-O-Si).

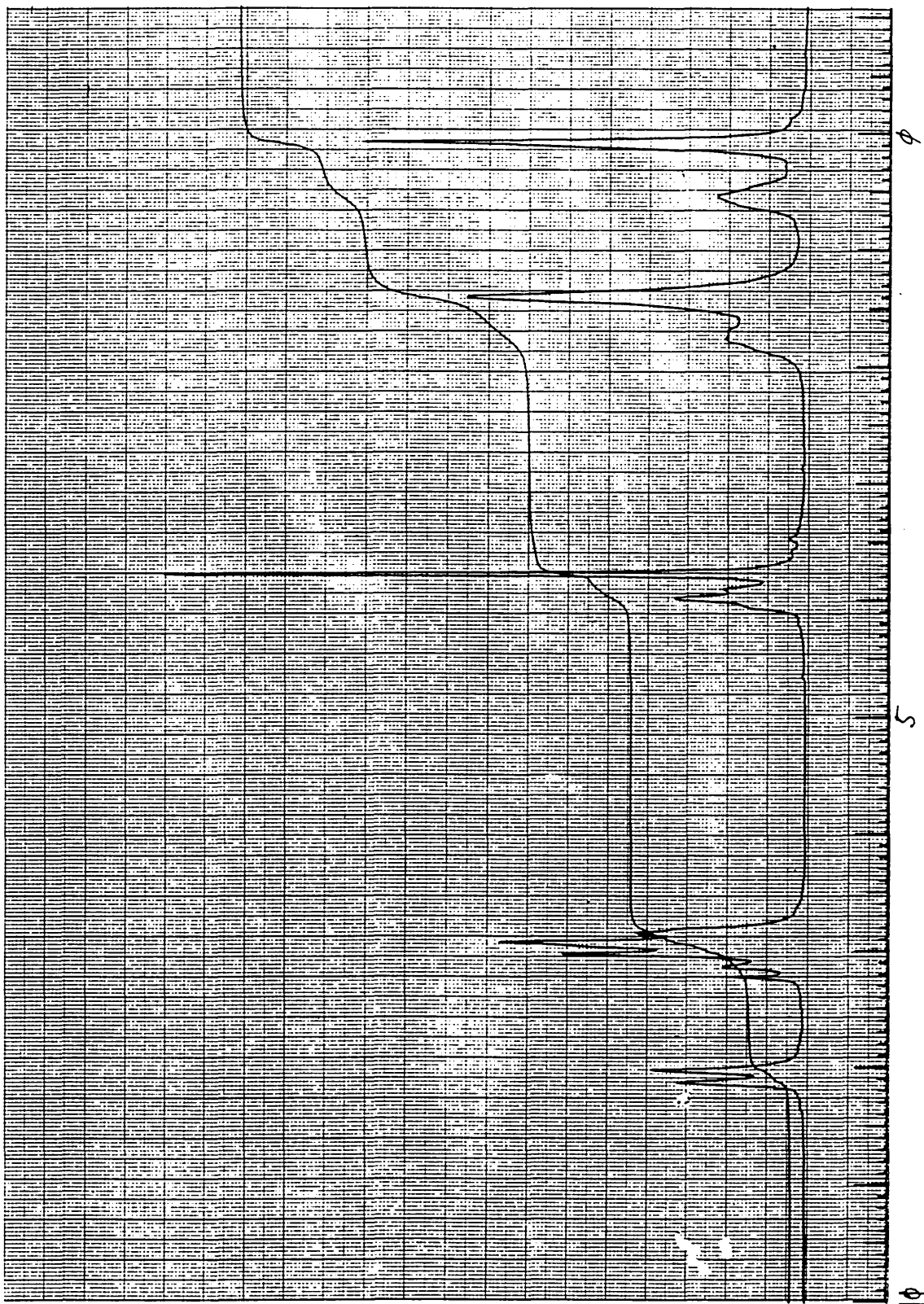


Figure 4.16  $^1\text{H}$  nmr spectrum of  $\text{D}_4\text{C}_6$  (see figure 8.1 for key to nomenclature).  
 $^1\text{H}$  nmr signal (ppm): 0.1 (12H, s, Si- $\text{CH}_3$ ), 0.6 (8H, t, Si- $\text{CH}_2$ ), 1.5 (32H, m,  $\text{CH}_2$ ), 3.8 (12H, s,  $\text{OCH}_3$ ), 4.0 (8H, t,  $\text{OCH}_2$ ), 7.5 (32H, m, aromatic H).

#### 4.2.6.2 Cyclic Amphiphilic Oligomers

After removal of the solvent, the excess monomeric amphiphile was distilled off (100°C, 0.3mm.Hg, 4 hours). The residue was stirred in ethanol (4 hours at 50°C) to liberate the carboxylic acid groups. The ethanol was removed under reduced pressure, and the product obtained by phase-separation from acetone/water (80/20) 7 times. Finally, an acetone solution of the product was dried ( $Mg_2SO_4$ ), filtered and evaporated to give the final product, which was then dried under vacuum. The  $^1H$  nmr spectra were consistent with the required structures (see figures 4.17).

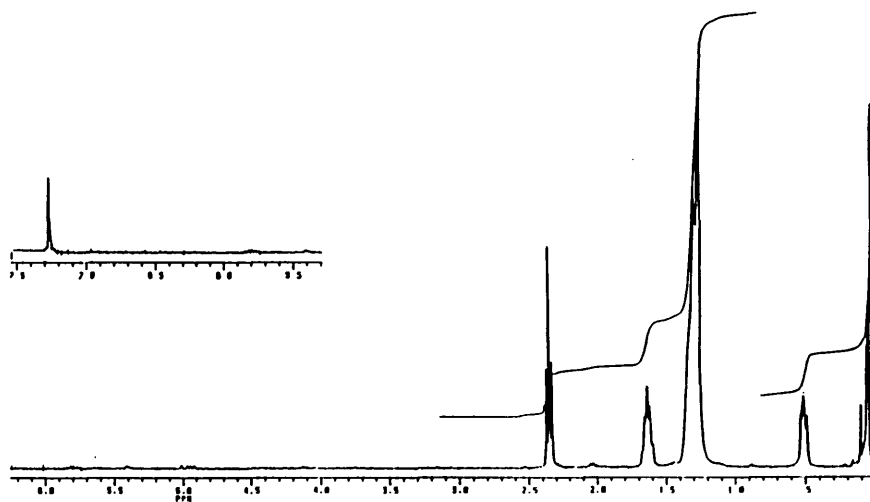


Figure 4.17  $^1H$  nmr spectrum of the acid form of the cyclic amphiphilic tetramer.

$^1H$  nmr signal (ppm); 0.05 (12H, s, Si- $CH_3$ ), 0.5 (8H, t, Si- $CH_2$ ), 1.3 (48H, m,  $CH_2$ ), 1.65 (8H, m,  $CH_2$ -C-acid), 2.35 (8H, m,  $CH_2$ -acid).

### 4.2.6.3 Linear Amphiphilic Polymers

After removal of the solvent, the product was isolated by phase-separation from acetone/water (80/20) seven times. The residue was stirred in ethanol (4 hours at 50°C) to liberate the carboxylic acid groups. After the ethanol was removed, the product was taken up in acetone, dried ( $Mg_2SO_4$ ) and filtered. The acetone was removed under reduced pressure and the product was dried under vacuum. The IR and  $^1H$  nmr spectra were consistent with the required structures (see figures 4.18 and 4.19).

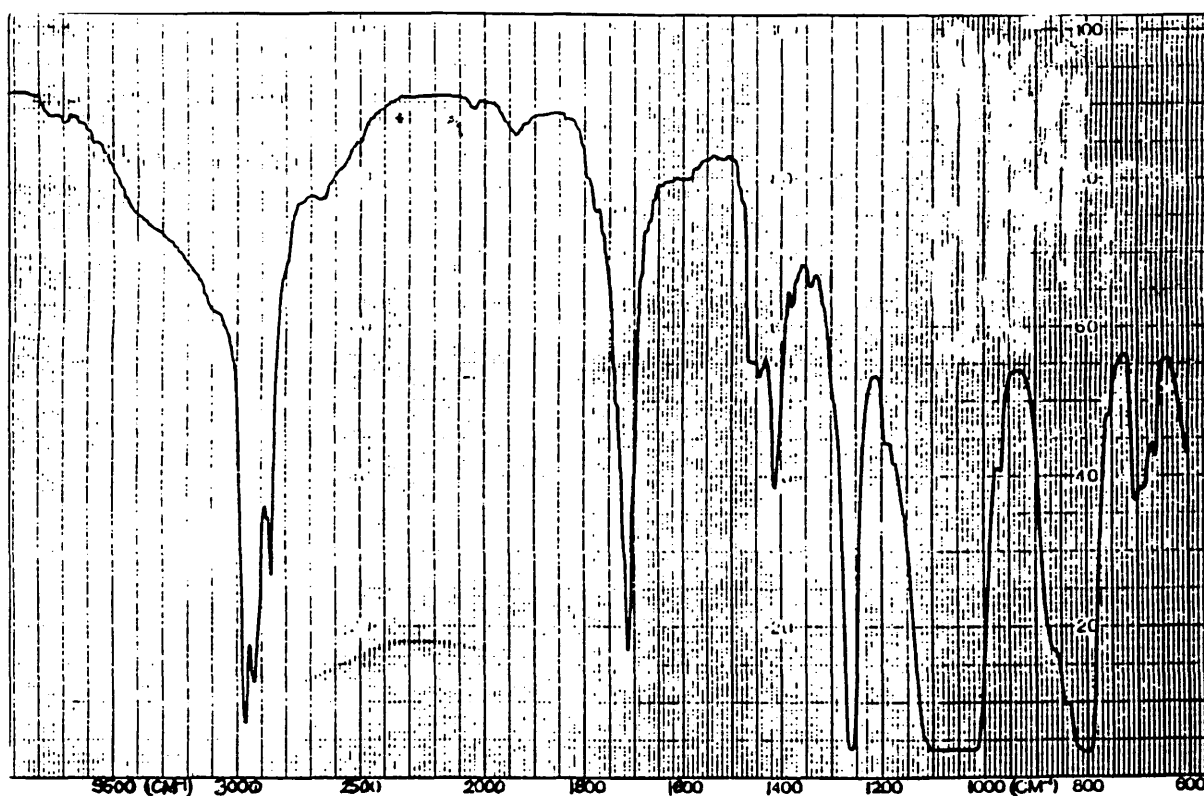


Figure 4.18 IR spectrum of linear amphiphilic polymer (nominal  $M_n=1000$ ).

IR signal ( $cm^{-1}$ ): 3500-3000 (C=O), 2950 (CH), 1710 (C=O),  
1300-750 (Si-O-Si).



## 4.2.7 Salts of the Amphiphilic Siloxanes. General Procedures

### 4.2.7.1 Sodium salts

#### a) Cyclic Oligomers.

Ethanolic solutions of the acid functionalised cyclic oligomers (2g in 20ml) were neutralised with ethanolic NaOH ( $0.025\text{M}\cdot\text{dm}^{-3}$ ). The precipitated sodium salts were filtered off, triturated with hot acetone and dried under reduced pressure (yield approximately 85%). The IR and  $^1\text{H}$  nmr spectra were consistent with the required structure (see figures 4.20 and 4.21).

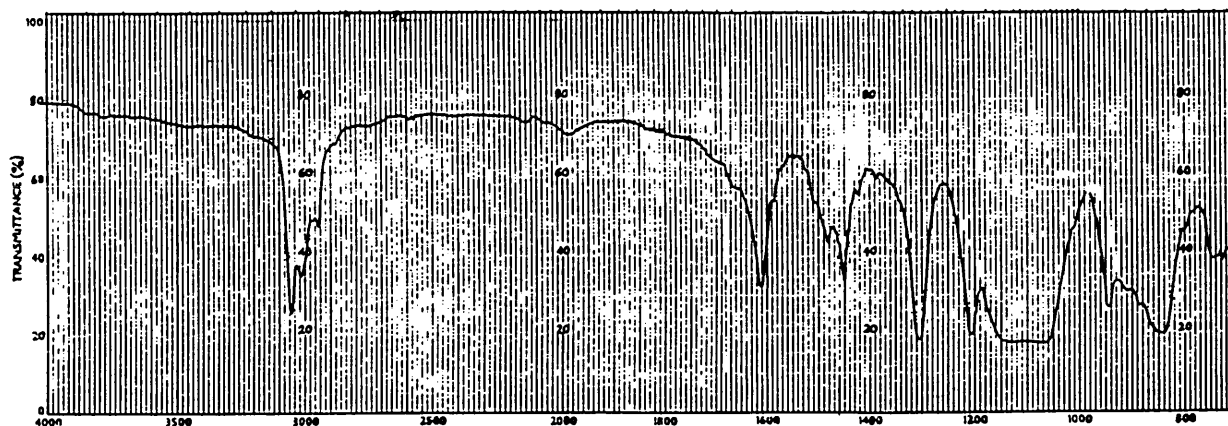


Figure 4.20 IR spectrum of the sodium salt of cyclic amphiphilic tetramer.

IR signal ( $\text{cm}^{-1}$ ): 2950 (CH), 1560 (C=O), 1300-750 (Si-O-Si).

Note: due to misalignment of the recording chart, peaks appear at  $50\text{ cm}^{-1}$  above actual. Therefore, subtract  $50\text{ cm}^{-1}$  from chart reading to obtain true wavenumber.

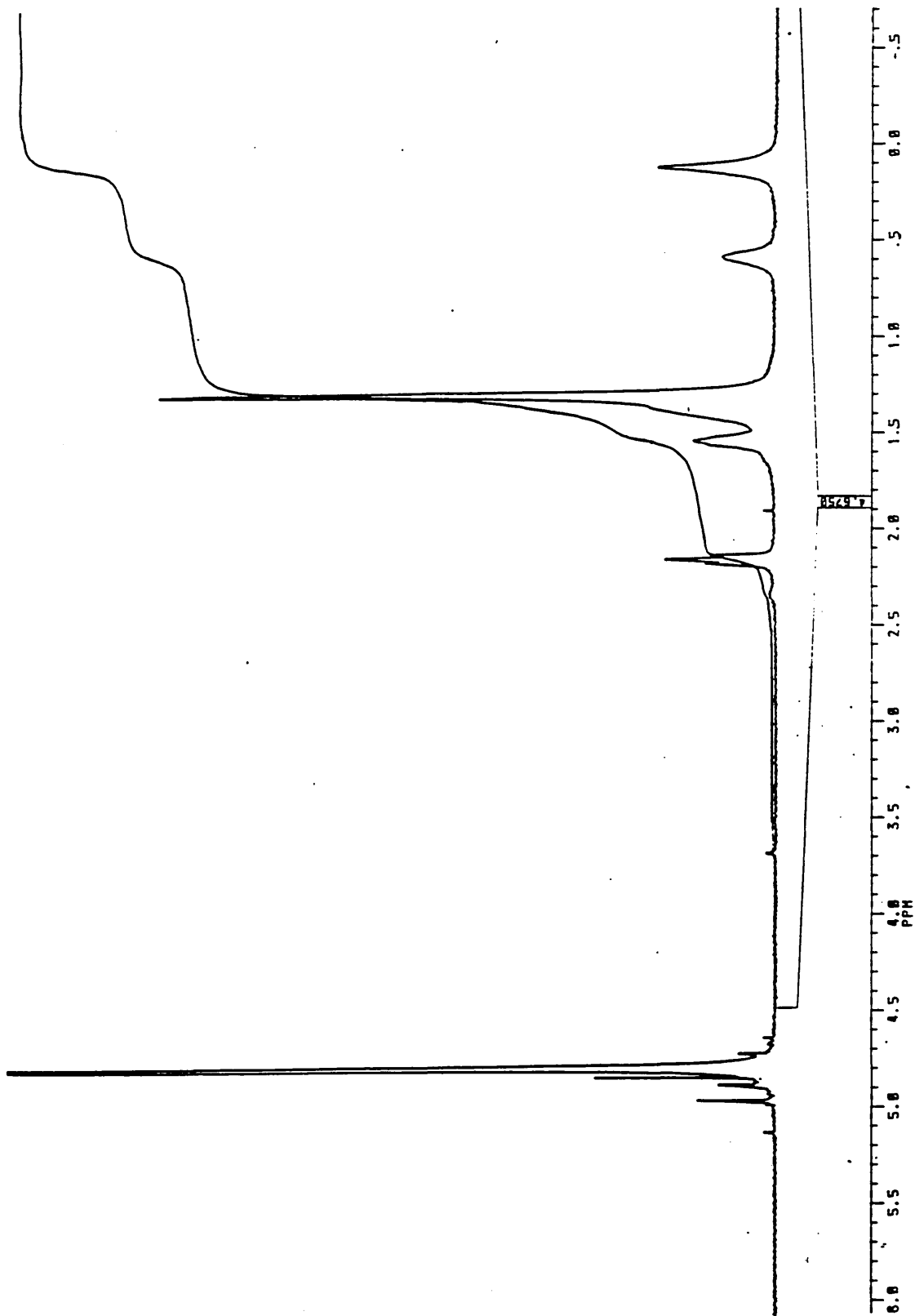


Figure 4.21. <sup>1</sup>H nmr spectrum of the sodium salt of the cyclic tetramer.

<sup>1</sup>H nmr signal (ppm): 0.1 (12H, s, Si-CH<sub>3</sub>), 0.6 (8H, t, Si-CH<sub>2</sub>), 1.3 (48H, m, CH<sub>2</sub>), 1.55 (8H, m, CH<sub>2</sub>-C-salt), 2.15 (8H, t, CH<sub>2</sub>-salt).

b) Linear Polymers

Ethanol solutions of the acid terminated linear polymers (2g in 20ml) were neutralised with ethanolic NaOH (0.025M.dm<sup>-3</sup>). The end-point was monitored by change in pH as a function of added NaOH using a pH meter. The solutions were reduced in volume, under reduced pressure, to their solubility limit and then excess acetone was added. Clear, viscous gums were deposited and the liquors were decanted off. The products were triturated in hot acetone and dried under vacuum. The IR and <sup>1</sup>H nmr spectra were consistent with the required structure (see figures 4.22 and 4.23). The molecular weights were determined by GLC (see table 4.4).

	nominal M <sub>n</sub> of siloxane segment plus butyl tail	observed M <sub>n</sub> <sup>*</sup> of siloxane segment ( <sup>1</sup> H nmr)	observed M <sub>n</sub> <sup>*</sup> of molecule as a whole ( <sup>1</sup> H nmr)
a)	500	510	717
	1000	960	1167
	1500	1530	1737
	2000	2200	2407
b)	2000	2100	2307

\*<sup>1</sup>H nmr spectra recorded on a Bruker 560 spectrometer. M<sub>n</sub> calculated by comparison of signal due to Siloxane with signal due to rest of the molecule.

Table 4.4 M<sub>n</sub> of the sodium salts of a) α- and b) α,ω-functionalised linear dimethylsiloxanes.

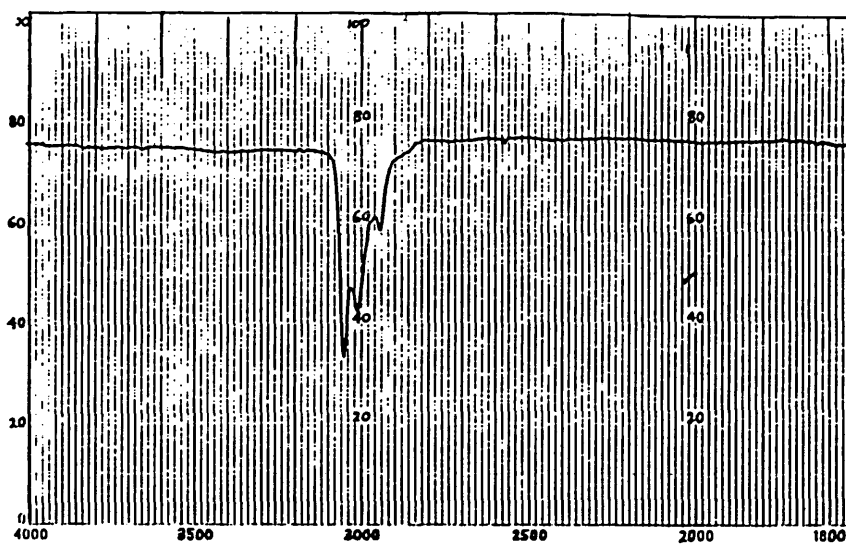
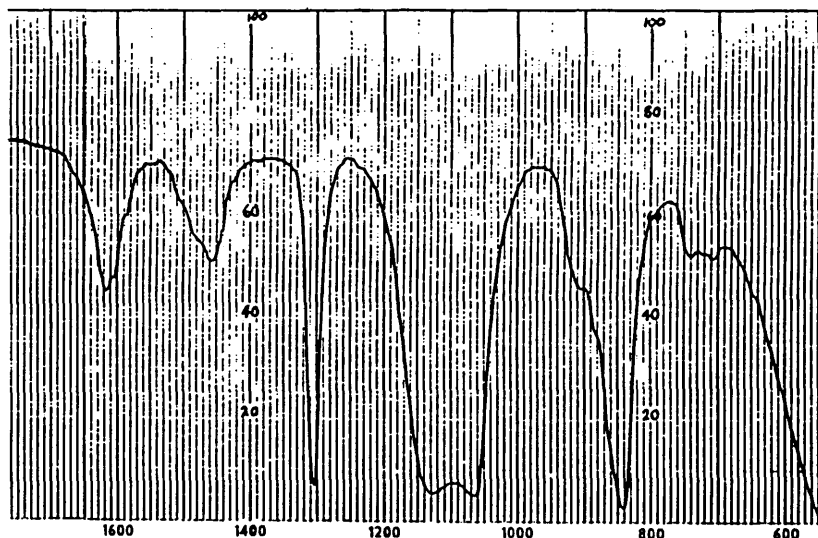


Figure 4.22 IR spectrum of the sodium salt of  $\alpha$ - functionalised linear dimethylsiloxane (nominal  $M_n=1000$ ).

IR signal ( $\text{cm}^{-1}$ ): 2950 (CH), 1570 (C=O), 1300-750 (Si-O-Si).

Note: due to misalignment of the recording chart, peaks appear at  $50 \text{ cm}^{-1}$  above actual. Therefore, subtract  $50 \text{ cm}^{-1}$  from chart reading to obtain true wavenumber.

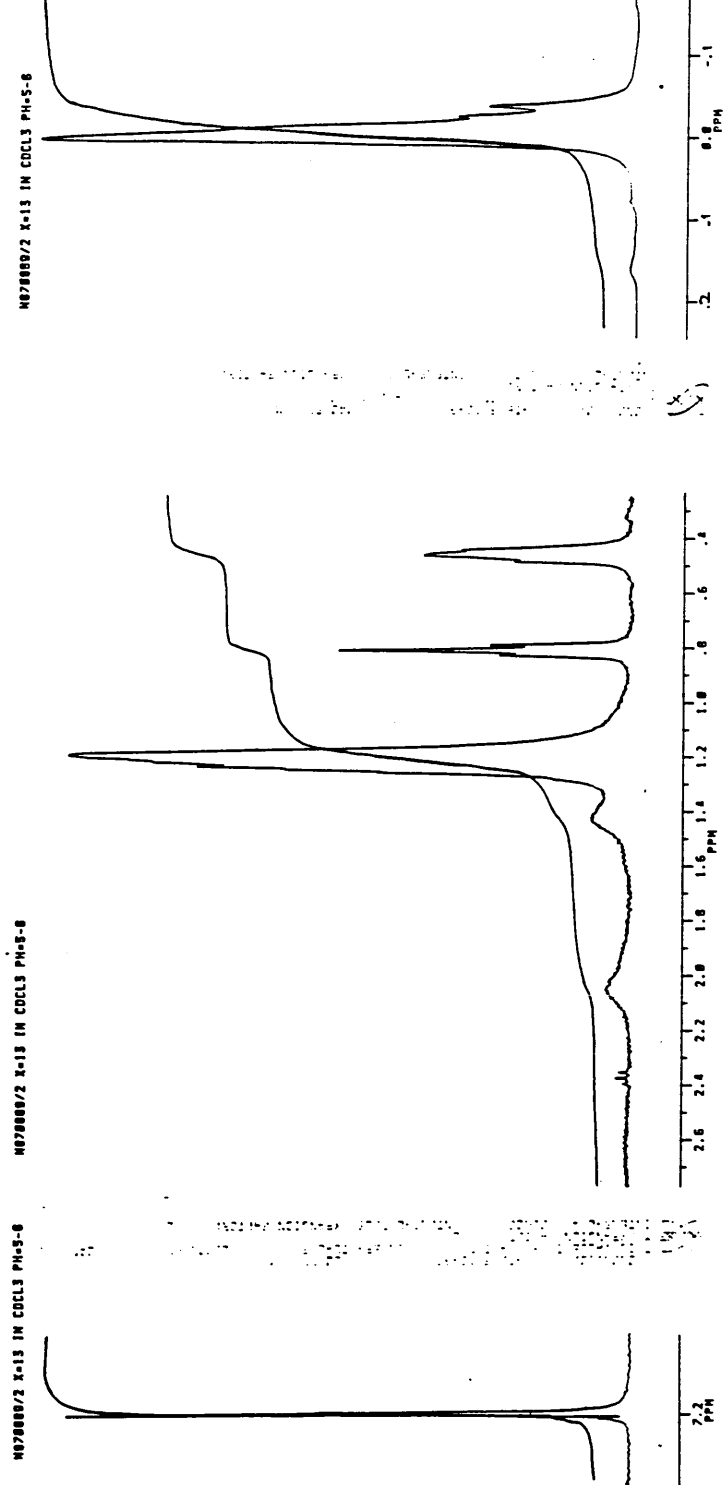


Figure 4.23  $^1\text{H}$  nmr spectrum of the sodium salt of  $\alpha$ -functionalised linear dimethylsiloxane (nominal  $M_n=1000$ ).

$^1\text{H}$  nmr signal (ppm); 0.0 (72H, s, Si- $\text{CH}_3$ ), 0.45 (4H, m, Si- $\text{CH}_2$ ), 0.8 (3H, t,  $\text{CH}_3$ ), 1.2 (18H, m,  $\text{CH}_2$ ), 1.45 (2H, m,  $\text{CH}_2$ -C-salt), 2.05 (2H, t,  $\text{CH}_2$ -salt).

#### 4.2.7.2 The Calcium Salts

##### a) The Cyclic Tetramer<sup>154</sup>

The tetrakis sodium salt of the cyclic tetramer (0.5g,  $4.7 \cdot 10^{-4}\text{M}$ ) was dissolved in deionised water (20ml) at 50 °C. Excess, saturated aqueous  $\text{CaCl}_2$  was added while stirring and a white, solid product precipitated out of solution. After centrifugation and filtration, the product was triturated in acetone, filtered and dried under vacuum (yield 0.39g, 79%).

##### b) The $\alpha$ -Functionalised Linear Polymer (nominal $M_n=500$ )

A solution of the acid  $\alpha$ -terminated linear dimethylsiloxane (0.5g) in acetone (50ml) was stirred at 50°C over excess  $\text{CaOH}_2$  for 4 hours. The solvent was removed under reduced pressure. The residue was then taken up in ethanol, filtered and the ethanol was removed under reduced pressure. The product was then dried under vacuum (yield 0.45g, 90%).

#### APPENDIX 4.1

This contains the GCMS data for the commercial mixture of cyclic hydrogenmethylsiloxanes obtained from Petrach Systems. All data was acquired using the following conditions:

Equipment	VG 305 Mass spectrometer
Injection temperature	225°C
Inlet lines	200°C
Column	1.25% Dexil 300
Initial temperature	60°C
Final temperature	200°C
Temperature gradient	10C.min <sup>-1</sup>
Carrier gas	Helium 16 lbs.in <sup>2</sup>
Electron beam energy	70eV

The gas chromatograph of the mixture, along with the structures subsequently assigned to the individual peaks, is shown in figure 4.24. Figures 4.25 to 4.29 show the mass spectra obtained for each of the major peaks in the chromatograph. Only the ions of particular importance have been referenced on the individual mass spectra, although the unmarked fragments do agree with the proposed structures. In all spectra 'M' represents the molecular ion.

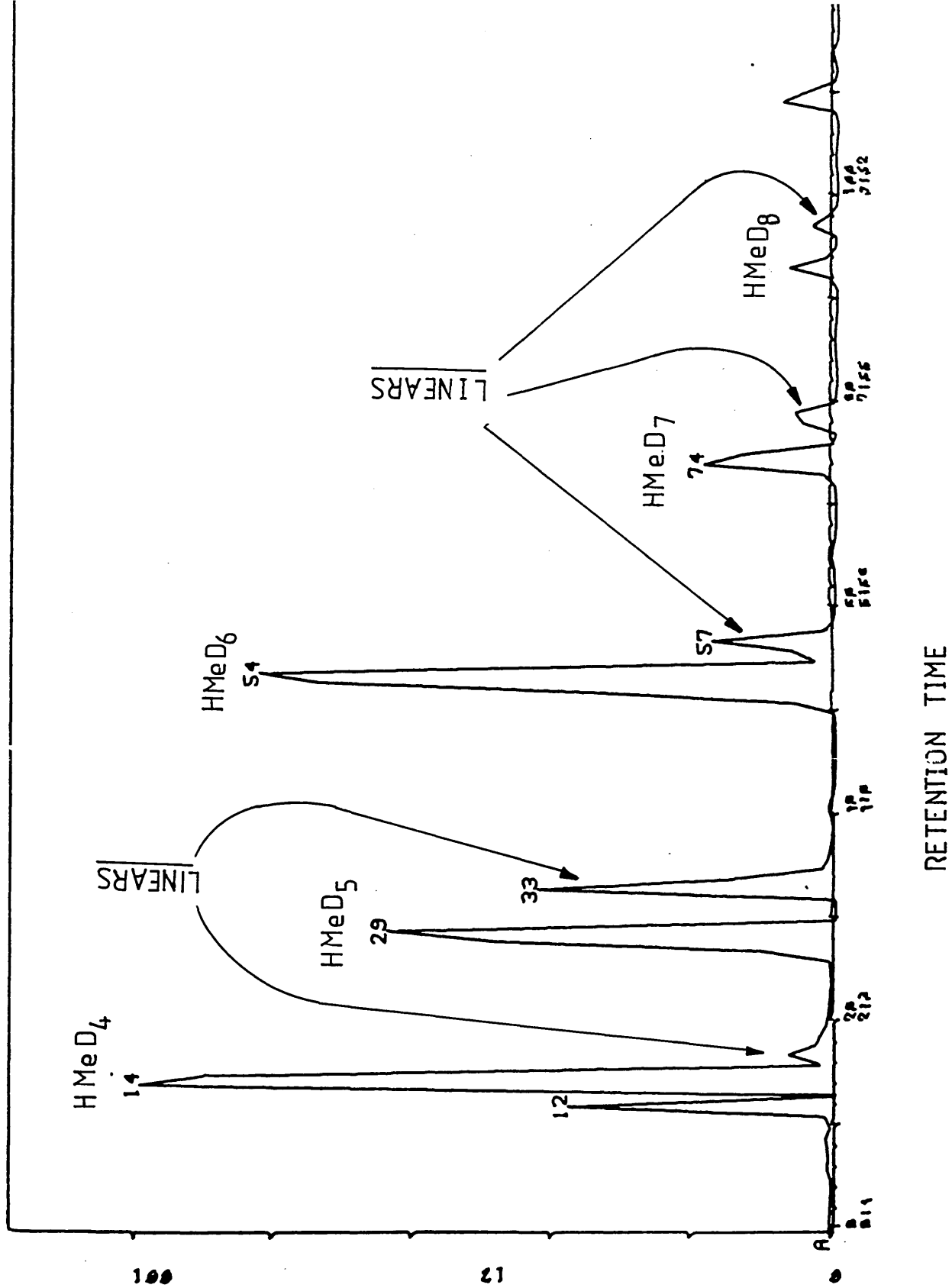


Figure 4.24 Gas chromatograph of the commercially available mixture of cyclic hydrogenmethylsiloxanes.

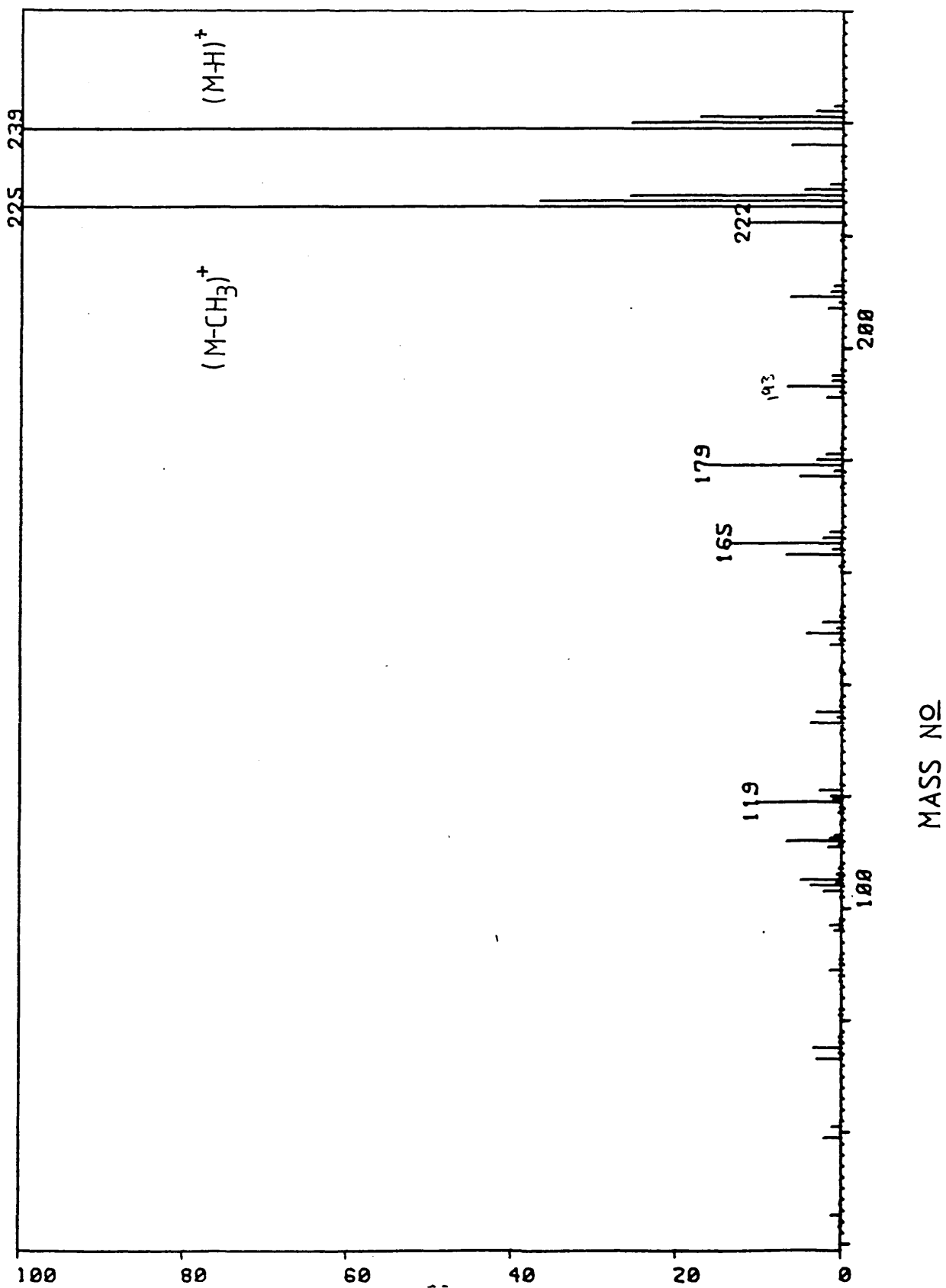


Figure 4.25 Mass spectrum of the compound corresponding to scan N° 15, i.e. the cyclic hydrogenmethyltetrasiloxane (hydrogenmethyl D<sub>4</sub>).

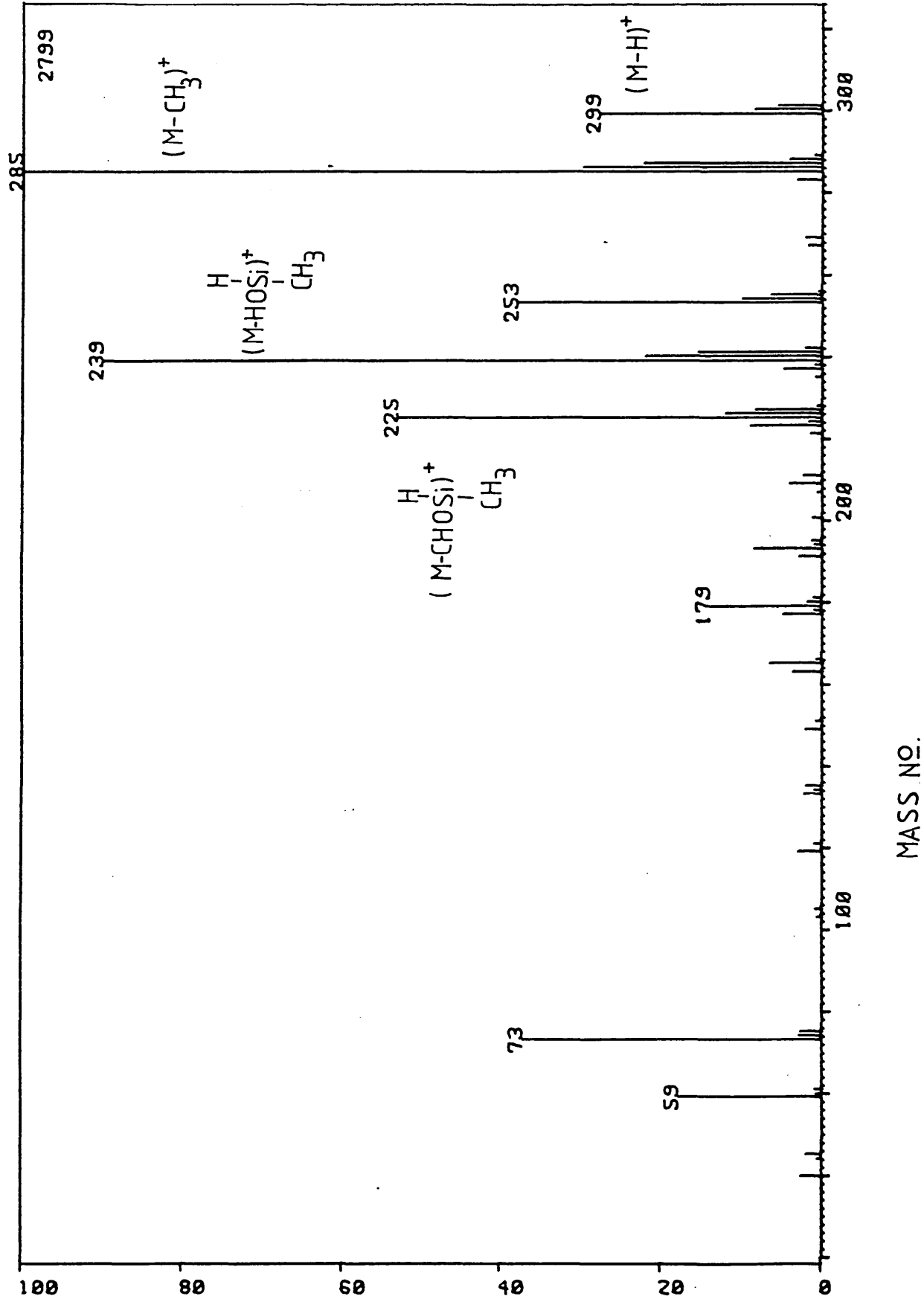


Figure 4.26 Mass spectrum of the compound corresponding to scan N° 28, i.e. the cyclic hydrogenmethylpentasiloxane (hydrogenmethyl D<sub>5</sub>).

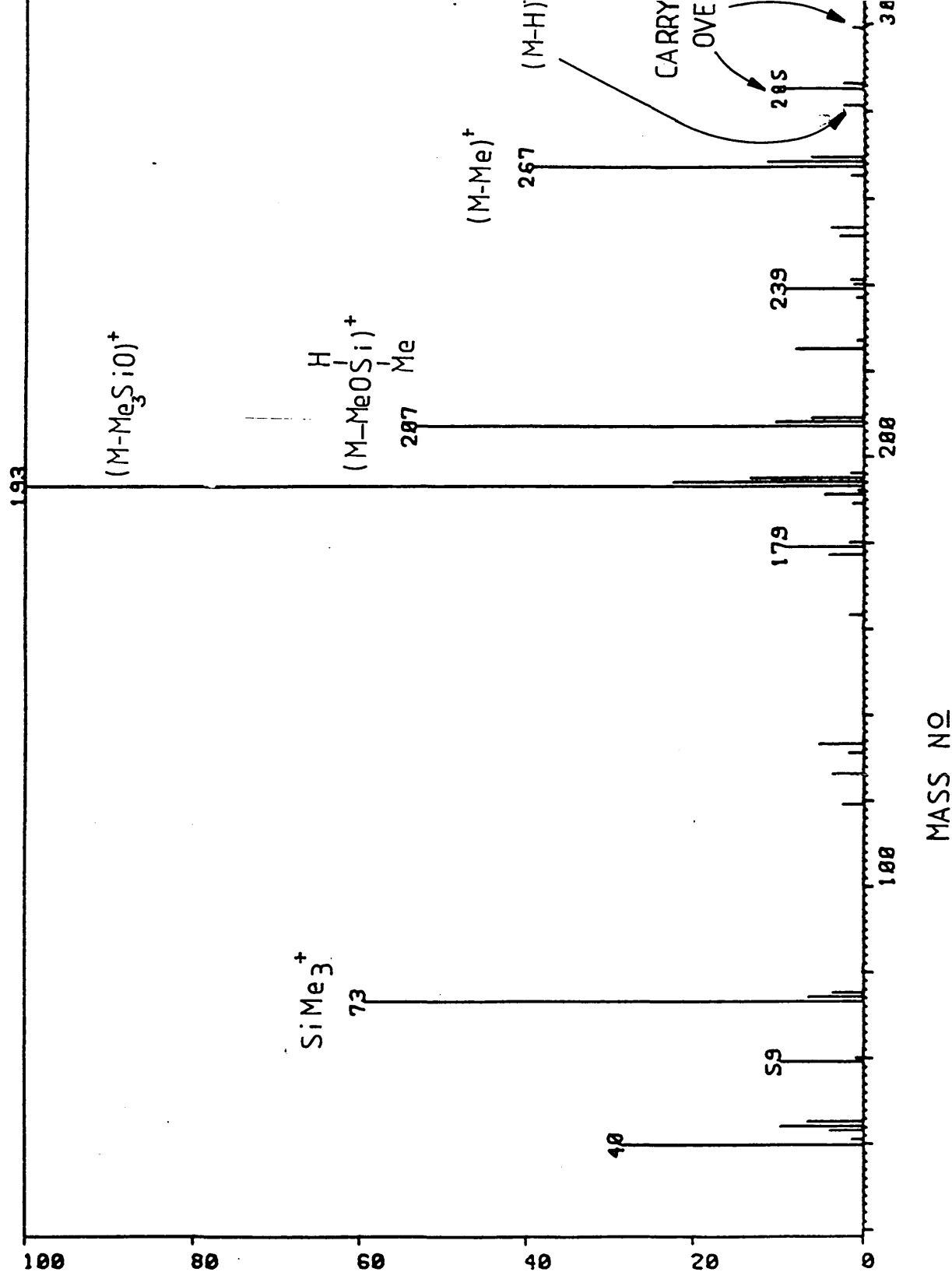
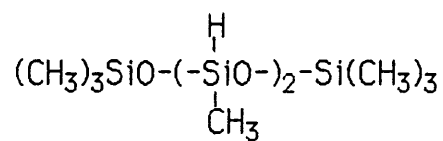


Figure 4.27 Mass spectrum of the compound corresponding to scan No 36, i.e. the linear hydrogenmethylsiloxane impurity:



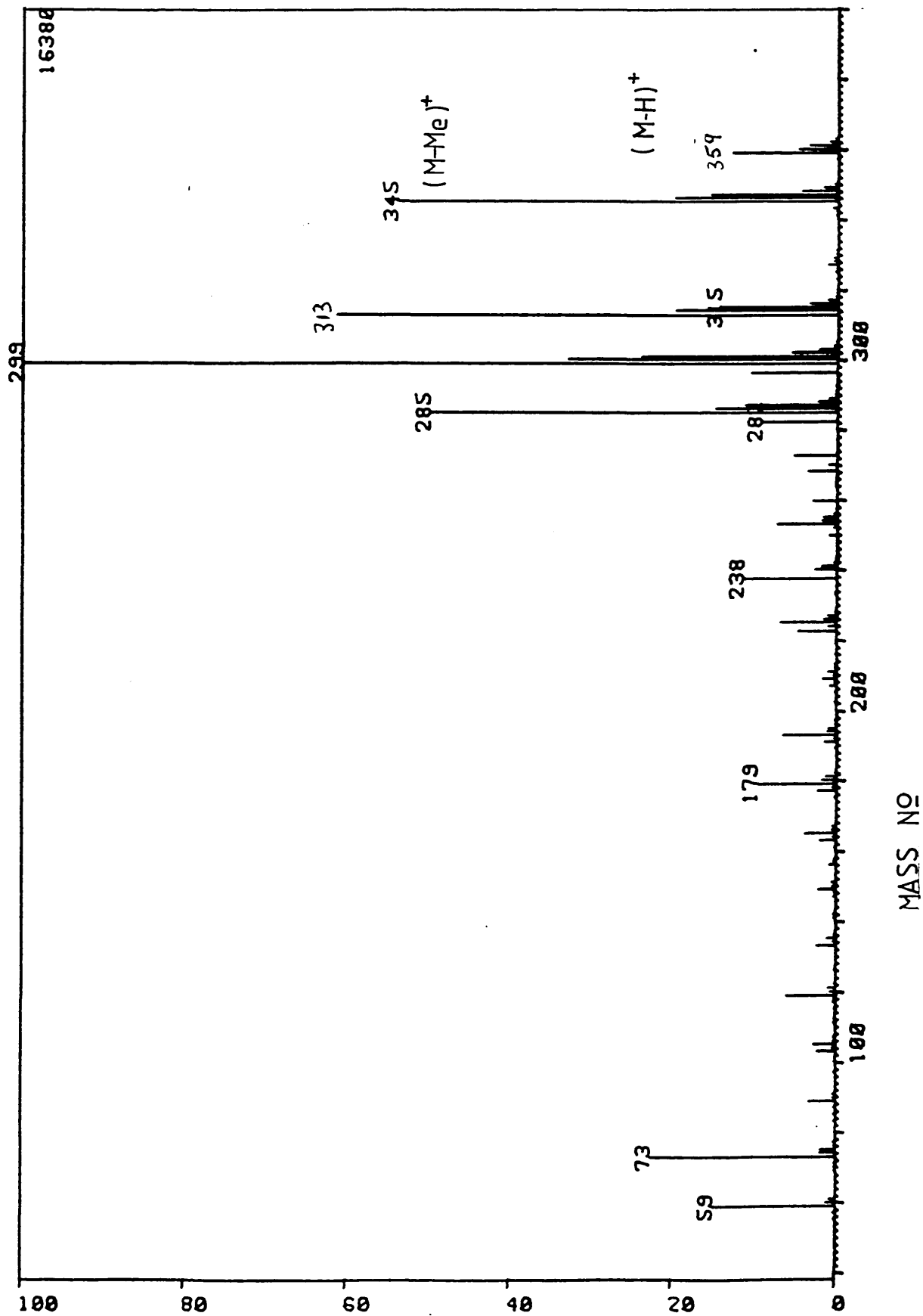


Figure 4.28 Mass spectrum of the compound corresponding to scan N° 54, i.e. the cyclic hydrogenmethylhexasiloxane (hydrogenmethyl D<sub>6</sub>).

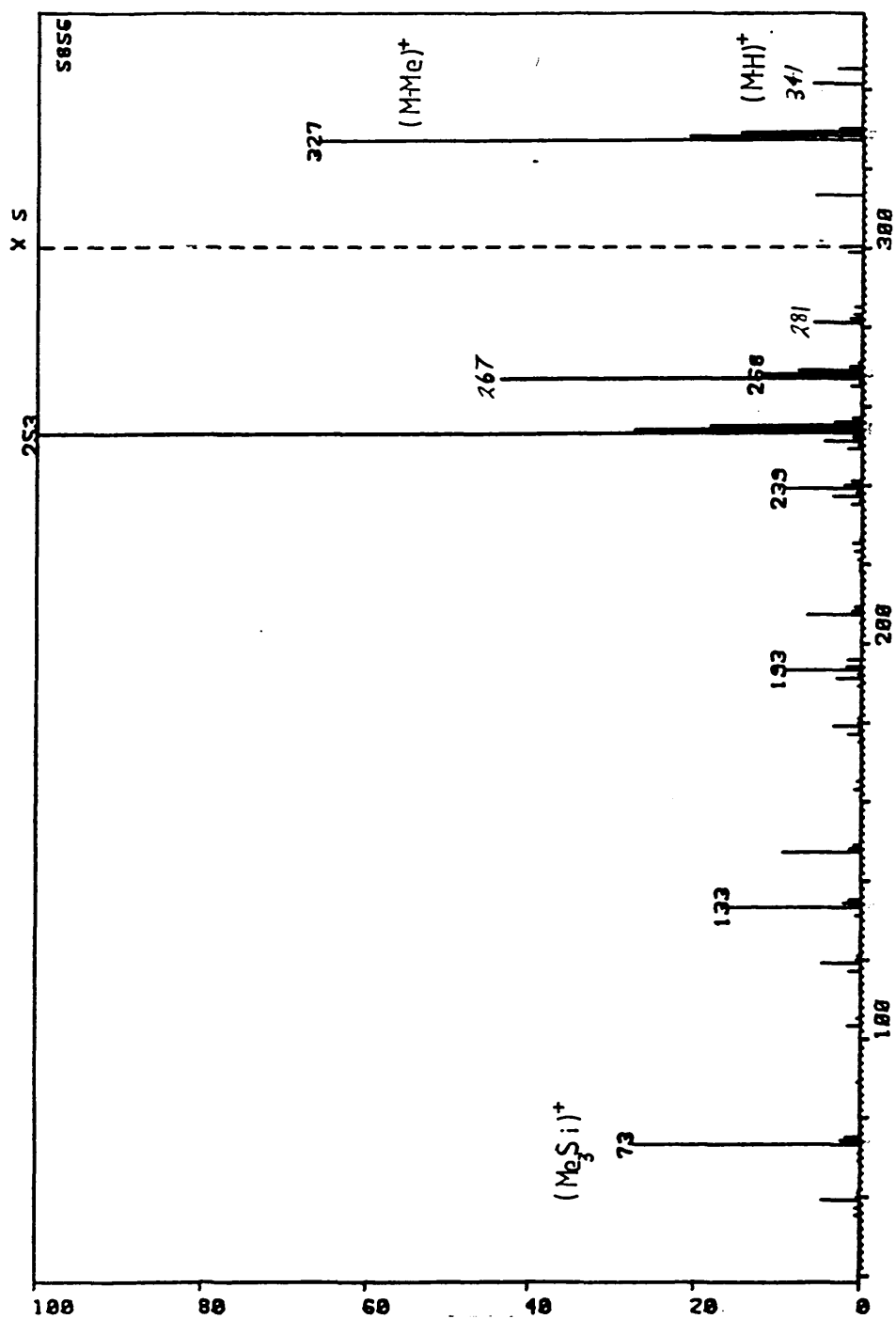
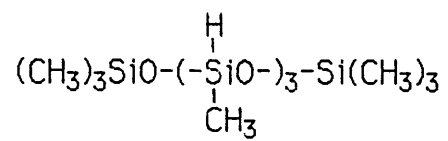


Figure 4.29 Mass spectrum of the compound corresponding to scan N° 57, i.e. the linear hydrogenmethylsiloxane impurity:



## **CHAPTER 5. CHARACTERISATION OF PHASE BEHAVIOUR**

### 5.1 Introduction

Having prepared the target materials (see chapters 3 and 4), the characterisation of their phase behaviour was undertaken. The majority of this work concentrated on the study of the thermotropic behaviour of the neat materials, in particular those that were amphiphilic in nature; this required the identification of the structural order present as a function of temperature alone. The remainder of the work focused on obtaining an overview of the lyotropic behaviour of the amphiphilic materials in concentrated aqueous solutions. This overview established the lyotropic mesophases present in the phase diagram—only as a qualitative function of concentration—and, where applicable, the upper and lower temperature limits of each phase within the range 0–100°C. A comprehensive characterisation of the lyotropic phase behaviour would have required the quantitative study of the effects of both composition and temperature on phase behaviour, which was not possible in the time available.

As no single technique can unequivocally determine the nature of a given mesophase, a number of different techniques—each offering supportive evidence—were employed during this work. Of the many techniques available for the characterisation of phase behaviour, those encountered during this work were:

- Polarising Microscopy
- Differential Scanning Calorimetry (DSC)
- X-ray Diffraction

These techniques—the underlying principles, experimental method and apparatus thereof—will form the basis of this chapter.

## 5.2 Polarising Microscopy

### 5.2.1 Introduction

When examined under the crossed-polars of a polarising microscope, a thin film of a mesophase will, in most cases, exhibit an optical pattern and a rheology, that may be indicative of the structural order present. Hence, a polarising microscope fitted with a heating stage may allow the initial assignment of structural order, and the visual observation of the transitions between the crystalline, mesomorphic and isotropic liquid phases, as a function of the temperature<sup>263,264</sup> and/or the concentration of added solvent<sup>264-267</sup>.

Due to the simplicity of the experimental method, and the amount of information thus obtained, the technique of optical microscopy has found wide-spread use in the study of both thermotropic and lyotropic mesophases. Hence, although supportive evidence is also required, optical microscopy would generally be the first technique employed in the characterisation of phase behaviour.

### 5.2.2 Principles

As the molecules that constitute the majority of mesophases are birefringent (i.e. they possess different refractive indices for light vibrating normal and parallel to their long axes), the ordered arrangements of the aggregates of these molecules that are found in most mesophases, are themselves birefringent. These mesophases therefore transmit polarised light and exhibit characteristic patterns (referred to as textures) when viewed through crossed-polars. The exceptions to this birefringence are the cubic phases, which because of their three-dimensional order are generally optically isotropic and appear as a uniform dark field. The relationship

between molecular structure and the observed optical properties of all these phases has been well established<sup>264</sup>. The description and classification of textures is a lengthy procedure that has been reviewed elsewhere<sup>25,264-268</sup> and will not be attempted here. However, simple microscopic observations of the relative viscosity (assessed by pressing on the cover-slip) and the texture of a mesophase may, with experience and by comparison with literature photomicrographs<sup>25,264-268</sup>, allow the initial assignment of phase structure.

### 5.2.3 Experimental

Observations of texture and viscosity were made on sample films, prepared between glass microscope slides and cover-slips, using a Vickers M41 Photoplan polarising microscope equipped with a heating stage. The temperature and rate of heating of the stage, and hence the sample, were controlled with a variable rheostat.

The initial assignment of the thermotropic mesophase structure of anhydrous samples was carried out with the observations of texture and viscosity as outlined above. The upper and lower temperature limits of a phase, and the temperature of any transitions that occurred, were determined by slowly heating and cooling the sample at a rate of approximately  $2^{\circ}\text{C}\cdot\text{min}^{-1}$ . Transition temperatures are quoted to the nearest  $0.5^{\circ}\text{C}$ .

Whilst the thermotropic behaviour of neat materials varies with temperature alone, the phase behaviour of lyotropic systems is both composition and temperature dependent. The comprehensive characterisation of lyotropic systems therefore requires the construction

of a phase diagram relating phase behaviour to variation of temperature and composition. As this was not possible here, an overview of the lyotropic phase behaviour of materials was obtained using the penetration technique of Lawrence<sup>219,269</sup>. In this technique, a small sample is placed between a microscope slide and a cover-slip. Solvent is added to the slide and allowed to diffuse into the sample. Thus, a concentration gradient, with decreasing solvent concentration towards the anhydrous sample, is established and lyotropic mesophases may develop as separate bands around the anhydrous sample. Each of these bands may exhibit a texture and viscosity that allows the initial assignment of phase structure. Due to their three-dimensional order, the cubic phases are optically isotropic and therefore do not exhibit an optical texture. These phases may nevertheless be identified with the appearance of a distinct, highly viscous, dark band. With heating or cooling of the sample, it is then possible to determine the upper and lower temperature limits of each of the phases present and an overview of the phase diagram for both temperature and composition can be established.

To construct a complete phase diagram, homogeneous samples of varying, but known, composition would have to be prepared and the thermotropic behaviour of thin films of these samples determined. Alternatively, macroscopic visual observations using the method of Void *et al.*<sup>137,270</sup> may be used. This method entails preparing bulk samples in sealed glass vials and observing the samples through illuminated polaroid windows. With this technique, there is no observation of a texture as such, but it is possible to follow the thermotropic phase behaviour of a sample by monitoring changes in appearance and viscosity. Repeating this operation with samples of varying composition would quantify the effects of both temperature and

composition and thus complete the phase diagram. This technique overcomes the problem of solvent loss which may be encountered in the penetration technique at elevated temperatures.

### 5.3 Differential Scanning Calorimetry

#### 5.3.1 Introduction

Differential scanning calorimetry (DSC) is a rapid and powerful technique for the study of thermally induced transitions. It is a modification of differential thermal analysis (DTA) that can be used to determine transition temperatures and the enthalpy changes involved. DSC, therefore, acts as a complement to optical microscopy, finding widespread application in the study of the thermotropic phase behaviour of both single<sup>89,150,151,201,271-278</sup> and multi-component<sup>176,201,202,208,279-281</sup> systems.

#### 5.3.2 Principles

In DSC, the sample and an inert reference (i.e. a material that does not undergo a thermal transition in the temperature range of interest) are heated at an identical rate. The control unit attempts to maintain a gradually increasing and equivalent temperature in both sample and reference, and records the electrical power required to achieve this. If no thermally induced transition is taking place in the sample, then the relative rates at which power is supplied to the sample and the reference cells will remain constant. If a thermally induced transition takes place in the sample, then the control unit supplies enough electrical power to the sample or the reference—depending on whether the transition is exothermic or endothermic—to maintain the two at the same temperature. Hence, the electrical power input necessary to maintain the sample and the reference cells at an equivalent rate of temperature increase throughout the analysis

is plotted against time. As the rate of temperature increase is known this can be related to temperature. The resulting plot, or thermogram, provides information on the thermally induced events occurring throughout the temperature range of interest. This includes transition temperatures, the range over which a transition occurs, the magnitude of a transition, and whether the transition is of first or second order (i.e. involves a change in enthalpy or specific heat capacity, respectively).

### 5.3.3. Experimental

DSC thermograms were recorded using a Mettler TA 3000 thermal analysis system. The use of this system is outlined in the Mettler TA 3000 operating manual. This system consisted of a TC10 TA control unit, and a DSC 30 measuring cell with an operating range of  $-170^{\circ}\text{C}$  to  $+600^{\circ}\text{C}$ . Controlled cooling was achieved using liquid nitrogen. In addition to recording the measuring curve, the processor was used to calculate the transition temperatures and enthalpy changes occurring. The measuring sensor used to monitor the difference in temperature between sample and reference cells, was a vapour-deposited, five-fold gold-nickel thermopile. This ensured high instrumental accuracy and precision in the determination of enthalpy values (Mettler quoted values of 2% and 0.5%, respectively).

The baseline curve, i.e. empty sample and reference pans, was checked at regular intervals to ensure that it was free of peaks and discontinuities due to impurities in the cell.

The rate at which the cell furnace was heated in order to provide a linear temperature increase was controlled with a platinum resistance thermometer (Pt 100). Temperature measurement with the Pt 100 sensor

was calibrated every six months. The processor has the capability to automatically recalibrate from the fusion of pure indium, lead and zinc samples at 156.6 °C, 327.4 °C and 419.5 °C respectively.

As the measurements carried out were all on one-component samples (i.e. no solvent present), the loss of volatiles was not a problem. Hence, samples of 5 to 15 mg were contained in standard aluminium pans (40 µl net volume) as supplied by Mettler AG, Switzerland. Empty pans were used as the reference. To minimise the effects of sample oxidation at high temperature, a steady stream of dry nitrogen ( $60\text{cm}^3\cdot\text{min}^{-1}$ ) was passed through the DSC cell. If measurements were to be carried out with solvent present, then high pressure pans would be required. Steel pans which can be hermetically sealed to withstand a maximum pressure of approximately 100 bar are commercially available.

When carrying out DSC experiments, a fast heating rate gives sharp well defined peaks. Alternatively, a slow heating rate results in conditions closer to equilibrium but also small poorly defined peaks. Hence, a compromise was made, and a heating rate of  $10^\circ\text{C}\cdot\text{min}^{-1}$  was employed during this study. Although experiments were mostly conducted with heating, some cooling analyses were carried out. These cooling runs will be referred to in subsequent sections by the subscripts C.

During the evaluation of thermograms, the control unit was used to calculate the transition temperatures and enthalpy changes involved. The temperatures of first-order transitions were taken as the apex of the curve of heat supplied versus temperature. For a symmetrical peak, this represents the temperature at which the transition is 50% complete. The

temperatures of second-order transitions were also taken at the point of the curve at which the transition was 50% complete. Due to the broad transitions observed during this study—the basis of which will be discussed in chapters 6, 7 and 8—transition temperatures will be quoted to the nearest degree C ( $^{\circ}\text{C}$ ) and changes in enthalpy will be quoted to the nearest  $\text{kJ}\cdot\text{mol}^{-1}$ .

## 5.4 X-ray Diffraction

### 5.4.1 Introduction

A characteristic of mesophase structures is that while there is no short range order (i.e.  $<5\text{\AA}$ ), there is some long range order in one, two or three dimensions<sup>24,149,282-284</sup>. The interaction of X-rays with electrons in these ordered materials and the subsequent diffraction patterns that occur, can be related to atomic positions within the sample. Hence, X-ray diffraction may be used to establish mesophase structure and dimensions.

X-ray diffraction techniques<sup>285</sup> are usually categorised into wide-angle X-ray scattering (WAXS) and small-angle X-ray scattering (SAXS). Such a distinction is required because the instrumental requirements, and on occasion the method of analysing data, are very different. In the former, the required structural information is contained in the intensities at large scattering angles and is used to obtain structural information on a scale of 1 nm or smaller. In the latter, the required structural information is contained in the intensities at small scattering angles and is used to obtain structural information on a scale of 1-1000 nm. Hence, small-angle X-ray diffraction is generally the most widely used of the two techniques in the study of mesophase structures (i.e. to investigate aggregate dimensions and/or inter-molecule spacings).

During this work, SAXS has been used to study amphiphilic materials only, although the following basic principles apply to both WAXS as a technique and, also, to the study of non-amphiphilic materials in general.

#### 5.4.2 Principles

When a beam of X-rays is incident to a material, it is partly absorbed and partly scattered, with the rest being transmitted unmodified. The scattering occurs as a result of interaction of the X-rays with electrons in the material. The X-rays scattered from different electrons in ordered materials, interfere with each other and produce a diffraction pattern that varies with scattering angle. The variation of the scattered and diffracted intensity with angle provides information on the electron density distribution, and hence the atomic positions within the sample<sup>285</sup>.

The analysis of data is generally based upon treating the X-ray diffraction patterns as powder patterns. The positions of the reflections can be related to the interplanar spacings by means of the Bragg equation:

$$n\lambda=2d \sin \theta \quad \text{(Equation 5.1)}$$

where  $n$  = order of reflection  
 $\lambda$  = wavelength of incident radiation  
 $d$  = interplanar spacing  
 $2\theta$  = diffraction angle

The symmetry of the lattice is obtained by fitting the observed spacings to a proposed structure. The patterns may be so distinctive as to allow the assignment of phase structure from the visual inspection of the X-ray diffraction pattern alone. The number and intensities of reflections depend upon the material, the structural order present, and the composition (i.e. multi-component systems). If the number of observed reflections is small,

which is generally the case, it may not be possible to categorise phases according to their one-, two- or three-dimensional order. Here, complementary information obtained from optical microscopy<sup>263-267</sup>, NMR<sup>286</sup>, etc, is required to determine a phase structure.

Having assigned a structure, either from the X-ray patterns alone, or from a combination of techniques, the positions of the reflections can then be used to calculate the structural dimensions of the phase. Alternative methods of calculating the dimensions for each of the more common mesophases appear in the literature<sup>24,142,149,166</sup>. By considering the proposed structure and the composition of the phase—this requires some estimation of the volume fractions of polar and non-polar moieties present; see section 5.4.3.4—these methods use the derived interaggregate distances to calculate the structural parameters involved. With phases of two- and three-dimensional periodicity (i.e. hexagonal and cubic, respectively) these calculated values will be dependent on this approximation. With a phase of one-dimensional periodicity (i.e. lamellar) the surface area per molecule will be independent of this approximation. With a knowledge of composition and the chemical structures involved, these calculated parameters can be used to indicate the validity of the proposed structure.

### 5.4.3 Assignment of Structure and Calculation of Lattice Parameters

#### 5.4.3.1 Phases with One-dimensional Periodicity

Here, we are concerned with the lamellar phase. This phase is thought to be composed of alternating extended polar and non-polar layers (see figure 1.3). The polar layers are made up of the polar moieties of the amphiphile plus any polar solvent present. The non-polar layers are made up of the non-polar moieties of the amphiphile plus any non-polar solvent present.

Lamellar phases usually exhibit a series of sharp reflections in the small-angle region with d-values in the ratio of 1:1/2:1/3:1/4. The intensity of the higher order reflections fall off rapidly and with solvent present, often it is only the first reflection which may be observed.

For the lamellar phase of an amphiphile/water system, the thickness of the amphiphile bilayer,  $d_a$ , is given by<sup>24,149</sup>:

$$d_a = d_0 \varnothing_a \quad (\text{Equation 5.2})$$

where  $d_0$  = the principle reflection (equal to interplanar distance)

$\varnothing_a$  = the volume fraction of the hydrophobic chains

Similarly, the thickness of the water layer,  $d_w$ , is given by<sup>287</sup>:

$$d_w = (1-C_a)d_0 \quad (\text{Equation 5.3})$$

where  $C_a$  = the weight fraction of the amphiphile plus combined water

The area per molecule at the alkyl chain/water interface ( $S$ ) is given by<sup>24</sup>:

$$S = \frac{2 V_a M \cdot 10^{24}}{d_0 \varnothing_a N} \quad (\text{Equation 5.4})$$

where  $V_a$  = the partial specific volume of the amphiphile ( $\text{cm}^3 \text{g}^{-1}$ )

$M$  = the molecular weight of the amphiphile

$N$  = Avogadros number ( $6.022 \times 10^{23} \text{ mol}^{-1}$ )

Assuming that  $V_a = V_w$  (partial specific volume of water) =  $1.0 \text{ cm}^3 \text{g}^{-1}$  and

$\varnothing_a = C_a$ , a simplified expression for  $S$  is obtained<sup>178,287</sup>:

$$S = \frac{2M \cdot 10^{24}}{d_a N} \quad (\text{Equation 5.5})$$

### 5.4.3.2 Phases with Two-dimensional Periodicity.

The most common phase with two-dimensional periodicity is the hexagonal phase. This phase consists of parallel rod shaped micelles of indefinite length packed in a two-dimensional hexagonal lattice. Other phases with two-dimensional periodicity have been proposed<sup>24</sup>. These phases have square or rectangular lattices, but only the hexagonal type will be considered here.

The hexagonal phase, both normal and reversed hexagonal (see figure 1.2 a and b), exhibit a series of sharp reflections in the small-angle region with d-values in the ratio of  $1 : 1/\sqrt{3} : 1/\sqrt{4} : 1/\sqrt{7}$ . The calculation of structural parameters for the hexagonal phase used here is based upon that derived by Spegt and Skoulios<sup>164,166-168</sup>, for the thermotropic reversed hexagonal phases of anhydrous divalent metal soaps. The lattice parameter, a (i.e. the distance between the centres of the rod micelles), is obtained from the first order reflection,  $d_0$ , by the following equation:

$$a = \frac{2 d_0}{\sqrt{3}} \quad \text{(Equation 5.6)}$$

The number of polar groups per unit length of rod, n, can be calculated from the following expression:

$$n = \frac{\sqrt{3} N a^2 \delta}{2M} \quad \text{(Equation 5.7)}$$

where N = the Avogadro number

a = the lattice parameter, as derived from equation 5.6

$\delta$  = the density of the amphiphile

M = the molecular weight of the amphiphile

The radius,  $r_c$ , of the rod micelle is obtained from the following equation.

$$r_c = \left[ \frac{n \cdot V_{pol}}{N\pi} \right]^{1/2} \quad (\text{Equation 5.8})$$

where  $n$  = the number of polar groups per unit length of rod, as derived from equation 5.7

$V_{pol}$  = the molar volume of the polar group

The interfacial area per polar group,  $S$ , can now be obtained from the expression:

$$S = \frac{2\pi r_c}{n} \quad (\text{Equation 5.9})$$

where  $r_c$  is defined as in equation 5.8

$n$  is defined as in equation 5.7.

#### 5.4.3.3 Phases with Three-dimensional Periodicity.

Various structures with three-dimensional periodicity have been proposed<sup>13,25,26,288-293</sup>. The most common appear to be the body centred cubic structures<sup>26,167,171,294</sup>. These, and other more complex structures, have been reviewed by Fontell<sup>149</sup>, and as they were not encountered during this work will not be discussed further here.

#### 5.4.3.4 Estimates of the Volumes of Polar and Non-polar Moieties.

Applying the appropriate calculation, the interfacial area per polar group thus can be calculated from the principle reflection of the X-ray pattern and a knowledge of the chemical structure of the amphiphile itself. Using data for the temperature dependence of the density of a linear poly(dimethylsiloxane) ( $M_n=1220$  and  $M_w/M_n=1.01$ ), and literature values for

sodium stearate, and the CH<sub>2</sub> and CH<sub>3</sub> moieties, estimates of the volumes of these groups at a number of temperatures were calculated<sup>301,315,316</sup>. Table 5.1 lists these values, which have been used to estimate the densities of the amphiphiles for which structural parameters have been calculated in chapters 6 and 7. Subsequently, these values have been employed in the calculation of the surface areas per polar group.

TEMPERATURE (°C)	VOLUME (Å <sup>3</sup> )			
	CH <sub>2</sub>	CH <sub>3</sub>	D unit	NaCO <sub>2</sub>
25	27	54	130	20
50	27	58	134	21
100	28	66	141	25
200	29	82	157	29
230	30	86	163	33
300	32	97	182	48

Table 5.1 Estimated volumes for the CH<sub>2</sub>, CH<sub>3</sub>, dimethylsiloxane and sodium carboxylate groups at a range of temperatures.

#### 5.4.4 Experimental

X-ray diffraction experiments were carried out using a Kratky camera (manufactured by Anton Paar KG, Graz, Austria) equipped with a slit collimator system. The camera length was 203mm, the divergence slit was 200µm and the receiving slit 300µm.

Samples were sealed in quartz capillary cells. Room temperature measurements were carried out at 25°C. Elevated temperatures were attained by electrically heating the sample holder using an Anton Paar K-HR temperature control unit with a operating range of 25-300°C ± 1.5°C.

Samples were allowed to equilibrate for 20 minutes at each temperature before data collection was started.

Copper  $K_{\alpha}$  irradiation ( $\lambda = 1.5418 \text{ \AA}$ ), supplied by a copper target tube equipped with beryllium windows operating at 50 KV and 40 mA and powered by a Phillips PW 1730 generator, was used to irradiate samples. Cooling of the X-ray tube was achieved with a constant flow of cold water. A monochromatic X-ray beam was obtained by means of a focusing quartz crystal monochromator.

The scattered radiation was detected by a proportional counter whose output was fed into a scaling circuit via a pulse height discriminator. The scattering curve (i.e. scattering intensity versus scattering angle) was scanned step-wise with a sequential mode of data collection. The collected data was smoothed, de-smearred and fitted using computer methods to yield the Bragg spacings and peak intensities, which were then used to verify proposed structures and to calculate lattice parameters, as previously outlined.

## CHAPTER 6 PHASE BEHAVIOUR OF THE CYCLIC AMPHIPHILIC SILOXANES

### 6.1 Introduction

The amphiphilic cyclic siloxanes consisted of a cyclic methylsiloxane oligomer (tetramer and pentamer), to which an eleven-carbon alkyl chain was attached at each of the silicon atoms of the siloxane ring. The terminal carbon atom of each alkyl chain constituted part of a carboxyl moiety. The sodium, and in the case of the tetramer, the calcium salts of these carboxylated cyclic siloxanes were prepared. The structures of these molecules are shown below:

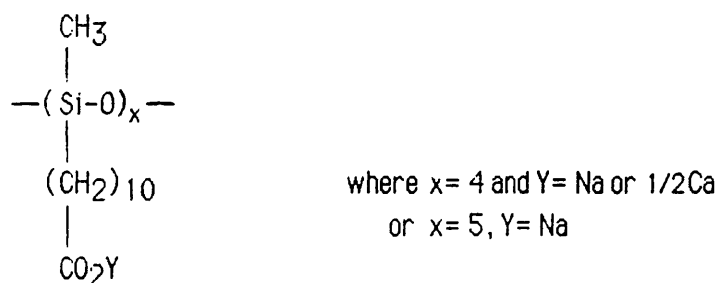


Figure 6.1 Cyclic amphiphilic siloxanes

Although there are examples in the patent literature regarding the use of cyclic amphiphilic siloxanes as surfactants<sup>295</sup>, no systematic investigation of their phase behaviour has been reported. Hence, having synthesised a number of novel molecules, the main priority was to gain an overview of their lyotropic and thermotropic behaviour and thus, to investigate the effects of incorporating anionic amphiphiles onto an oligomeric cyclic siloxane backbone. This overview was obtained with a combination of techniques, as described in chapter 5. The thermotropic behaviour of neat materials was investigated using polarising optical microscopy, DSC and

X-ray diffraction. The lyotropic behaviour of amphiphile/solvent systems was studied using polarising optical microscopy in combination with the penetration technique of Lawrence<sup>219</sup>.

As we have seen in chapter 2, the lyotropic phase behaviour of linear amphiphilic side-chain polymers is very much dependent on the chemical nature and the structure of both the amphiphile itself, and the repeat unit of the polymer backbone. The differences in the lyotropic phase behaviour of these amphiphilic polymers and the equivalent monomeric amphiphiles, has been explained in terms of<sup>68-72,215</sup>:

- the relative ability of the polymer to pack into a particular micelle geometry (i.e. changes in the packing constraints and the possible restriction of the packing of side-chains due to the nature of the backbone itself)
- the subsequent stability of these micelles (i.e. the kinetics of the formation/breakdown of micelles formed by multi-molecular units)
- changes in the hydrophilic and lipophilic balance of the amphiphile repeat unit due to polymerisation.

The cyclic side-chain amphiphiles studied here, being oligomeric, may represent a 'halfway house' between monomeric amphiphiles and the linear amphiphilic side-chain polymers. The study of these molecules may therefore result in some additional understanding of the effects on lyotropic phase behaviour of:

- polymer fixation of monomeric amphiphiles
- variation in the DP of such side-chain amphiphiles
- the micelle kinetics of multi-molecular units.

Previous studies of the lyotropic phase behaviour of amphiphilic side-chain polymers have indicated that the flexibility of a linear siloxane backbone is such that the influence on the translational or rotational motions of side-chains attached to it, is not sufficient to alter the shape of the micelle structures that are characteristic of the parent monomeric amphiphile<sup>66,67</sup>. As such, the attachment of amphiphiles to every unit of a linear siloxane backbone is thought to have an effect similar to a lengthening of the hydrophobic chain of the parent amphiphile by around 3-4 methylene units<sup>66,67</sup>. As the oligomeric cyclic siloxanes are more rigid than their linear counterparts<sup>296</sup>, it was of interest to see if the same would be true for the lyotropic behaviour of the cyclic amphiphilic side-chain oligomers.

As the literature concentrates on the lyotropic behaviour of amphiphilic polymers, it was the intention of this study to also gain an overview of the thermotropic behaviour of the cyclic amphiphilic side-chain oligomers. As no previous investigations of the thermotropic behaviour of similar molecules have been carried out, the rationalisation of the observed behaviour of these cyclic systems was not straight-forward. In attempting to understand and to explain their behaviour, comparisons were sought with the behaviour of conventional monomeric soaps<sup>16,142,144,151,166,170,171,177,185,297-303</sup>; considering the structures of these cyclic siloxanes (see figure 6.1), this was thought to be a valid initial comparison, particularly so, in view of the study of the lyotropic phase behaviour of linear amphiphilic side-chain siloxanes referred to above<sup>66,67</sup>. Also, it was of interest to see what effect the higher rigidity of cyclic siloxane oligomers<sup>296</sup> would have on the thermotropic phase behaviour of the cyclic amphiphilic siloxanes.

In summary, the intention was to gain an overview of the thermotropic and lyotropic phase behaviour of these novel cyclic amphiphilic side-chain oligomers, and contrast this behaviour with that of monomeric amphiphiles and, where appropriate, the linear side-chain amphiphilic polymers.

## 6.2 Thermotropic Phase Behaviour

### 6.2.1 The Sodium Salts

#### 6.2.1.1 Results

##### 6.2.1.1.1 Polarising Optical Microscopy

The microscopy of previously unmelted powdered samples of the sodium salts of the cyclic tetramer and pentamer (figure 6.1;  $Y = \text{Na}$ ,  $x = 4$  and  $5$ ; hereafter referred to as  $\text{NaD}_4$  and  $\text{NaD}_5$ , respectively), was characterised by two main optical events in the temperature range  $0$ - $450^\circ\text{C}$ . These events were:

- the formation of a birefringent fluid phase at  $248^\circ\text{C}$  for  $\text{NaD}_4$  and  $242^\circ\text{C}$  for  $\text{NaD}_5$
- the transition of this fluid phase to the low viscosity isotropic liquid at approximately  $430^\circ\text{C}$ .

The mesophase formed by both  $\text{NaD}_4$  and  $\text{NaD}_5$  exhibited a bright non-geometric texture and a viscosity, which were indicative of a hexagonal mesophase (see figure 6.2)<sup>16</sup>.

At about  $280^\circ\text{C}$ , there was a slight 'darkening' of the edge of the samples, which was believed to indicate the onset of thermal degradation of the material in contact with the atmosphere and, by the transition to the low viscosity isotropic liquid at approximately  $430^\circ\text{C}$ , considerable degradation had occurred.

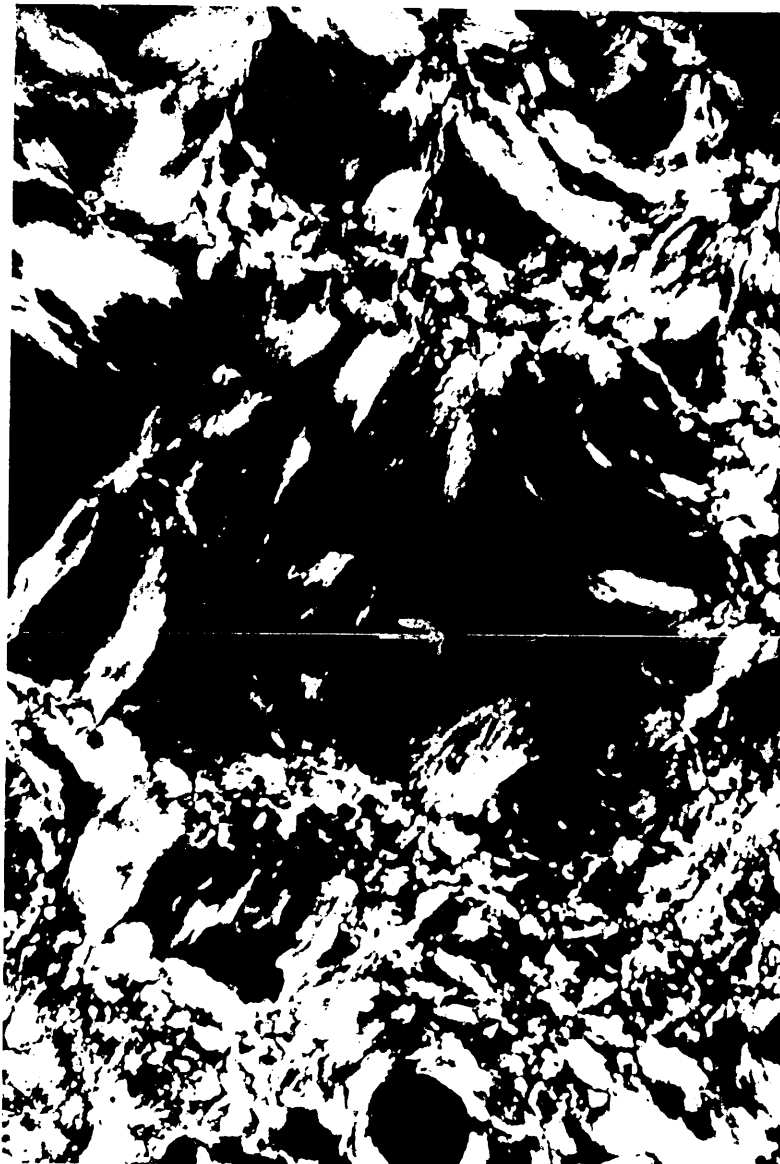


Figure 6.2 Optical texture of the fluid birefringent phase of  $\text{NaD}_4$  at  $274^\circ\text{C}$ .

Thin sample films of  $\text{NaD}_4$  and  $\text{NaD}_5$  were then prepared by placing powdered samples between a cover-slip and a microscope slide at  $270^\circ\text{C}$ , depressing the cover-slip and then, in order to minimise thermal degradation, rapidly cooling to room temperature. Microscopy of these films indicated a birefringent solid phase at room temperature. This phase exhibited a texture similar to that of the mesophase from which it had been prepared (see figure 6.2). As the temperature was increased, the depression of the cover-slip indicated a very slight softening of the samples at  $145^\circ\text{C}$  and  $142.5^\circ\text{C}$  for  $\text{NaD}_4$  and  $\text{NaD}_5$ , respectively. This softening was not accompanied by an obvious change in optical texture. As the temperature was gradually increased, a significant reduction in viscosity occurred at  $250^\circ\text{C}$  for  $\text{NaD}_4$  and  $245^\circ\text{C}$  for  $\text{NaD}_5$ , with the formation of the birefringent fluid phase described above. Again, this phase was stable up to temperatures that were concomitant with a degree of thermal degradation.

#### 6.2.1.1.2 Differential Scanning Calorimetry (DSC)

Thermograms were initially recorded on heating previously unmelted samples of  $\text{NaD}_4$  and  $\text{NaD}_5$  between  $-170^\circ\text{C}$  and  $450^\circ\text{C}$ . These thermograms were characterised by three first order endothermic transitions (hereafter denoted T1, T2 and T3 in order of increasing temperature). There was also a large exothermic transition occurring at about  $420^\circ\text{C}$ , which was thought to correspond to the onset of severe thermal degradation of the sample. No peak was observed corresponding to the optical observation of the transition to the isotropic liquid at approximately  $430^\circ\text{C}$ . Figure 6.3 shows typical thermograms for previously unmelted samples of  $\text{NaD}_4$  and  $\text{NaD}_5$  (dried over  $\text{P}_2\text{O}_5$  at  $100^\circ\text{C}$  for 24 hours) and table 6.1 summarises the results of these analysis.

TRANSITION	TRANSITION TEMPERATURE (°C) AND ENTHALPY (KJ.mol <sup>-1</sup> )			
	NaD <sub>4</sub>		NaD <sub>5</sub>	
	°C	KJ.mol <sup>-1</sup>	°C	KJ.mol <sup>-1</sup>
T1	62	20	44	19
T2	147	7	144	10
T3	258	26	245	22

Table 6.1 The transition temperatures and corresponding enthalpy changes, observed during the initial heating of samples of NaD<sub>4</sub> and NaD<sub>5</sub> from -170 to 450°C, at a heating rate of 10°C.min<sup>-1</sup>.

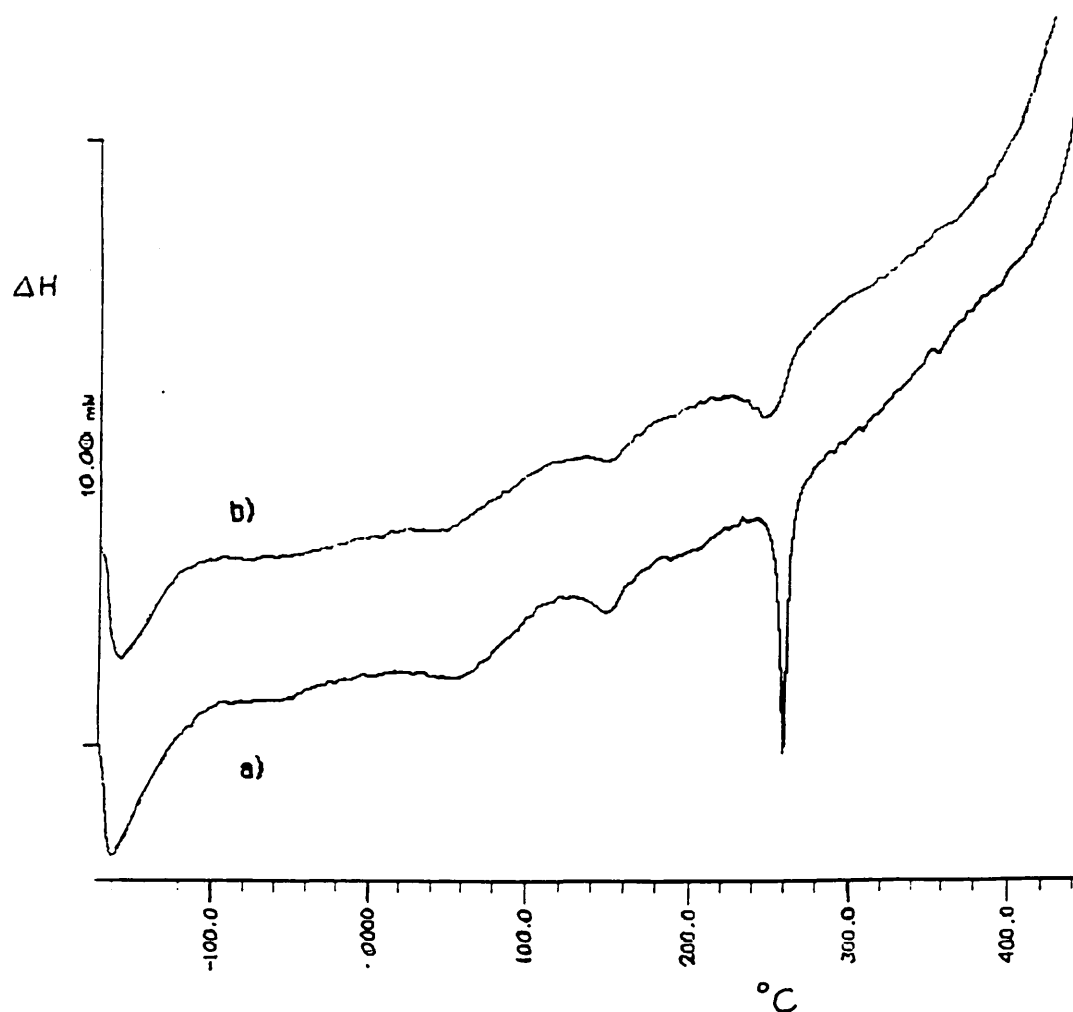


Figure 6.3 Thermograms for previously unmelted samples of a) NaD<sub>4</sub> and b) NaD<sub>5</sub> which have been dried over P<sub>2</sub>O<sub>5</sub> at 100 °C for 24 hours, and heated from -170 to 450°C at a rate of 10°C.min<sup>-1</sup>

In order to assess the effects of heating and cooling, repeated analysis of previously unmelted samples of NaD<sub>4</sub> and NaD<sub>5</sub> were then carried out between -50 and 320°C, at a heating rate of 10°C.min<sup>-1</sup>; 320°C was chosen as the upper temperature limit in an attempt to limit the degree of thermal degradation occurring with repeated heating. As previously outlined, the initial thermogram of both NaD<sub>4</sub> and NaD<sub>5</sub> was characterised by three endothermic transitions over this temperature range. The thermograms obtained during the subsequent reheating of these samples over the same range and the identical heating rate, were characterised by only one endothermic transition (see figure 6.4). The temperature of this transition gradually increased to a maximum after several heating cycles. As the temperature and enthalpy of this transition corresponded closely to that of the T3 transitions previously outlined, and as optical microscopy had demonstrated the reversibility of the solid to mesophase transition, this transition was therefore assigned the reference T3'; thus, reflecting the possible connection with the T3 transition obtained on initial heating. Table 6.2 records the transition temperatures and corresponding enthalpy changes, observed during the repeated heating of NaD<sub>4</sub> and NaD<sub>5</sub>.

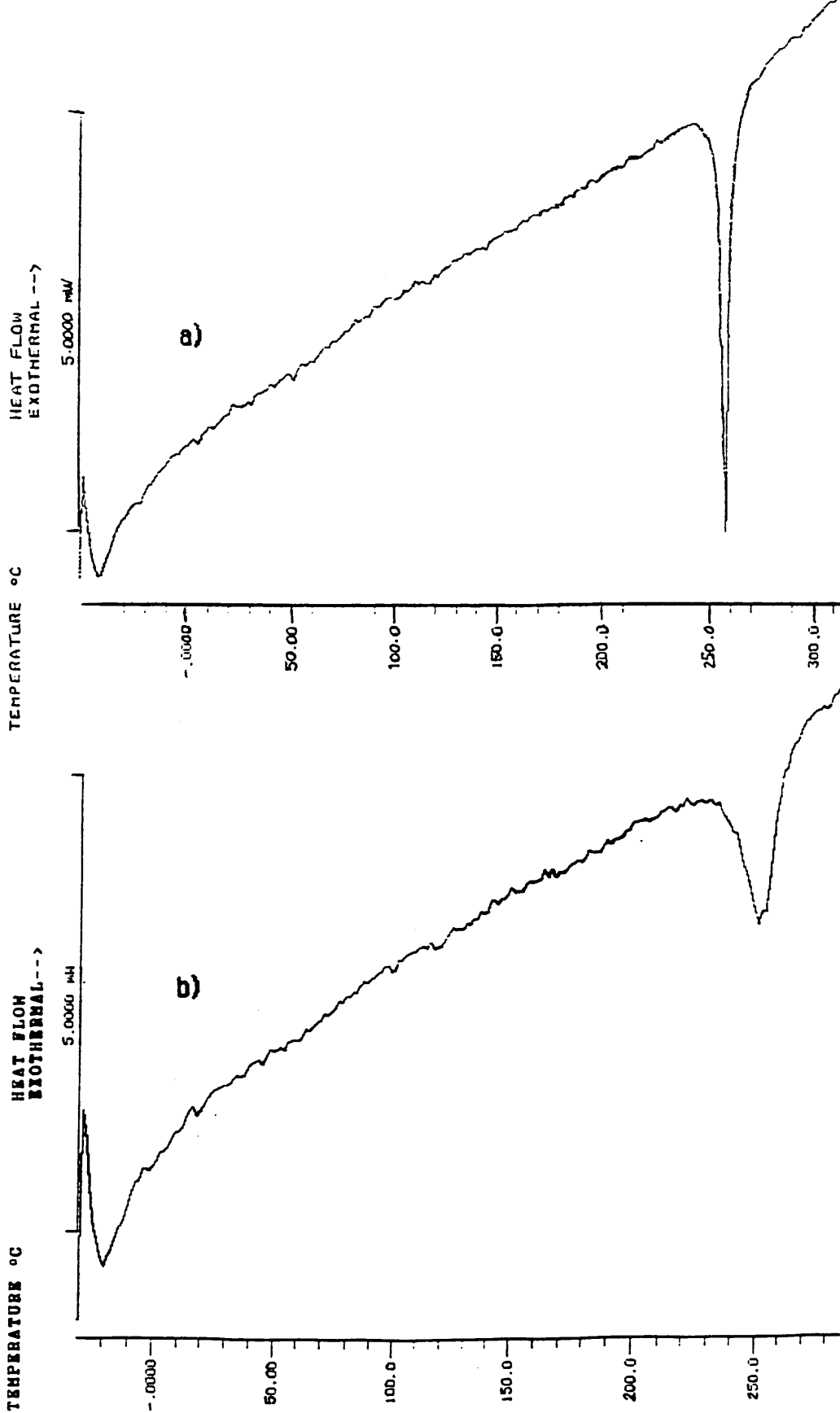


Figure 6.4 Thermograms obtained on the reheating of samples of a) NaD<sub>4</sub> and b) NaD<sub>5</sub> from -50 to 320°C at a rate of 10°C.min.<sup>-1</sup>

TRANSITION	TEMPERATURE (°C) AND ENTHALPY CHANGE (KJ.MOLE <sup>-1</sup> )					
	RUN N°					
	1	2	3	4	5	6
T1	62(20)	←----- none observed -----→				
T2	147(7)	←----- none observed -----→				
T3 or T3'	258(26)	259(28)	262(25)	262(22)	262(25)	263(24)

a) NaD<sub>4</sub>

TRANSITION	RUN N°				
	1	2	3	4	5
T1	50(14)	←----- none observed -----→			
T2	145(9)	←----- none observed -----→			
T3 or T3'	242(21)	251(26)	252(24)	252(20)	252(19)

b) NaD<sub>5</sub>

Table 6.2 The transition temperatures and the corresponding enthalpy changes (in parentheses) occurring during repeated thermal analysis from -50 to 320°C for samples of a) NaD<sub>4</sub> and b) NaD<sub>5</sub>.

Following these analyses, the sample vials were reweighed. A reduction in the mass of the samples of 2-3% had occurred over the course of the heating cycles. These samples were then retained in atmospheric conditions, for subsequent re-evaluation. After two months storage, the thermograms recorded on the reheating of these samples between 30 and 300°C, again exhibited only one exothermic transition. The temperature and enthalpy of this transition corresponded closely to that of the final T3' transitions outlined above. Figure 6.5 shows the thermograms obtained for NaD<sub>4</sub> and NaD<sub>5</sub>, whilst table 6.3 summarises the results of these analyses.

TRANSITION	TRANSITION TEMPERATURE (°C)/ENTHALPY (KJ.mol <sup>-1</sup> )	
	NaD <sub>4</sub>	NaD <sub>5</sub>
T3'	262(22)	252(20.5)

Table 6.3 The transition temperatures and enthalpy changes (in parentheses) observed during the reheating of NaD<sub>4</sub> and NaD<sub>5</sub> from 30 to 300°C, at a heating rate of 10°C.min<sup>-1</sup>. These samples had been stored for two months following the initial heating outlined in table 6.2.

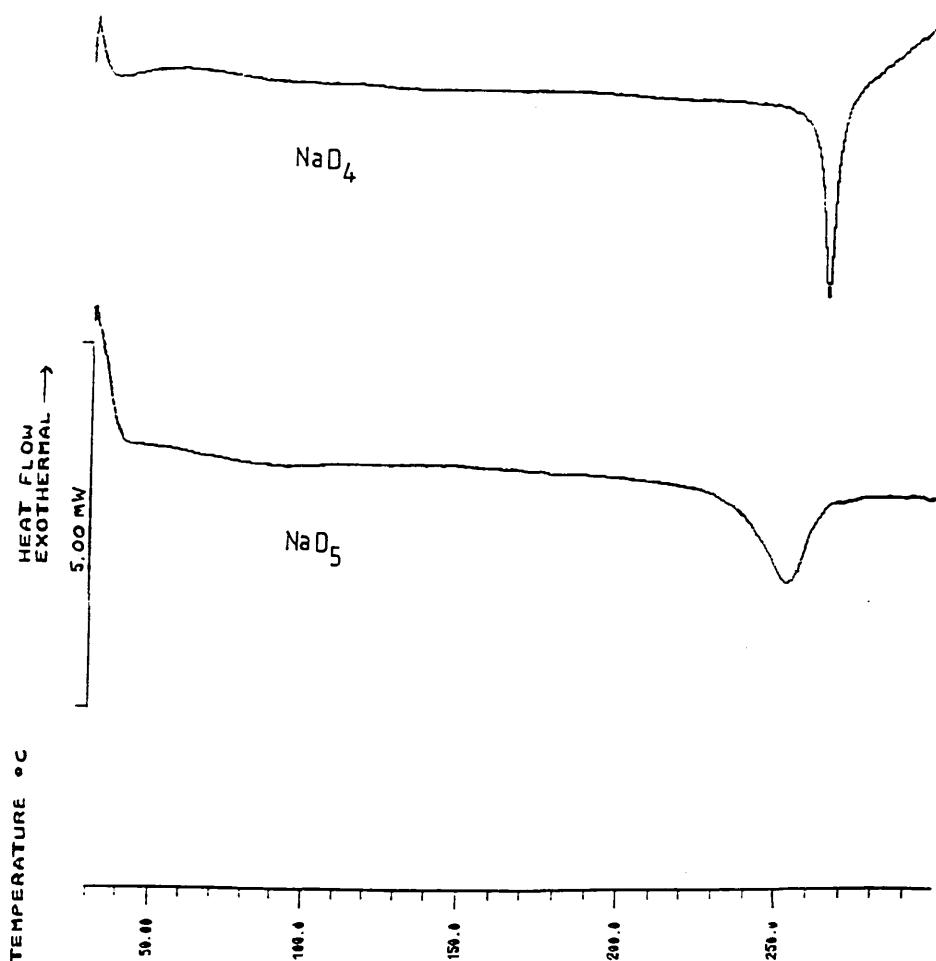


Figure 6.5 Thermograms obtained on heating NaD<sub>4</sub> and NaD<sub>5</sub> from 30 to 300°C at a rate of 10°C.min<sup>-1</sup>, after storing the sample for two months subsequent to the initial heating analysis.

Thermograms were subsequently recorded on cooling fresh samples of  $\text{NaD}_4$  and  $\text{NaD}_5$  from 320 to 0°C at a rate of  $2^\circ\text{C}\cdot\text{min}^{-1}$  (see figure 6.6). In both cases, the thermograms were characterised by one first order exothermic transition. Although the temperature of this transition was not determined instrumentally, visual inspection of the thermograms indicated that the transition temperature was similar to that of the T3 transition occurring in both  $\text{NaD}_4$  and  $\text{NaD}_5$  during the initial heating analysis. The transition occurring during the cooling cycle has therefore been assigned the reference  $\text{T3}_c$ ; thus, reflecting the possible connection with the T3 transition observed during the initial heating.

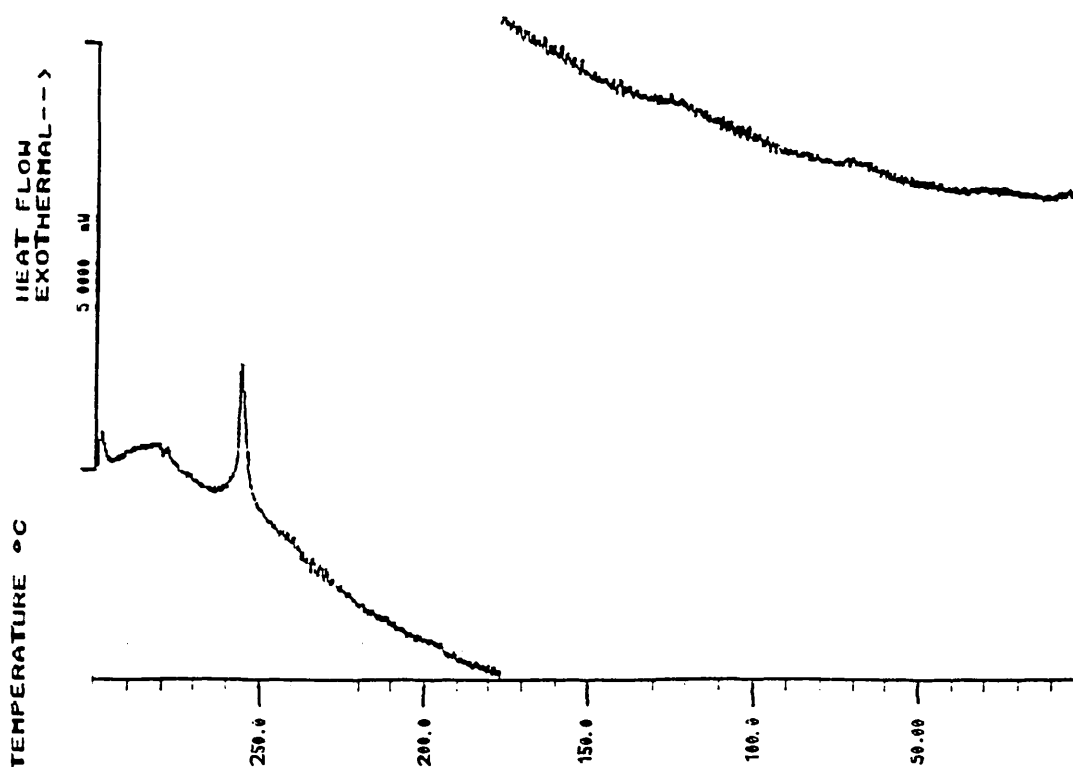


Figure 6.6 Thermogram obtained on the cooling a sample of  $\text{NaD}_4$  from 300 to 0°C at a rate of  $2^\circ\text{C}\cdot\text{min}^{-1}$

These cooling runs were followed by an immediate reheating from 0 to 320°C (see figure 6.7). These thermograms exhibited one endothermic transition. Again, visual inspection of the thermograms indicated that the transition temperature corresponded closely to that of the final T3' transition outlined above.

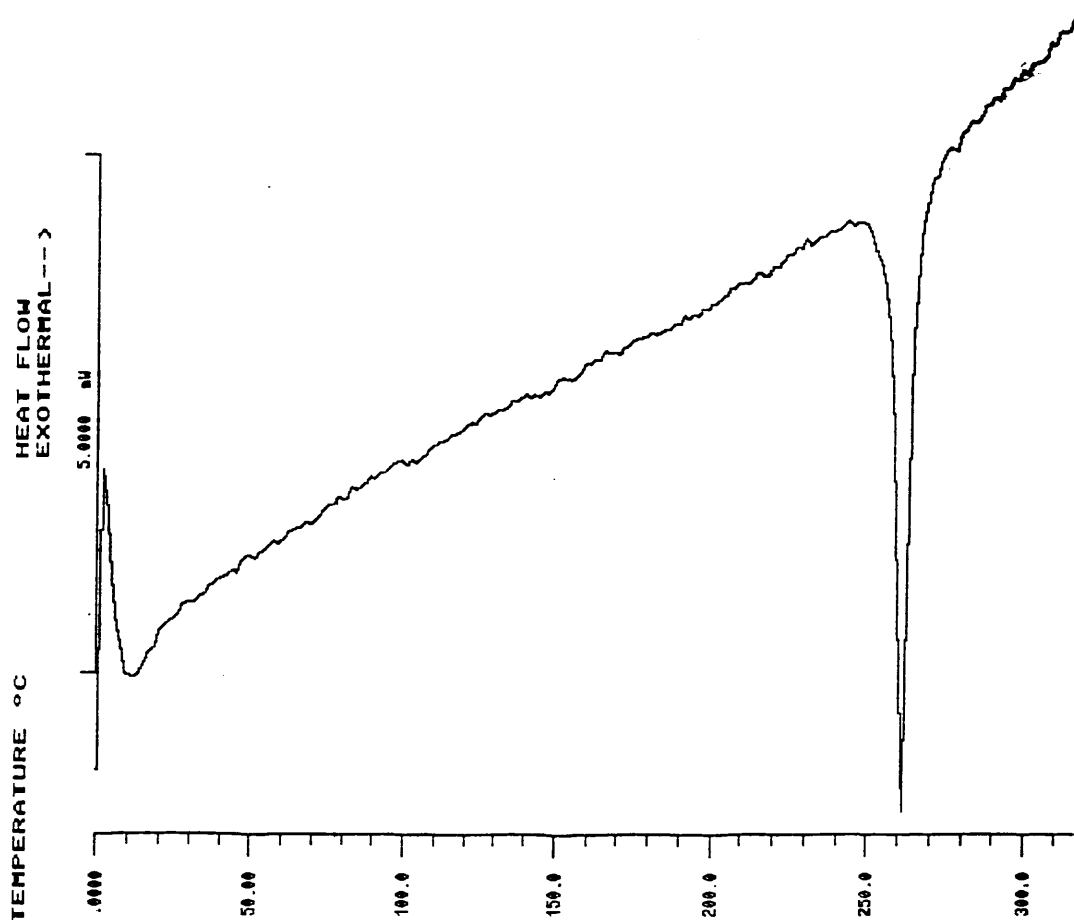


Figure 6.7 Thermogram obtained on reheating a sample of  $\text{NaD}_4$  from 0 to 320°C at a rate of  $10^\circ\text{C}\cdot\text{min}^{-1}$ , immediately following a controlled cooling cycle (rate of cooling  $2^\circ\text{C}\cdot\text{min}^{-1}$ )

### 6.2.1.1.3 Thermo-Gravimetric Analysis (TG)

A thermogram was recorded on the heating of a previously unmelted sample of  $\text{NaD}_4$  between  $35^\circ\text{C}$  and  $420^\circ\text{C}$ . This thermogram exhibited no significant weight loss up to about  $280^\circ\text{C}$ , at which point there was a gradual and increasing loss in weight, up to the termination of the evaluation at  $420^\circ\text{C}$ . This loss in weight was believed to reflect the thermal degradation of the sample. Figure 6.8 shows a thermogram obtained for a sample of  $\text{NaD}_4$  which had been dried over  $\text{P}_2\text{O}_5$  at  $100^\circ\text{C}$  for 24 hours.

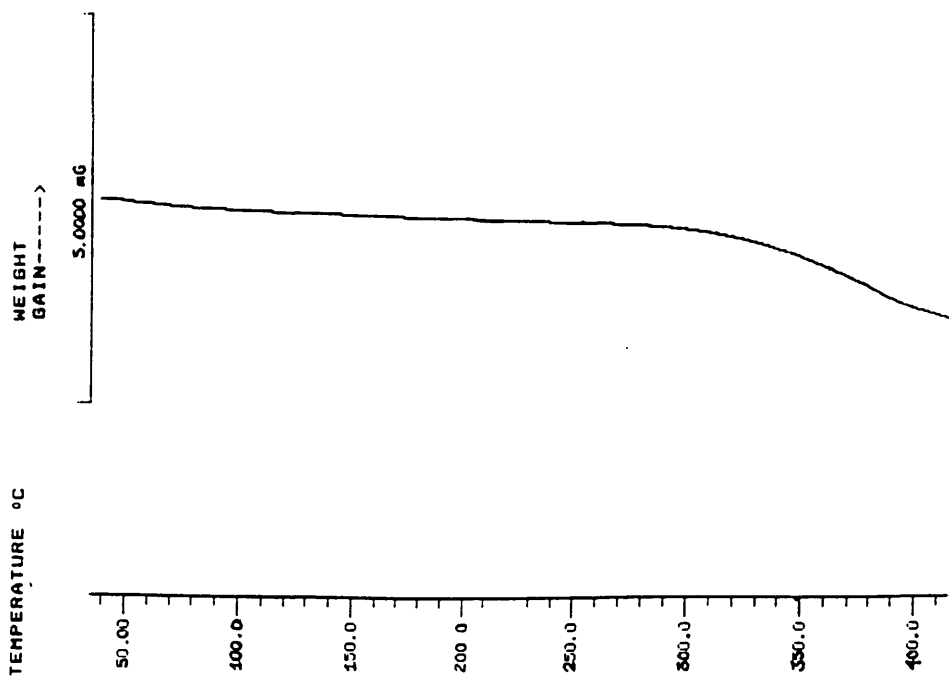


Figure 6.8 TG thermogram obtained on heating a sample of  $\text{NaD}_4$  from  $35$  to  $420^\circ\text{C}$  at a heating rate of  $10^\circ\text{C}\cdot\text{min}^{-1}$ .

### 6.2.1.1.4 X-Ray Diffraction

Diffraction patterns were obtained for a sample of  $\text{NaD}_4$  in the low-angle region at various temperatures. Figure 6.9 shows the diffraction patterns obtained and table 6.4 summarises the spacings observed.

SIGNAL	SPACING (Å) OF PEAKS OBSERVED AT VARIOUS TEMPERATURE		
	50°C	200°C	300°C
$d_0$	30.0	28.8	28.2
$d_1$	14.4	14.4	24.7
$d_2$	none	none	17.3
$d_3$	none	none	14.1

Table 6.4 The spacings observed in the X-ray diffraction pattern for  $\text{NaD}_4$  at 50, 200 and 300°C.

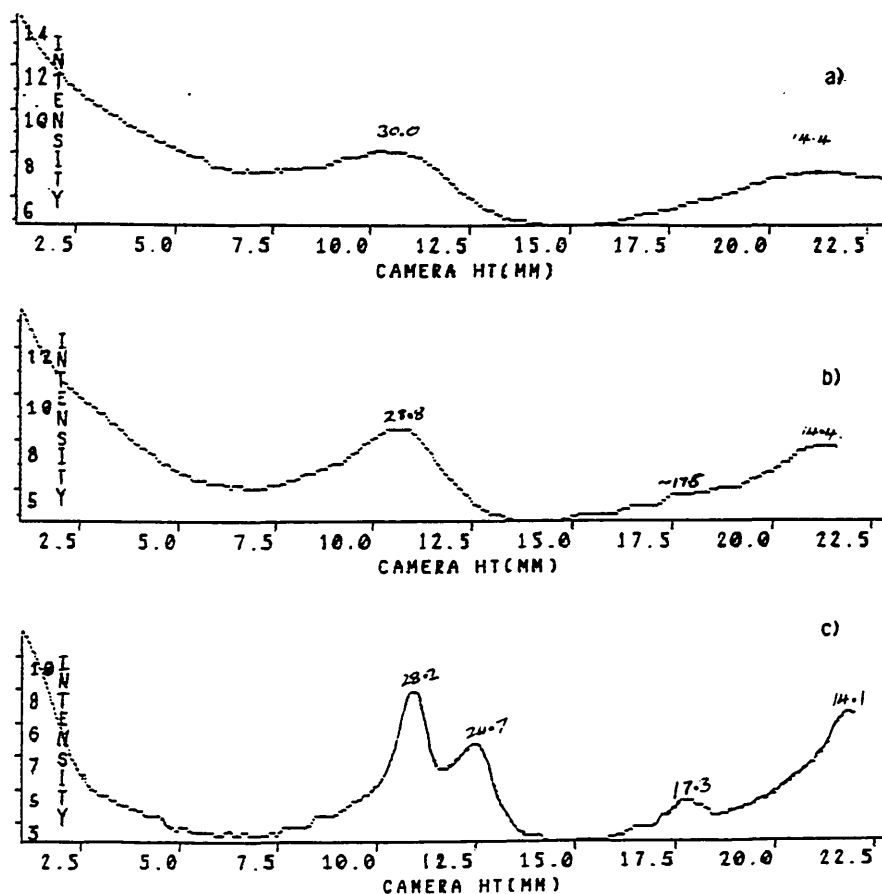


Figure 6.9 X-ray patterns for  $\text{NaD}_4$  at a) 50°C, b) 200°C and c) 300°C.

At 50 and 200°C, the peaks observed were very broad with only the principle and the second order reflections identifiable (see table 6.4). The positions of these two reflections were, within experimental error, in the ratio of 1:1/2.

At 300°C, the peaks observed were less broad and it was possible to distinguish four reflections at 28.2, 24.7, 17.3 and 14.1Å. The indexing of these reflections was not straight-forward and will be discussed in further detail later.

#### 6.2.1.2 Discussion

Optical microscopy of films of NaD<sub>4</sub> and NaD<sub>5</sub> indicated that these materials existed as ordered solids at room temperature. The non-geometric texture of these birefringent films was indicative of a hexagonal phase<sup>16</sup>. At approximately 145°C a very slight—almost imperceptible—softening of this crystalline solid was observed. This softening was not accompanied by a change in optical texture. On further heating, a birefringent fluid phase formed at about 250°C. The non-geometric texture and the viscosity of this phase were indicative of a hexagonal phase (see figure 6.2). This phase was stable up to the transition to the isotropic liquid at about 430°C. It was not possible to be precise about the temperature of this transition due to the thermal degradation also occurring.

The transitions observed during the DSC analysis of previously unmelted samples of NaD<sub>4</sub> and NaD<sub>5</sub> were in general agreement with the observations from the optical study. Of the three endothermic transitions in the range -170 to 450°C, the temperature of the T2 and T3 transitions corresponded to the observations under the microscope of the initial softening of the

crystalline solid, and the transition to the birefringent fluid phase, respectively; the T2 transition occurring at 147°C for NaD<sub>4</sub> and 144°C for NaD<sub>5</sub>, corresponded to the initial softening of the respective crystalline solids at 145 and 142°C, and the T3 transition occurring at 258°C for NaD<sub>4</sub> and 245°C for NaD<sub>5</sub>, corresponded to the transition to the fluid birefringent phase at 250 and 245°C for NaD<sub>4</sub> and NaD<sub>5</sub>, respectively. There were, however, some apparent discrepancies between the observations resulting from these two techniques. The T1 transition occurring at about 60°C during the initial DSC analysis, had no corresponding transition when viewed under the microscope. This presumably indicated that this transition was not associated with a significant change in the overall structural arrangement within the sample. In addition, the optical observation of the transition from the mesophase to the isotropic liquid, had no corresponding identifiable thermal transition during DSC analysis. This presumably indicated that only a small enthalpy change was involved in this transition. The magnitude of this enthalpy change may, in turn, indicate that the order inherent to the crystalline solid has been essentially lost, prior to the formation of the isotropic liquid. This would be consistent with the birefringent fluid phase being a fused mesophase<sup>151</sup>. The nature of all these transitions will be discussed in greater detail later.

The absence of an identifiable thermal event in the range -170°C up to T1, indicates that no thermal induced transitions are taking place in this range. However, it should be remembered that whilst the the presence of a peak in the DSC curve denotes a transition, the converse is not necessarily true.

As the transition from the mesophase to the isotropic liquid occurred at a temperature at which considerable thermal degradation of the samples had taken place, all subsequent DSC investigations of the effects of repeatedly heating and cooling were carried out on samples that had not been heated to greater than 320°C (i.e. the samples were not heated above the mesophase to isotropic liquid transition). It is worth noting that the first evidence of degradation of the samples during the DSC occurred with the exothermic peak at about 420°C, whilst microscopy and TG indicated the onset of degradation to be approximately 280°C (i.e. the observations of a slight browning of the sample and a loss in weight of the sample, respectively). These differences in the apparent onset of thermal degradation, presumably arose as a result of the relative sensitivity of the techniques themselves to the degradation occurring, and not as a result of any differences in the thermal stability of the individual samples used.

Whilst the thermograms obtained on the initial heating of NaD<sub>4</sub> and NaD<sub>5</sub> from -170 to 320°C were characterised by three endothermic transitions (i.e. T<sub>1</sub>, T<sub>2</sub> and T<sub>3</sub>), the reheating of these samples over the same temperature range, either within minutes of the initial heating analysis, or after two months storage, gave only one endothermal transition (T<sub>3</sub>'). The cooling of samples from 300 to 0°C at a rate of 2°C.min<sup>-1</sup>, gave one exothermal transition (T<sub>3c</sub>). As the temperature of the T<sub>3</sub>, T<sub>3</sub>' and T<sub>3c</sub> transitions were similar, and optical microscopy had demonstrated the reversibility of the solid to mesophase transition, it seems reasonable to suggest that all these thermal events correspond to the same solid/mesophase transition. As no instrumental analysis of the transition temperature of T<sub>3c</sub> was carried out, it is not possible to judge if any supercooling of mesophase to solid transition occurred.

The absence of the T1 and T2 transitions from all thermograms, other than those recorded on the initial heating of the samples, may indicate that:

- these transitions were due to one or more impurities that were volatilised from, or dissolved in, the matrix during heating to 320°C, and/or
- the structural aspect(s) responsible for T1 and/or T2 on initial heating, had not reformed on cooling.

Considering the spectroscopic characterisation and the TG analysis of NaD<sub>4</sub> and NaD<sub>5</sub> (see chapter 4 and section 6.2.1.1.3), the suggestion of impurities as an explanation for the absence of the T1 and T2 transitions during repeated heating analysis seems unlikely. It is, therefore, proposed that the structural aspect(s) responsible for these transitions during the initial heating, had not reformed on cooling. This may be explained by:

- an annealing of the samples during heating, and thus the formation of an alternative equilibrium structure on cooling, or
- the formation of a non-equilibrium structure as a result of a quenching of the samples during the 'rapid' cooling that followed the heating analysis (i.e. the structural features responsible for these transitions were not allowed to reform during cooling).

This latter effect has been reported in other amphiphiles, in which some structural aspects of a high temperature phase have been retained at lower temperatures due to super-cooling<sup>153,304,305</sup>.

Having used thermal analysis and optical microscopy of NaD<sub>4</sub> and NaD<sub>5</sub> to establish the temperature 'boundaries' of individual phases and to supply some initial indication of the structures present within these boundaries, X-ray diffraction data for a sample of NaD<sub>4</sub> was used as corroborative evidence, and to calculate some structural parameters<sup>149</sup>. As the similar

behaviour of NaD<sub>4</sub> and NaD<sub>5</sub> had been demonstrated, and both molecules being adjacent members of a homologous series of compounds, the general conclusions derived from X-ray analysis of NaD<sub>4</sub>, will be applied to NaD<sub>5</sub> during the following discussions.

At 50 and 200°C, the low-angle X-ray diffraction pattern of NaD<sub>4</sub> exhibited two broad peaks, corresponding to the principle and the second order reflections respectively (see table 6.4). At both temperatures, the positions of these reflections were, within experimental error, in the ratio of 1:1/2. A number of structures have been proposed for birefringent phases whose principle and second order reflections are in this ratio<sup>24,149</sup>. These include the crystalline and mesomorphic lamellar and the tetragonal phases (i.e. the C and K phases, presumed to be two dimensional tetragonal arrangements of normal and reversed rod micelles, respectively). Whilst the lamellar phases have been encountered in many single and multi-component systems and are generally accepted phase structures, the tetragonal phases have been observed only in lyotropic systems and over very narrow composition ranges<sup>267,306,307</sup>, and remain to be established. It has also been pointed out that the structure of the tetragonal phase would imply the presence of a X-ray reflection corresponding to the diagonal of the square lattice, but this has not been observed<sup>308,309</sup>. In addition, recent studies of the compositions where these phases were thought to exist, have reinterpreted the observed behaviour in terms of well established phase structures<sup>16,310-314</sup>. The existence of the tetragonal phase therefore remains to be established and, in the absence of the X-ray reflection corresponding to the diagonal of the square lattice, will not be invoked here. Consequently, the X-ray pattern indicates that NaD<sub>4</sub> exists as a lamellar phase structure at both 50 and 200°C. However, when the number of peaks

in the X-ray pattern is so small, it is not possible to unequivocally propose a structure on the basis of this data alone<sup>149</sup>, and guidance is required from other techniques. Although the X-ray pattern indicated a lamellar structure, the optical texture exhibited by solid films of NaD<sub>4</sub> was more characteristic of a hexagonal phase, the X-ray diffraction pattern of which exhibits principle and second order reflections in the ratio of 1:1/√3<sup>24,149</sup>. Thus, at this stage, the data from X-ray diffraction of powdered samples and optical microscopy of solid films were at odds.

In view of this, the experimental method employed in the optical study was re-examined. To limit the effects of thermal degradation, the solid sample films were prepared by rapidly cooling a film of the high fluid phase from 270°C to room temperature. This 'quenching' of the samples could have frozen the structure and texture of the fluid phase into the solid sample films, i.e. the formation of a non-equilibrium structure. This structure would have been reflected in the subsequent observations under the microscope at all temperatures below the transition to the fluid phase, but not in the X-ray diffraction patterns obtained from a previously unmelted powdered sample. A similar 'quenching' of the cyclic amphiphiles during DSC analysis has already been proposed as a possible explanation for the absence of the T1 and T2 transitions from all thermograms other than those obtained on initial heating<sup>153,304,305</sup>.

Having tentatively proposed a lamellar structure on the basis of diffraction patterns, the interfacial area per amphiphile polar group in such a structure, may be derived<sup>149</sup>. For NaD<sub>4</sub> at 50 and 200°C, the area per polar group that would result for a lamellar phase was calculated to be 28.4 and 34.1 Å<sup>2</sup>, respectively. It should be pointed out that as no density values specific to

NaD<sub>4</sub> exist, the densities of the different polar and non-polar moieties were estimated at each temperature using data from several sources<sup>301,315,316</sup> (see section 5.4). Nevertheless, these derived values should be representative, providing the proposed structure is valid.

As the area per polar group is a measure of the lateral packing density of the head groups, it is reasonable to expect that the value of this parameter will be similar at equivalent temperatures for all straight chain sodium soaps of equivalent phase structures. Thus, the comparison of the area per polar group of monomeric sodium soaps (see table 6.5) and the calculated value for NaD<sub>4</sub>, is of particular interest.

PHASE PRESENT	PARAMETER	VARIATION IN SURFACE AREA PER POLR GROUP (S) WITH TEMPERATURE (t) AND CHAIN LENGHT (C <sub>n</sub> ) FOR A NUMBER OF STRIAGTH CHAIN SODIUM SOAPS			
		C <sub>12</sub>	C <sub>14</sub>	C <sub>16</sub>	C <sub>18</sub>
Waxy	t (°C)	142	142	140	133
	S (Å <sup>2</sup> )	24	23	23	25
Superwaxy	t (°C)	183	182	176	175
	S (Å <sup>2</sup> )	*	*	24	*
Subneat	t (°C)	215	210	211	210
	S (Å <sup>2</sup> )	*	24	24	22
Neat (lamellar)	t (°C)	252	248	254	256
	t <sub>1</sub> (°C)	290	271	278	285
	S (Å <sup>2</sup> )	36	38	40	42

Where t = the transition temperature for the formation of the phase in question (with the exception of the lamellar mesophase, the lattice dimensions within each phase are essentially independent of temperature)

t<sub>1</sub> = the temperature for which the dimensions of the lamellar mesophase are given.

\* = no values given

Table 6.5 The variation of area per polar group for convention straight sodim soaps with temperature (values taken from reference 24).

As table 6.5 shows, although the straight chain sodium soaps exist as a number of different polymorphs with increasing temperature, the surface area per polar group for this homologous series of soaps ( $C_{12}$ - $C_{18}$ ), is relatively constant at about  $23$ - $25\text{\AA}^2$ , in all the crystalline and semi-crystalline phases (i.e. all those phases in which the head groups are not fully fused). Only in the high temperature lamellar mesophase is this not the case, and the surface area becomes temperature dependent.

The value derived for  $\text{NaD}_4$  at  $50^\circ\text{C}$  is, therefore, in reasonable agreement with that of the monomeric soaps at this temperature. Whilst this supports the proposal of the lamellar structure for  $\text{NaD}_4$  at this temperature, the slight increase in the area per polar group indicates that there exists either:

- a less dense packing of the head groups in  $\text{NaD}_4$  than is present in the monomeric straight chain sodium soaps of this structure, or
- some interdigitation of the soap molecules within the bilayers.

As the derived area per polar group is only slightly larger than that of the monomeric soaps this would seem to favour a less dense packing of the molecules within the bilayers, rather than an interdigitated arrangement.

The derived value of  $34.1\text{\AA}^2$  at  $200^\circ\text{C}$ , is significantly larger than that of the monomeric soaps at the equivalent temperature. This indicates a significantly less dense packing of the head groups of  $\text{NaD}_4$  compared to the monomeric soaps. In view of the macroscopic properties of  $\text{NaD}_4$  at this temperature (i.e. semi-crystalline solid) the significant increase in the area per polar group at this higher temperature is surprising; by analogy with the behaviour of monomeric soaps, the surface area per polar group would be expected to be relatively constant in all phases in which the head groups are

not fully fused. Indeed, the similar packing density of the polar groups within this 'solid' phase of NaD<sub>4</sub> and within the high temperature lamellar mesophase of monomeric soaps seems unlikely, and as such, requires further investigation.

Having proposed a lamellar structure, it was of interest to compare the bilayer thickness of such a structure with the molecular dimensions of NaD<sub>4</sub>. In considering the structure of NaD<sub>4</sub>, it should be remembered that the oligomeric cyclic siloxane backbones are much more rigid than their linear counterparts, and are essentially planar in geometry<sup>296</sup>. It therefore seems reasonable to consider the structure of NaD<sub>4</sub> as four C<sub>11</sub> carboxylates, emanating from a central planar siloxane 'disc'. If all head groups have to reside at the non-polar/polar interfaces of the bilayer and there are no voids present, then the maximum bilayer thickness will be dictated by the maximum distance between two polar groups<sup>24,149</sup>. The maximum distance between the centres of two polar groups will be twice the length of an 'all trans' amphiphile chain; one chain representing one C<sub>11</sub> sodium carboxylate plus one methylsiloxane unit (see figure 6.10). Assuming that the Si-C bond approximates to the length of the C-C bond and that the sodium carboxylate head group is about 5Å in length, then twice the length of an 'all trans' chain approximates to 40.5Å<sup>317</sup>.

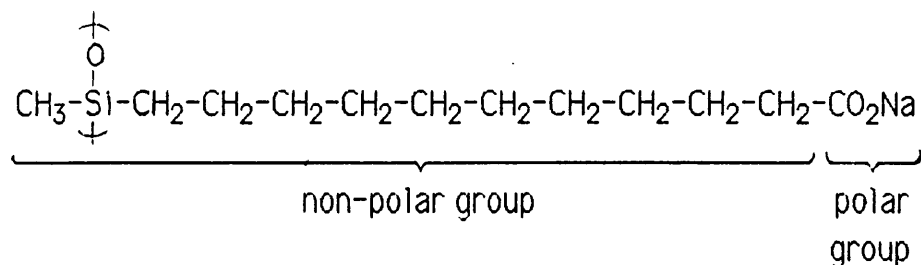


Figure 6.10 Schematic representation of the amphiphilic repeat unit of NaD<sub>4</sub>.

The actual bilayer thickness, given by  $d_0$ , was 30Å at 50°C and 28.8Å at 200°C. Hence, the bilayer thickness was less than the length of two 'all trans' amphiphile units. By analogy with other amphiphiles, this can be explained by a tilting of the chains within the bilayers.

The absence of a DSC transition from T2 (~145°C) up to T3 (~250°C), would indicate that the lamellar structure proposed at 200°C, remains essentially unaltered up to the transition to the birefringent fluid phase. Above this transition, but below the transition to the isotropic liquid, the optical texture of NaD<sub>4</sub> and NaD<sub>5</sub> was indicative of a hexagonal phase (H<sub>2</sub>). As has been seen, the transition corresponding to the formation of the low viscosity isotropic liquid could not be resolved from the exothermal transition arising from the thermal degradation of the sample. This indicated that a relatively small enthalpy change was involved in the transition to the isotropic liquid. Hence, any remnants of crystalline order inherent to the birefringent fluid phase prior to this final melting transition, must have been relatively low. This in turn indicated that the birefringent fluid phase was of the fused type (mesophase)<sup>151</sup>.

The X-ray diffraction pattern of a H<sub>2</sub> mesophase would be expected to exhibit peaks in the ratio of  $1:1/\sqrt{3}:1/\sqrt{4}:1/\sqrt{7}$ <sup>24,149</sup>. However, the X-ray pattern obtained for NaD<sub>4</sub> at 300°C, contained four peaks at 28.2, 24.7, 17.3 and 14.1Å, which cannot be reconciled with a conventional hexagonal structure. It is, however, possible to index all four reflections to a body centred cubic structure, which exhibits low-angle reflections in the ratio  $1/\sqrt{3}:1/\sqrt{4}:1/\sqrt{8}:1/\sqrt{11}$ <sup>316</sup>. Taking the value of  $d_0$  as equal to 28.2Å, and applying the above relationship, the second, third and fourth reflections

would be 24.42, 17.26 and 14.72Å, respectively. Although these values are in approximate agreement with the values obtained experimentally, the body centred cubic phase would be expected to be optically isotropic<sup>318</sup>, which was not the case.

An important parameter in judging the plausibility of a structure proposed on the basis of X-ray diffraction data, is the area per amphiphile polar group that would result in such a structure. The area per polar group that would result from the proposal of a H<sub>2</sub> structure was calculated to be 17.7Å<sup>2</sup> (see section 5.4). The facts that the lateral packing densities of the apparently fused polar groups of NaD<sub>4</sub> and the monomeric soaps are so different at equivalent temperatures (see table 6.5), and that the area per polar group of the lower temperature forms of NaD<sub>4</sub> are substantially larger than 17.7Å<sup>2</sup> (i.e. 28.4 and 34.1Å<sup>2</sup>, at 50 and 200°C, respectively), indicates the implausibility of the H<sub>2</sub> structure. Indeed, a change from the lamellar mesophase formed by monomeric sodium soaps to the H<sub>2</sub> mesophase proposed for NaD<sub>4</sub>, would necessitate a negative change in the surface curvature of the polar/non-polar interface of the micelles that constitute these mesophases. Whilst a methylsiloxane group is a relatively bulky unit (~74Å<sup>3</sup> at 25°C), the attachment of one of these units to the ends of each of the hydrophobic chains—i.e. ten carbon atoms removed from the polar group—would not be expected to result in a such a significant change in the packing of the individual amphiphiles or the surface curvature of the polar/non-polar interface. As NaD<sub>4</sub> and NaD<sub>5</sub> are multi-amphiphile molecules, it is possible that the formation of isotropic spherical micelles may be destabilised due to the finite aggregation number of such structures<sup>67</sup>. However, this effect could not explain the fact that NaD<sub>4</sub> and

NaD<sub>5</sub> do not form the lamellar mesophase which is so typical of conventional straight chain sodium soaps, because the growth of bilayers is unrestricted in two dimensions.

Hence, the identification of an optical texture typical of a H<sub>2</sub> phase may have been misleading. Whilst this texture probably signifies some sort of intermediate phase, it is not possible on the basis of the evidence available here, to propose a structure for the mesophase formed by NaD<sub>4</sub> and NaD<sub>5</sub>. However, the optical study and the X-ray diffraction pattern of NaD<sub>4</sub> have demonstrated that, unlike the monomeric straight chain sodium soaps, NaD<sub>4</sub> does not form a lamellar mesophase immediately preceding the formation of the low viscosity isotropic liquid. No explanation for this behaviour can be offered at this stage.

Having obtained an overview of the thermotropic behaviour of NaD<sub>4</sub> and NaD<sub>5</sub>, we can attempt to explain this behaviour in terms of the established principle of the step-wise melting of mesomorphic materials, and contrast this behaviour with that of the monomeric sodium soaps (see chapter 2). At room temperature, X-ray diffraction indicated that NaD<sub>4</sub> and NaD<sub>5</sub> exist as lamellar crystalline phases similar to that of the monomeric sodium soaps at the equivalent temperature, but with a slightly less compact packing of the individual amphiphiles<sup>24</sup>. X-ray diffraction at 200°C, in combination with DSC data, indicated that although this overall structure remained essentially unchanged from room temperature up to the transition to the mesophase at about 250°C, there was a further reduction in the packing density of these amphiphiles at the higher temperature.

Between room temperature and the transition to the mesophase, two transitions (T1 and T2) occurred during the initial DSC heating of NaD<sub>4</sub> and NaD<sub>5</sub>. The first of these transitions (T1) was a broad endothermic transition (~20KJ.mole<sup>-1</sup>) occurring at about 60°C. In view of the relatively low temperature at which this transition takes place, and by comparison with the melting behaviour of fatty acids and other soaps, it seems reasonable to attribute this primarily to a change occurring in the weakly interacting non-polar regions of these amphiphiles<sup>24,142,151</sup>. In this context, it should be remembered that the non-polar regions of NaD<sub>4</sub> and NaD<sub>5</sub> are made up of C<sub>10</sub> alkyl chains attached to each of the repeat units of the tetrameric and pentameric cyclosiloxane backbones. As the non-substituted cyclic dimethylsiloxane tetramer and pentamer (i.e. D<sub>4</sub> and D<sub>5</sub>) melt at 17 and -40°C, respectively<sup>319</sup>, and the T1 transition for both NaD<sub>4</sub> and NaD<sub>5</sub> occurs at around 60°C, it is proposed that the C<sub>10</sub> alkyl chains dominate the melting behaviour of the non-polar regions of the amphiphilic repeat units of NaD<sub>4</sub> and NaD<sub>5</sub>. By analogy with the behaviour of the monomeric sodium soaps<sup>24,142,151</sup>, T1 could therefore be:

- an intercrystalline transition, i.e. similar to the curd-curd transition occurring in some long-chain sodium soaps at 80-90°C, or
- the initiation of the step-wise melting of the non-polar chains of the crystalline phase, i.e. similar to the curd-subwaxy transition occurring in long-chain sodium soaps at 100-130°C.

The intercrystalline transition of monomeric soaps is thought to consist of a change in the angle of tilt of the hydrocarbon chain axis, while the packing of the polar groups remains essentially unaffected. The enthalpy change involved in this type of transition varies typically from 1 to 5

$\text{KJ.mole}^{-1}(142,299)$ . The curd-subwaxy transition is attributed to a change in the binding of the hydrocarbon chains as a result of the initiation of the step-wise melting of these chains. The enthalpy change involved in this transition is generally greater than the intercrystalline transition, and is in the region of  $12-13 \text{ KJ.mole}^{-1}(142,299)$ . Whilst the enthalpy of the T1 transition is about  $20\text{KJ.mole}^{-1}$ , it should be remembered that  $\text{NaD}_4$  and  $\text{NaD}_5$  are 'multi-amphiphile' molecules. Hence, when comparing the enthalpy changes occurring in  $\text{NaD}_4$  and  $\text{NaD}_5$  with those of monomeric sodium soaps, comparisons should be made on the basis of the changes associated with individual amphiphilic units. Ideally, comparisons of  $\Delta H/T$  are required, however, as the temperature of the transitions being compared are similar, comparisons of  $\Delta H$  will be a reasonable approximation.

Dividing the enthalpy changes of  $\text{NaD}_4$  and  $\text{NaD}_5$  pro rata per amphiphilic unit of these molecules, the enthalpy change involved in the T1 transition becomes equal to  $4-5 \text{ KJ.mole}^{-1}$  of amphiphilic repeat unit. Whilst the magnitude of this enthalpy change and the transition temperature approximate to that of the intercrystalline transition of monomeric soaps, this is not sufficient evidence to classify T1 as some type of intercrystalline transition.

The higher temperature transition (T2, typically  $7-9 \text{ KJ.mole}^{-1}$ ) occurred at about  $145^\circ\text{C}$ . Again, if this enthalpy change is divided pro rata per amphiphilic unit of  $\text{NaD}_4$  and  $\text{NaD}_5$ , this then becomes just less than  $2 \text{ KJ.mole}^{-1}$  of amphiphile. Around this temperature the samples did undergo a very slight softening, reflecting at least a partial melting of the crystalline structure. By analogy with the behaviour of the monomeric

sodium soaps, this transition could thus be a stage in the<sup>142,299</sup>:

- step-wise melting of the non-polar chains, and/or
- step-wise melting of the polar groups.

As the X-ray diffraction patterns were identical at temperatures above and below T<sub>2</sub> (i.e. at 50 and 200°C), the overall phase structure remains unaffected by this transition. Remembering that the monomeric sodium soaps undergo transitions ascribed to the melting of the alkyl chains at temperatures similar to T<sub>2</sub>,<sup>142,299</sup>, it seems reasonable to propose that the T<sub>2</sub> transition is primarily associated with the non-polar regions. However, the reduced packing density of the molecules also indicates that the polar groups themselves have undergone some structural changes. As has been seen, the packing of the polar groups within monomeric sodium soaps is independent of temperature in all the crystalline and semi-crystalline phases and hence, this is something of a surprising observation.

The limited experimental evidence available here indicates that, as is the case with the monomeric straight chain sodium soaps, NaD<sub>4</sub> and NaD<sub>5</sub> exist as a lamellar crystalline phase at room temperature, and initially melt via the step-wise melting of the hydrophobic chains. Unlike the monomeric soaps this melting of the hydrophobic chains of NaD<sub>4</sub> and NaD<sub>5</sub> results in a less compact packing of the polar groups. In addition, X-ray data indicates that the melting of the hydrophobic chains of NaD<sub>4</sub> and NaD<sub>5</sub> does not result in the formation of the ribbon phases which are characteristic of monomeric sodium soaps at temperatures between the lamellar crystalline and the formation of the lamellar mesophase<sup>24,142</sup> (see figure 6.11).

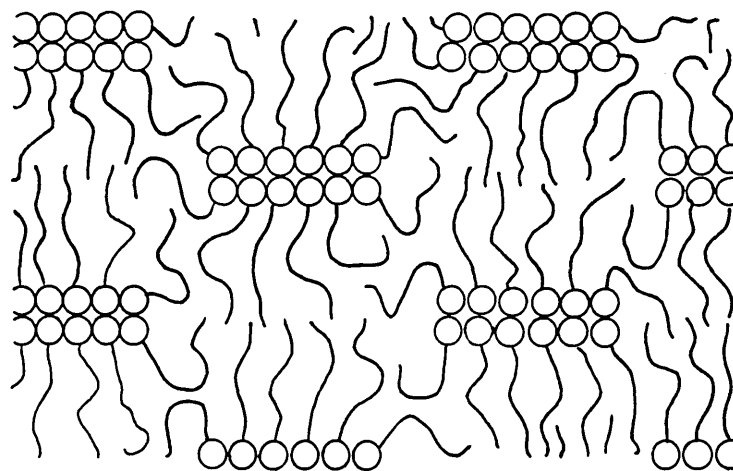


Figure 6.11 Schematic representation of the ribbon phase of anhydrous monomeric sodium soaps at elevated temperatures (see ref.24).

The presence of these semi-crystalline ribbon phases in monomeric sodium soaps has been explained by the melting and disordering of the alkyl chains, whilst the polar head groups retain their crystalline arrangement<sup>24</sup>. In these soaps, the alkyl chains are attached to the head groups, which are effectively anchored in closely packed and fixed positions in the polar regions. On the other hand, the alkyl chains themselves, which are partially or wholly fused, are only anchored in a fixed position via the carbon atom covalently bonded to the polar group. Thus, the mobility of the alkyl chain is very small near the polar group, but increases towards the methyl end group

and with increasing temperature. At some temperature, the mobility and subsequent disorder in the alkyl chains of the monomeric soaps, is such that the average orientation of the fused chains is fan-wise, and at some distance from the polar groups, the chains are sufficiently disordered to overtake the edge of the ordered polar region. This process results in the formation of the ribbon type phases.

As NaD<sub>4</sub> and NaD<sub>5</sub> also undergo a step-wise melting of the non-polar chains, the absence of the ribbon phases during the melting of NaD<sub>4</sub> and NaD<sub>5</sub> is presumably explained by some mechanism that precludes this fan-wise orientation of their fused or partly fused hydrophobic chains. As the attachment of the non-polar chains to the cyclic siloxane backbone in NaD<sub>4</sub> and NaD<sub>5</sub> must result in a restriction of the degree of freedom of these chains at the opposite end from the polar group, this may preclude the fan-wise orientation of the non-polar groups. In addition, the significant increase in the surface area per polar group of NaD<sub>4</sub> at 200°C, would tend to counteract the tendency of the alkyl chains to adopt a fan-wise orientation. Whether this increase in the area per polar group of NaD<sub>4</sub> at 200°C, arises as a consequence of, or in addition to, the restricted freedom of the alkyl chains at the opposite end from the polar group of each amphiphilic unit, is a mute question which cannot be answered here. It is, however, worth noting that the absence of the ribbon phases, as explained above, does not seem compatible with the absence of a lamellar structure for the high temperature mesophase of NaD<sub>4</sub> and NaD<sub>5</sub>. Whatever the structure of this mesophase, excluding the lamellar phase and any phase with a positive surface curvature of the non-polar/polar interface, the mesophase structure would presumably result from a negative surface curvature of the

polar/non-polar interface; presumably requiring an average fan-wise orientation of the non-polar chains. Why this fan-wise orientation should be permitted above the melting point of polar groups (i.e. in the mesophase) but not below (i.e. in the semi-crystalline phase) is not obvious.

At about 250°C, both NaD<sub>4</sub> and NaD<sub>5</sub> undergo a transition to a mesophase (T3). Owing to the high temperature at which this transition occurs, it seems reasonable to attribute this transition primarily to a melting of the polar groups. As we have seen, the absence of an identifiable DSC signal corresponding to the subsequent transition to the isotropic liquid, indicated that only a small enthalpy change was involved in the melting of this mesophase. The magnitude of this enthalpy change, indicates that most of the 'bonds' present in the original crystal structure have been broken down prior to this final melting and, reflects a step-wise melting similar to that encountered in monomeric sodium soaps<sup>142,151,299</sup>.

Having proposed that the T3 transition is associated with the melting of the polar groups, it is expected that this transition would be susceptible to the presence of water. The observation that the temperature of the transition to the mesophase gradually increased to a maximum after several DSC analyses (see table 6.2) may reflect this, and may indicate that initially the samples were not truly anhydrous. With non-anhydrous samples, repeated heating would tend to drive off any water associated with the polar groups and lead to successively increasing transition temperatures (i.e. T3 to T3'). Due to the relatively high temperature at which T3 occurred, there is also a possibility of thermal degradation. The 3% reduction in the mass of samples and the increase in the transition temperature of T3 with repeated heating, may have been due to either of these effects.

An interesting result of this work, is the observation that the total heat of fusion for each amphiphile unit of NaD<sub>4</sub> and NaD<sub>5</sub> (13.3 and 10.3 kJ.mol<sup>-1</sup>, respectively) is substantially less than that of the monomeric straight chain sodium soaps of approximately equivalent hydrophobic chain length (typically 30 to 40 kJ.mol<sup>-1</sup> for sodium laurate and myristate, respectively)<sup>151</sup>. Remembering that the majority of the heat of fusion for monomeric sodium soaps is associated with the melting of the alkyl chains<sup>151</sup>, and comparing the structures of NaD<sub>4</sub> and NaD<sub>5</sub> with those of the monomeric sodium soaps, it may be reasonable to assume that the major differences in the melting behaviour of these oligomers and the related monomers would be associated with the non-polar regions of the respective molecules. Indeed, the total enthalpy changes ascribed to the melting of the non-polar chains of NaD<sub>4</sub> and NaD<sub>5</sub> (i.e. 6 to 7 KJ.mol<sup>-1</sup> per amphiphile repeat unit; T1 plus T2) is much less than the corresponding transitions of the monomeric sodium soaps of equivalent hydrophobic chain length (typically 20 to 35 kJ.mol<sup>-1</sup> for sodium laurate and myristate, respectively)<sup>151</sup>. On the other hand, the total enthalpy changes ascribed to the melting of the polar groups of NaD<sub>4</sub> and NaD<sub>5</sub> (i.e. T3; 4 to 6 KJ.mol<sup>-1</sup> per amphiphile repeat unit) is typical of the equivalent transition in monomeric soaps (i.e. approximately 6 KJ.mol<sup>-1</sup>)<sup>151</sup>. Hence, the attachment of amphiphiles to the siloxane rings in NaD<sub>4</sub> and NaD<sub>5</sub> may have disrupted the packing of the hydrocarbon chains of these amphiphiles, in particular, restricting their close contact. A similar effect has been reported for sodium oleate, in which the presence of a cis double bond in the nine position is thought to disrupt the efficient packing of the non-polar chains<sup>151</sup>. Thus, the total heat of fusion for sodium oleate is reported to be 35.5 kJ.mol<sup>-1</sup>, as opposed to the 58 kJ.mol<sup>-1</sup> of the corresponding saturated soap, sodium stearate.

Although it seems unlikely, the relatively low enthalpy of melting of the non-polar chains of NaD<sub>4</sub> and NaD<sub>5</sub> may, in part, be attributed to a more organised character of the melted soaps. However, if the attachment to the siloxane backbone does disrupt the packing of the hydrocarbons chains of NaD<sub>4</sub> and NaD<sub>5</sub>, a similarly low heat of fusion would be expected to occur in the fatty acids of these cyclic amphiphiles. To check this, DSC was carried out on the fatty acid of NaD<sub>4</sub> (hereafter referred to as D<sub>4</sub>COOH; see figure 6.12).

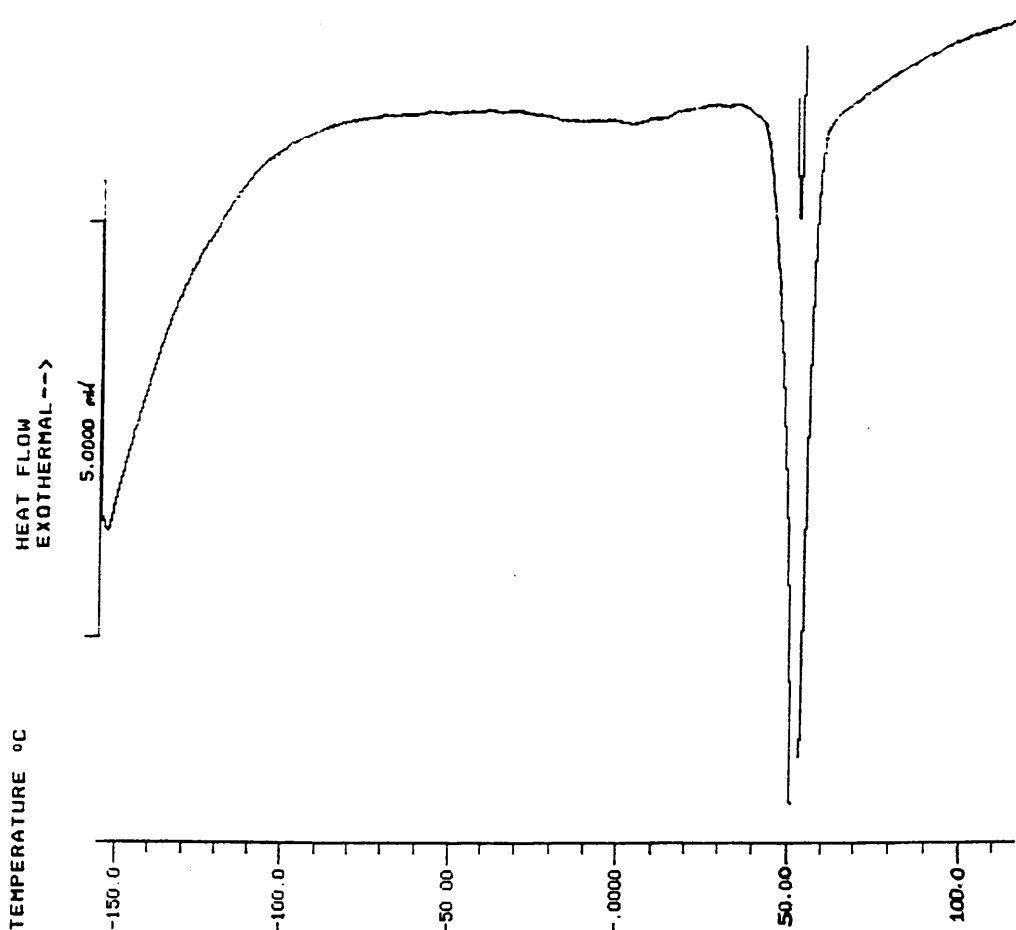


Figure 6.12 Thermogram of D<sub>4</sub>CO<sub>2</sub>H obtained on heating from -160 to 120°C at a rate of 10°C.min<sup>-1</sup>.

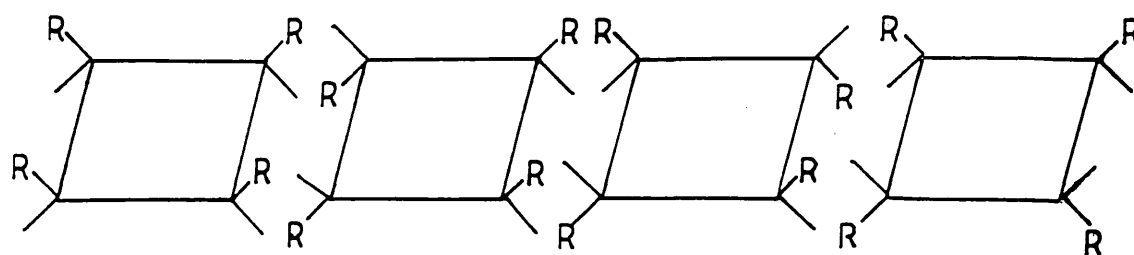
The enthalpy of fusion for this non-mesomorphic material was  $38 \text{ kJ.mol}^{-1}$  (i.e.  $9.5 \text{ kJ.mol}^{-1}$  of repeat unit). This is similar to the total heat of fusion of the repeat unit of  $\text{NaD}_4$ , but when compared with the heat of fusion of the straight chain fatty acids (approximately  $30 \text{ kJ.mol}^{-1}$  for lauric acid) it is unusually low<sup>297</sup>. Therefore, attaching hydrocarbon chains to a siloxane ring does appear to have a significant effect on the packing of these chains and thus, the total enthalpy of fusion of  $\text{NaD}_4$  and  $\text{NaD}_5$ .

This proposal apparently conflicts with the conclusions drawn from earlier studies of the lyotropic behaviour of linear amphiphilic side-chain siloxanes, in which the attachment to a linear siloxane backbone is said to have had little effect on the rotational or translation motion of amphiphilic side-chains<sup>66,67</sup>. In attempting to understand these apparently conflicting observations two factors should be considered. Firstly,  $\text{NaD}_4$  and  $\text{NaD}_5$  consist of a cyclic siloxane backbone, and cyclic dimethylsiloxane oligomers are relatively rigid compared with their oligomeric and polymeric linear counterparts<sup>296</sup>. Therefore, the attachment of amphiphiles to these rigid backbones may have an adverse effect on the free motions of these side-chains<sup>72</sup>. Secondly, the lyotropic mesophases studied previously<sup>66,67</sup>, are made up of fused non-polar chains, as opposed to the room temperature crystalline structures of  $\text{NaD}_4$  and  $\text{NaD}_5$  being studied here. Thus, the reduced ability of the non-polar chains of  $\text{NaD}_4$  and  $\text{NaD}_5$  to pack closely in the crystalline form may not necessarily be reflected in the previous studies of the lyotropic behaviour of the fused amphiphiles (the discussion of the lyotropic phase behaviour of  $\text{NaD}_4$  follows in section 6.3.1.2).

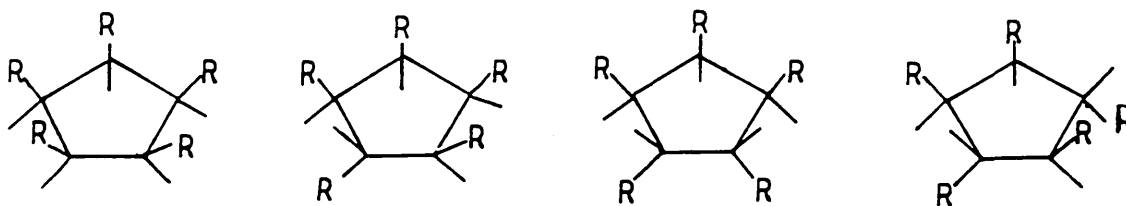
On the basis of the results obtained during this study, attaching hydrocarbon chains to a rigid siloxane ring does have a significant effect on the packing of the hydrophobic chains attached to it. The fact that the enthalpies of melting of the polar groups of NaD<sub>4</sub> and NaD<sub>5</sub> are similar to those of monomeric sodium soaps, indicates that the polar groups are less affected by the attachment to the siloxane. This may be understood by considering the alkyl chain which links the polar group to the siloxane ring as acting as a type of spacer group, and decoupling the motions and the steric effects of these moieties. It is also envisaged that this disruptive effect of the attachment to the siloxane rings will vary along the length of the alkyl chain. Hence, the packing of the methylene units closest to the polar group may be similar to that encountered in monomeric sodium soaps, but the closer to the siloxane ring, the less efficient the packing of these methylene units would be. It may also follow that it is primarily the melting of the methylene units closest to the head group that gives rise to T1 and T2.

Having noted that the cyclic oligomers are relatively rigid compared with their linear oligomeric and polymeric equivalents, it is interesting to note that cyclic chains also differ from the corresponding linear systems in that their chain backbone atoms are arranged into covalently bonded rings, without any chain ends. This imposes restricted freedom of movement about the silicon-oxygen bonds, compared with the corresponding linear backbones, and the shorter the chain length, the greater this restriction becomes. Thus, unlike their linear equivalents, cyclic side-chain structures such as NaD<sub>4</sub> and NaD<sub>5</sub>, also contain a number of geometric isomers which cannot interchange (see figure 6.13). These isomers may have affected the X-ray patterns observed and may have contributed to the broad X-ray lines

of  $\text{NaD}_4$ . The presence of these isomers—each isomer having a distinct melting point—may also be expected to result in the depression of the melting point of the mixture, relative to the individual isomers, and the occurrence of relatively broad thermal transitions. Whilst both  $\text{NaD}_4$  and  $\text{NaD}_5$  certainly did give rise to broad thermal transitions, it is not possible to judge if the presence of the geometric isomers is the root cause of this effect or, at this stage, to fully understand the effects of the presence of these isomers.



a)  $\text{NaD}_4$



b)  $\text{NaD}_5$

**Figure 6.13** A schematic diagram of the geometric isomers of a)  $\text{NaD}_4$  and b)  $\text{NaD}_5$ ; where the square and the pentagon represent the cyclic siloxane tetramer and pentamer backbones respectively. The corners of each geometric form represent silicon, the centre of each side represent oxygen, R represents the side-chain amphiphile and each unspecified equatorial bond represents a methyl group.

In general, the samples of NaD<sub>4</sub> and NaD<sub>5</sub> exhibited very similar thermal behaviour, despite their different degree of polymerisation. There was, however, a trend for NaD<sub>5</sub> to undergo thermal transitions at slightly lower temperatures than NaD<sub>4</sub>, and for these transitions to occur over a broader temperature range. These observations may be explained by the different amounts of higher members of this homologous series of amphiphilic side-chain siloxanes (i.e. NaD<sub>n</sub>) that would have been present in NaD<sub>4</sub> and NaD<sub>5</sub> as a result of the polydispersed nature of the siloxane precursors used in their preparation. These siloxane precursors were used as obtained from Petrach, and contained 1 and 5 wt% of the higher cyclic homologues, respectively<sup>322</sup>. The preparation and characterisation of mono-dispersed samples of each member of the homologous series—possibly using preparative Gas Chromatography<sup>323</sup> or spinning band distillation, as outlined in chapter 2—may have been of assistance in assessing the possible effects of these 'impurities'.

A significant result of this work, is the increased thermal stability of the mesophase region of NaD<sub>4</sub> and NaD<sub>5</sub>, relative to that of the monomeric sodium soaps of equivalent chain length<sup>142,151,299</sup>. The transition to the low viscosity isotropic liquid of NaD<sub>4</sub> and NaD<sub>5</sub> occurred at approximately 430°C. This is at least 100°C greater than that of sodium laurate and sodium myristate (i.e. 320 and 316°C, respectively)<sup>300</sup>. As the chemical nature of NaD<sub>4</sub> and NaD<sub>5</sub> are not dissimilar to that of the monomeric sodium soaps, specific inter-molecular forces of attraction cannot explain the enhanced thermal stability of the mesophase region of NaD<sub>4</sub> and NaD<sub>5</sub>. Hence, it is tentatively proposed that this increased thermal stability of the mesophase region of these multi-amphiphile molecules, may arise as a result of the

oligomeric nature of the molecules themselves. This may be qualitatively understood by considering that the amphiphilic side-chain repeat units of these oligomers cannot escape from the micelle as individual units due to their covalent bonding to the other amphiphiles of the oligomers (i.e. there are 4/5 'bonds' per molecule to hold the amphiphile structure together). Hence, the micelles and the mesophases which are built up of these micelles, are stabilised. This explanation has been proposed for the enhanced thermal stability of the aqueous lyotropic mesophases of linear amphiphilic side-chain siloxanes<sup>67,69,70</sup>, although the major effect in these systems is now believed to be the increased length of the hydrophobic chain of the amphiphilic repeat units, due to the attachment to the siloxane backbone<sup>66,67</sup>. An additional consequence of the multi-amphiphile nature of NaD<sub>4</sub> and NaD<sub>5</sub>, is that all the polar groups of each oligomer may not be isolated to the same polar/non-polar interface. These molecules may, therefore, act as 'molecular cross-links' between micelles, maintaining the mutual orientation of the micelles and thus, also enhancing the stability of the mesophase region.

### 6.2.1.3 Conclusions

The thermotropic behaviour of NaD<sub>4</sub> and NaD<sub>5</sub> has much in common with that of monomeric sodium soaps, although there are also significant differences that require further and more in-depth research in order to fully elucidate these differences and to assist in our understanding of these systems, and the factors that govern the resulting thermotropic behaviour. Nevertheless, the following general conclusions may be drawn:

1. The well established principles explaining the behaviour of monomeric amphiphiles seem to be generally applicable to the phase behaviour of these novel cyclic amphiphilic oligomers.

2. As these principles dictate, the non-polar and polar moieties of these amphiphiles tend to aggregate in the neat state. The driving force for this aggregation will be the enthalpic contribution from the association of the polar groups.
3. Due to the molecular structure of these amphiphiles (i.e. packing constraints), the phase structure at ambient is that of a bilayer.
4. The absence of an identifiable thermal event from  $-170^{\circ}\text{C}$  up to room temperature, probably indicates that no thermal induced transitions are taking place in this range. Thus, the bilayer phase remains at the lower temperatures.
5. At room temperature, the non-polar chains and the polar groups appear to be crystalline, although the attachment of the  $\text{C}_{11}$  carboxylates to the rigid cyclic siloxane backbone seems to limit the degree of crystallinity within the  $\text{C}_{10}$  alkyl chains of these molecules, and the packing of the amphiphiles.
6. At around  $60$  and  $145^{\circ}\text{C}$ , it seems likely that the non-polar chains of these cyclic amphiphiles undergo a two stage melting process that results in a less compact packing of the amphiphiles within the bilayers (i.e.  $T_1$  and  $T_2$ , respectively). This process may be analogous to the initial stages in the step-wise melting of monomeric straight-chain sodium soaps.
7. Unlike the monomeric straight-chain sodium soaps of equivalent chain length, the melting of the non-polar chains (i.e. the formation of a semi-crystalline phase) does not result in the formation of ribbon type structures. This may be due to a restriction of the alkyl chain freedom, as a result of the attachment to the comparatively rigid siloxane ring. The structure of the intermediate phase region therefore requires further investigation.

8. At around 250°C, the polar groups of these amphiphiles melt. This is also analogous to the step-wise melting of monomeric amphiphiles. This melting of the head groups has a significant effect on the behaviour of this series of amphiphiles, giving rise to a mesophase.

9. The structure of the mesophase formed by these molecules is atypical of the straight chain sodium soaps, and requires further investigation.

10. The attachment of the C<sub>11</sub> sodium carboxylates to the cyclic siloxane ring increases the thermal stability of the mesophase regions of these oligomeric amphiphiles by at least 100°C, relative to the equivalent monomeric soaps. The presence of a number of 'bonds' per multi-amphiphile molecule holding the micelle structures together may explain this effect. In addition, the formation of 'molecular cross-links' between micelles may become important.

## 6.2.2 The Calcium Salt

### 6.2.2.1 Results

#### 6.2.2.1.1 Polarising Optical Microscopy

The microscopy of previously unmelted powdered samples of the calcium salt of the cyclic tetramer (Figure 6.1; X=4 and Y= 1/2Ca, hereafter referred to as CaD<sub>4</sub>) was characterised by three main optical events in the temperature range 0-550°C. These events were:

- the formation of a birefringent fluid phase at 156°C
- the gradual loss of the birefringency of this viscous liquid from 275-295°C
- the formation of a low viscosity isotropic liquid phase at 490°C.

The non-geometric texture and the viscosity of the mesophase were possibly indicative of a hexagonal type structure (see figure 6.14)<sup>16</sup>. At

about 280°C, there was evidence of the onset of thermal degradation of the sample, and by the transition to the isotropic low viscosity liquid at about 490°C, considerable degradation had occurred.



Figure 6.14 Optical texture of the fluid birefringent phase of  $\text{CaD}_4$  at 200°C.

A film of  $\text{CaD}_4$  was then prepared by placing a powdered sample between a cover-slip and a microscope slide at  $200^\circ\text{C}$ , depressing the cover-slip and then, rapidly cooling to room temperature. Microscopy of this film indicated a birefringent solid phase at room temperature. This phase exhibited a texture similar to that of the mesophase from which it had been prepared. As the temperature was gradually increased, a significant reduction in viscosity occurred at  $154^\circ\text{C}$ , with the formation of the bright birefringent fluid phase described previously. Again, this mesophase was stable up to temperatures that were concomitant with a significant degree of thermal degradation of the sample.

#### 6.2.2.1.2 Differential Scanning Calorimetry (DSC)

The thermogram recorded on heating a previously unmelted sample of  $\text{CaD}_4$  between  $-170$  and  $550^\circ\text{C}$  was characterised by two first order endothermic transitions (hereafter referred to as T1 and T2 in order of increasing temperature). Figure 6.15 shows a typical thermogram for a sample which had been dried under vacuum over  $\text{P}_2\text{O}_5$  at  $100^\circ\text{C}$  for 24 hours, whilst table 6.6 summarises the results of this analysis.

TRANSITION	TRANSITION TEMPERATURE ( $^\circ\text{C}$ )	ENTHALPY ( $\text{KJ.mol}^{-1}$ )
T1	159	17
T2	478	42

Table 6.6 The transition temperatures and enthalpy changes observed during the initial heating of  $\text{CaD}_4$  ( $-170$  to  $550^\circ\text{C}$ ;  $10^\circ\text{C.min}^{-1}$ ).

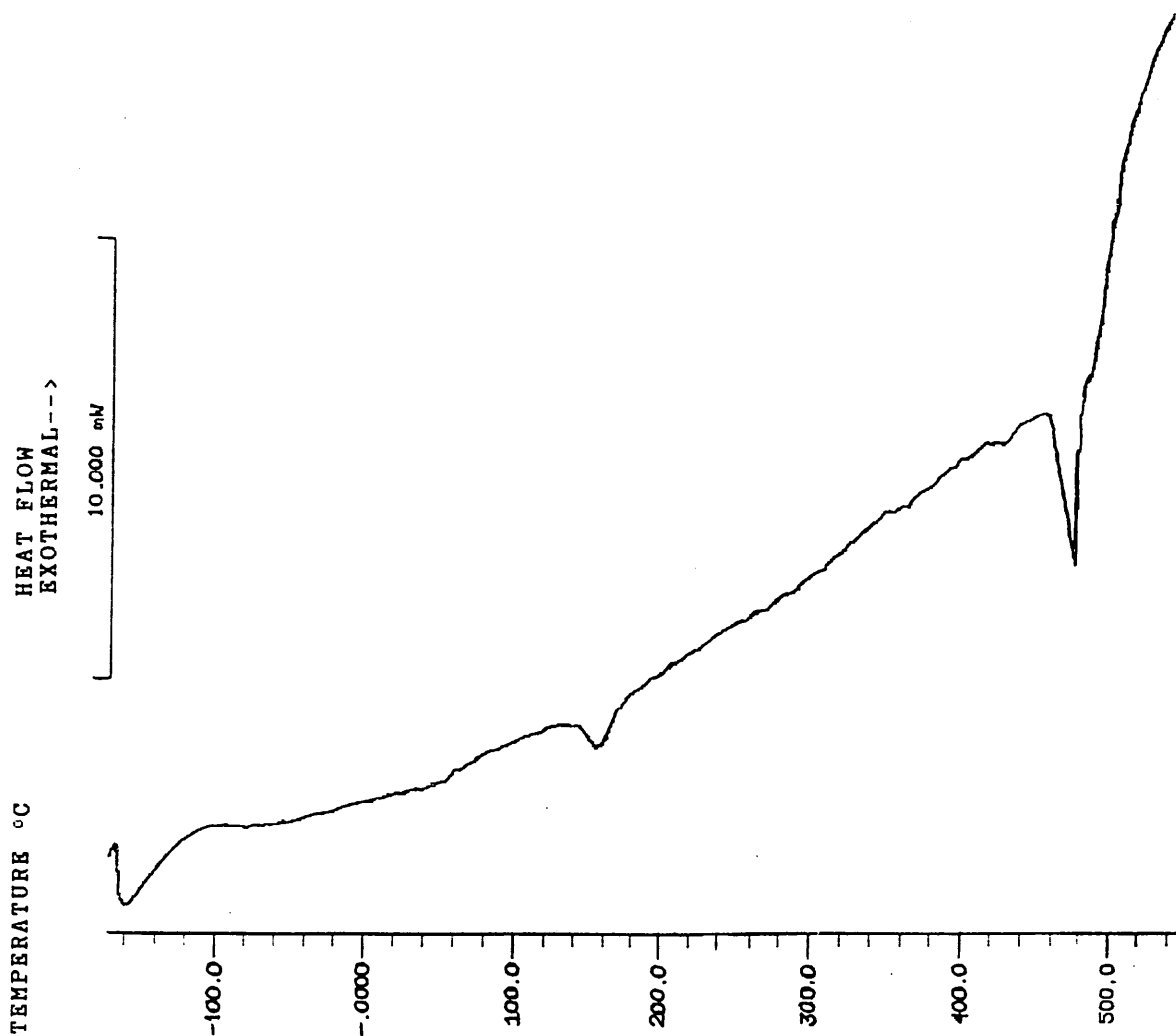


Figure 6.15 The thermogram of a previously unmelted sample of  $\text{CaD}_4$  which had been heated from  $-170$  to  $550^\circ\text{C}$  at a rate of  $10^\circ\text{C}\cdot\text{min}^{-1}$ .

In order to assess the effects of heating and cooling the samples, repeated thermal analysis of a fresh sample of  $\text{CaD}_4$  was carried out between  $-50$  and  $320^\circ\text{C}$ ;  $320^\circ\text{C}$  was arbitrarily chosen as the maximum temperature in an attempt to limit the thermal degradation occurring with repeated heating. Whilst the initial thermogram was characterised by one endothermic transition in this temperature range, no transition was identified during the reheating (see figure 6.16).

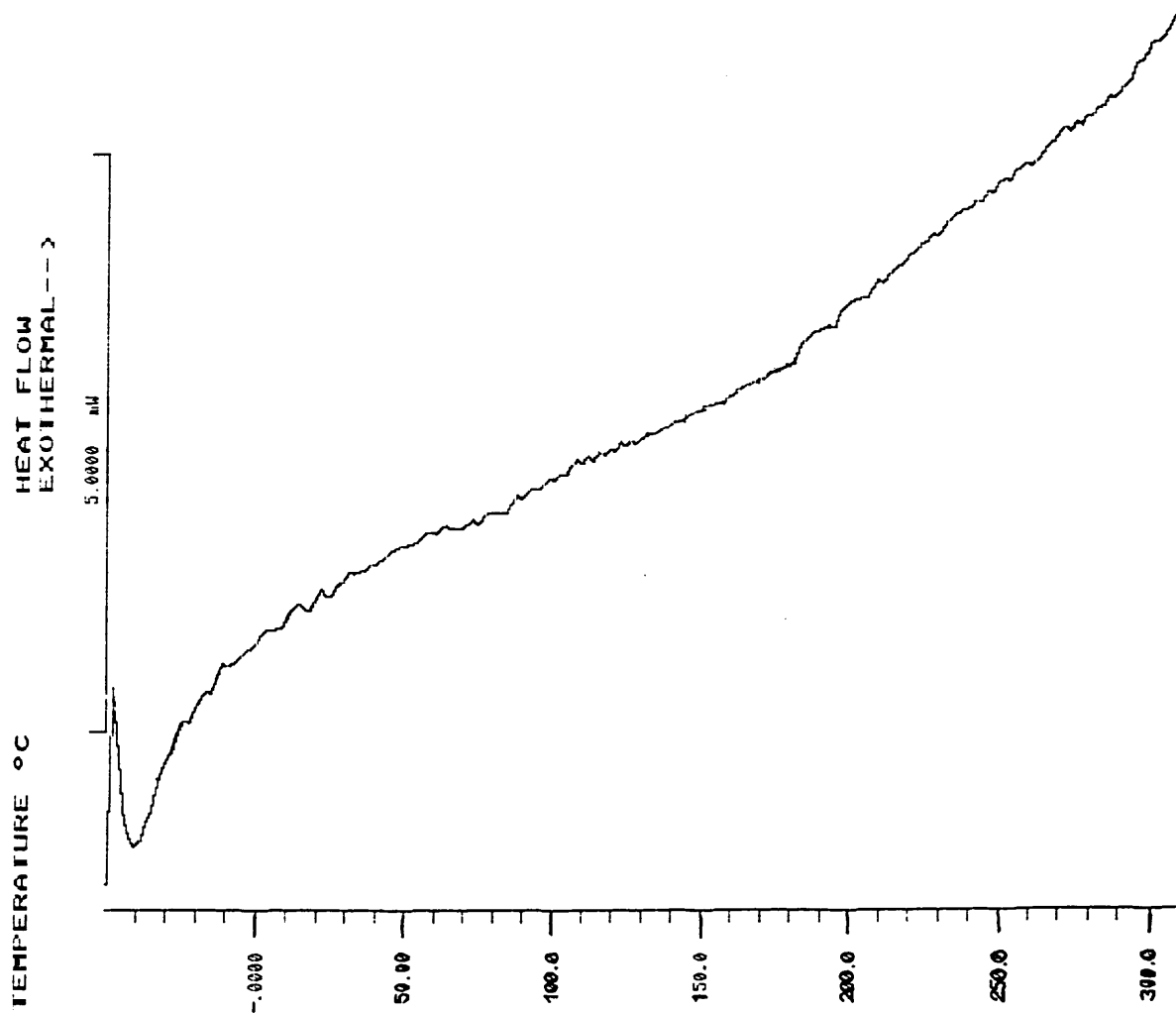


Figure 6.16 Thermogram obtained on the reheating of a sample of CaD<sub>4</sub> from -50 to 320°C at a rate of 10°C.min<sup>-1</sup>

A thermogram was then recorded for a fresh sample of CaD<sub>4</sub> from 220 to 20°C at a cooling rate of 2°C.min<sup>-1</sup>. No transitions were identified during this analysis (see figure 6.17A), or the subsequent reheating of the sample between 20 and 220°C at a rate of 10°C.min<sup>-1</sup> (see figure 6.17B).

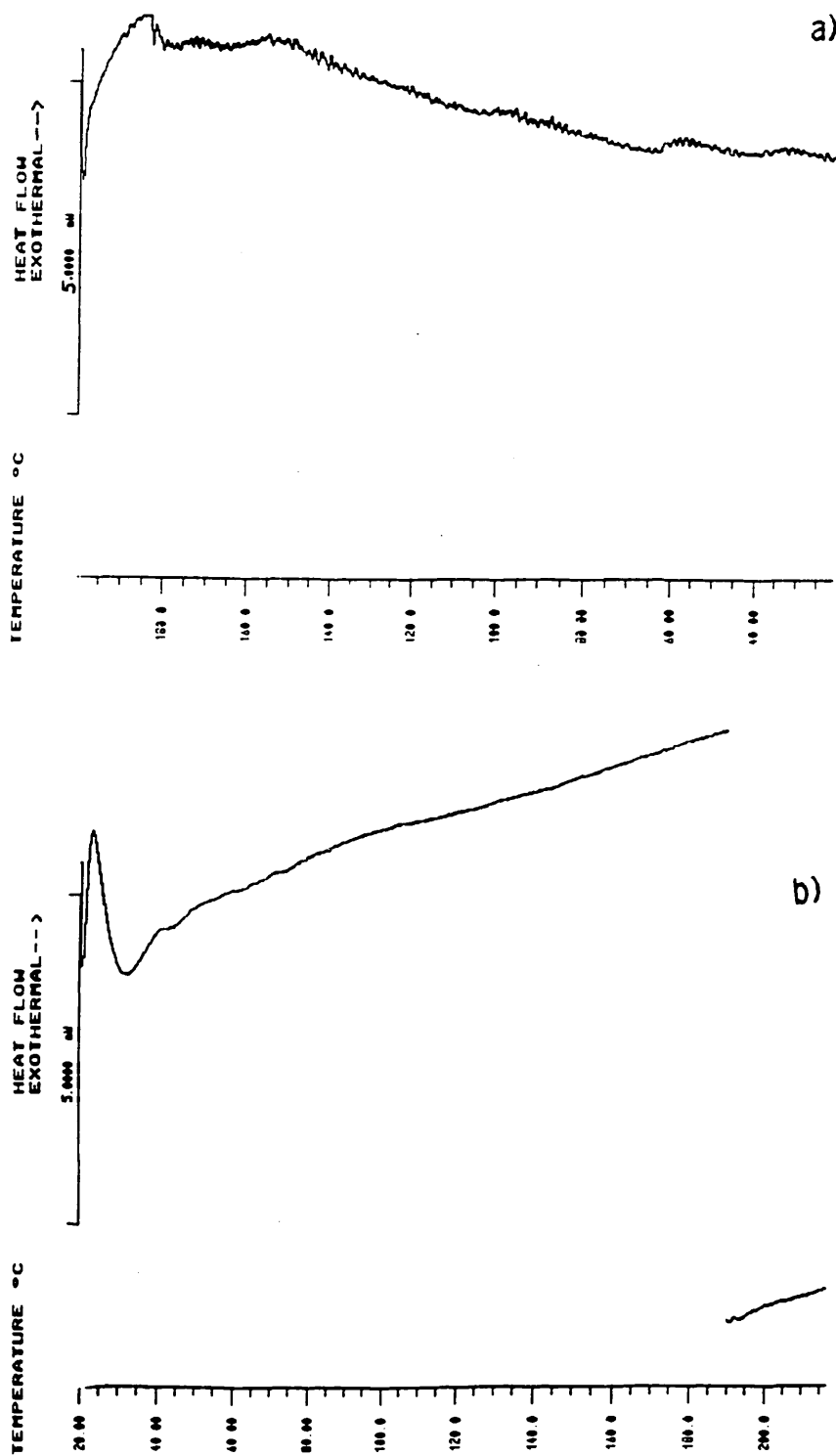


Figure 6.17 Thermogram obtained for a sample of  $\text{CaD}_4$  on a) cooling from 200 to 20°C at a rate of  $2^\circ\text{C}\cdot\text{min}^{-1}$  and b) on the immediate reheating from 20 to 220°C at a rate of  $10^\circ\text{C}\cdot\text{min}^{-1}$ .

### 6.2.2.1.3 Thermo-Gravimetric Analysis (TG)

A thermogram was recorded on heating a previously unmelted sample of  $\text{CaD}_4$  between 35 and 550°C. This thermogram exhibited no significant weight loss up to about 250°C, at which point there was a gradual and increasing loss in weight up to the termination of the evaluation at 550°C. This loss in weight was believed to correspond to the onset of thermal degradation of the sample. Figure 6.18 shows the thermogram obtained for a sample of  $\text{CaD}_4$  which had been dried over  $\text{P}_2\text{O}_5$  at 100°C for 24 hour.

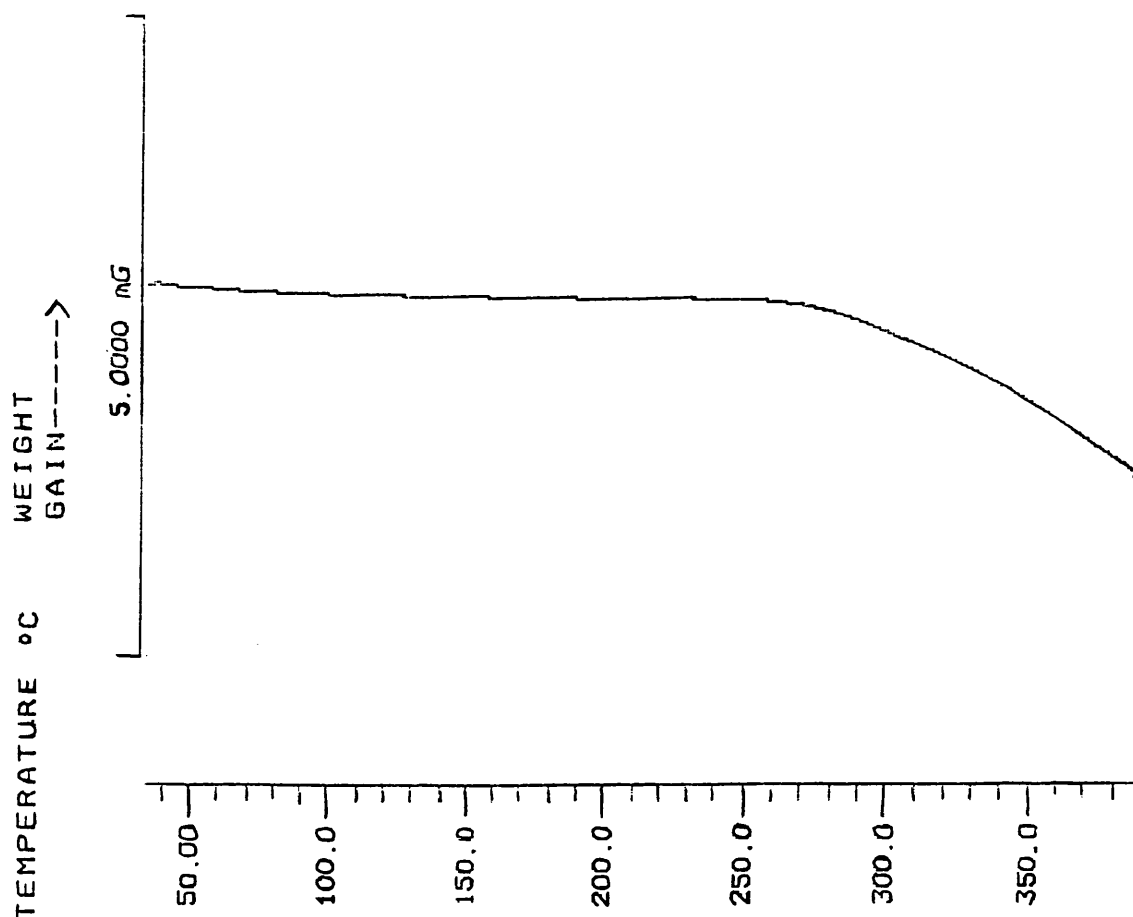


Figure 6.18 Thermogram of  $\text{CaD}_4$  obtained on heating from 35 to 550°C at a rate of 10°C.min<sup>-1</sup>.

### 6.2.2.1.4 X-Ray Diffraction

Diffraction patterns were obtained for a sample of  $\text{CaD}_4$  in both the low- and wide-angle regions. Figure 6.19 shows the diffraction patterns obtained in the low-angle region, while table 6.7 shows the corresponding spacings observed at 25 and 200°C.

SIGNAL	VARIATION OF SPACINGS (Å) OF PEAKS OBSERVED WITH TEMPERATURES	
	25°C	200°C
$d_0$	30.8	27.7
$d_1$	15.4	13.8

Table 6.7 Spacings observed in the X-ray diffraction pattern for  $\text{NaD}_4$  at 25 and 200°C.

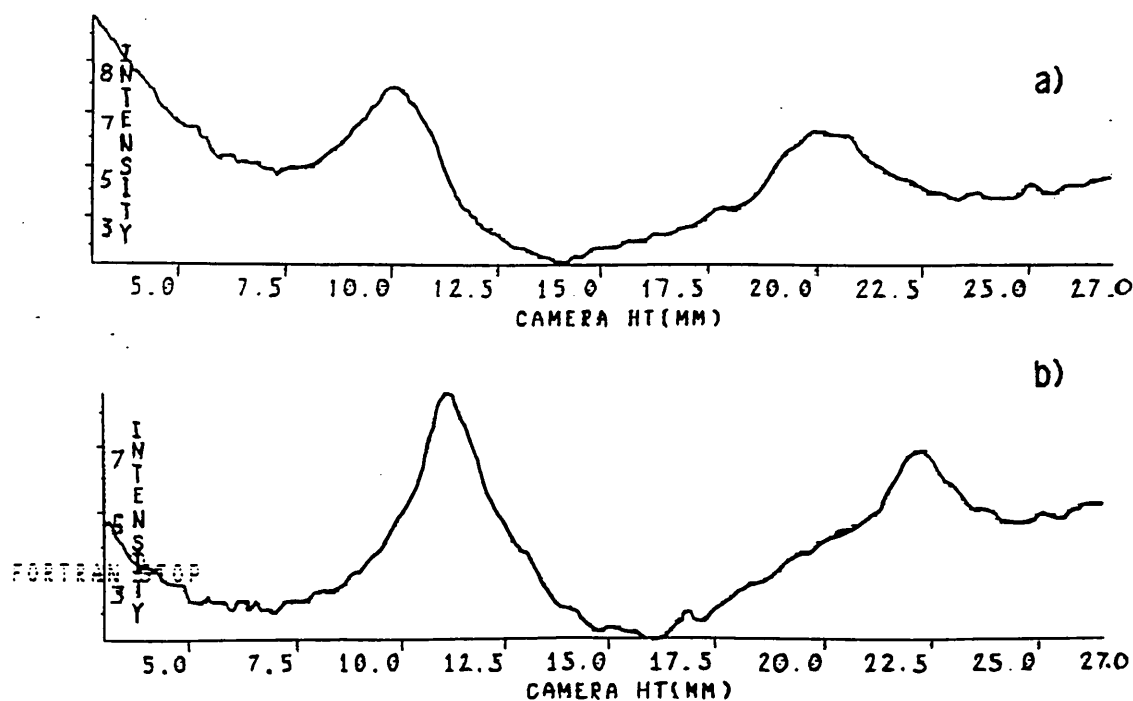


Figure 6.19 X-ray diffraction pattern obtained for  $\text{CaD}_4$  in the low angle region at a) 25°C and b) 200°C.

At 25 and 200°C the main peaks observed were very broad. In each case, the major peaks were in the ratio of 1:1/2, and there was some evidence of a very weak broad peak around  $d_0/\sqrt{3}$ . No peaks of any real intensity were observed in the wide-angle region at either temperature. An attempt to record an X-ray diffraction pattern at 300°C was abandoned, as considerable thermal degradation of the sample had obviously occurred.

#### 6.2.2.2 Discussion

Optical microscopy of films of  $\text{CaD}_4$  indicated that this material exists as an ordered solid at room temperature. The non-geometric texture of this birefringent solid was indicative of a hexagonal phase<sup>16</sup>. At about 154°C, a birefringent fluid phase formed. The non-geometric texture and the viscosity of this fluid phase were also indicative of a hexagonal phase. The birefringency of this phase gradually diminished over a broad temperature range from 275 to 295°C. The loss of birefringence was not accompanied by a significant change in viscosity. This optically isotropic viscous fluid phase was stable up to the transition to the low viscosity isotropic liquid at about 480°C. It was not possible to be precise about the temperature of this transition because of the severe thermal degradation of the sample.

The transitions observed during the DSC heating of previously unmelted samples of  $\text{CaD}_4$  were in general agreement with these observations. The temperature of the two main endothermic transitions occurring in the range -170 to 550°C (i.e. T1 and T2 at 159 and 480°C, respectively), corresponded to the observations under the microscope of the transition to the fluid birefringent phase and the formation of the low viscosity isotropic liquid, respectively. No transition was identified for the loss of birefringence of the viscous fluid phase.

There is some evidence of a small endothermic transition occurring over a broad temperature range at around 50°C. A transition occurring at a similar temperature was observed in NaD<sub>4</sub> and NaD<sub>5</sub> and was believed to be an intercrystalline transition or the initiation of the step-wise melting of the non-polar chains of the crystalline phase (see section 6.2.1.2). However, the intensity of the DSC signal occurring in CaD<sub>4</sub> is such that no firm conclusions may be drawn with respect to this 'transition'.

As the transition to the isotropic liquid occurred at a temperature at which considerable thermal degradation of the samples had also occurred, all subsequent DSC investigations of the effects of repeatedly heating and cooling CaD<sub>4</sub> were carried out on samples that had not been heated to greater than 320°C. The thermograms obtained on the reheating of CaD<sub>4</sub> from -50 to 320°C, gave no transitions.

During controlled cooling of samples from 200 to 20°C (2°C.min<sup>-1</sup>), there was some evidence of two small, broad enthalpy transitions occurring at around 155 and 55°C. As the higher temperature transition corresponds to the T1 transition occurring during initial heating, it may be that the thermal events occurring around 155°C corresponded to this same transition. This being the case, no significant supercooling of the solid/fluid phase transition occurred. The weak signal occurring at around 55°C on cooling, may indicate that a transition does indeed occur at a similar temperature during the initial heating of CaD<sub>4</sub>. If this were the case, the absence of any evidence of this transition during the reheating of a sample—remembering that these samples were initially heated and then cooled rapidly—may be explained by a quenching of the sample during the rapid cooling that

followed the initial heating analysis (see section 6.2.1.2). However, the low intensity of these signals do not allow for an unambiguous interpretation of these 'transitions'.

Having used thermal analysis and optical microscopy of  $\text{CaD}_4$  to establish the temperature 'boundaries' of individual phase regions, and to supply some initial indication of the structures present within these boundaries, X-ray diffraction data was used as corroborative evidence for these observations. At 50 and 200 °C, the low-angle patterns of  $\text{CaD}_4$  exhibited two strong broad peaks (see table 6.7 and figure 6.19). At both temperatures, the positions of these reflections were, within experimental error, in the ratio of 1:1/2. No peaks of any real intensity were observed in the wide-angle region at either temperature.

A number of phase structures have been proposed, whose principle and second order reflections in the low-angle region are in the ratio of 1:1/2. These include the crystalline and mesomorphic lamellar and the tetragonal phases (i.e. C and K). However, as discussed in section 6.2.1.2, only the generally accepted lamellar phase structure will be invoked here.

In attempting to rationalise the behaviour of  $\text{CaD}_4$ , the optical studies—which indicated a hexagonal phase below the transition to the viscous isotropic phase at 275 to 295°C—cannot be reconciled with the X-ray diffraction patterns at 25 and 200°C, which did not exhibit the strong  $d_0/\sqrt{3}$  reflection that is generally characteristic of the hexagonal phase<sup>24,149</sup>. In attempting to proposing a structure for the crystalline phase of  $\text{CaD}_4$  (i.e. at temperatures less than 155°C) on the basis of this

conflicting data, it is worth remembering the experience with the equivalent sodium salt (see 6.2.1.2). This work indicated that the optical study of solid films may have been misleading because of the method employed in the preparation of the films themselves (i.e. the rapid quenching of the sample from the higher temperature fluid phase, freezes the structure of this high temperature phase into the solid film). A similar quenching of molecular orientation during rapid cooling has been noted in a number of studies<sup>153,304,305</sup>. In fact, during an early X-ray study of calcium stearate<sup>153</sup>, in the absence of a cell for obtaining diffraction patterns at elevated temperatures, this effect was used to advantage, with samples which had been quenched from various higher temperatures being examined at room temperature, in the hope that the molecules would be frozen into the relative orientations characteristic of each of the higher temperature forms. This, and the fact that the crystalline lamellar is the phase structure encountered in monomeric straight chain soaps of the alkali and alkaline earth metals, may indicate that the optical texture of the solid film of  $\text{CaD}_4$  at 25°C was not characteristic of an equilibrium structure. Hence, the X-ray diffraction pattern obtained from a unmelted sample at 25°C, may be more representative of the equilibrium crystalline structure of  $\text{CaD}_4$ . On this basis, the experimental evidence indicates that a lamellar phase similar to that encountered in monomeric calcium soaps<sup>24,149,166</sup>, and  $\text{NaD}_4$  and  $\text{NaD}_5$  (see 6.2.1.2), may also be characteristic of the crystalline form of  $\text{CaD}_4$ .

Having proposed the lamellar structure at 25°C, the area per polar group that would result in this structure can be calculated<sup>149</sup>. The comparison of the area per polar group of monomeric calcium soaps of the lamellar structure (see table 6.8) with this derived value is obviously of interest.

PARAMETERS	PHASE PRESENT					
	A	B	C	D	E	F
t (°C)	<100	100-110	110-127	133-165	166-180	240*
S (Å <sup>2</sup> )	**	20.1-20.3	26.3-29.4	31.4-33.5	34.7	43.8

Where A and B represent modifications of the crystalline lamellar phase

t = temperature stability range of the phase

\* = the temperature for which the dimensions of the phase are given

\*\* = no values given, but is expected to be just less than the value of the phase B, which entails slightly less compact packing of the head groups

Table 6.8 The variation of area per polar group of calcium myristate (C<sub>14</sub>) with temperature and phase structure (values from ref.166).

The surface area per polar group for the homologous series of straight chain calcium soaps (C<sub>12</sub>-C<sub>18</sub>) is relatively independent of chain length<sup>166</sup>. Hence, the values for calcium myristate (C<sub>14</sub>Ca) given in table 6.8, are representative of this series of soaps. For CaD<sub>4</sub> at 25°C, the surface area per head group that would result in a lamellar structure was calculated to be 28.4Å<sup>2</sup> (see chapter 5). This is significantly larger than the area per head group of calcium myristate at the equivalent temperature, which would indicate that either:

- a less dense packing of the head groups in exists CaD<sub>4</sub> than is present in the monomeric straight chain calcium soaps of this structure, or
- there is some interdigitation of the soap molecules within the bilayers.

A comparison of the bilayer thickness resulting from the proposed lamellar structure at 25°C (i.e. d<sub>0</sub> = 30.8Å), with the molecular dimensions of CaD<sub>4</sub> (i.e two 'all trans' amphiphile repeat units, each of 20.25Å in length; see section 6.2.1.2) would indicate an inclination of non-interdigitated hydrophobic chains to the basal planes of the lamellae, of 49.5°. This degree

of tilting is considerably less than the  $73^\circ$  found in calcium myristate (this value was calculated from data presented by Spegt and Skoulios<sup>166</sup>).

The structural parameters derived from the proposed lamellar structure for  $\text{CaD}_4$  at  $25^\circ\text{C}$  cannot be used to differentiate between the non-interdigitated or interdigitated bilayer structures and, do not preclude the possibility of either of these lamellar modifications. However, these parameters do indicate a packing of the molecules that is significantly different to that found in the crystalline lamellar structure of monomeric straight chain calcium soaps. As this tentative proposal of the lamellar phase is based on a diffraction pattern containing only two diffraction signals, further work is obviously required to verify this proposition and to fully characterise the crystalline structure of  $\text{CaD}_4$ .

The proposal that, the optical texture of the solid film was not indicative of the equilibrium structure of  $\text{CaD}_4$  at  $25^\circ\text{C}$ , due to the previous quenching of the sample, cannot explain the different structures indicated by the optical and X-ray studies of the birefringent fluid phase of  $\text{CaD}_4$  (i.e. the samples were not cooled prior to carrying out the experimental observations at  $200^\circ\text{C}$ ). Whilst a convincing explanation for these discrepancies eludes us, and it is not possible to propose a structure for the birefringent fluid phase of  $\text{CaD}_4$ , the following points should be noted. Firstly, aggregates of rod micelles have been proposed as the structures of the intermediate phases formed by monomeric straight chain calcium soaps<sup>170</sup>. Hence, although the structures proposed for the monomeric calcium soaps are not regarded as definite, the possible occurrence of a hexagonal phase for  $\text{CaD}_4$  (as is indicated by microscopy) would be in keeping with the generally accepted

behaviour of these soaps (i.e. based on rod micelles). Secondly, the proposal of a lamellar structure for  $\text{CaD}_4$  at  $200^\circ\text{C}$ , would give rise to an area per polar group of  $37.2\text{\AA}^2$ , which is very similar to that found in monomeric straight chain soaps at equivalent temperatures (see table 6.8). Although the phase structures involved may not be identical, this indicates similar packing densities in these related amphiphiles at similar temperatures and may therefore support the proposal of the lamellar phase.

In addition, the positions of the principle and second order reflection of the X-ray patterns of  $\text{CaD}_4$  and  $\text{NaD}_4$  in the range 25 to  $200^\circ\text{C}$ , are almost identical (see tables 6.4 and 6.7). Considering the obvious molecular similarities between these sodium and calcium salts, this would seem to be strong evidence of a similarity of phase structure. Unfortunately, this can be interpreted in one of two ways, firstly, as supporting the proposition that the lamellar phase as the structure present in both classes of oligomeric amphiphilic siloxanes at temperatures at least up to  $200^\circ\text{C}$ , or, secondly, putting in doubt the previous proposal of the lamellar structure for the semi-crystalline phase of  $\text{NaD}_4$ .

Although additional work is obviously required to characterise the structures of the individual phase regions of  $\text{CaD}_4$ , some comparisons between the phase behaviour of  $\text{CaD}_4$  and the monomeric straight chain calcium soaps, may be made. Whilst the behaviour of the monomeric calcium soaps varies with the length of the hydrocarbon chain, the overall behaviour of this homologous series of amphiphiles is very similar<sup>24,153,166,170,304</sup>. With increasing temperature, the structure of these anhydrous soaps changes from the lamellar crystalline state at  $120^\circ\text{C}$ ,

through a number of intermediate phases of various degrees of order, to a reverse hexagonal fluid phase at 180°C, and to the isotropic liquid at greater than 350°C. This step-wise melting from the crystalline state to the isotropic liquid, occurs via the melting of the hydrocarbon chains, followed by the melting of the polar groups. The structure of the intermediate phases, although known to involve disordered alkyl chains, has not been fully resolved. The structure of the high temperature reverse hexagonal phase is established.

At room temperature, X-ray diffraction indicates that  $\text{CaD}_4$  exists as a crystalline lamellar phase, which is also the crystalline structure of the monomeric straight chain calcium soaps and  $\text{NaD}_4$ . However, the X-ray spacings also indicate that there exists:

- a less dense packing, with a greater angle of tilt, of the non-interdigitated amphiphiles of  $\text{CaD}_4$ , than is found in monomeric calcium soaps, or,
- an interdigitated arrangement of the molecules themselves within the bilayer.

X-ray diffraction indicates that the lamellar structure remains essentially unchanged at 200°C, although the optical observations, which were indicative of a hexagonal fluid phase at temperatures greater than 155°C, do not support this.

DSC indicates a weak transition occurring at around 50°C, during the initial heating and subsequent controlled cooling of samples. Whilst the enthalpy of this 'transition' is such that no firm conclusions may be drawn, it is interesting to note that similar transitions have been identified for calcium

stearate at 50°C<sup>155</sup>, and NaD<sub>4</sub> and NaD<sub>5</sub> at 60°C (see 6.2.1.2). X-ray diffraction indicates that, as is the case in the monomeric calcium soaps<sup>166</sup> and NaD<sub>4</sub>, this 'transition' does not result in a significant change in the overall crystalline lamellar structure of CaD<sub>4</sub>.

The monomeric calcium soaps undergo a number of additional transitions between 50°C and the formation of the reverse hexagonal phase at about 180°C. Of these, the transition occurring at about 110°C, is believed to result from a change in the packing of the soap molecules within the lamellar phase<sup>166</sup>. A transition at about 120°C, is thought to represent the melting of the hydrocarbon chains and the formation of a body centred tetragonal lattice made up of reverse rod micelles of finite length<sup>170</sup>. At about 160°C, a further modification to the phase structure results in the formation of the birefringent fluid phase. The nature of this phase region has yet to be fully established<sup>170</sup>. At about 180°C, the reverse hexagonal phase is the accepted structure of all the straight long-chain calcium soaps<sup>24,149,166,170</sup>.

In the case of CaD<sub>4</sub>, only one transition has been observed in the range 50 to 480°C during DSC analysis. This transition (i.e T1 at 159°C) corresponds to the formation of the fluid phase of CaD<sub>4</sub> and, occurs at a temperature similar to the formation of the fluid phase of the monomeric calcium soaps. This may indicate that for CaD<sub>4</sub>, T1 embodies all the changes occurring in the multiple steps of the monomeric calcium soaps up to the formation of the birefringent fluid phase. However, in the absence of established structures for the phases of CaD<sub>4</sub> above or below T1, no firm conclusions may be drawn.

Whatever the nature of T1, in view of the relatively high temperature at which this transition takes place and the fluidity of the resulting phase, it seems reasonable to attribute this to a complete melting of the weakly interacting non-polar regions of these amphiphiles and some partial melting of the polar groups. In comparison with the monomeric calcium soaps, it is reasonable to propose that the polar groups will retain some aspects of an ordered arrangement up to the transition to the low viscosity isotropic liquid at around 480°C.

It is interesting to note, that the wide-angle X-ray diffraction patterns at 50 and 200°C did not exhibit spacings corresponding to either a crystalline or liquid-like arrangements of the C<sub>10</sub> alkyl moieties of the hydrophobic chains of CaD<sub>4</sub>. Hence, no direct evidence regarding the nature of the non-polar chains is available. This may be very important, indicating that the structure is rather irregular.

If T1 does represent the complete melting of the non-polar chains and some partial melting of the polar groups, the enthalpy change of T1 (i.e. 16 KJ.mole<sup>-1</sup>) must be equal to or greater than the maximum enthalpy of fusion of the non-polar chains of CaD<sub>4</sub>. Remembering that CaD<sub>4</sub> is a 'multi-amphiphile' molecule, the enthalpy changes occurring per amphiphile repeat unit is equal to 4 KJ.mole<sup>-1</sup>. This is much less than the enthalpy change associated with the melting of fatty acids of equivalent chain length. As was the case with NaD<sub>4</sub> and NaD<sub>5</sub>, this may reflect the reduced packing efficiency of the non-polar chains as a result of their attachment to the siloxane backbone (see 6.2.1.2). This reduced packing efficiency may also be reflected in the increased area per polar group in the proposed

lamellar crystalline phase of  $\text{CaD}_4$ , relative to that of the monomeric calcium soaps of this structure. This behaviour is also analogous to that of  $\text{NaD}_4$ .

The enthalpy change and the temperature of the transition to the low viscosity isotropic liquid could not be measured accurately because of the width of the DSC peak and the degree of thermal degradation also occurring. However, the magnitude of the enthalpy change occurring during this endothermic transition (i.e. approximately  $10 \text{ kJmol}^{-1}$  of amphiphile repeat unit) would indicate that considerable structural order remains in the viscous isotropic phase of  $\text{CaD}_4$ . Due to the high temperature at which this transition occurred it is reasonable to assume that this reflects the order inherent in the polar groups. The fact that considerable order remains within the polar groups of  $\text{CaD}_4$  prior to the formation of the isotropic liquid, is analogous to the behaviour of the monomeric straight chain calcium soaps<sup>160</sup>.

What is not analogous to the behaviour of the monomeric calcium soaps, is the formation of a viscous isotropic phase preceding the transition to the low viscosity isotropic liquid. Whilst a number of structures have been proposed for the isotropic phases encountered in anhydrous amphiphiles<sup>24,149</sup>, as an attempt to obtain diffraction data at  $300^\circ\text{C}$  was abandoned due to the degradation of the sample, it is not possible to propose a phase structure for the isotropic viscous phase observed here. Indeed, the possibility that this degradation was not implicated in the transition can not be ruled out. In addition, no DSC transition was observed corresponding to the transition from the birefringent fluid phase to this viscous isotropic phase. A small enthalpy change, coupled with the broad temperature range

over which this transition occurred could explain the absence of a DSC signal corresponding to this optical event. However, in the absence of a sound understanding of the structures of the birefringent and isotropic viscous fluid phases of  $\text{CaD}_4$ , no real conclusions may be drawn here.

A significant observation is the increased thermal stability of the ordered phase region of  $\text{CaD}_4$ , relative to that of the monomeric calcium soaps. The transition to the low viscosity isotropic phase occurred at a temperature approximately  $140^\circ\text{C}$  greater than is found in calcium stearate<sup>160,166</sup>. At the temperature at which the transition to the low viscosity isotropic liquid occurs, it is reasonable to propose that this transition is primarily associated with the polar groups. As the individual polar groups of  $\text{CaD}_4$  are in a chemical environment that is essentially identical to that found in monomeric calcium soaps, it is also reasonable to suggest that the difference in the behaviour of these related monomeric and oligomeric calcium soaps arises as a consequence of the multi-amphiphile nature of  $\text{CaD}_4$ . As was the case with the oligomeric sodium salts, this may be qualitatively understood by considering that the amphiphilic side-chain repeat units of these oligomers cannot escape from the micelle as individual amphiphiles due to their covalent bonding to the other amphiphiles. Hence the micelle, and the mesophases which are built up by these micelles, are stabilised. In addition, the individual amphiphilic side-chain units of each oligomer may not be isolated to the same polar/non-polar interface. Hence, these molecules may act as 'molecular cross-links' between micelles thus maintaining the mutual orientation of the micelles and enhancing the stability of the ordered phase region.

### 6.2.2.3 Conclusions

The thermotropic behaviour of  $\text{CaD}_4$  seems to have much in common with that of the monomeric straight chain calcium soaps and, some aspects of the behaviour of the equivalent sodium soaps,  $\text{NaD}_4$  and  $\text{NaD}_5$  (see section 6.2.1.2). Hence, although there are significant differences that require a more in-depth study, the following general conclusions may be drawn:

1. The well established principles explaining the phase behaviour of monomeric amphiphiles seem to be generally applicable to these novel cyclic amphiphiles.
2. As these principles dictate, the non-polar and polar moieties of these amphiphiles tend to aggregate in the neat state. The driving force for this aggregation will be the enthalpic contribution from the association of the polar groups.
3. Due to the molecular structure of these amphiphiles (i.e. packing constraints), the crystalline structure at room temperature is probably that of a bilayer, although the arrangement within the bilayer is less clear. It is interesting to note that  $\text{NaD}_4$  and  $\text{NaD}_5$  exhibit a similar crystalline structure.
4. The absence of an identifiable thermal event in the range  $-170$  to  $25^\circ\text{C}$ , probably indicates that no thermal induced transitions are taking place in this range. Thus, the proposed lamellar phase would also remain at the lower temperatures.
5. In these lamellar phases, the non-polar chains and the polar head groups appear to be crystalline. However, the enthalpy change ascribed to the melting of the individual hydrophobic (i.e.  $\leq 4$   $\text{KJ.mole}^{-1}$ ), indicates that the attachment of the  $\text{C}_{11}$  carboxylates to the rigid cyclic siloxane backbone limits the degree of crystallinity of

the C<sub>10</sub> alkyl chains, and the efficient packing of the amphiphiles.

6. At around 155°C, there appears to be a one-stage melting of the non-polar chains of these cyclic amphiphiles as well as a partial melting of the polar groups (i.e. T1). This process results in the formation of a birefringent fluid phase. This melting of the non-polar chains, may entail all the changes occurring in the step-wise melting of the alkyl chains of monomeric straight chain calcium soaps. However, as the structure of the resulting birefringent phase remains to be established, it is unclear whether T1 is also accompanied by a change in the overall phase structure.

7. The formation of the birefringent fluid phase of CaD<sub>4</sub> occurs at a temperature similar to that of the monomeric calcium soaps, although the structure of this phase may not be typical of the monomeric soaps. The structure of this phase requires further investigation.

8. At around 275-295°C, a viscous isotropic liquid formed. Although no structure can be proposed for this phase, this behaviour is not typical of the monomeric soaps and warrants further investigation.

9. At around 480°C, the polar groups of these amphiphiles melt completely. Again, this is analogous to the step-wise melting of monomeric calcium soaps. The melting of the polar groups coincides with the formation of the low viscosity isotropic liquid.

10. The attachment of the C<sub>11</sub> calcium carboxylates to the cyclic siloxane increases the thermal stability of the ordered phase regions of this amphiphile. The formation of multi-amphiphile molecules may explain this effect. In addition the formation of molecular cross-links between micelles may become important.

### 6.3. The Lyotropic Phase Behaviour

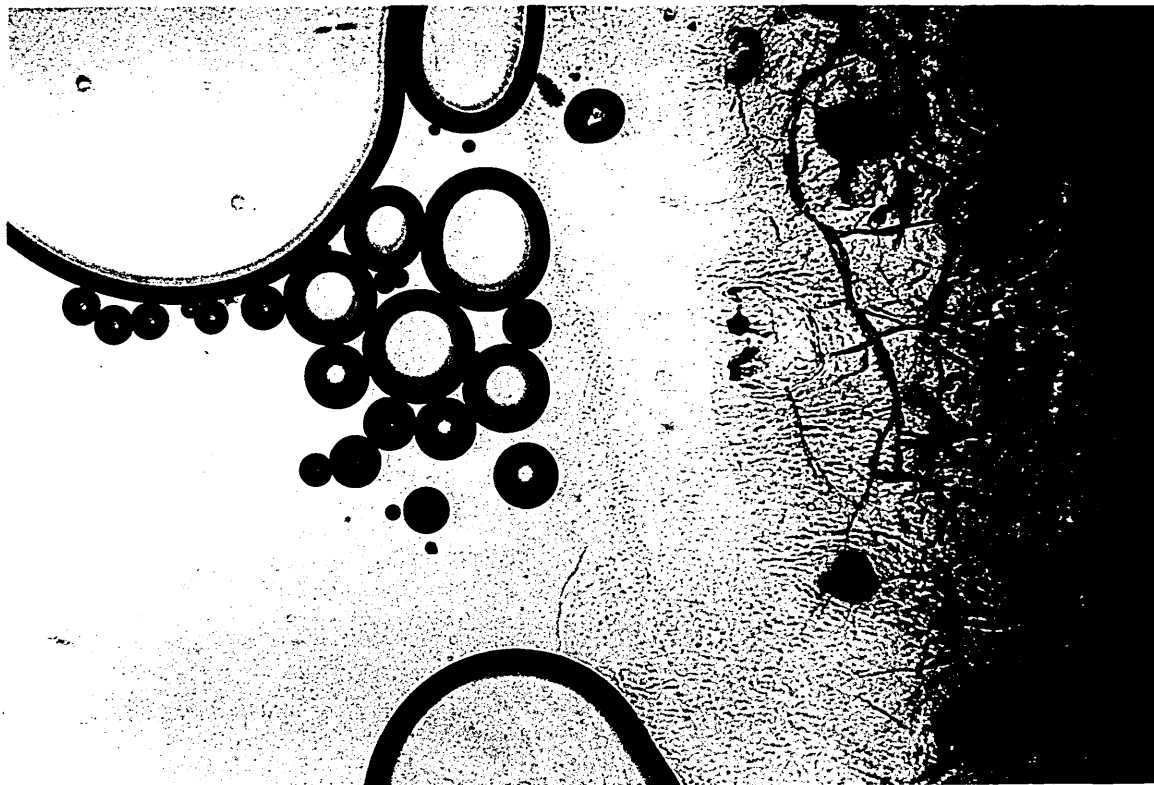
#### 6.3.1. The Sodium Salt, NaD<sub>4</sub>

##### 6.3.1.1 Results

##### 6.3.1.1.1 Polarising Optical Microscopy

A film of NaD<sub>4</sub> was prepared by placing a powdered sample between a cover-slip and a microscope slide at 270°C, depressing the cover-slip and then rapidly cooling to room temperature. Microscopy of this film indicated a birefringent solid phase at room temperature. The texture of this solid was indicative of a hexagonal phase (see figure 6.2). Water was contacted with the edge of the amphiphile at 5°C. After 10 minutes, the sample was gradually heated up to 100°C.

At 20-21°C, a thin mesophase region, which exhibited a non-geometric texture and a viscosity characteristic of the hexagonal phase<sup>16</sup>, was formed (see figure 6.20). As the temperature was increased, this band became gradually wider. At 45°C two additional mesophase regions were identified (see figure 6.21). At amphiphile concentrations between the hexagonal region and the solid amphiphile, a low viscosity birefringent phase formed. This phase exhibited a mosaic texture and a viscosity typical of the lamellar mesophase<sup>16</sup>. With the polars removed, the lamellar/hexagonal phase boundary was marked by a refractive index discontinuity (see figure 6.21). In addition, close examination of the high surfactant concentration side of the hexagonal region, indicated the presence of an area of slightly different texture, and of a slightly lower viscosity, compared to the majority of the hexagonal mesophase region (see figures 6.21). The transition between these regions was not marked by a clear discontinuity in refractive index. All three mesophases were stable to greater than 100°C. No cooling of the samples was carried out.



$L_{\alpha}$

SOLID

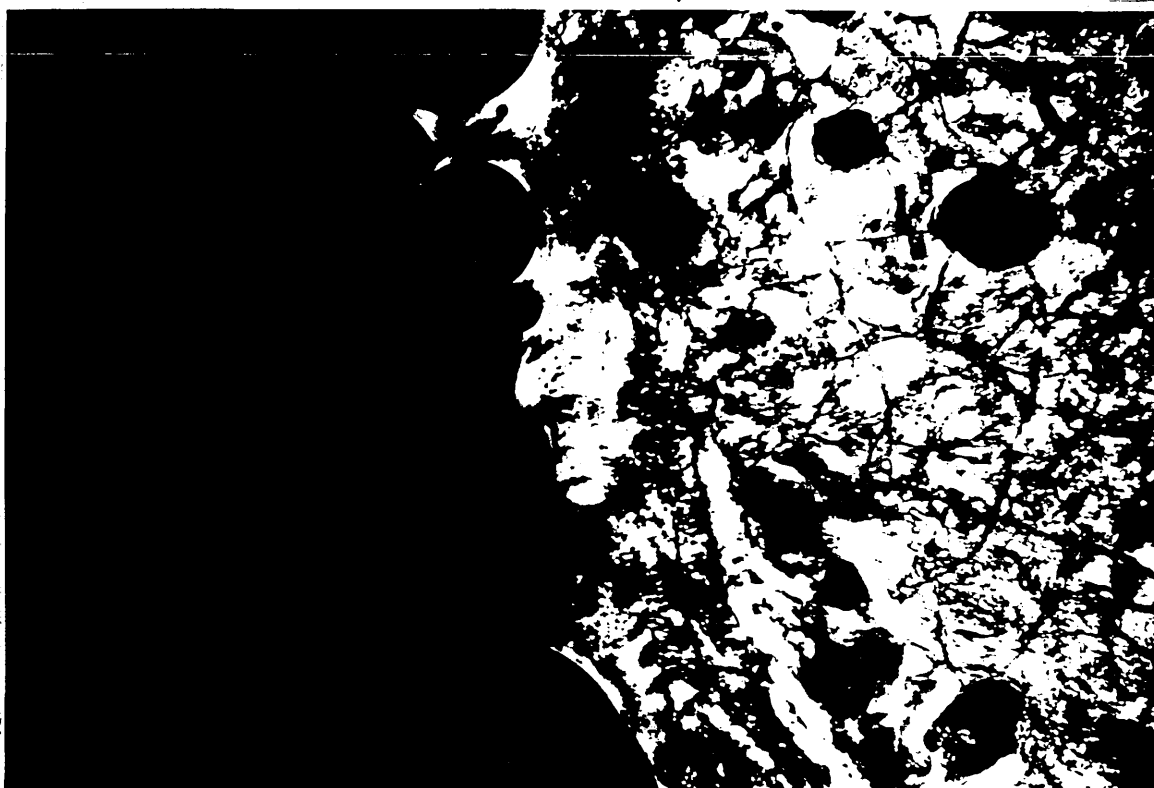


Figure 6.20. A sample of  $\text{NaD}_4$  in contact with water at  $30^\circ\text{C}$ . a) with cross-polars in place and b) with cross-polars removed.

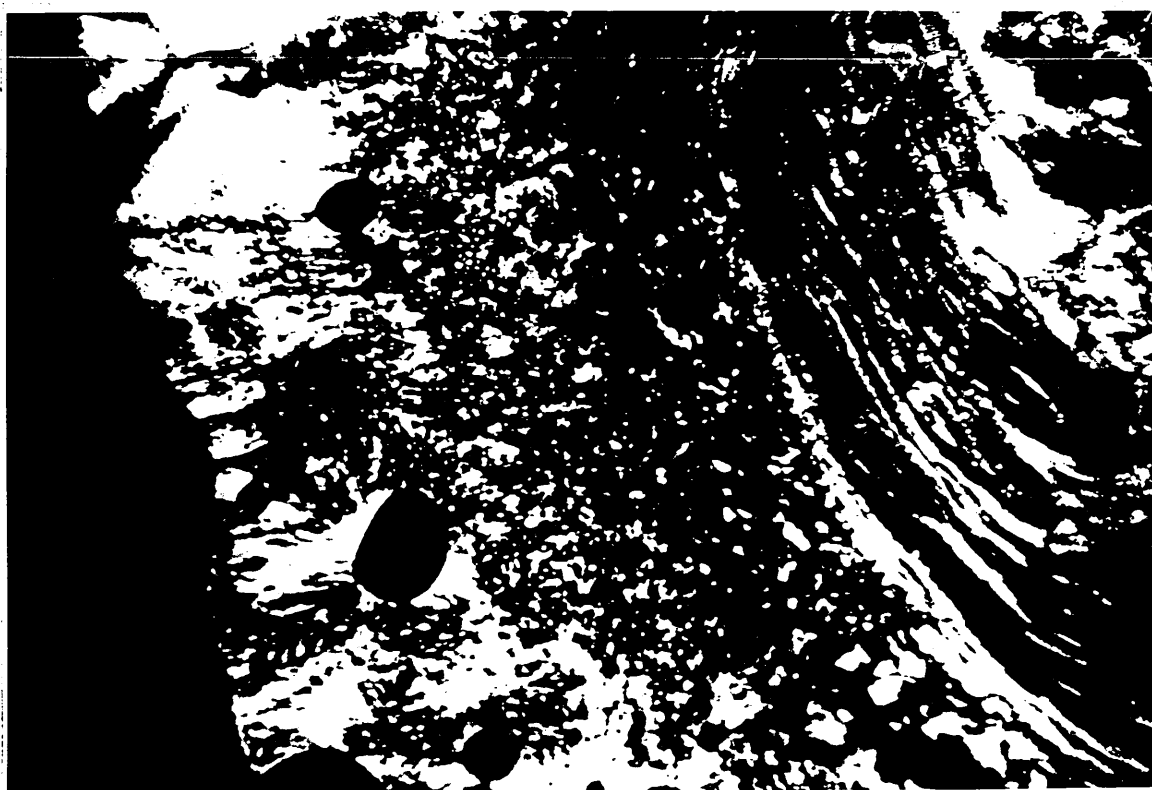


Figure 6.21 A sample of  $\text{NaD}_4$  in contact with water at  $55^\circ\text{C}$ . a) with cross-polars in place and b) with cross-polars removed.

### 6.3.1.2 Discussion

Time did not permit an in-depth study of the lyotropic phase behaviour of this amphiphile. Instead, an overview of the phase behaviour of the amphiphile/water system between 5 and 100°C was established using the penetration technique of Lawrence<sup>219</sup>. The phase behaviour outside this temperature range was not investigated, as this represents the practical temperature range for soaps in aqueous systems and a number of experimental difficulties are encountered when determining aqueous phase behaviour above and below these limits. It is worth repeating that the penetration technique indicates the phases that form with changing amphiphile concentration and, where applicable, gives the upper and lower temperature limits of each phase; no quantitative information regarding the composition of a phase can be derived from this technique.

During penetration experiments, NaD<sub>4</sub> formed a number of lyotropic mesophases with water. At 5°C, only the solid amphiphile and water were observed. As the temperature was increased, three birefringent mesophase regions were formed; each mesophase occurring at a particular temperature. This lower temperature limit for formation is the 'penetration' temperature,  $T_{pen}$ . The first of these mesophases exhibited a non-geometric texture and an intermediate viscosity that was characteristic of a hexagonal phase ( $H_1$ )<sup>16</sup>. At higher temperature and higher concentration, an intermediate and the lamellar ( $L_\alpha$ ) mesophases formed simultaneously. The lamellar phase, which occurred at highest amphiphile concentration (i.e. adjacent to solid amphiphile) was characterised by a mosaic texture and a relatively low viscosity<sup>16</sup>. The intermediate phase region, occurring at amphiphile concentrations between  $H_1$  and  $L_\alpha$ , had a non-geometric texture and a viscosity typical of a hexagonal phase. Whilst, there was a distinct first

order boundary between the lamellar and the intermediate phase, no such boundary was observed between the intermediate and the 'normal' hexagonal phase regions. Despite this, the hexagonal and intermediate phase regions were distinguishable.

The absence of a phase boundary between the 'normal' hexagonal and the intermediate phase regions, and their similar textures, may indicate that the intermediate phase is a variant of the conventional hexagonal phase. This leads us to propose a deformed hexagonal ( $H_{1d}$ )—thought to consist of rod micelles arranged on a deformed hexagonal lattice—as the structure for this region<sup>16,185</sup> (see figure 6.22).

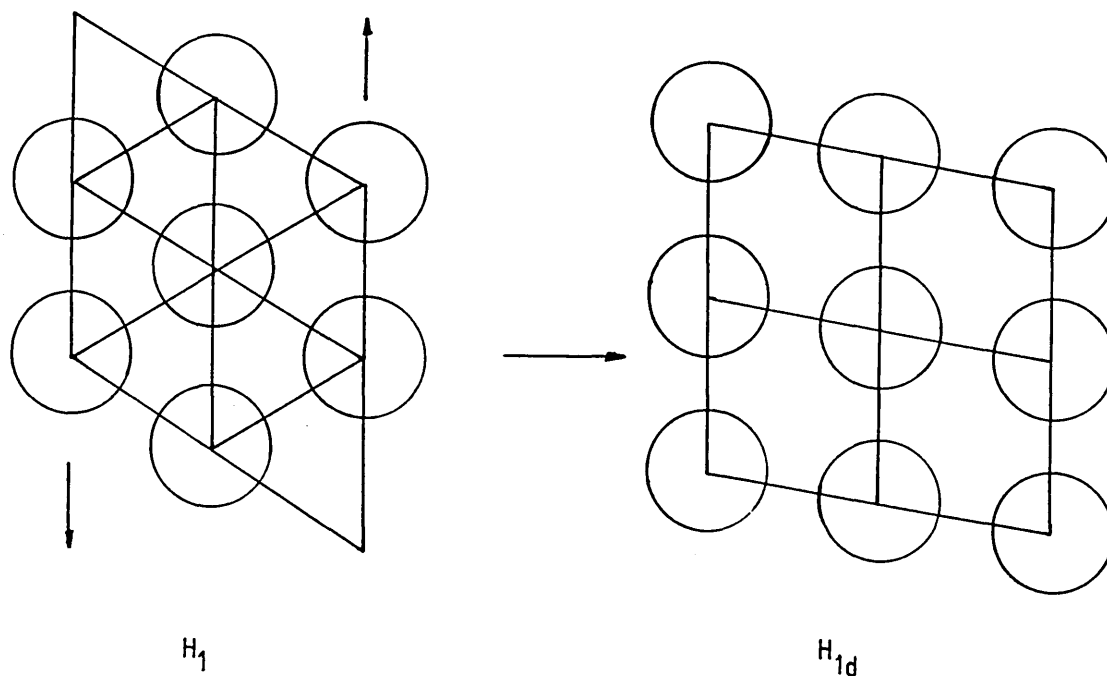


Figure 6.22 A schematic representation of the deformed hexagonal phase ( $H_{1d}$ ) compared to the normal hexagonal phase ( $H_1$ ).

A summary of the sequence of phases observed for NaD<sub>4</sub> with increasing temperature and concentration is given in table 6.9 below.

Temperature (°C)	Phase sequence	Observation
21-22	S-H <sub>1</sub> -L <sub>1</sub>	Formation of the H <sub>1</sub> phase
45	S-L <sub>α</sub> -H <sub>1d</sub> -H <sub>1</sub> -L <sub>1</sub>	Formation of the L <sub>α</sub> phase and an additional region, that was distinct from, but continuous with, the hexagonal phase region
100	As above	All phases present at 45°C, still present

Where S = solid amphiphile; L<sub>α</sub> = lamellar mesophase; H<sub>1d</sub> = intermediate region; H<sub>1</sub> = hexagonal mesophase; L<sub>1</sub> = isotropic liquid

Table 6.9 Summary of the lyotropic phase sequences of NaD<sub>4</sub> developed with increasing temperature.

Having established the main features of the aqueous phase behaviour of this oligomeric amphiphile from 5 to 100°C, it was of interest to compare this behaviour with that of related systems (see chapter 2 for review of the related monomeric and polymeric amphiphiles). In this respect, the results of two studies, which have also employed the penetration technique to separately investigate the aqueous phase behaviour of monomeric sodium alkanoates<sup>185</sup> and an amphiphilic side-chain polymer with C<sub>11</sub> sodium alkanoate moieties attached to every unit of a linear siloxane backbone<sup>66</sup>, are of particular interest. The results of these studies have been summarised in table 6.10, along with those obtained here for NaD<sub>4</sub>.

Amphiphile	Phase				
	H <sub>1</sub>	(int.1)	V <sub>1</sub>	(Int.2)	L <sub>α</sub>
C <sub>8</sub> Na	<23	-	66	-	77
C <sub>10</sub> Na	29	67	69	-	72
C <sub>12</sub> Na	42	65	-	69-85	74
C <sub>14</sub> Na	54	68	-	-	73
C <sub>16</sub> Na	67	-	-	78	82
C <sub>18</sub> Na	75	-	-	83	85
*Polymer	<20	-	-	-	70
NaD <sub>4</sub>	21-22	45	-	-	45

where C<sub>n</sub>Na = the homologous series of sodium alkanoates; the T<sub>pen</sub> values for these sodium soaps taken from reference (185).

Int.1 and Int.2 thought to be the deformed hexagonal and a thin bilayer structure, respectively.

\*polymer = the ionic polymer studied by Hall in reference (66).

Table 6.10 A comparison of the mesophase penetration temperatures (T<sub>pen</sub>) for NaD<sub>4</sub>, the related monomeric sodium alkanoates and the linear amphiphilic side-chain siloxane.

As can be seen from table 6.10, the sequence of mesophases formed by monomeric sodium alkanoates (i.e. the sodium soaps) with increasing temperature and/or increasing concentration is the hexagonal followed by the lamellar, with a variety of birefringent and non-birefringent mesophases occurring over a narrow concentration around the hexagonal to lamellar transition region<sup>185</sup>. The nature of the phases formed at intermediate soap concentrations depends on the length of the hydrocarbon chain. With short hydrocarbon chain derivatives, the non-birefringent bicontinuous cubic phase (V<sub>1</sub>) occurs, while at higher chain lengths the

birefringent deformed hexagonal ( $H_{1d}$ ) and/or a thin bilayer structure occur (where these phases coexist, the bilayer structure occurs at higher amphiphile concentration). The critical chain length for the cross-over from the cubic to the birefringent intermediate phases for monomeric sodium soaps occurs at around the  $C_{10}$  soap.

Comparing the phase behaviour of the ionic polymer with that of the monomeric sodium soaps<sup>185</sup>, and from previous experience with a non-ionic side-chain polysiloxane, Hall concluded that<sup>66</sup>:

- the attachment of amphiphilic units to a polysiloxane backbone does not significantly restrict the translational motion and micelle packing of the amphiphiles
- there is little difference between the phase behaviour of the polymeric amphiphile from that of the monomeric sodium alkanoate systems
- the general behaviour of this ionic polysiloxane could be explained in terms of the increase in alkyl chain length of the amphiphile due to fixation to the siloxane backbone.

Despite these similarities, it was noted that the behaviour of the ionic polymer and the monomers of similar lipophilic/hydrophilic balance was not identical. The mesophases formed by the polymer were, once formed, more stable at lower temperatures and, the intermediate phases that are characteristic of sodium soaps of similar chain length did not occur. No explanations for the different behaviour of the polymer and the monomers was offered.

Comparing the behaviour of  $\text{NaD}_4$  with that of the monomeric sodium soaps, the sequence of phases formed by  $\text{NaD}_4$  with increasing temperature is identical to that of sodium myristate (i.e.  $\text{C}_{14}\text{Na}$ , see table 6.10). At this point, it should be noted that in the absence of supporting spectroscopic or X-ray diffraction data, the assignments of structures for the individual phase regions of  $\text{NaD}_4$  should be viewed with some caution<sup>24,149</sup>. However, the fact that the overall proposed behaviour of  $\text{NaD}_4$  is so similar to that of the related monomers and the ionic polymer, seems to indicate the validity of these proposals. Hence, the fact that  $\text{NaD}_4$  forms three mesophases common to the monomeric sodium soaps would seem to indicate that the attachment of  $\text{C}_{11}$  sodium alkanoates to every unit of a cyclic siloxane backbone does not significantly restrict the translational and rotational motions and the micelle packing of these amphiphiles. The fact that the sequence of phases formed by  $\text{NaD}_4$  is identical to that of sodium myristate ( $\text{C}_{14}\text{Na}$ ) seems to indicate that the result of coupling these  $\text{C}_{11}$  amphiphiles to the siloxane backbone is, therefore, to effectively lengthen the non-polar chain of the amphiphilic units by approximately three methylene groups. These observations support the results of previous studies<sup>66,67</sup>.

Unlike the polymeric equivalent,  $\text{NaD}_4$  did form an intermediate phase at concentrations around the hexagonal to lamellar transition region and this behaviour is typical of the monomeric sodium soaps of a similar hydrophilic/hydrophobic balance<sup>185</sup>. As the amphiphilic repeat units of the polymer and  $\text{NaD}_4$  are chemically identical, it seems reasonable to propose that the occurrence of this intermediate phase in the phase sequence of the oligomer, but not the polymer, was determined by an effect other than the

chemical nature of the respective amphiphiles (i.e not subtle changes in the hydrophobic/hydrophilic balance of the amphiphilic repeat units of the oligomer and the polymer). The rationalisation of the different behaviour of the oligomer and the polymer should therefore consider:

- the degree of polymerisation of these multi-amphiphile molecules (i.e. ~50 for the polymer and 4 for NaD<sub>4</sub>)
- the probable increased polydispersity of the polymeric amphiphile (see chapter 3)
- the cyclic and linear natures of the backbones of NaD<sub>4</sub> and the polymer, respectively.

As the deformed hexagonal phase structure is made up of micelles that are not restricted in aggregation number by the dimensions of the micelle (i.e. the micelle may expand in one dimension to accommodate additional amphiphilic units), it is not easy to envisage how the increased degree of polymerisation or the probable increased polydispersity of the linear polymer may preclude the formation of this intermediate structure<sup>67</sup>. Whilst the study of the thermotropic phase behaviour of NaD<sub>4</sub> indicated that the attachment of C<sub>11</sub> sodium alkanoates to the cyclic methylsiloxane backbone limited the efficient packing of the non-polar chains of these amphiphiles in the crystalline state, the fact that NaD<sub>4</sub> exhibits a lyotropic mesophase sequence identical to C<sub>14</sub>Na may indicate that this limitation applies only to the crystalline close packing of the non-polar chains, and not to the packing of the fused non-polar chains (as is the case in these lyotropic mesophases). Hence, at this stage, no convincing explanation for the difference in the phase behaviour of NaD<sub>4</sub> and the linear polymer of the same amphiphilic repeat unit, may be offered.

Although  $\text{NaD}_4$  exhibits the same sequence of phases as  $\text{C}_{14}\text{Na}$ , the oligomer forms these mesophases at much lower temperatures. The polymeric amphiphile<sup>66</sup> also forms the hexagonal and a lamellar mesophase at lower temperatures than any of the long-chain monomeric sodium soaps and, once formed, these mesophases are stable to a much lower temperature than those of the monomers. In the absence of any cooling of the samples during the penetration experiments carried out during this work, no comment on the low temperature stability of the phases formed by  $\text{NaD}_4$  may be made. However,  $\text{NaD}_4$  and  $\text{C}_{14}\text{Na}$  form the same sequence of mesophases and the factors determining the packing of the amphiphilic units of these molecules are probably essentially the same (i.e. packing constraints)<sup>16</sup>.

The fact that  $\text{NaD}_4$  forms these phases at much lower temperatures could indicate that the water solubility of the amphiphilic repeat units of the oligomer is greater than that of the monomeric sodium soaps. As the sodium carboxylate moiety is the polar group common to the monomeric soaps and  $\text{NaD}_4$ , it is reasonable to attribute any changes in solubility to the nature of the respective hydrophobic chains. The hydrophobicity of a non-polar chain is proportional to the surface area of the chain and the interfacial tension between the chain and water<sup>17</sup>. Considering that the volume of the non-polar chain of  $\text{C}_{14}\text{Na}$  is slightly larger than the non-polar chain of the repeat unit of  $\text{NaD}_4$  (i.e. approximately  $378$  and  $340\text{\AA}^3$ , respectively, assuming that the volumes of the  $\text{CH}_2$ ,  $\text{CH}_3$ , and  $\text{OSi}(\text{CH}_3)$  groups are  $27$ ,  $54$  and  $73\text{\AA}^3$ , respectively), and the oil/water interfacial tension of a hydrocarbon is also greater than that of a dimethylsiloxane (i.e.  $52$  and  $42$  dynes. $\text{cm}^{-1}$ , respectively<sup>324</sup>), the hydrophobicity of the repeat unit

of NaD<sub>4</sub> would indeed be slightly less than that of C<sub>14</sub>Na. However, as NaD<sub>4</sub> forms hexagonal and lamellar mesophases at temperatures below even C<sub>8</sub>Na (see table 6.10), this can not be the major factor determining the lower T<sub>pen</sub> for the mesophases of NaD<sub>4</sub>.

Remembering the conclusions drawn from the thermotropic behaviour of NaD<sub>4</sub>, an additional effect that may contribute to an increase in the water solubility of the amphiphilic units of this oligomeric amphiphile, is the reduced efficiency of chain packing within the non-polar chains of NaD<sub>4</sub>, relative to that of the alkyl chains of monomeric sodium soaps (see section 6.2.1.2). Thus, the dissolution of the amphiphilic repeat units of NaD<sub>4</sub> in an aqueous medium, should require less energy to mix with the solvent than the equivalent sodium soaps (i.e. in proportion to the respective heats of fusion of these amphiphiles). A similar consideration may also explain the lower T<sub>pen</sub> of the polymer studied by Hall<sup>66</sup>.

### 6.3.1.3 Conclusions

The proposed lyotropic phase behaviour of NaD<sub>4</sub> requires further corroboration through the use of additional spectroscopic techniques (see chapter 5), and further research is required to fully understand the implications of the results obtained during this study. However, the following general conclusions may be drawn:

1. The attachment of a C<sub>11</sub> sodium alkanoate to every unit of a cyclic methylsiloxane does not significantly restrict the translational and rotational motion and the micelle packing of these amphiphiles in lyotropic mesophases (i.e. there is no significant restriction imposed on the conformations of the fused non-polar chains).

2. As has been the case with previous studies of linear amphiphilic side-chain siloxanes, the result of coupling these  $C_{11}$  amphiphiles to the cyclic siloxane backbone is to effectively lengthen the non-polar chain of each amphiphilic unit by approximately 3 methylene units. Hence,  $NaD_4$  forms the same sequence of mesophases as sodium myristate ( $C_{14}Na$ ).

3. The oligomeric amphiphiles form mesophases at temperatures significantly below those of monomeric sodium soaps of similar hydrophobic/hydrophilic balance. This may be explained by a less efficient crystalline packing of the non-polar chains of these oligomers.

### 6.3.2 The Calcium Salt

#### 6.3.2.1 Results of Polarising Optical Microscopy

A film of  $CaD_4$  was prepared by placing a powdered sample between a cover-slip and a microscope slide at  $200^\circ\text{C}$ , depressing the cover-slip and then rapidly cooling to room temperature. Microscopy of this film indicated a birefringent solid phase at room temperature. The texture of this solid was indicative of a hexagonal phase (see figure 6.14). Water was then contacted with the edge of the amphiphile at  $5^\circ\text{C}$ . After 10 minutes the sample was gradually heated to  $100^\circ\text{C}$ . There was no evidence of any interaction between the sample and the water in this temperature range.

#### 6.3.2.2 Discussion

Having suggested that the attachment of  $C_{11}$  sodium alkanoate moieties to every unit of a cyclic siloxane backbone has an effect similar to an extension of the non-polar chains of the individual units of these molecules

by approximately 3 methylene units, it seems reasonable to propose that a similar attachment of C<sub>11</sub> calcium alkanoates would have an analogous effect. This would give rise to an oligomer with similar phase behaviour to calcium myristate (i.e. C<sub>14</sub>Ca). It is, therefore, perhaps not surprising that CaD<sub>4</sub> did not show any interaction with water in the range 5 to 100°C. This is analogous to the behaviour of the monomeric calcium soaps and reflects the strong forces of attraction between the polar groups of these soaps.

#### 6.3.2.3 Conclusions

CaD<sub>4</sub> did not form any lyotropic mesophases with water in the temperature range 5 to 100°C. This is analogous to the behaviour of the monomeric calcium soaps and presumably reflects the strong forces of attraction between the polar groups of these soaps.



crystalline at room temperature and become insoluble in water with relatively short hydrophobic chains (i.e.  $n_c > 18$  and  $> 12$  for the hydrocarbon and fluorocarbon chains, respectively)<sup>13,328</sup>. The linear amphiphiles studied here are based on a dimethylsiloxane non-polar moiety and, therefore, represent novel variants of the conventional amphiphiles. Unlike the conventional amphiphiles, due to the high chain mobility and the low  $T_g$  of the siloxane backbone ( $\approx -125^\circ\text{C}$ )<sup>327</sup>, these amphiphilic siloxanes represent extremely long straight chain amphiphiles with highly flexible, low melting hydrophobic segments. Such amphiphiles may be water soluble even at low temperatures amphiphiles with relatively long-chain non-polar moieties.

This potential for the synthesis of amphiphiles with extremely long, low melting, hydrophobic segments, may also give rise to interesting properties in the area of oil soluble soaps. The lengthening of the hydrophobic backbone, whilst the polar group remains constant, will tend to shift the hydrophobic/hydrophilic balance of the amphiphile towards the hydrophobic, possibly resulting in the formation of oil soluble anionic soaps<sup>328</sup>.

The investigation of the thermotropic and lyotropic phase behaviour of these novel amphiphiles was, therefore, of interest as the dimethylsiloxane chain represents a novel hydrophobe and, the combination of a very long, and yet highly flexible, hydrophobic chain has been hitherto unachievable with conventional amphiphiles. Having synthesised the materials the main priority was to gain an overview of their lyotropic and thermotropic phase behaviour and to investigate the effects of incorporating an anionic amphiphile onto the terminal silicon atom of a number of oligomeric and polymeric linear dimethylsiloxane backbones. This overview was obtained with a combination of techniques as outlined previously in chapters 5 and 6.

## 7.2 Thermotropic Phase Behaviour

### 7.2.1 The Sodium Salts (see figure 7.1; $x \approx 4, 10, 17.5$ & $26.5$ ; $Y = \text{Na}$ )

#### 7.2.1.1 Results

##### 7.2.1.1.1 Polarising Optical Microscopy

A film of the shortest chain length amphiphile (figure 7.1,  $x \approx 4.0$ , hereafter referred to as  $\text{Na}_{500}$ ; the subscript referring to the approximate molar mass of the n-butyl PDMS backbone) was examined under the microscope in the temperature range  $0$ – $350^\circ\text{C}$ . This material existed as a birefringent viscous fluid at  $0^\circ\text{C}$  and exhibited a non-geometric texture and an intermediate viscosity typical of a hexagonal phase (see figure 7.2). On heating, a gradual decrease in viscosity and a gradual increase in birefringence was observed, although no obvious phase transition occurred up to  $251^\circ\text{C}$ . At this temperature, there was a slight, but definite, reduction in viscosity and a slight modification to the texture of the phase. Nevertheless, this high temperature phase also exhibited the viscosity and the non-geometric texture typical of a hexagonal phase (see figure 7.3). This phase remained up to the transition to the isotropic liquid at  $312^\circ\text{C}$ .

With the three longer chain amphiphiles (figure 7.1,  $x \approx 10.0$ ,  $17.5$  and  $26.5$ ; hereafter, referred to as  $\text{Na}_{1000}$ ,  $\text{Na}_{1500}$  and  $\text{Na}_{2000}$ , respectively) their phase behaviour was, with the exception of the absence of the high temperature phase region above  $250^\circ\text{C}$ , very similar to that outlined for  $\text{Na}_{500}$ . All these amphiphiles existed as birefringent viscous fluids at  $0^\circ\text{C}$ . Although there was a slight decrease in viscosity and, possibly, birefringence with increasing amphiphile chain length, the viscosity and texture of the fluid phases of these amphiphiles were typical of a hexagonal phase and, were very similar to that exhibited by  $\text{Na}_{500}$  at equivalent temperatures (see figures 7.4–7.6).

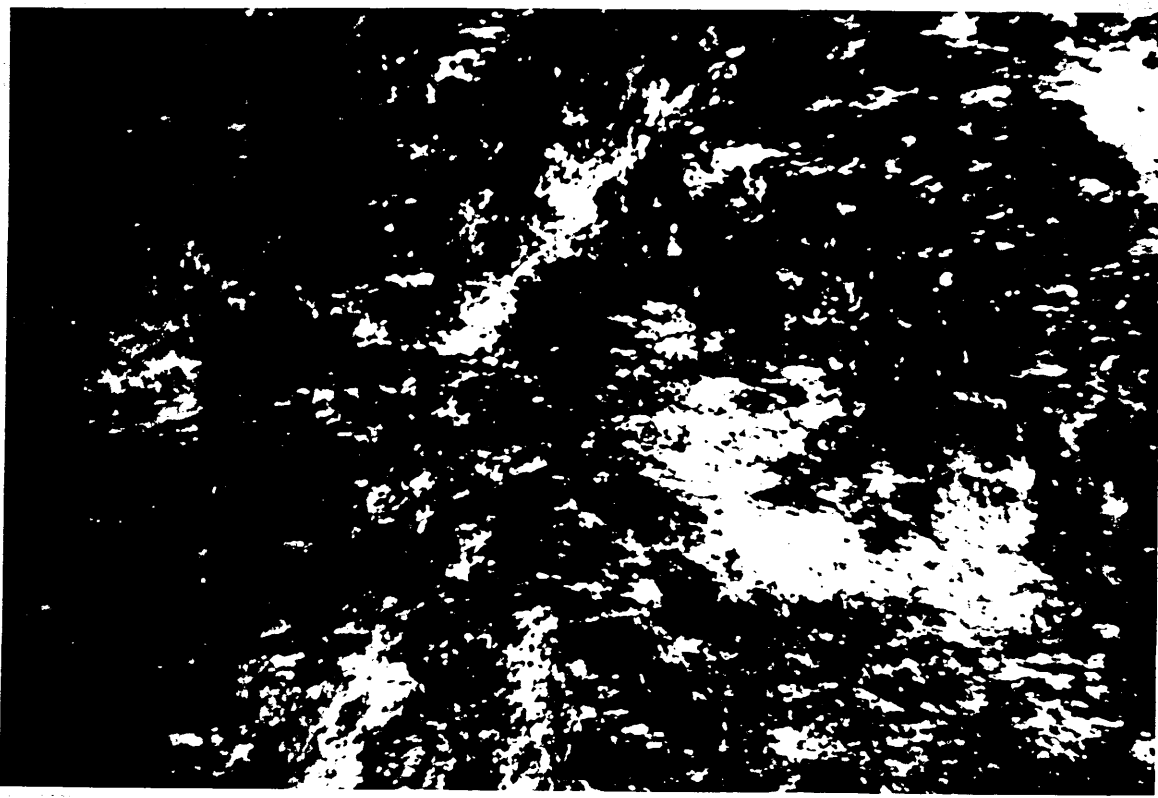


Figure 7.2 Optical texture of  $\text{Na}_{500}$  at  $50^\circ\text{C}$ .



Figure 7.3 Optical texture of  $\text{Na}_{500}$  at  $280^\circ\text{C}$ .



Figure 7.4 Optical texture of  $\text{Na}_{1000}$  at  $50^\circ\text{C}$ .



Figure 7.5 Optical texture of  $\text{Na}_{1500}$  at  $50^\circ\text{C}$ .



Figure 7.6 Optical texture of  $\text{Na}_{2000}$  at  $50^\circ\text{C}$ .

On heating samples of  $\text{Na}_{1000}$ ,  $\text{Na}_{1500}$  and  $\text{Na}_{2000}$ , there was a gradual decrease in the viscosity and a gradual increase in the birefringence of the samples, although no obvious phase transition occurred until  $252$ ,  $252.5$  and  $248.5^\circ\text{C}$ , respectively. The transition occurring at these temperatures resulted in the formation of the low viscosity isotropic liquid.

For all the amphiphiles of this series, a slight 'darkening' of the edge of the sample occurring at about  $285^\circ\text{C}$  was thought to indicated the onset of thermal degradation.

### 7.2.1.1.2 Differential Scanning Calorimetry (DSC)

Thermograms were initially recorded on the heating of previously unmelted samples of all the members of this homologous series between  $-170^{\circ}\text{C}$  and  $350^{\circ}\text{C}$ . These thermograms were characterised by up to five endothermic transitions (hereafter denoted T1, T2, T3, T4 and T5 in order of increasing temperature) and a final large exothermic transition at around  $320^{\circ}\text{C}$ , believed to correspond to the onset of extensive thermal degradation. T1 was a second order transition, whilst T2, T3, T4 and T5 were all first order. Figures 7.7 and 7.8 show representative thermograms for this series of amphiphiles, whilst table 7.1 summarises the results of these analyses.

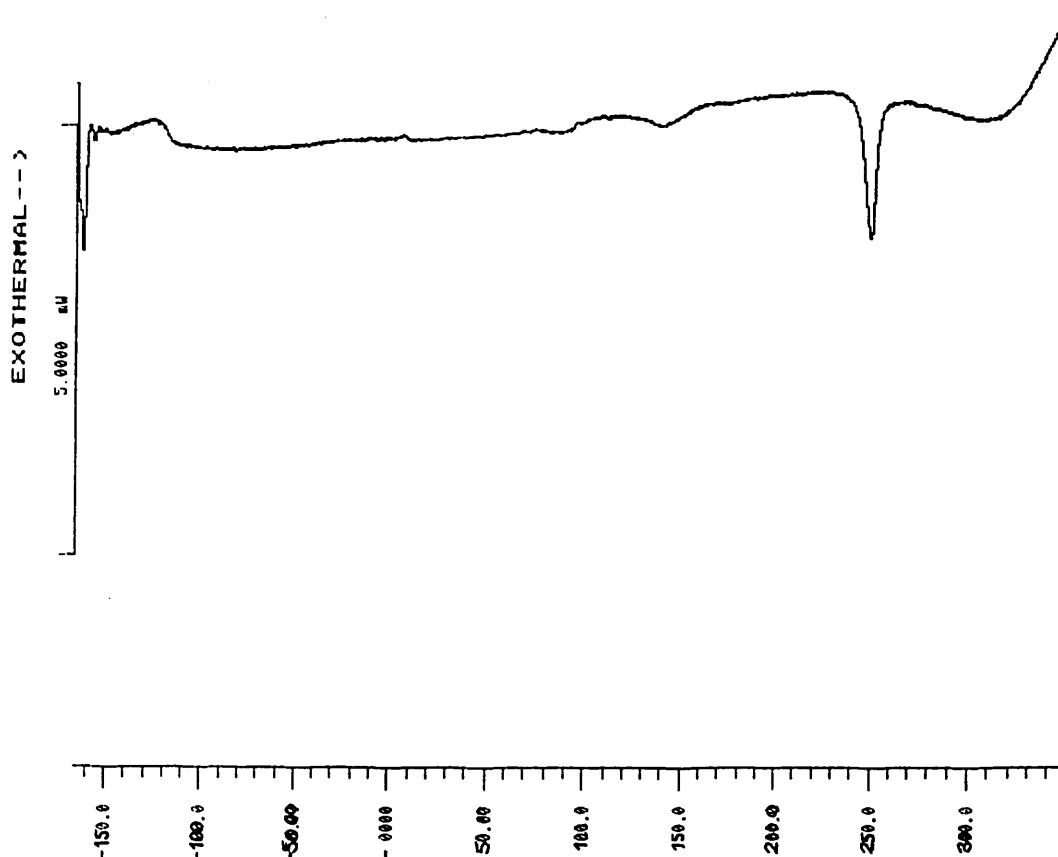


Figure 7.7 Representative thermogram for a previously unmelted sample of  $\text{Na}_{500}$  which had been dried over  $\text{P}_2\text{O}_5$  at  $100^{\circ}\text{C}$  for 24 hours, and heated from  $-170$  to  $350^{\circ}\text{C}$  at a rate of  $10^{\circ}\text{C}\cdot\text{min}^{-1}$

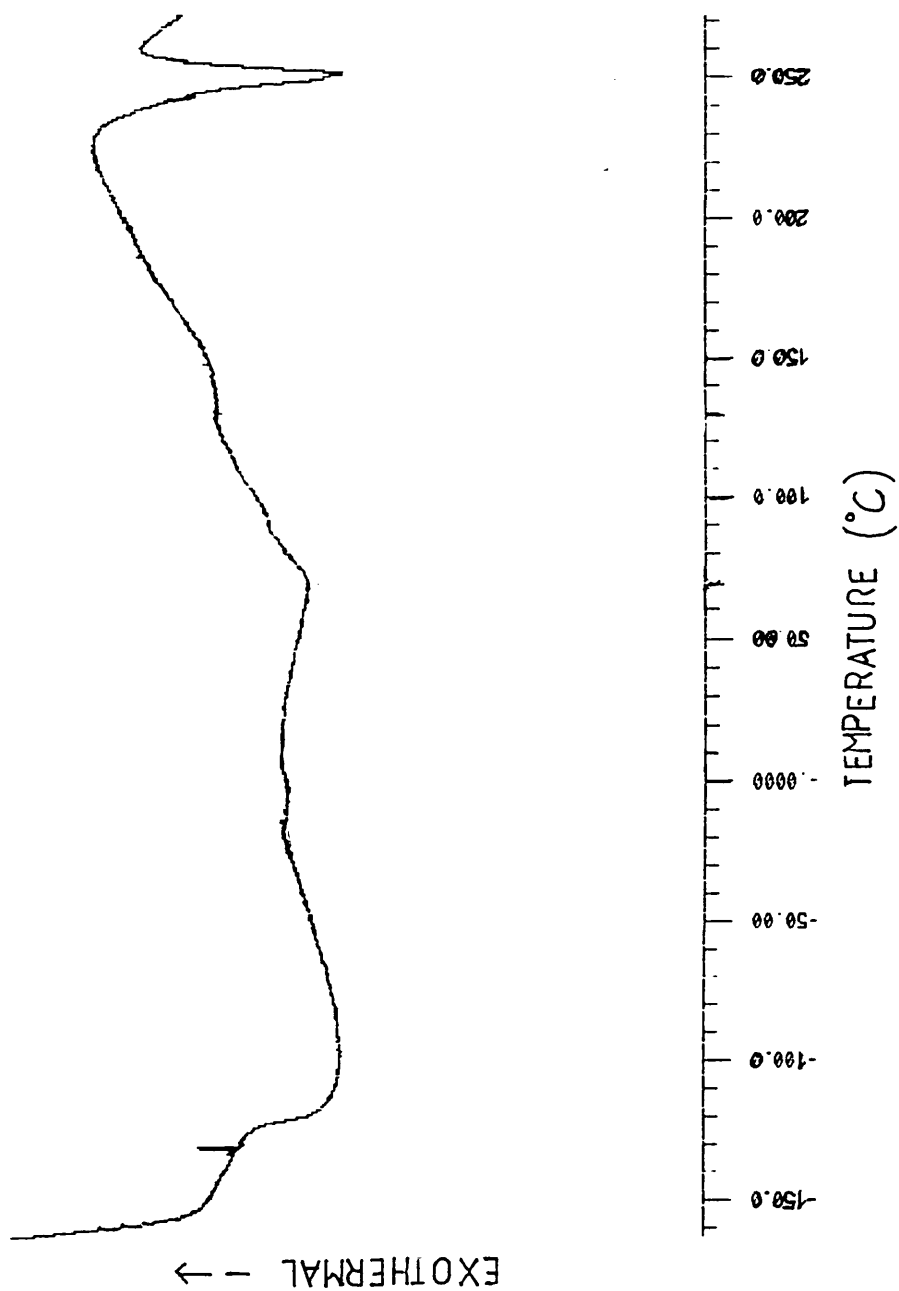


Figure 7.8 Representative thermogram for a previously unmelted sample of  $\text{Na}_{1000}$  which had been dried over  $\text{P}_2\text{O}_5$  at  $100^\circ\text{C}$  for 24 hours, and heated from  $-170$  to  $350^\circ\text{C}$  at a rate of  $10^\circ\text{C}\cdot\text{min}^{-1}$

TRANSITION	TRANSITION TEMPERATURE (°C) AND CORRESPONDING ENTHALPY (KJ.mol <sup>-1</sup> ) OR CHANGE IN SPECIFIC HEAT CAPACITY (J.g <sup>-1</sup> .K <sup>-1</sup> )			
	Na500	Na1000	Na1500	Na2000
T1 sample 1	-120 (0.40)	-120 (0.36)	-122 (0.37)	122 (0.5)
T2 sample 1	85 (*)	65 (*)	75 (*)	none observed
sample 2	90 (*)	85 (*)		
sample 3	83 (2)			
T3 sample 1	140 (2)	150 (*)	180 (*)	165 (3)
sample 2	122 (2)	none observed		
sample 3	140 (3)			
T4 sample 1	248 (10)	250 (13)	252 (14)	250 (13)
sample 2	243 (10)	251 (9)		
sample 3	249 (10)			
T5 sample 1	none observed	not applicable		
sample 2	none observed			
sample 3	315 (*)			

note -T1 is a second order transition and represents a change in the specific heat capacity of the sample, the units of which are J.g<sup>-1</sup>.K<sup>-1</sup>

T2-T5 are first order transitions and represent changes in enthalpy, the units of which are KJ.mol<sup>-1</sup>

\* indicates that although there was evidence of a transition, the signal was very broad and therefore it was not possible to accurately evaluate the enthalpy change occurring; hence, the transition temperatures quoted are approximate.

**Table 7.1** The transition temperatures and corresponding changes in enthalpy and specific heat capacity (both in parentheses) observed during the initial heating of this series of linear amphiphiles at a heating rate 1.0°C.min<sup>-1</sup> (In each case, sample 1 was heated from -170 to 350°C, and samples 2 and 3 were heated from 0 to 350°C).

Although not all the members of this homologous series exhibited the same number of transitions, for ease of reference and discussion, the various transitions occurring with each amphiphile have been arbitrarily categorised on the basis of their temperature of occurrence, and the similarity of the enthalpy changes involved; the validity of this classification will be discussed later. Consequently, it should be pointed out that T5 corresponds to the transition to the low viscosity isotropic liquid for Na<sub>500</sub> only; Na<sub>1000</sub>, Na<sub>1500</sub> and Na<sub>2000</sub> undergoing the transition to the isotropic liquid at T4. In addition, T3 and where applicable, T2 and T5 were small enthalpy transitions occurring over a broad temperature range. Thus, it was not always possible to accurately determine the enthalpy changes occurring. T2 was not observed during the initial heating of Na<sub>2000</sub>.

In order to assess the effects of heating and cooling, repeat analyses of a previously unmelted sample of Na<sub>500</sub> were carried out between room temperature and 280°C. The temperature and enthalpy change of the transitions observed during these analyses are summarised in Table 7.2.

TRANSITION	TRANSITION TEMPERATURE (°C)/ENTHALPY CHANGES(KJ.mol <sup>-1</sup> )				
	run 1	run 2	run 3	run 4	run 5
T2	90(note <sup>1</sup> )	none*	none*	none*	none*
T3	122 (2)	180 (note <sup>1</sup> )	none*	none*	199 (3)
T4	243 (10)	265 (13)	264 (12)	264 (12)	264 (12)

none\* - no peak observed in this region of the evaluation

note<sup>1</sup> - although peak was observed, it was very small and broad and no evaluation of the enthalpy change occurring was carried out.

Table 7.2 The transition temperatures and corresponding enthalpy changes (in parentheses) observed during the repeated heating of a sample of Na<sub>500</sub> from 0 to 280°C, at a heating rate 10°C.min<sup>-1</sup>.

Following these repeat evaluations, the sample vial was reweighed. A reduction in the mass of the sample of about 35% had occurred. Visual inspection of the sample indicated that considerable thermal degradation had also taken place. No thermograms were determined for these amphiphiles during cooling cycles.

### 7.2.1.1.3 X-Ray Diffraction

Diffraction patterns were obtained for all materials in the low-angle region at various temperatures. Figures 7.9 to 7.12 show the diffraction patterns obtained, whilst table 7.3 summarises the results of these experiments.

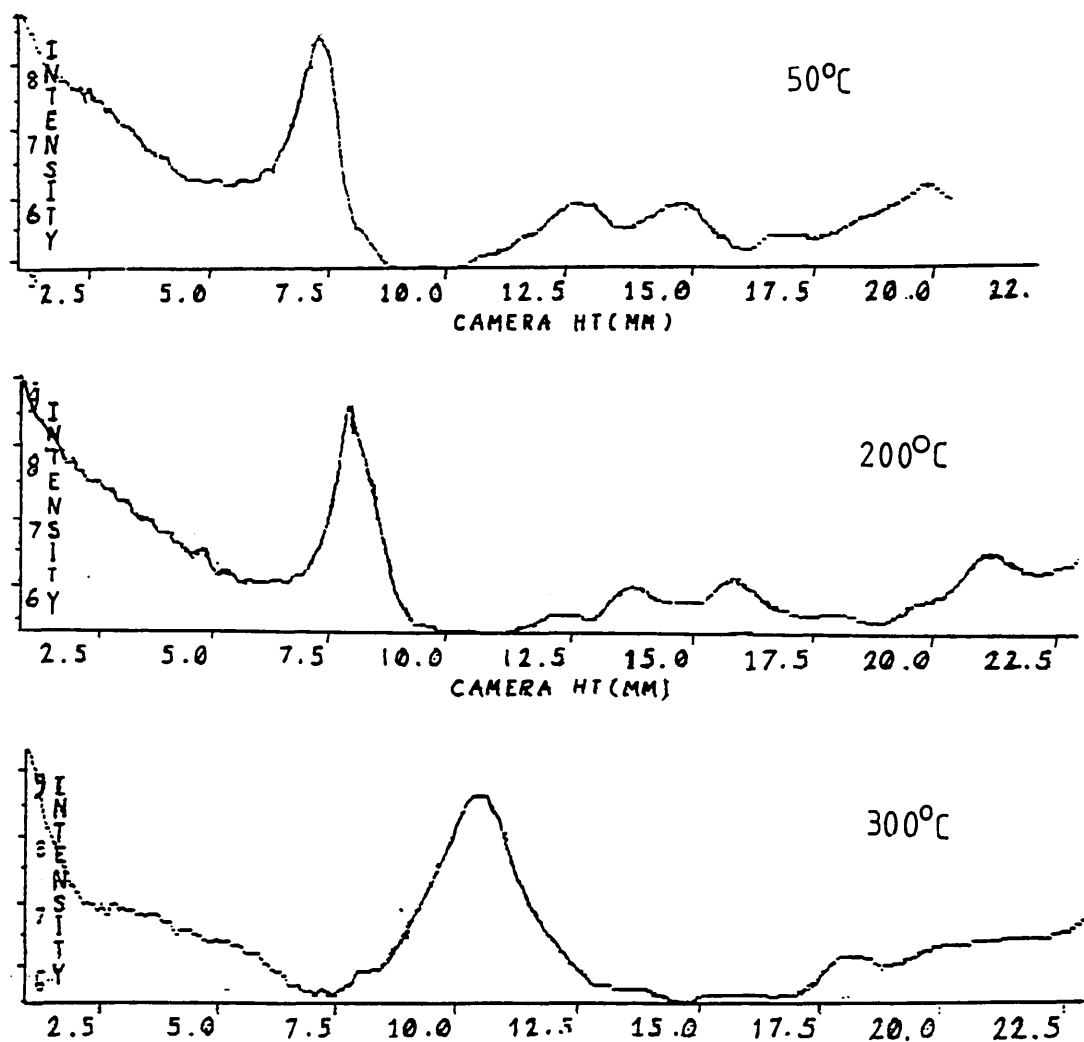


Figure 7.9 Low angle X-ray diffraction patterns for Na<sub>500</sub>

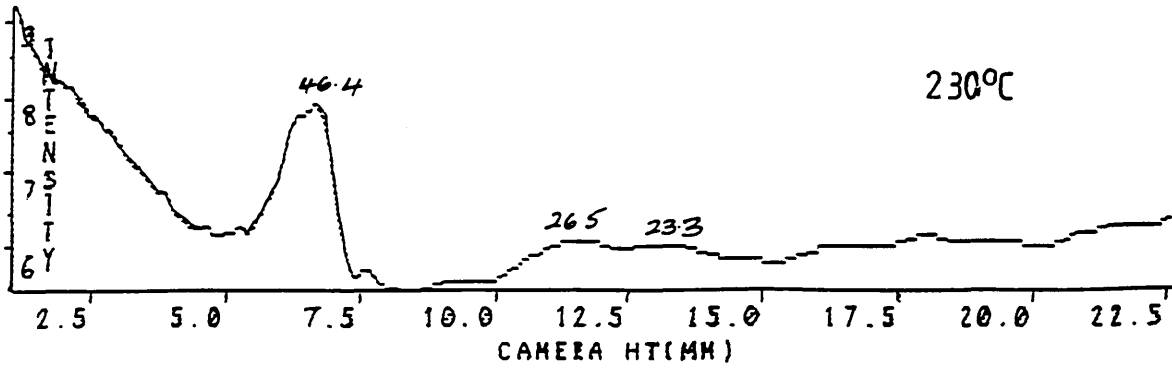
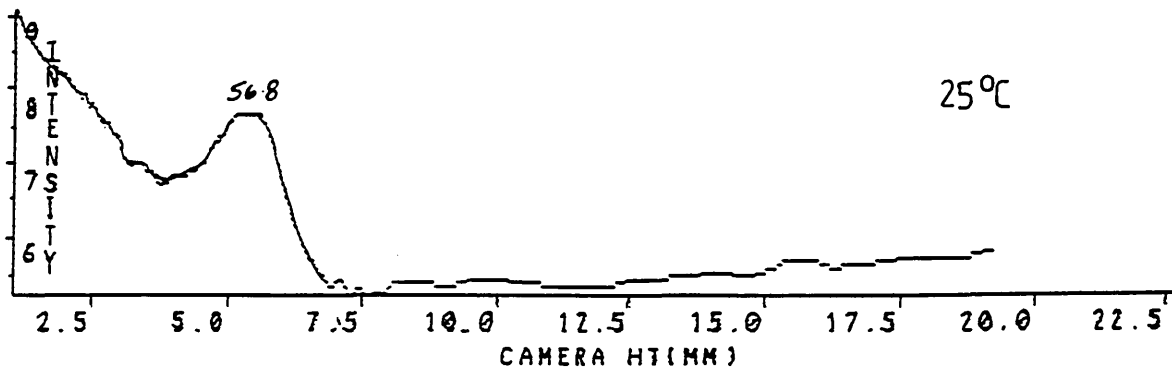


Figure 7.10 Low angle X-ray diffraction patterns for  $\text{Na}_{1000}$ .

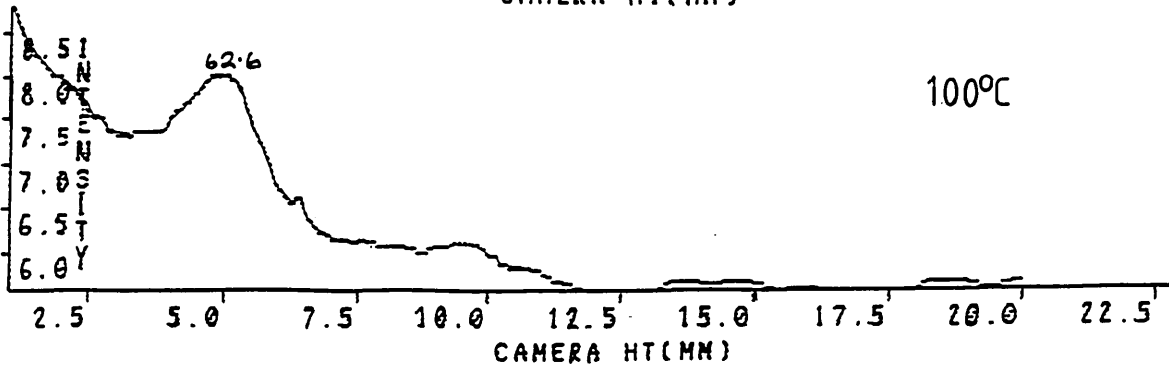
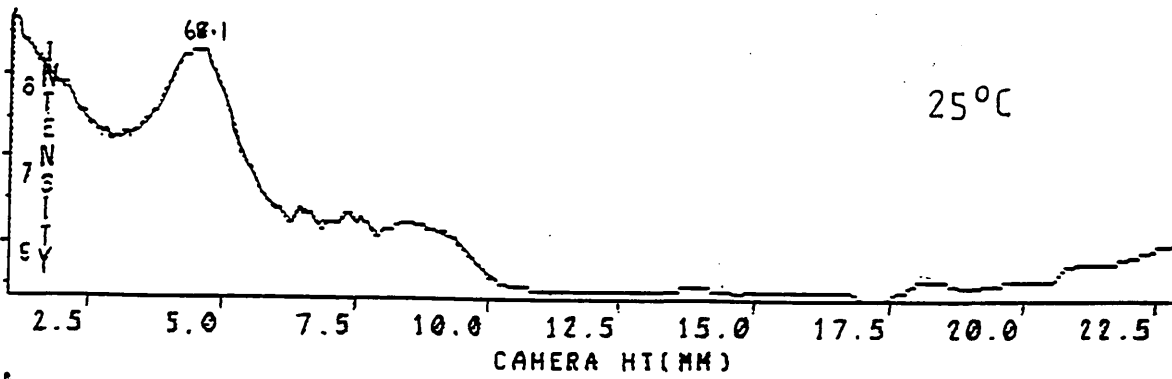


Figure 7.11 Low angle X-ray diffraction patterns for  $\text{Na}_{1500}$ .

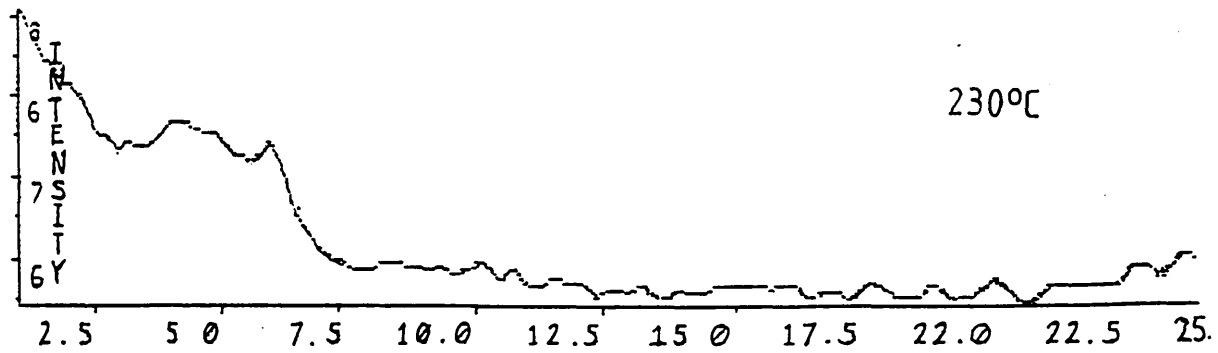
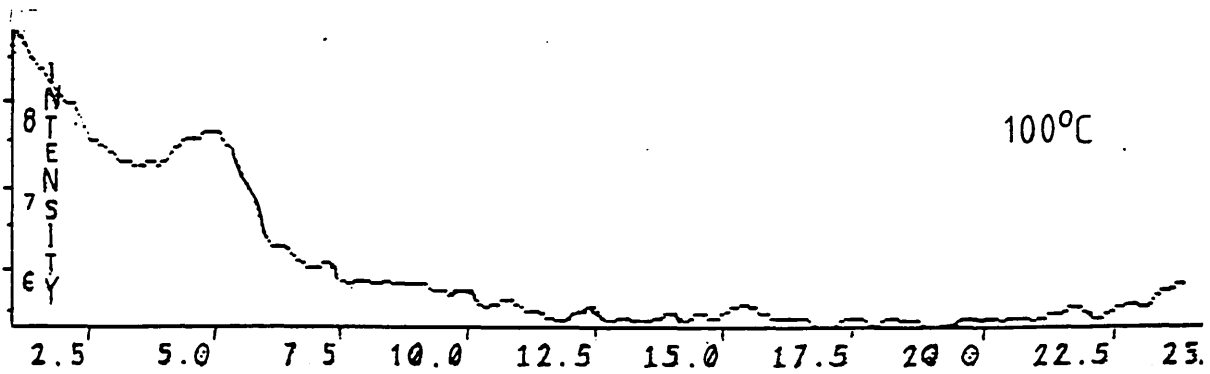
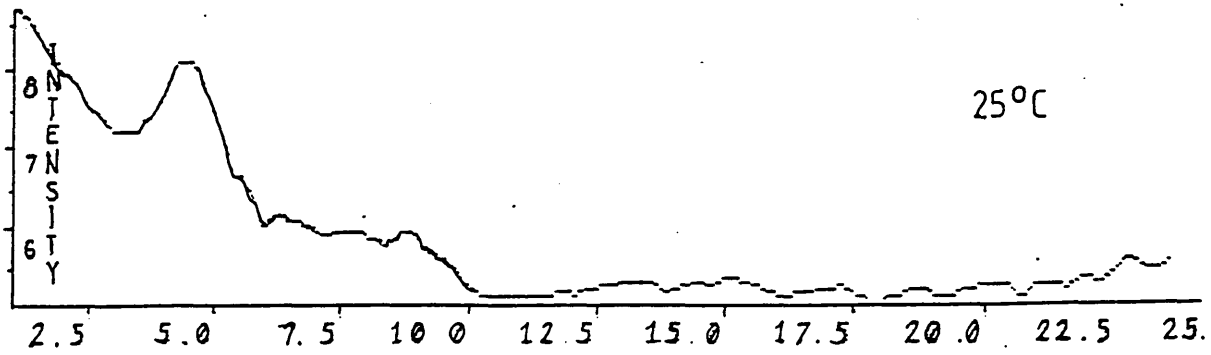


Figure 7.12 Low angle X-ray diffraction patterns for  $\text{Na}_{2000}$ .

SIGNAL	Na <sub>500</sub>	Na <sub>1000</sub>	Na <sub>1500</sub>	Na <sub>2000</sub>
<u>At 25°C</u> d <sub>0</sub> d <sub>1</sub> d <sub>2</sub>		59.9 (d <sub>0</sub> ) 34.5 (d <sub>1</sub> /√3) 30.7 (d <sub>1</sub> /√4)	68.1 (d <sub>0</sub> )	69.3 (d <sub>0</sub> )
<u>At 50°C</u> d <sub>0</sub> d <sub>1</sub> d <sub>2</sub> d <sub>3</sub>	41.8 (d <sub>0</sub> ) 24.5 (d <sub>1</sub> /√3) 21.3 (d <sub>1</sub> /√4) 15.3 (d <sub>1</sub> /√7)			
<u>At 100°C</u> d <sub>0</sub>			62.6 (d <sub>0</sub> )	62.0 (d <sub>0</sub> )
<u>At 200°C</u> d <sub>0</sub> d <sub>1</sub> d <sub>2</sub> d <sub>3</sub>	38.9 (d <sub>0</sub> ) 22.7 (d <sub>1</sub> /√3) 19.7 (d <sub>1</sub> /√4) 14.9 (d <sub>1</sub> /√7)			
<u>At 230°C</u> d <sub>0</sub>		47.6 (d <sub>0</sub> )	52.0 (d <sub>0</sub> )	52.0 (d <sub>0</sub> )
<u>At 300°C</u> d <sub>0</sub> d <sub>1</sub>	29.2 (d <sub>0</sub> ) 16.9 (d <sub>1</sub> /√3)			

Note - blank areas indicate no diffraction patterns recorded at that temperature for that particular sample

Table 7.3 The d-spacings observed and the reflections assigned to each of the major peaks in the X-ray diffraction patterns for the linear amphiphiles in the low-angle region at various temperatures.

Na<sub>500</sub> and Na<sub>2000</sub> showed a broad diffuse peak in the wide-angle region at approximately 6.3Å. No investigation of this region was carried out for the remaining members of this series of amphiphiles.

#### 7.2.1.1.4 Thermo Gravimetric Analysis (TG)

A thermogram was recorded on the heating of a previously unmelted sample of  $\text{Na}_{500}$  between  $35^\circ\text{C}$  and  $420^\circ\text{C}$ . This thermogram exhibited no significant weight loss up to about  $280^\circ\text{C}$ , at which point there was a gradual and increasing loss in weight up to the termination of the evaluation at  $450^\circ\text{C}$ . This loss in weight was thought to indicate the onset of thermal degradation of the sample. Figure 7.13 shows the thermogram obtained during the heating of a sample of  $\text{Na}_{500}$  which had been dried over  $\text{P}_2\text{O}_5$  at  $100^\circ\text{C}$  for 24 hour.

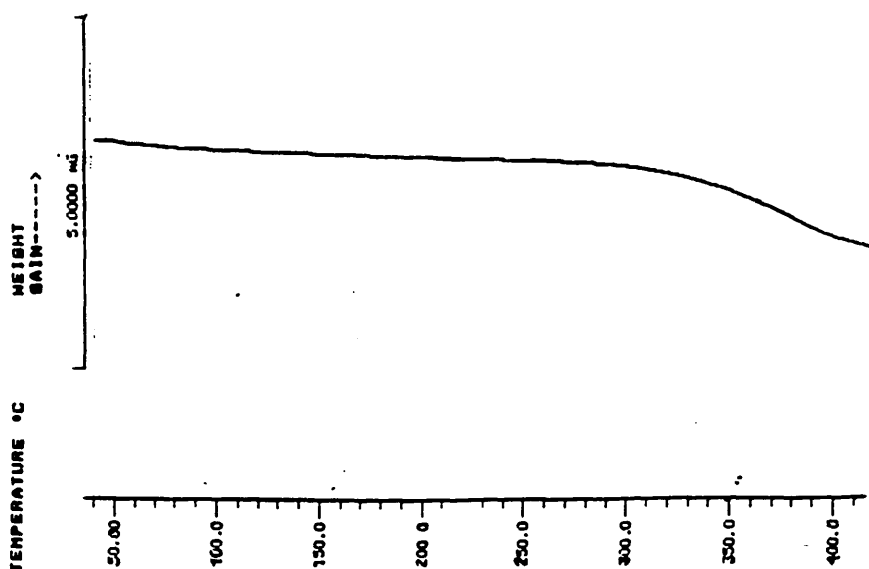


Figure 7.13 TG thermogram obtained on heating a sample of  $\text{Na}_{500}$  from  $35$  to  $420^\circ\text{C}$  at a heating rate of  $10^\circ\text{C}\cdot\text{min}^{-1}$ .

### 7.2.1.2 Discussion

Optical microscopy indicated that this homologous series of amphiphiles existed as ordered fluids at 0°C. The non-geometric texture and the viscosity of these birefringent fluid phases were similar for all the members of this series and were characteristic of a hexagonal phase<sup>16</sup>. For all these amphiphiles, this phase was stable up to around 250°C (see table 7.1 for exact transition temperatures). With Na<sub>1000</sub>, Na<sub>1500</sub> and Na<sub>2000</sub> (i.e. the three longer chain amphiphiles) the transition occurring around this temperature (i.e. T<sub>4</sub>) resulted in the formation of the low viscosity isotropic liquid. With Na<sub>500</sub>, the transition occurring at this temperature resulted in the formation of an additional ordered fluid phase. Although this inter-phase transition resulted in a definite reduction in viscosity, the viscosity and the non-geometric texture of this high temperature phase of Na<sub>500</sub> were also characteristic of a hexagonal structure. This phase remained up to the transition to the low viscosity isotropic liquid at 312 °C.

Having used optical microscopy to establish the upper temperature 'boundary' of the ordered phase regions of these amphiphiles and to supply some initial indication of the structures present, X-ray diffraction data obtained at various temperatures was used as a source of corroborative evidence (see table 7.3).

In general, where the diffraction pattern exhibited more than one reflection, the observed pattern was characteristic of a hexagonal phase and thus, supported the conclusions drawn from microscopy (i.e depending on the number of reflections observed, the reciprocal spacings were in the ratio  $1:\sqrt{3}:\sqrt{4}:\sqrt{7}$ )<sup>24,149</sup>. In some cases the patterns possessed additional peaks of low intensity. However, the intensity scale in this technique is a

logarithmic relationship and small 'peaks' are not necessarily valid. Where the diffraction patterns exhibited only one peak it was not possible to propose a structure from this data or to corroborate the conclusions derived from optical microscopy. However, the absence of peaks other than the principle reflection does not mean that the optical study was flawed. Indeed higher order reflections often have very low intensities and in polydisperse samples of the type studied here, may be too broad to be seen.

Having proposed phase structures for these amphiphiles from 0°C up to the transition to the low viscosity isotropic liquid, DSC was used to provide additional information on the number and the nature of the transitions occurring in this temperature range and, also to provide some data on the low temperature behaviour. As the number, temperature, and enthalpy change of the transitions occurring in the thermograms of the individual amphiphiles were so similar (see table 7.1), it seems reasonable to suggest that the transitions occurring at similar temperatures were due to related thermal processes.

The thermograms of all the linear amphiphiles were characterised by a second order transition occurring at around -120°C (T1). Considering their molecular structure, the temperature and second order nature of T1 indicated that this transition was primarily associated with the linear poly(dimethylsiloxane) (PDMS) backbone of the amphiphiles<sup>327</sup>. For example, it has been reported that whilst high molar mass linear PDMS is highly crystalline, linear polymer of comparable molar mass to the siloxane chains of these amphiphiles is amorphous and undergoes a glass transition in the range -135 to -125°C<sup>327</sup>. Thus, the absence of a transition(s) corresponding to the melting of crystalline linear PDMS in the range -60 to -20°C, and the

presence of the second order transition at around  $-120^{\circ}\text{C}$ , indicated that the siloxane segments of these amphiphiles were amorphous and in an environment similar to that of the equivalent bulk non-substituted linear PDMS. The implications of this would be that the siloxane backbone would be able to rotate and be essentially liquid-like above  $T_1$ , whilst below this transition, the liquid-like structure of the polymer would be frozen into a glassy state<sup>331</sup>.

Having established that these amphiphiles existed as ordered fluids at  $0^{\circ}\text{C}$ , the absence of a transition in between  $T_1$  and  $0^{\circ}\text{C}$ , suggested—although, was not conclusive evidence—that these ordered fluids were themselves stable to  $T_1$  (i.e. approximately  $-120^{\circ}\text{C}$ ). Bearing in mind the proposal that the siloxane chains constitute the continuous phase of these reversed hexagonal structures and that  $T_1$  represents the glass transition of this continuous phase, it seems unlikely that the established macroscopic fluidity of these amphiphiles at  $0^{\circ}\text{C}$  would be maintained at temperatures below  $T_1$ . Thus, below  $T_1$ , these amphiphiles would be expected to exist as reversed hexagonal structures with a glass-like continuous phase, whose macroscopic properties would be that of a glassy solid.

As a corollary of establishing the amorphous nature of the siloxane chains, it follows that the structural order within the phases of these amphiphiles (above or below  $T_1$ ) must primarily entail the  $\text{C}_{11}$  sodium carboxylate moieties. This is supported by the fact that the total enthalpy change associated with the first order endothermic transitions occurring in these amphiphiles between  $T_1$  and the transition to the low viscosity isotropic liquid (i.e.  $T_2$ ,  $T_3$ ,  $T_4$  and, where applicable,  $T_5$ ) seemed to be independent of the siloxane chain length of the individual amphiphiles (see table 7.1).

Therefore, these transitions were most likely associated with thermal processes primarily involving the C<sub>11</sub> sodium carboxylate moiety and, the structural order within these phases (above or below T1) must also primarily entail this moiety.

At this stage, it is worth pointing out that whilst the phase behaviour of these linear amphiphilic siloxanes differs significantly from that of the cyclic amphiphiles discussed in chapter 6, there are similarities in the number and temperature of the thermal transitions that occur in these two classes of novel amphiphiles above 0°C (see table 7.4).

TRANSITION SAMPLE N <sup>o</sup>	TRANSITION TEMPERATURE (°C) AND CORRESPONDING ENTHALPY(KJ.mol <sup>-1</sup> )						
	Na500	Na1000	Na1500	Na2000	TRANSITION	NaD <sub>4</sub>	NaD <sub>5</sub>
T2 1 2 3	85(*) 90(*) 83(2)	65(*) 85(*)	75(*)	none obs.	T1	62(20)	44(19)
T3 1 2 3	140(2) 122(2) 140(3)	150(*) none obs.	180(*)	165(3)	T2	147(7)	144(10)
T4 1 2 3	248(10) 243(10) 249(10)	250(13) 251(9)	252(14)	250(13)	T3	258(26)	245(22)
T5 1 2 3	none obs. none obs. 315(*)	not applicable				none obs.	none obs.

note - \* indicates that the transition observed was very broad and therefore it was not possible to accurately evaluate the enthalpy change occurring or the transition temperatures.

Table 7.4 The transition temperatures and corresponding enthalpy changes (in parenthesis) observed above 0°C during the initial heating of the sodium salts of the linear and cyclic amphiphilic siloxanes.

As can be seen in table 7.4, the cyclic amphiphiles undergo a number of transitions above 0°C which are comparable to those occurring in the linear amphiphiles. For instance, two transitions occurring at approximately the same temperature and of similar enthalpy, were observed during the initial heating of the cyclic (i.e. T1 and T2) and the linear amphiphiles (i.e. T2 and T3). In the cyclic amphiphiles, which were crystalline at room temperature, it was concluded that these transitions were primarily associated with a rearrangement/melting of the non-polar chains and that the processes occurring were analogous to the initial stages in the step-wise melting of monomeric straight long-chain sodium soaps. In addition, a transition occurring at around 250°C was characteristic of both the linear and the cyclic amphiphiles. This transition was ascribed to the melting of the crystalline polar groups of the cyclic amphiphiles and again, was believed to represent a further stage in the step-wise melting of these amphiphiles and similarly, was analogous to the behaviour of monomeric straight chain sodium soaps.

The fact that the sodium salts of these linear amphiphiles undergo a number of transitions similar to those previously ascribed to the step-wise melting of the crystalline cyclic amphiphiles seems to indicate that the C<sub>11</sub> sodium carboxylate moieties of both the linear and the cyclic amphiphiles were undergoing thermal transitions that were related to similar physical processes. Consequently, despite the novel molecular structure of the linear amphiphilic siloxanes and the resulting structure and properties of the phases formed by these amphiphiles, it seemed likely that the C<sub>10</sub> alkyl chains and the polar groups of the linear amphiphiles may have retained some degree of crystalline order within the macroscopically fluid hexagonal phase observed between T1 and T4. This would in turn indicate that the

fluid hexagonal phases formed by these linear amphiphiles are semi-crystalline below T<sub>4</sub>, with the C<sub>11</sub> sodium carboxylates having some structural order and the siloxane chains being essentially amorphous.

The fact that the T<sub>3</sub> and, where applicable, the T<sub>2</sub> transitions of the linear amphiphiles did not result in corresponding transitions when viewed under the microscope, indicated that these DSC transitions were not associated with a significant change in the overall structural arrangement of the phase.

Thus far, we have considered the phase behaviour of all the members of this series of amphiphiles to be identical below T<sub>4</sub>. However, whilst this is generally the case, Na<sub>2000</sub> did not exhibit the T<sub>2</sub> transition, that was typical of the shorter chain length linear amphiphiles. Whilst it is possible that this transition does not occur with this, the longest chain amphiphile, it is not obvious why this should be the case if this transition is—as proposed—associated with the melting of the C<sub>10</sub> alkyl chain. Alternatively, if this low enthalpy transition is associated with the melting of the C<sub>10</sub> alkyl chain of these amphiphiles, the reduced volume fraction of this chain in this, the longest chain amphiphile, may have resulted in a transition that was approaching the limit of detection of the DSC measuring cell. This coupled with the polydispersity of the sample could explain the different thermograms of the respected samples. At present, no further explanation of this observation can be offered.

In attempting to rationalise the behaviour of this series of linear amphiphiles, the magnitude of the enthalpy changes occurring gives an insight into the structural order present and the changes taking place. An

interesting result arising from the study of the cyclic amphiphiles, was the low total heat of fusion for each amphiphile of NaD<sub>4</sub> and NaD<sub>5</sub> (13 and 10 kJ.mol<sup>-1</sup>, respectively) relative to that of the corresponding monomeric straight chain sodium soaps (typically 30 kJ.mol<sup>-1</sup> for sodium laurate<sup>151</sup>). In comparing the structures of NaD<sub>4</sub> and NaD<sub>5</sub> with those of conventional sodium soaps, it was assumed that the major differences in their melting behaviour would be associated with the non-polar regions of the respective amphiphiles. As the enthalpy changes ascribed to the melting of the C<sub>10</sub> alkyl chains of these cyclic amphiphiles (i.e. T1 and T2) were relatively low, and the packing density of the polar group at 50°C were similar for NaD<sub>4</sub> and the monomeric sodium soaps, this seemed to support this proposition. Therefore, the attachment of amphiphiles to the siloxane ring in these cyclic amphiphiles was thought to disrupt the packing of the C<sub>10</sub> alkyl side-chains and, in particular, to restrict their close contact.

A comparison of the enthalpy changes associated with the melting of the alkyl chains of the linear amphiphilic siloxanes with those of the cyclic amphiphiles and conventional straight chain sodium soaps, shows a similarly reduced enthalpy change occurring in the linear amphiphilic siloxanes. For example, the total enthalpy change ascribed to the melting of the C<sub>10</sub> alkyl chains in the linear amphiphiles (i.e. T2 plus T3, <5KJ.mol<sup>-1</sup>), is slightly less than the corresponding enthalpy change in the sodium salts of the cyclic amphiphiles (6 to 7 KJ.mol<sup>-1</sup>per amphiphile repeat unit). Both of these are considerably less than those of the corresponding transitions of monomeric straight chain sodium soaps of similar alkyl chain length (typically 20KJ.mol<sup>-1</sup> for sodium laurate<sup>151</sup>). As was the case with the cyclic amphiphiles, although the presence of T2 and T3 indicates some

crystalline order within the C<sub>10</sub> alkyl chains of the linear amphiphiles, the attachment of the alkyl chains to the linear siloxane backbone seems to have restricted their ability to crystallise. Considering the relative volume of the dimethylsiloxane repeat unit (i.e.  $\approx 130\text{\AA}^3$  at 25°C) and the flexibility of the linear siloxane backbone, this is perhaps not surprising, as the thermal motions and steric effects of this chain cannot be fully divorced from those of the C<sub>10</sub> alkyl chains, due to the covalent bond that exists between them. Thus, the siloxane chains, which are mobile (above T<sub>g</sub>) bulky polymers, would be expected to restrict the effective packing of the C<sub>10</sub> alkyl chains to which they are attached.

By the same token, one end of the siloxane chain is constrained by the attachment to the terminal carbon atom of the C<sub>10</sub> alkyl chain and, therefore, this constraint would also be expected to affect the flexibility of the siloxane backbone itself. As it has been reported that the T<sub>g</sub> of linear PDMS varies from -135 to -125°C for polymer of comparable molar mass to that of these linear amphiphiles (i.e. M<sub>n</sub> in the range 500 to 2000)<sup>327</sup>, the occurrence of T<sub>1</sub> at about -120°C may also reflect the kinetic and steric interactions occurring between the siloxane and C<sub>10</sub> alkyl moieties of these amphiphiles. It is worth emphasising that the T<sub>g</sub> of non-substituted linear PDMS reaches a maximum at approximately -123.2°C for high molar mass polymer<sup>327</sup>. Thus, unless the macroscopic structural arrangement within the hexagonal phases formed by these amphiphiles exerts a significant influence on the flexibility of the siloxane chains, the interaction between the alkyl and siloxane moieties of these amphiphiles is the only plausible explanation for the both the observed shift in T<sub>g</sub> of the siloxane to higher temperatures and the reduced packing efficiency of the alkyl chains.

If the reduced crystallinity of the C<sub>10</sub> alkyl chains in these linear amphiphiles is due to the attachment of the siloxane chains, it is reasonable to assume that the order within these alkyl chains will not be uniform along the length of the chain. Thus, the order would be expected to increase along the alkyl chain from the amorphous siloxane regions to the crystalline polar groups. At this stage, no supporting evidence can be presented for this proposal.

Whilst the melting of the C<sub>10</sub> alkyl chains of these linear amphiphiles involves a relatively small enthalpy change compared with the equivalent processes in conventional sodium soaps, the enthalpy change ascribed to the melting of the polar groups (i.e. ~10KJ.mol<sup>-1</sup> for T4) approximates to that straight chain sodium soaps (i.e. ~8 KJ.mol<sup>-1</sup> for the semi-crystalline to mesophase transition of sodium laurate<sup>151</sup>) and, NaD<sub>4</sub> and NaD<sub>5</sub> (see chapter 6). This seems to indicate that the order within the polar group of these amphiphiles prior to T4, is comparable to that of the conventional sodium soaps, and is further evidence of the semi-crystalline nature of the fluid phase of all these linear amphiphiles below this transition. The fact that the polar groups pack efficiently despite their indirect attachment to the bulky siloxane chains, may reflect the 'spacer group' effect<sup>332</sup> of the C<sub>10</sub> alkyl chain which covalently links these two moieties.

Whilst the melting of the polar groups (i.e. T4) resulted in the formation of the low viscosity isotropic liquid for Na<sub>1000</sub>, Na<sub>1500</sub> and Na<sub>2000</sub>, the equivalent transition of Na<sub>500</sub> gave rise to an additional lower viscosity hexagonal phase region. Compared with the final melting transition of the longer chain amphiphiles (i.e. T4), the final melting transition of Na<sub>500</sub> (i.e.

T5) entailed a relatively small enthalpy change (see table 7.1). As the low viscosity isotropic liquid entails little order, this indicated that most of the structural order within the high temperature hexagonal phase of Na<sub>500</sub> had been lost prior to formation of this phase (i.e at T4). The small enthalpy change associated with T5 and the reduced viscosity of the phase prior to this transition, are therefore consistent with a fused phase region (i.e. a mesophase). This is also indirect evidence that the other members of this series of amphiphiles are, as proposed, semi-crystalline up to the transition to the isotropic liquid at T4. This being the case, by analogy with the behaviour of monomeric sodium soaps, the interfacial area per amphiphile polar group would be expected to be essentially independent of temperature for all these linear amphiphiles below T4 (i.e the semi-crystalline phase) and dependent on temperature above T4 for Na<sub>500</sub> (i.e the mesophase)<sup>24,149</sup>. The values for the area per polar group derived from the X-ray study of these amphiphiles at various temperatures are compared in table 7.5 (see section 5.4).

Phase	Parameter	amphiphile			
		Na500	Na1000	Na1500	Na2000
Semi-crystalline H <sub>2</sub>	t (°C)	50	25	25	25
	S (Å <sup>2</sup> )	13	11/12	12	14
	t (°C)	200	200	100	100
mesomorphic H <sub>2</sub>	S (Å <sup>2</sup> )	17	19	22	18
	t (°C)		230	211	210
	S (Å <sup>2</sup> )		19	23	26
	t (°C)	300		not applicable	
	S (Å <sup>2</sup> )	32			

Table 7.5 The variation of the area per polar group for the linear amphiphilic siloxanes with temperature.

Table 7.5 shows that there is generally reasonable agreement between the area per polar group of the various amphiphiles at equivalent temperatures. This seemed to indicate that this parameter is essentially independent of the siloxane chain length. This is perhaps surprising, as the increased tendency of the siloxane chains to adopt a coiled conformation and, the reduced electrostatic interaction between micelles—both effects resulting from an increase in siloxane chain length—might be expected to influence the area per polar group within these structures.

The derived areas per polar group at temperatures of 25 and 50°C range from 11–14Å<sup>2</sup>. By comparison with the typical values for the area per polar group of conventional sodium soaps, which are in the range 20–25Å<sup>2</sup> in the semi-crystalline phases (table 6.7), these values appear to be much too small. Whilst the area per polar group of the linear amphiphilic siloxanes cannot be compared quantitatively with those of monomeric sodium soaps, which although based on the same polar group are of a different phase structure, the much reduced area per polar group of these novel amphiphiles would require a more compact packing of the polar groups than found in conventional sodium soaps. This observation, therefore, warrants further investigation and may indicate that the polar cores of the rod micelles are non-circular in this temperature region.

The values obtained at the higher temperatures (i.e. 17–32Å<sup>2</sup>) appear to be more reasonable. Table 7.5 also indicates that the values derived for the area per polar group of these amphiphiles in the supposedly semi-crystalline phases (i.e. at temperatures below T<sub>4</sub>), do not appear to be independent of temperature. This is not as expected<sup>24,149</sup>, but may reflect the unusually small values calculated at 25 and 50°C, indicating that there

is some rearrangement of the polar groups above this temperature range (i.e. a transition from a non-cylindrical to a cylindrical arrangement of the polar cores).

In discussing these observations, it should be pointed out that no density measurements for this series of amphiphiles have been made and the densities of the polar and non-polar regions of these molecules were estimated using data from several sources<sup>301,315,316</sup> (see section 5.4). Thus, the values of the area per polar group derived using these figures are only approximations. To facilitate the accurate calculation of these parameters, and the subsequent improved interpretation of the phase behaviour of these amphiphiles, accurate density values would be required. In the absence of this work, it is possible to suggest that compared with the values for all these amphiphiles at the lower temperatures, the relatively large value of the area per polar group for Na<sub>500</sub> at 300°C reflects the fused nature of the high temperature mesophase.

Having outlined the phase behaviour of this series of linear amphiphiles, we may now attempt to rationalise this behaviour in terms of the well established principles applied to conventional amphiphiles and, contrast this behaviour with that of the cyclic amphiphiles discussed in chapter 6.

It has been proposed that the micelles formed by these linear amphiphiles below the transition to the low viscosity isotropic liquid, are reversed micelles with the polar groups constituting the cores of the micelles. These micelles are very different to the micelles formed by monomeric straight chain sodium soaps and the cyclic amphiphiles discussed previously. The different geometries of the micelles formed by these

related classes of amphiphiles may be understood on the basis of their different molecular structures. The constraint on micelle shapes arising from chain packing have led to the assumption that a micelle radius cannot be longer than the maximum length of the hydrophobic moiety ( $l$ ) of an amphiphile<sup>15,16</sup>. Thus, there is a relationship between the volume and maximum length of an amphiphile, and the micelle shape adopted by that amphiphile. This leads to minimum areas per molecule ( $a_{\min}$ ) for normal spherical, cylindrical and bilayer micelles, given by:

$$\begin{aligned} \text{sphere} \quad (a_{\min}) &= 3 v/l \\ \text{cylinder} \quad (a_{\min}) &= 2 v/l \\ \text{bilayer} \quad (a_{\min}) &= v/l \quad \text{where } v = \text{volume of the hydrophobic moiety} \end{aligned}$$

For a  $C_{12}$  hydrocarbon chain, assuming a maximum extension of  $15\text{\AA}$  and that the volume of the  $\text{CH}_2$  and  $\text{CH}_3$  groups is  $27$  and  $54\text{\AA}^3$  respectively, this gives<sup>16</sup>:

$$\begin{aligned} \text{sphere} \quad a_{\min} &= 70\text{\AA}^2 \\ \text{cylinder} \quad a_{\min} &= 47\text{\AA}^2 \\ \text{bilayer} \quad a_{\min} &= 23.5\text{\AA}^2 \end{aligned}$$

The values for other chain lengths vary slightly from these because of the different fractions of  $\text{CH}_3$  groups within the micelle interior.

Similarly, the relationship between the volume and the maximum length of the linear amphiphilic siloxanes should also, at least in part, determine the micelle shapes adopted by these amphiphiles. Employing approximations for the maximum length of the amphiphilic siloxanes and the volumes of the dimethylsiloxane unit (see section 5.4), limiting values for the surface area per chain may be estimated for these amphiphilic siloxanes. If we apply the

above relationships to  $\text{Na}_{1000}$  at  $25^\circ\text{C}$  and assume that the volumes of the dimethylsiloxane,  $\text{CH}_2$  and  $\text{CH}_3$  moieties are  $130\text{\AA}^3$ ,  $27\text{\AA}^3$  and  $54\text{\AA}^3$  respectively, and that the length of  $\text{Na}_{1000}$  is  $47\text{\AA}$ , then the limiting values are as follows:

$$\begin{array}{ll} \text{sphere} & a_{\min} = 130\text{\AA}^2 \\ \text{cylinder} & a_{\min} = 86\text{\AA}^2 \\ \text{bilayer} & a = 43\text{\AA}^2 \end{array}$$

Although these values will obviously vary with the ratios of the siloxane to alkyl chain moieties of these amphiphile and also with the temperature,  $\text{Na}_{1000}$  should be representative of this series. Thus, for these linear amphiphilic siloxanes with sodium carboxylate polar groups, the observed reversed phase structures are qualitatively as expected (i.e. less than the bilayer  $a_{\min}$ ). In addition, the shape of the hydrophobic moiety of these amphiphiles is not of a uniform cross-section along the length of the chain, as is assumed in the above calculations. Indeed, these shapes may be visualised as a sort of wedge, with the bulky siloxane units furthest away from the polar head group. This effect could contribute to a negative surface curvature of the non-polar/polar interface of the micelles and thus the formation of reversed micelles and reversed phase structures.

The exact surface area per polar group at this interface, and, thus the degree of surface curvature of the interface, will be dependent on the balance between intra-micelle and inter-micelle forces. The electrostatic and steric forces of repulsion between adjacent polar groups will tend to maximise the area per polar group and thus, minimise inter-micelle distance, whilst the inter-micellar forces of repulsion (also electrostatic and steric) would tend to have the opposite effect.

An additional effect which could be envisaged to be important for the longer chain amphiphiles of this series, is the tendency of the siloxane chains to coil. This effect would be expected to act so as to minimise inter-micelle distance and increase the area per polar group. However, as the area per polar group appears to be essentially independent of siloxane chain length (see table 7.5), this factor does not seem to be significant.

As packing constraints dictate the formation of reversed rod-like micelles, inter-micelle repulsive interactions give rise to a hexagonal packing of these micelles. Below  $T_1$  (i.e. the glass transition of the siloxane chain), it is reasonable to assume that the phase is essentially made up of an amorphous glass-like continuum, with the micelle cores (polar groups) distributed in a two-dimensional hexagonal array. Although no attempt was made to study the physical properties of these amphiphiles at these low temperatures, the macroscopic properties of such a phase would be expected to be that of a glassy solid.

Above  $T_1$ , the  $T_g$  of the siloxane continuum presumably results in the formation of a fluid-like amorphous siloxane phase, whilst the cores of the micelles remain essentially crystalline. Consequently, the ordered, but yet also fluid, nature of the hexagonal phase formed by the linear amphiphilic siloxanes above  $T_1$  but below  $T_4$ , may be rationalised by this combination of an amorphous siloxane continuum and the partially ordered  $C_{11}$  sodium carboxylate moieties. Thus, the siloxane chains, which are essentially liquid-like above their  $T_g$  ( $T_1$ ), give rise to the macroscopic fluidity of these phases, whilst the  $C_{11}$  sodium carboxylates moieties, which constitute the core of the reversed micelles, maintain the intra and inter-micelle order below the transition to the isotropic liquid.

With increasing temperature above T<sub>1</sub>, no transitions were observed before approximately 75°C. At this temperature it seemed likely that the C<sub>10</sub> alkyl chains began a process of a step-wise melting (i.e. T<sub>2</sub>, which occurred over a range of temperatures from 67 to 90°C for the different amphiphiles/samples). Further increased temperature resulted in a second transition in the range 120-150°C (i.e. T<sub>3</sub>), which is also thought to correspond to a stage in the melting of the alkyl chains. The melting of these chains did not result in a significant change to the overall phase structure.

The fact that the polar groups of the linear amphiphiles apparently retain crystalline order, despite their attachment to the bulky siloxane chains, may reflect the 'spacer group' effect of the C<sub>10</sub> alkyl chains<sup>332</sup>. This may be contrasted with the behaviour of long chain soaps in which the non-polar chains are of a non-compact branched type and, therefore, do not crystallise. In these soaps, the relatively large cross-sectional area of the bulky side-chains may also restrict the efficient packing of the polar groups<sup>173-175</sup> and, hence, mesophases may result at room temperature. This is not the case with these linear siloxane-containing amphiphiles, as the C<sub>10</sub> alkyl chain must effectively decouple the steric and kinetic interactions of the polar groups and the siloxane chains, thereby, allowing the crystallisation of the polar groups.

Increasing the temperature above the melting of the alkyl chains eventually results in the melting of the polar groups themselves. This process of step-wise melting is very similar to that occurring in monomeric sodium soaps and the cyclic amphiphilic siloxanes (see chapters 2 and 6). For Na<sub>1000</sub>, Na<sub>1500</sub> and Na<sub>2000</sub>, the melting of the polar groups resulted in the

formation of the low viscosity isotropic liquid (i.e. T4). This loss of the ordered arrangement of micelles, indicating that the inter-micelle forces which maintain the hexagonal arrangement of these micelles within the semi-crystalline fluid phases have broken down.

Unlike the longer chain amphiphiles, the melting of the polar groups of Na<sub>500</sub> (also T4), and the resulting loss of crystalline order that occurred at this transition, did not result in a corresponding loss of the inter-micelle order. Consequently, at T4, Na<sub>500</sub> forms a fused H<sub>2</sub> phase rather than the isotropic liquid formed by the longer chain amphiphiles. As steric and, to a lesser degree, electrostatic repulsive forces are responsible for maintaining the mutual arrangement of these micelles<sup>16</sup>, the different behaviour of the members of this series of amphiphiles presumably results from the differing separations of the strongly interacting micelle cores (i.e. the polar groups). That is to say, the inter-micellar forces arise essentially from the polar regions of these molecules and with the shortest chain length amphiphile, the closer proximity of the polar group is sufficient to maintain the order above T4. The fact that unlike the longer chain amphiphiles, Na<sub>500</sub> forms a mesophase above the melting of the polar groups, indicates that the behaviour of this amphiphile is, in this respect, more akin to the behaviour of the conventional straight sodium soaps (i.e. in both conventional sodium soaps and Na<sub>500</sub> inter-micellar forces are sufficient to maintain some inter-micelle order above the melting of the polar groups). This is perhaps not surprising as Na<sub>500</sub>, which is the shortest chain length amphiphile of this series, possesses a molecular structure which is closest to that of the conventional monomeric straight chain sodium soaps (i.e. Na<sub>500</sub> has the addition of approximately 6 dimethylsiloxane units).

Having obtained an overview of the thermotropic phase behaviour of this series of amphiphiles, the effects of repeated heating and cooling a sample of Na<sub>500</sub> between 25 and 280°C were investigated. Whilst the thermogram obtained on the initial heating of this amphiphile was characterised by three first order endothermic transitions in this range, the reheating was characterised by a maximum of two exothermic transitions (see table 7.2). The temperature of these transitions seemed to rise with each analysis, especially so for the lower temperature transition. The replacement of the T2 and T3 transitions which occur during the initial heating of the sample, with one higher temperature transition or the absence of a transition during reheating, may indicate that a different structural arrangement of the alkyl chains is favoured on cooling from the mesophase. The gradual increase in the temperature of the T4 transition with repeated heating may indicate that the polar groups were not initially truly anhydrous and that the repeated heating was driving off any remaining water. However, it is also worth noting that the repeated heating of this sample also resulted in a 2-3% loss in weight and obvious thermal degradation of the sample. Thus, either of these effects may explain the modification of the thermal behaviour of this amphiphile on reheating.

At this stage, it is worth contrasting the effects of the respective siloxane backbones on the phase behaviour of the linear and cyclic amphiphiles studied. In discussing the melting behaviour of the sodium salts of the cyclic amphiphiles (see chapter 6), it was noted that the total heat of fusion for each monomer unit of these oligomeric amphiphiles was substantially less than that of the corresponding monomeric straight chain sodium soaps. It was concluded that the reduced melting enthalpy was primarily associated with a disruption of the packing of the hydrocarbon

chains of the cyclic amphiphiles as a result of the attachment of amphiphiles to a relatively rigid siloxane ring.

A similarly reduced enthalpy of fusion has been noted for the linear amphiphilic siloxanes. Here, the disruption of the packing of the C<sub>10</sub> alkyl chains may be qualitatively understood by the size of the repeat units of the linear dimethylsiloxane chain and, possibly, also some influence of the motions of this very flexible backbone. On the other hand, the repeat unit of the oligomeric methylsiloxane ring is not so large or so flexible. Hence, the detailed mechanism by which the crystalline packing of the alkyl chain is disrupted may not be identical in these different classes of siloxane-containing, amphiphiles.

#### 7.2.1.3 Conclusions

Although this was not an exhaustive study of the thermotropic behaviour of these linear amphiphiles, the following general conclusions may be drawn:

1. The well established principles explaining the phase behaviour of conventional amphiphiles seem to be generally applicable to the rationalisation of the phase behaviour of these novel amphiphiles.
2. As these principles dictate, the non-polar and polar moieties of these amphiphiles tend to aggregate to form micelles in the neat state. The driving force for this aggregation will be the enthalpic contribution from the association of the polar groups.
3. Due to the molecular structure of these amphiphiles (i.e. packing constraints), the structure of these micelles appears to be that of a reversed rod-like micelle.
4. The steric repulsive forces between the polar cores of these micelles result in a two-dimensional hexagonal arrangement of the

micelles, and thus, the formation of hexagonal phases.

5. Within these phases, the siloxane chains form an amorphous continuous phase. Thus, below the  $T_g$  of the siloxane chains (i.e. below  $T1$ ), the properties of these phases would be expected to be those of a solid, whilst above the  $T_g$ , the properties of these phases are known to be those of an ordered fluid.

6. Whilst the siloxane continuous phase is amorphous, the  $C_{11}$  sodium carboxylate groups maintain some crystalline order at temperatures below the melting of the polar head groups (i.e below  $T4$ ). Consequently, below  $T4$ , the fluid phases of these amphiphiles may be considered to be semi-crystalline.

7. Above room temperature, the  $C_{10}$  alkyl chains undergo a two stage melting process,  $T2$  and  $T3$ . This process is analogous to initial stages in the step-wise melting of conventional monomeric straight chain sodium soaps. The complete melting of the alkyl chains does not result in a significant change in the structure or properties of the fluid phases formed by these amphiphiles.

8. The enthalpy changes associated with the melting of the  $C_{10}$  alkyl chains indicates that the attachment of these chains to the siloxane backbone reduces their ability to crystallise. This effect may be more pronounced for the methylene units closest to the siloxane chain, and may be less significant for the methylene units adjacent to the crystalline polar groups.

9. At around  $250^\circ\text{C}$ , the polar groups of these amphiphiles melt. Again, this is analogous to the step-wise melting of related monomeric amphiphiles.

10. The melting of the polar groups has a significant effect on the behaviour of this series of amphiphiles. For the shortest chain length amphiphile ( $\text{Na}_{500}$ ), this transition results in the formation of a hexagonal mesophase. For the longer chain soaps ( $\text{Na}_{1000}$ ,  $\text{Na}_{1500}$  and  $\text{Na}_{2000}$ ), this transition gives rise to the low viscosity isotropic liquid.

11. As inter-micellar forces of repulsion are responsible for maintaining the mutual order arrangement of micelles, the decreased separation of the rod micelles of the shortest chain length amphiphile ( $\text{Na}_{500}$ ) maintains the ordered arrangement of these micelles above the melting of the polar groups. Hence, a mesophase is formed prior to the formation of the low viscosity isotropic liquid. This is analogous to the behaviour of the conventional straight chain sodium carboxylates, to which  $\text{Na}_{500}$  is similar in terms of molecular structure.

12. The relative increased separation of the sodium carboxylate groups of the longer chain length amphiphiles ( $\text{Na}_{1000}$ ,  $\text{Na}_{1500}$  and  $\text{Na}_{2000}$ ) reduces the inter-micelle forces of repulsion and, hence, these amphiphiles form the isotropic liquid once the polar groups have melted.

13. The fact that these linear amphiphiles undergo a number of transitions which are very similar to those occurring in the cyclic amphiphiles discussed in chapter 6, reflects the contribution of the  $\text{C}_{11}$  sodium carboxylate amphiphilic units, which are common to both types of amphiphile, in determining the phase behaviour of these novel amphiphiles.

## 7.2.2 The Calcium Salt of the Shortest Chain Length Amphiphile

### 7.2.2.1 Results

#### 7.2.2.1.1 Polarising Optical Microscopy

A film of the calcium salt of the shortest chain length amphiphile (figure 7.1,  $x=4.0$ ;  $Y=1/2Ca$ ; hereafter referred to as  $Ca_{500}$ ) was examined under the microscope in the temperature range 0–500°C. This material existed as a birefringent viscous fluid at 0°C. This fluid phase exhibited a non-geometric texture and an intermediate viscosity typical of an hexagonal phase (see figure 7.14).



Figure 7.14 Optical texture of the fluid birefringent phase of  $Ca_{500}$  at 50°C.

On heating, a gradual decrease in viscosity and a gradual increase in the birefringence of the phase was observed, although no obvious phase transition occurred up to the transition to the low viscosity isotropic liquid at approximately 450°C. It was not possible to be accurate about the temperature of this transition because of the severe thermal degradation of the sample.

#### 7.2.2.1.2 Differential Scanning Calorimetry (DSC)

A thermogram was recorded on the heating of a previously unmelted sample of Ca<sub>500</sub> between -160°C and 500°C. This thermogram was characterised by three transitions (hereafter denoted as T1, T2, and T3, in order of increasing temperature) and a final large exothermic transition, believed to correspond to the onset of thermal degradation. T1 was second order, whilst T2 and T3 were first order transitions. Figure 7.15 shows a representative thermogram for Ca<sub>500</sub>, whilst table 7.6 summarises the results of this analysis. No cooling or repeated heating analyses were carried out.

TRANSITION	TRANSITION TEMPERATURE (°C) AND CORRESPONDING CHANGES IN ENTHALPY (KJ.mol <sup>-1</sup> ) AND SPECIFIC HEAT CAPACITY (J.g <sup>-1</sup> .K <sup>-1</sup> )
T1	-120 (*)
T2	70 (*)
T3	458 (54)

note - \* indicates that although a transition was observed, the signal was very broad and, therefore, it was not possible to accurately evaluate the enthalpy change occurring; hence, the transition temperatures quoted are approximate.

- the M<sub>n</sub> of Ca<sub>500</sub> is an approximation based on the M<sub>n</sub> of Na<sub>500</sub> from which it was prepared.

Table 7.6 The transition temperatures and corresponding enthalpy changes (in parentheses) observed during the initial heating of a sample of Ca<sub>500</sub> from -160 to 500°C, at a heating rate 10°C.min<sup>-1</sup>.

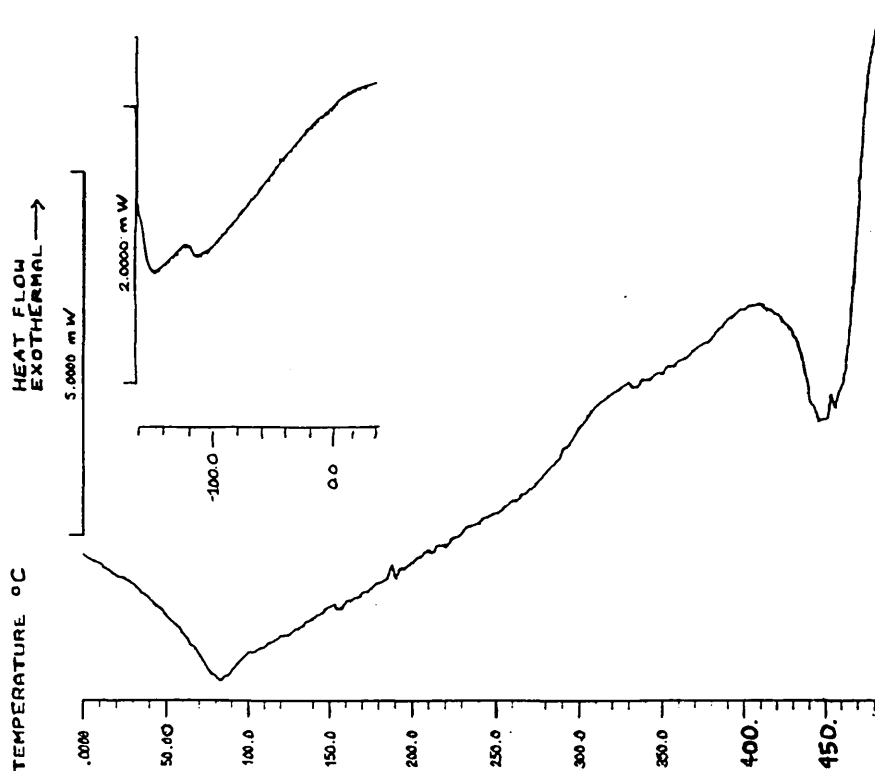


Figure 7.15 Thermograms of a previously unmelted sample of  $\text{Ca}_{500}$  which has been dried over  $\text{P}_2\text{O}_5$  at  $100^\circ\text{C}$  for 24 hours, and heated from  $-160$  to  $0^\circ\text{C}$  and  $0$  to  $500^\circ\text{C}$  at a heating rate of  $10^\circ\text{C}\cdot\text{min}^{-1}$ .

#### 7.2.2.2 Discussion

As this was not an in-depth study, the rationalisation of the observations made has been carried out with particular reference to the behaviour of the related linear and cyclic amphiphiles discussed in previous sections. The non-geometric texture and the intermediate viscosity of  $\text{Ca}_{500}$  from  $0^\circ\text{C}$  up to the transition to the low viscosity isotropic liquid at around  $458^\circ\text{C}$ , were thought to be characteristic of a hexagonal phase<sup>16</sup>. In the absence of any independent supporting evidence (i.e. X-ray diffraction), any interpretation of these observations can only be a tentative one. However, considering the

previous experience with the equivalent sodium salt, Na<sub>500</sub>, it is proposed that the non-geometric texture of Ca<sub>500</sub> was indicative of a hexagonal phase, and that this phase would be made up of a two dimensional hexagonal array of reversed rod micelles (H<sub>2</sub>), containing the polar groups in a non-polar siloxane continuum.

The DSC thermogram obtained during the initial heating of Ca<sub>500</sub> was characterised by a second order transition occurring at around -120°C (T1) and two first order transitions occurring at 70 and 458°C (T2 and T3, respectively). Based on the proposal that Ca<sub>500</sub> forms a phase structure similar to the H<sub>2</sub> phase formed by Na<sub>500</sub>, T1 was believed to be primarily associated with the T<sub>g</sub> of the linear PDMS backbone<sup>327</sup>(see section 7.2.1.2). Thus, the siloxane backbone of Ca<sub>500</sub> would be able to rotate and essentially be liquid-like above T1, whilst below this transition, the liquid-like structure of the polymer would be frozen into a glassy state. The similar optical textures and the presence of a common second order transition at around -120°C seems to indicate that the behaviour of Ca<sub>500</sub> and Na<sub>500</sub> was indeed very similar, particularly at low temperature.

The absence of a transition between T1 and 0°C, suggested that the fluid hexagonal phase of Ca<sub>500</sub> was stable to T1. However, at temperatures below T1 (i.e. the glass transition of the continuous phase), it seems unlikely that the established macroscopic fluidity of this amphiphile at 0°C would be maintained. It thus follows that below T1, Ca<sub>500</sub> would exist as a reversed hexagonal structure with a glass like continuous phase, whose macroscopic properties would be that of a glassy solid.

As a corollary of the proposed amorphous nature of the siloxane continuous phase, it also follows that the structural order within the phases formed by  $\text{Ca}_{500}$  (i.e. above or below  $T_1$ ) must primarily entail the  $\text{C}_{11}$  calcium carboxylate moieties. Hence, the two first order DSC transitions occurring at approximately 70 and 458°C ( $T_2$  and  $T_3$ , respectively) must reflect the melting of these  $\text{C}_{11}$  calcium carboxylate groups, and the ordered fluid phase formed by  $\text{Ca}_{500}$  at temperatures greater than  $T_1$  would appear to be semi-crystalline. Experience with the equivalent sodium salt ( $\text{Na}_{500}$ ) and the calcium salt of the cyclic amphiphile ( $\text{CaD}_4$ ) would indicate that these transitions reflect a step-wise melting of the  $\text{C}_{10}$  alkyl chains followed by the polar groups. This step-wise melting is also analogous to the behaviour of the conventional monomeric calcium soaps<sup>24,149,153,155,166,170</sup>. Whilst the melting of the alkyl chains does not result in a significant change in the phase structure, the complete melting of the polar groups corresponds to the formation of the low viscosity isotropic liquid.

During the study of the sodium salts of the linear and cyclic amphiphiles, it was noted that these related molecules underwent a number of similar transitions above 0°C; it was concluded that this reflected the presence of a common  $\text{C}_{11}$  sodium carboxylate. Having established that the low temperature behaviour of the calcium and sodium salts of the shortest chain linear amphiphiles ( $\text{Ca}_{500}$  and  $\text{Na}_{500}$ ) were similar, and that this reflects the presence of a common non-polar moiety, it was of interest to contrast the high temperature behaviour of the calcium salts of the linear and cyclic amphiphiles (i.e.  $\text{Ca}_{500}$  and  $\text{CaD}_4$ , respectively), which should be determined by the presence of the common calcium carboxylate group (see table 7.7).

	TRANSITION TEMPERATURE AND CORRESPONDING ENTHALPY	
	(°C)	(KJ.mol <sup>-1</sup> )
	Ca <sub>500</sub>	CaD <sub>4</sub>
T2	70 (*)	159 (17)
T3	458 (54)	478 (42)

note - \* indicates that although transition observed, the signal was very broad and therefore it was not possible to accurately evaluate the enthalpy change occurring or the transition temperature.

Table 7.8 A comparison of the transition temperatures and corresponding enthalpy changes (in parentheses) occurring in Ca<sub>500</sub> and CaD<sub>4</sub> above 0°C.

As can be seen in table 7.7, both the cyclic and linear amphiphile undergo two transitions at temperatures greater than 0°C. Whilst there is a significant difference in the temperature at which the first of these transitions occur (i.e. 70 and 159°C for Ca<sub>500</sub> and CaD<sub>4</sub>, respectively), the temperature at which these amphiphiles undergo the transition to the isotropic liquid is very similar. This indicates that the high temperature behaviour of Ca<sub>500</sub> is dominated by the presence of the calcium carboxylate polar group, and in this respect is similar to that of CaD<sub>4</sub>. There is a also significant difference in the enthalpy change per amphiphile of these molecules for the transition to the isotropic liquid. However, due to the high temperature at which the transition to the isotropic liquid occurs and the severe thermal degradation known to be occurring at this temperature, a comparison of the enthalpy changes associated with these transition may be misleading.

Having proposed that the T2 transition primarily represents the melting of the C<sub>10</sub> alkyl chains of Ca<sub>500</sub>, it is of interest to note that the enthalpy

change involved in this transition was relatively small (see table 7.7). This seems to indicate a lack of crystalline order within the alkyl chains of this amphiphile. As was thought to be the case with the equivalent sodium salt, Na<sub>500</sub>, the steric and kinetic effects of the PDMS backbone may restrict the ability of the C<sub>10</sub> alkyl chains to pack, in particular restricting their close approach. Further work is required to confirm this proposal.

Unlike the equivalent sodium salt, Ca<sub>500</sub> did not form a fused mesophase following the melting of the polar groups (i.e. T3). This may presumably be explained by the high temperature at which this transition takes place relative to the sodium salt; The steric and electrostatic interactions between fused polar groups must not be sufficient to maintain a mutual arrangement of the micelles at such a temperature.

### 7.2.2.3 Conclusions

Although this was a limited investigation of the thermotropic phase behaviour of this linear amphiphile, the following general conclusions may be drawn:

1. The principles explaining the phase behaviour of conventional amphiphiles and the equivalent sodium salt, appear to be generally applicable to this novel amphiphile.
2. As these principles dictate, the non-polar and polar moieties of Ca<sub>500</sub> tend to aggregate to form micelles in the neat state. The driving force for this aggregation will be the enthalpic contribution from the association of the polar groups.
3. Due to the molecular structure of Ca<sub>500</sub> (i.e. packing constraints), the structure of these micelles appear to be that of a reversed rod.

4. The steric repulsive forces between the polar cores of these rod micelles result in a two-dimensional hexagonal arrangement of the micelles, and thus, the formation of a hexagonal phase.
5. Within this phase, the siloxane chains form an amorphous continuous phase. Thus, below the  $T_g$  of the siloxane chains (i.e. T1), the properties of this phase would be expected to be those of a solid, whilst above the  $T_g$ , the properties of the phase are known to be that of an ordered fluid.
6. Whilst the continuous siloxane phase is amorphous, the  $C_{11}$  calcium carboxylate groups maintain some crystalline order up to the melting of the polar groups at T3. Below the complete melting of the  $C_{11}$  calcium carboxylates (T3), the fluid phase of this amphiphile may be considered to be semi-crystalline.
7. Above room temperature, the  $C_{10}$  alkyl chains appear to undergo a one stage melting process (T2). This process may encompass all the stages encountered in the melting of the alkyl chains of conventional monomeric straight chain calcium soaps. This melting of the alkyl chains does not result in a significant change in the structure or properties of the fluid phase formed by this amphiphile.
8. The enthalpy changes associated with the melting of the  $C_{10}$  alkyl chains indicates that the attachment of these chains to the siloxane backbone reduces their ability to crystallise. This effect may be more pronounced for the methylene units closest to the siloxane chain, and less significant for the methylene units adjacent to the crystalline polar groups.
9. At around 458°C, the polar groups of these amphiphiles melt and the low viscosity isotropic liquid is formed. This is analogous to the

step-wise melting of related monomeric amphiphiles.

10. The absence of the fused mesophase that occurs above the melting of the polar groups of the equivalent sodium salt (i.e. Na<sub>500</sub>), is presumably a consequence of the relatively high temperature at which the melting of the polar groups of Ca<sub>500</sub> occurs. That is to say, that the inter-micellar forces of repulsion responsible for maintaining the mutual order arrangement of micelles, are not sufficient to maintain this order, at temperatures greater than the melting point of the calcium carboxylate polar groups (i.e at approximately 150°C above the melting point of the sodium carboxylate groups).

11. The fact that this linear amphiphile undergoes a number of transitions which are similar to those occurring in the cyclic amphiphile discussed in chapter 6, reflects the presence of the C<sub>11</sub> calcium carboxylate amphiphilic units, which are common to both classes of amphiphile.

12. The fact that the low temperature behaviour of Ca<sub>500</sub> and Na<sub>500</sub> is very similar, reflects the influence of the common hydrophobic moieties.

### 7.3. Lyotropic Phase Behaviour

#### 7.3.1. The sodium salt, Na<sub>1000</sub>

##### 7.3.1.1 Results

###### 7.3.1.1.1 Polarising Optical Microscopy

Films of Na<sub>1000</sub> were prepared by placing samples between a cover-slip and a microscope slide at room temperature and depressing the cover-slip. As has already been discussed, the optical texture of the neat material was indicative of a hexagonal phase (see section 7.2.1.2).

Water was then contacted with the edge of a sample at 5°C. After 10 minutes the sample was gradually heated up to 100°C. There was no evidence of any interaction between the amphiphile and the water in this temperature range.

Silicone fluid was also contacted with the edge of a sample of this amphiphile at 5°C. After 10 minutes the sample was gradually heated. There was no evidence of any interaction between the amphiphile and the silicone fluid, up to the formation of an isotropic liquid at 249°C.

##### 7.3.1.2 Discussion

###### 7.3.1.2.1 The Aqueous phase Behaviour

The overview of the lyotropic phase behaviour of Na<sub>1000</sub> afforded by the use of the penetration technique<sup>269</sup>, indicated no interaction between this amphiphile and water between 5 and 100°C. Bearing in mind that Na<sub>1000</sub> represents a modification of conventional straight chain sodium soaps, which are water soluble and known to form a number of lyotropic mesophases with water (see chapter 2), this is at first, a surprising observation. However, a consideration of the conclusions drawn from the

study of the thermotropic behaviour of this amphiphile, may assist in proposing a possible explanation for this behaviour, based on the phase structure formed by Na<sub>1000</sub> in the neat state.

The molecular structure of Na<sub>1000</sub> (i.e. the size and nature of the dimethylsiloxane chain) results in the formation of reversed rod micelles in the neat state. The packing of these micelles results in the formation of a two dimensional reversed hexagonal phase, in which the siloxane chains constitute the continuous phase. Hence, the existence of a non-polar continuum can be envisaged to limit the water solubility of this amphiphile, and results in the observed absence of any amphiphile/water interaction.

#### 7.3.1.2.2 The Non-Aqueous Phase Behaviour

The overview of the phase behaviour of the Na<sub>1000</sub>/silicone oil system between 5 and 300°C was obtained using the penetration technique. The observations resulting from this technique indicated no interaction of the amphiphile and the solvent within the temperature range studied (i.e. at a temperature below the transition to the low viscosity isotropic liquid at 249°C).

Previous studies of mixtures of anionic amphiphiles and non-polar hydrocarbon solvents<sup>131,151,201-205</sup> have indicated that crystalline anionic amphiphiles show very little solubility in hydrocarbons at room temperature due to the very strong bonding between the polar groups. The solubility of these soaps increases with temperature, the rate of increase depending on the soap and the solvent. As was discussed in chapter 2, these crystalline anionic amphiphiles undergo a step-wise melting process, in which the alkyl chains and then the polar groups melt. Over the intermediate temperature

range, a limited amount of the non-polar solvent may dissolved in the disordered hydrocarbon regions of the soap, while the polar groups retain their crystalline order<sup>206,207</sup>. Where the soap undergoes a thermotropic transition to a mesophase, complete solubility of this soap in non-polar solvents at temperatures above this transition is also thought to occur<sup>148,333</sup>. Bearing these observations in mind, the limited solubility of Na<sub>1000</sub> in the non-polar solvent is perhaps not surprising, as the reverse hexagonal structure proposed for Na<sub>1000</sub> below the transition to the low viscosity isotropic liquid is thought to be semi-crystalline (see section 7.2.1.2). Thus, the limited solubility of Na<sub>1000</sub> may be due to the strong bonding between the polar groups.

### 7.3.2 The Calcium Salt, Ca<sub>500</sub>

#### 7.3.2.1 Results

##### 7.3.2.1.1 Polarising Optical Microscopy

A film of Ca<sub>500</sub> was prepared by placing a sample between a cover-slip and a microscope slide at room temperature and depressing the cover-slip. As has been discussed, the texture of the phase observed, was indicative of a hexagonal phase (see section 7.2.2.2).

Water was then contacted with the edge of the sample at 5°C. After 10 minutes, the sample was gradually heated up to 100°C. There was no evidence of any interaction between the amphiphile and the water in this temperature range.

Penetration experiments using a non-polar solvent were not carried out.

### 7.3.2.2 Discussion

Again, the overview of the lyotropic phase behaviour of the amphiphile/water system between 5 and 100°C was obtained using the penetration technique. Within this temperature range, no interaction of the solvent and the amphiphile was evident. As was the case with the aqueous lyotropic behaviour of Na<sub>1000</sub>, the limited water solubility of Ca<sub>500</sub> may be explained with reference to the thermotropic phase behaviour of this amphiphile (see section 7.2.2.2).

As a result of the molecular structure of the amphiphile, the structure of the micelles formed by Ca<sub>500</sub> in the neat state is believed to be that of a reversed rod micelle. Thus, the packing of these micelles results in a two-dimensional hexagonal arrangement in which the siloxane chains constitute the continuous phase. Hence, as was the case with the sodium salt discussed previously, the limited water solubility of Ca<sub>500</sub> may be rationalised with reference to the non-polar nature of the continuous phase, in addition to the strong forces of attraction between adjacent polar groups.

## CHAPTER 8. THERMOTROPIC PHASE BEHAVIOUR OF THE CYCLIC NON-AMPHIPHILIC SILOXANES

### 8.1 Introduction

The cyclic non-amphiphilic siloxanes consisted of the cyclic tetramer or pentamer methylsiloxane backbone, to which a conventional non-amphiphilic mesogenic moiety (4'-methoxyphenyl 4-oxybenzoate) was attached at each of the silicon atoms of the siloxane ring, via an alkyl chain of three, five or six methylene units. The structures of these materials is shown below:

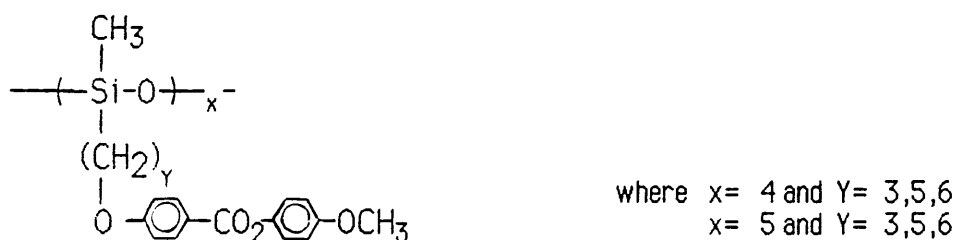


Figure 8.1 The cyclic non-amphiphilic siloxanes (hereafter referred to as  $D_xC_y$ , indicating the number of siloxane units in the backbone ( $D_x$ ) and the number of methylene units in the spacer group ( $C_y$ )).

Although a great deal of work has been published on the thermotropic phase behaviour of linear non-amphiphilic side-chain polymers<sup>64,73,81,82,84,89,92, 94,96-100,246,271,332,334-349</sup>, including siloxanes, relatively little work has been carried out on the corresponding cyclic systems (see chapter 1). Hence, in addition to the characterisation of the cyclic and linear amphiphiles which formed the major subject of this thesis (see chapters 6 and 7), the study of these cyclic non-amphiphilic siloxanes was thought to be a valuable supplement to this work. The main priority here was to gain an overview of the thermotropic phase behaviour of these novel cyclic oligomers, and then contrast this behaviour with that of the equivalent linear side-chain polymers<sup>64,99</sup>. This overview of phase behaviour was

obtained using a combination of DSC and optical microscopy as outlined in chapter 5.

As was discussed in chapter 1, the thermotropic phase behaviour of linear side-chain non-amphiphilic polymers is very much dependent upon the nature of the mesogenic moiety<sup>64,334</sup>, the repeat unit of the polymer backbone<sup>334,337,341</sup>, the degree of polymerisation<sup>64,349</sup> and, where appropriate, the spacer group used to covalently couple the backbone and the mesogen together<sup>99,271,332,334</sup>. Consequently, the study of these novel cyclic oligomers may result in some additional understanding of the effects on thermotropic phase behaviour of:

- polymer fixation of non-amphiphilic mesogens
- variation in the  $\overline{DP}$  of such side-chain structures
- the nature of the backbone itself

## 8.2 Results

### 8.2.1 Polarising Optical Microscopy

The initial microscopy of samples of the cyclic non-amphiphilic tetramer and pentamer with alkyl chain spacers of three methylene units (figure 8.1,  $x=4$  and  $5$ ,  $Y=3$ ; hereafter referred to as  $D_4C_3$  and  $D_5C_3$ , respectively) was characterised by one optical event, which was the transition from an opaque solid to a viscous isotropic liquid at  $24$  and  $20.5^\circ\text{C}$ , respectively. As the temperature was increased the viscosity of this phase gradually decreased.

The initial microscopy of samples of the cyclic siloxanes with alkyl chain spacers of five and six methylene units (figure 8.1,  $x=4$  and  $5$ ,  $Y= 5$  and  $6$ ; hereafter referred to as  $D_4C_5$ ,  $D_5C_5$ ,  $D_4C_6$  and  $D_5C_6$ , respectively) was characterised by two optical events (see table 8.1). These events were, the

transition from an opaque solid to a birefringent mesophase and the transition to the low viscosity isotropic liquid.

Sample	Transition Temperatures (°C )			
	Initial heating		Secondary heating of thin sample films	
	Initial softening	Loss of birefringence	Initial softening	Loss of birefringence
D <sub>4</sub> C <sub>3</sub>	24	not applicable	21	not applicable
D <sub>5</sub> C <sub>3</sub>	20.5	not applicable	17	not applicable
D <sub>4</sub> C <sub>5</sub>	11	92.5	10.5	92.5
D <sub>5</sub> C <sub>5</sub>	21.5	116.5	19.5	117
D <sub>4</sub> C <sub>6</sub>	10	99.5	9.5	100
D <sub>5</sub> C <sub>6</sub>	9	85.5	7.5	85

Table 8.1 Transition observed under microscope during the initial and secondary heating of this series of non-amphiphilic siloxanes.

Whilst it was difficult to assign a texture at low temperatures, the mesophases exhibited a bright texture which was more characteristic of a schlieren pattern at temperatures just below the transition to the isotropic liquid. The viscosity of these mesophases decreased as the temperature increased, and at temperatures just below the transition to the isotropic liquid was similar to that of the higher temperature low viscosity isotropic liquid. Thus, at temperatures about 10°C below the respective transitions to the isotropic liquid, the relatively low viscosity, the flickering birefringence and the textures were characteristic of nematic mesophases.

Films of all these materials were then prepared by placing samples between a cover-slip and a microscope slide, heating to about 10°C above the respective transitions to the isotropic liquids, and cooling slowly to room

temperature. Microscopy of these films indicated a non-birefringent solid phase for  $D_4C_3$  and  $D_5C_3$ , and a birefringent solid phase for  $D_4C_5$ ,  $D_5C_5$ ,  $D_4C_6$  and  $D_5C_6$ . The texture of the birefringent solids were not characteristic of any one pattern, possible due to a very fine structure. As the temperature was increased, the depression of the cover-slip indicated a softening of all these sample films (see table 8.1). This softening was not accompanied by an obvious change in the optical texture of the samples, i.e. for  $D_4C_3$  and  $D_5C_3$  there was a transition to the viscous isotropic liquid, and for  $D_4C_5$ ,  $D_5C_5$ ,  $D_4C_6$  and  $D_5C_6$  there was a transition to a viscous birefringent liquid. On further heating there was a gradual decrease in the viscosity of all these materials, and a final transition to the low viscosity isotropic liquid for  $D_4C_5$ ,  $D_5C_5$ ,  $D_4C_6$  and  $D_5C_6$ .

At temperatures just above the softening of the samples, the textures were not characteristic of any particular phase. However, as the temperature approached the transition to the isotropic liquid, the textures became more recognisable as characteristic schlieren patterns. It should be emphasised that as the temperature increased no mesophase-mesophase transitions were identified. Hence, although the textures observed at low temperatures were ambiguous, the patterns obtained at higher temperatures and the shimmering birefringence were thought to be indicative of the structures observed at lower temperatures.

Finally, fresh samples of  $D_4C_5$ ,  $D_5C_5$ ,  $D_4C_6$  and  $D_5C_6$  were prepared by cooling from the low viscosity isotropic liquid to approximately  $10^\circ\text{C}$  below the mesophase to isotropic liquid transition. These were then annealed at this temperature for 2 hours to allow textures to develop (figures 8.2 to 8.5).

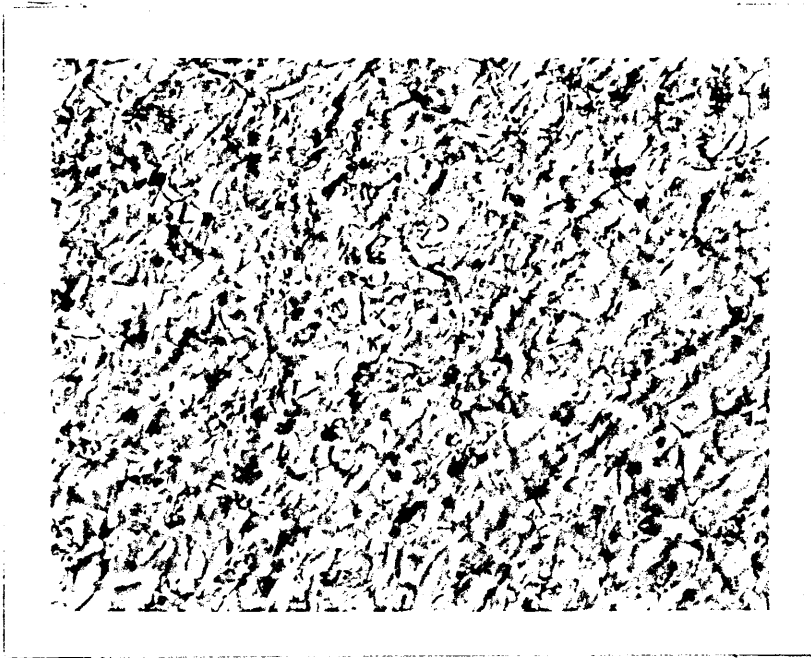


Figure 8.2 Schlieren texture of the birefringent mesophase of  $D_4C_5$  at  $82^\circ C$ .

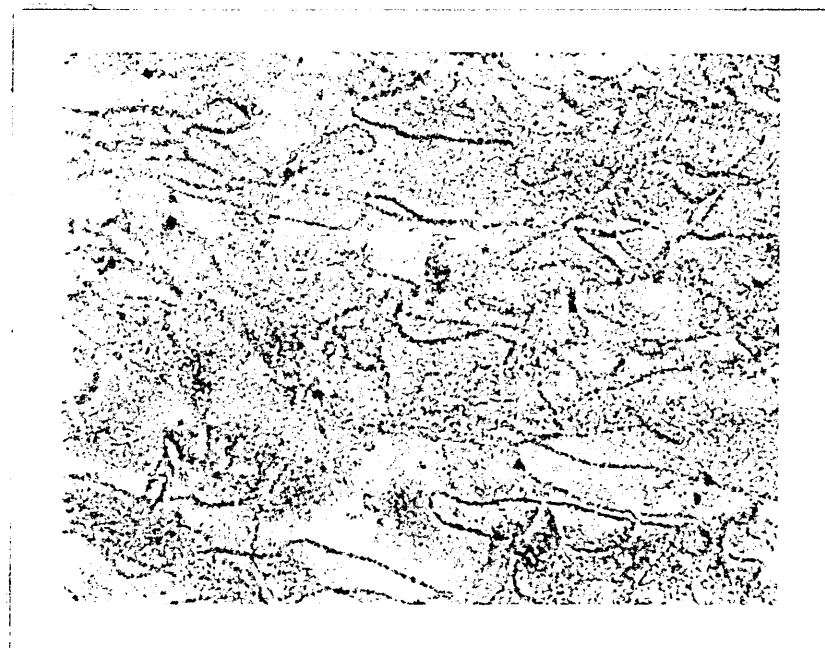


Figure 8.3 Schlieren texture of the birefringent mesophase of  $D_5C_5$  at  $107^\circ C$ .

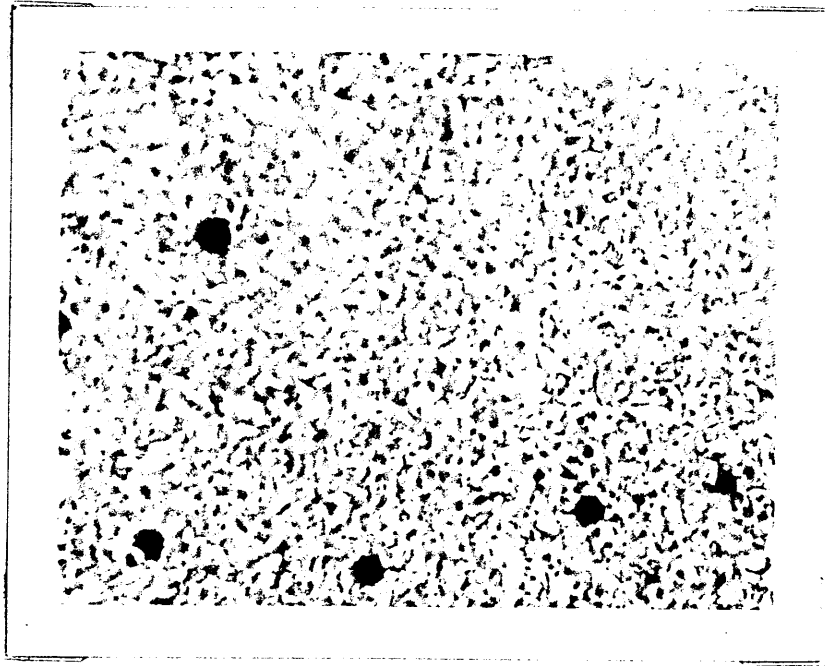


Figure 8.4 Fine schlieren texture of the mesophase of  $D_4C_6$  at  $89^\circ C$ .

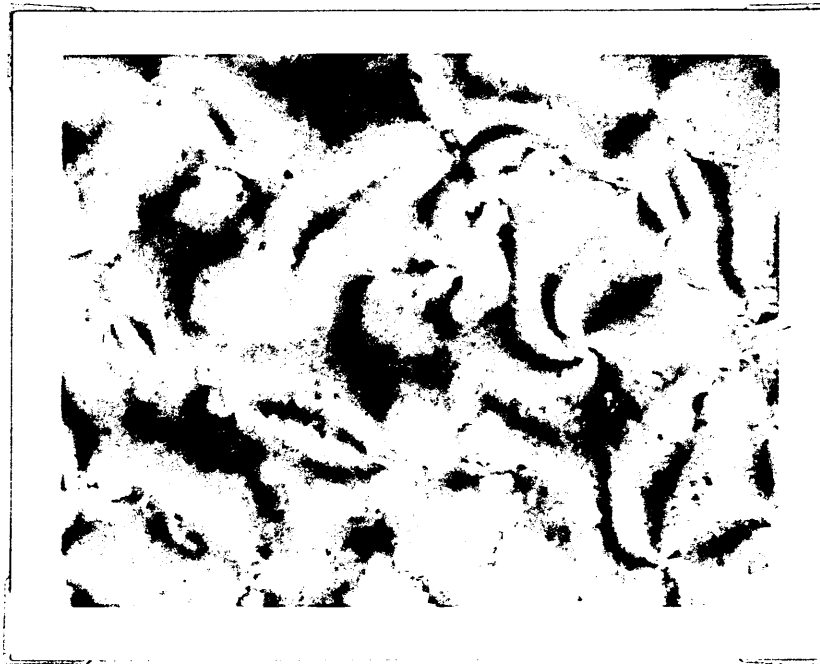


Figure 8.5 Schlieren texture of the birefringent mesophase of  $D_5C_6$  at  $75^\circ C$ .

## 8.2.2 Differential Scanning Calorimetry (DSC)

Thermograms were initially recorded during heating cycles with a heating rate of  $10^{\circ}\text{C}\cdot\text{min}^{-1}$ . These thermograms were characterised by up to 3 transitions (hereafter denoted as T1, T2, and T3, in order of increasing temperature). T1 was always a second order transition, whilst T2 and T3 were first order. Although not all the members of this series exhibited the same number of transitions, for ease of reference and discussion the transitions have been arbitrarily categorised on the basis of their temperature of occurrence (i.e. the lowest and highest temperature transitions were referenced T1 and T3, respectively; and, where appropriate, the transition occurring at an intermediate temperature was referenced T2). Figures 8.6-8.11 show the thermograms obtained, whilst table 8.2 summarises the results of these analyses.

SAMPLE	TRANSITION TEMPERATURE ( $^{\circ}\text{C}$ ) AND THE CORRESPONDING CHANGES IN ENTHALPY ( $\text{KJ}\cdot\text{mol}^{-1}$ ) OR SPECIFIC HEAT CAPACITY ( $\text{J}/\text{G}\cdot\text{K}$ )		
	T1 [ $\text{K}/\text{J}\cdot\text{g}^{-1}\cdot\text{K}^{-1}$ ]	T2 [ $\text{K}/\text{KJ}\cdot\text{mol}^{-1}$ ]	T3 [ $\text{K}/\text{KJ}\cdot\text{mol}^{-1}$ ]
D <sub>4</sub> C <sub>3</sub>	23/0.38	<-----not applicable----->	
D <sub>5</sub> C <sub>3</sub>	17/0.32	<-----not applicable----->	
D <sub>4</sub> C <sub>5</sub>	8/0.28	* 45	89/1
D <sub>5</sub> C <sub>5</sub>	* 19	39/2	112/2
D <sub>4</sub> C <sub>6</sub>	8/0.28	not applicable	92/1
D <sub>5</sub> C <sub>6</sub>	7/0.20	not applicable	* 75

note - \* although transition was observed, no evaluation of the enthalpy change occurring was carried out. Hence, the transition temperatures quoted are approximate.

Table 8.2 The transition temperatures and corresponding changes in enthalpy or specific heat capacity observed during the heating of the non-amphiphilic cyclic siloxanes at a heating rate  $10^{\circ}\text{C}\cdot\text{min}^{-1}$ .

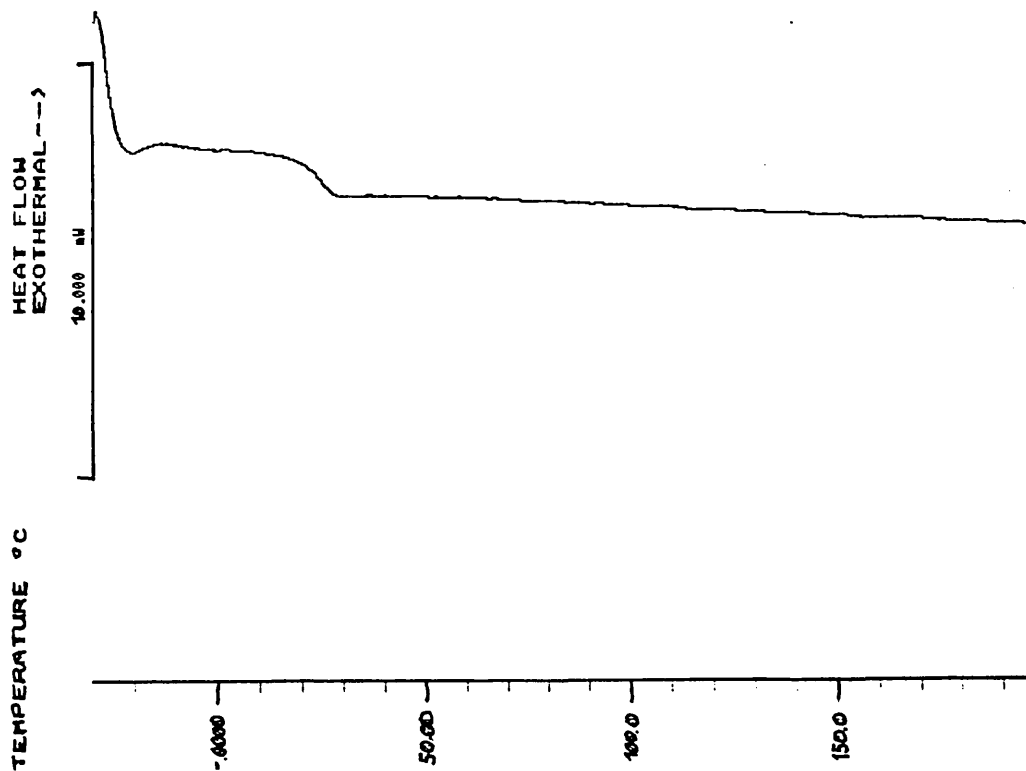


Figure 8.6 Thermogram obtained on heating a sample of  $D_4C_3$  from  $-30$  to  $200^\circ\text{C}$  at rate of  $10^\circ\text{C}\cdot\text{min}^{-1}$

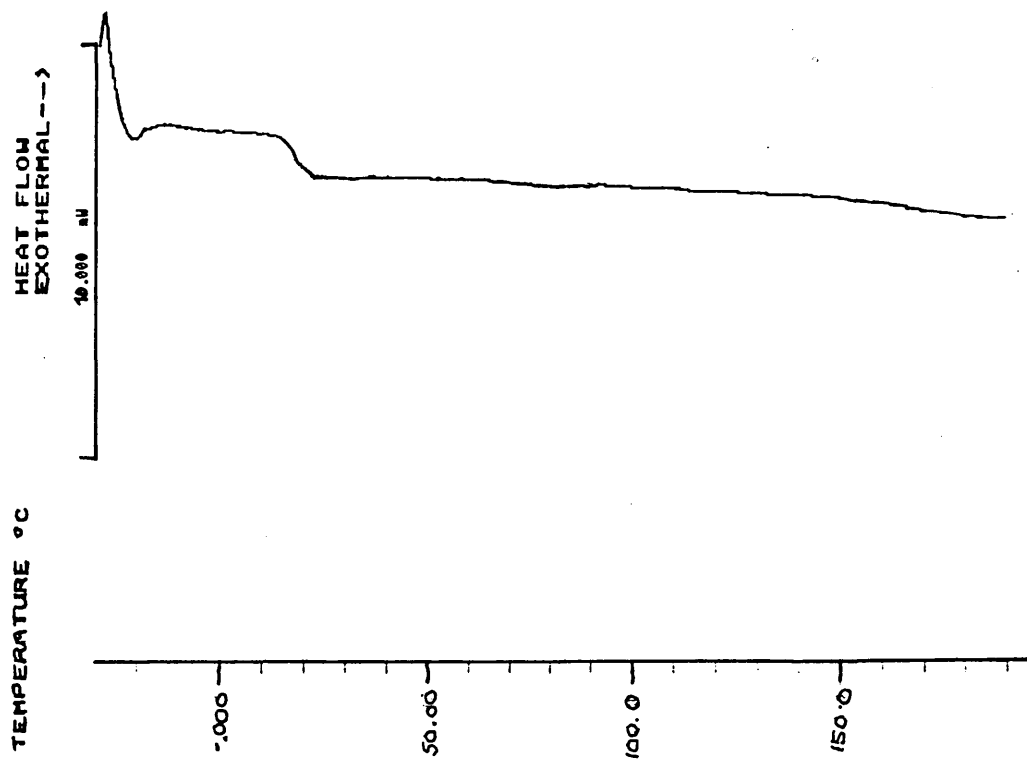


Figure 8.7 Thermogram obtained on heating a sample of  $D_5C_3$  from  $-30$  to  $200^\circ\text{C}$  at rate of  $10^\circ\text{C}\cdot\text{min}^{-1}$

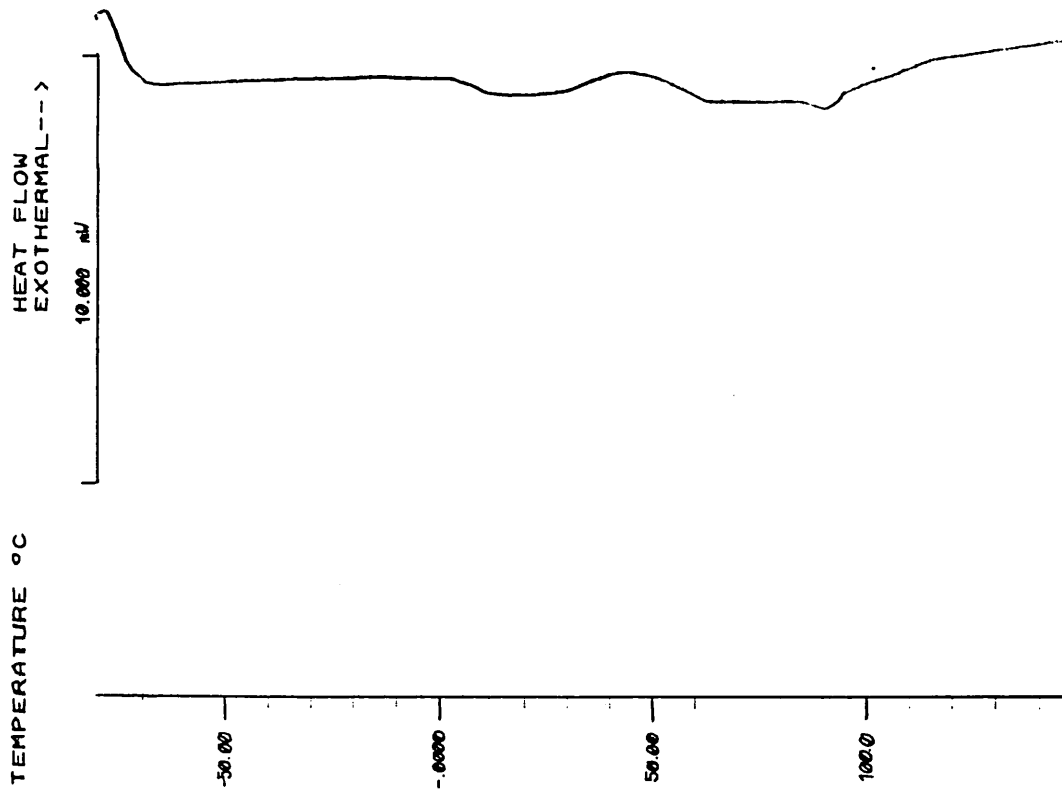


Figure 8.8 Thermogram obtained on heating a sample of  $D_4C_5$  from  $-80$  to  $150^\circ\text{C}$  at rate of  $10^\circ\text{C}\cdot\text{min}^{-1}$

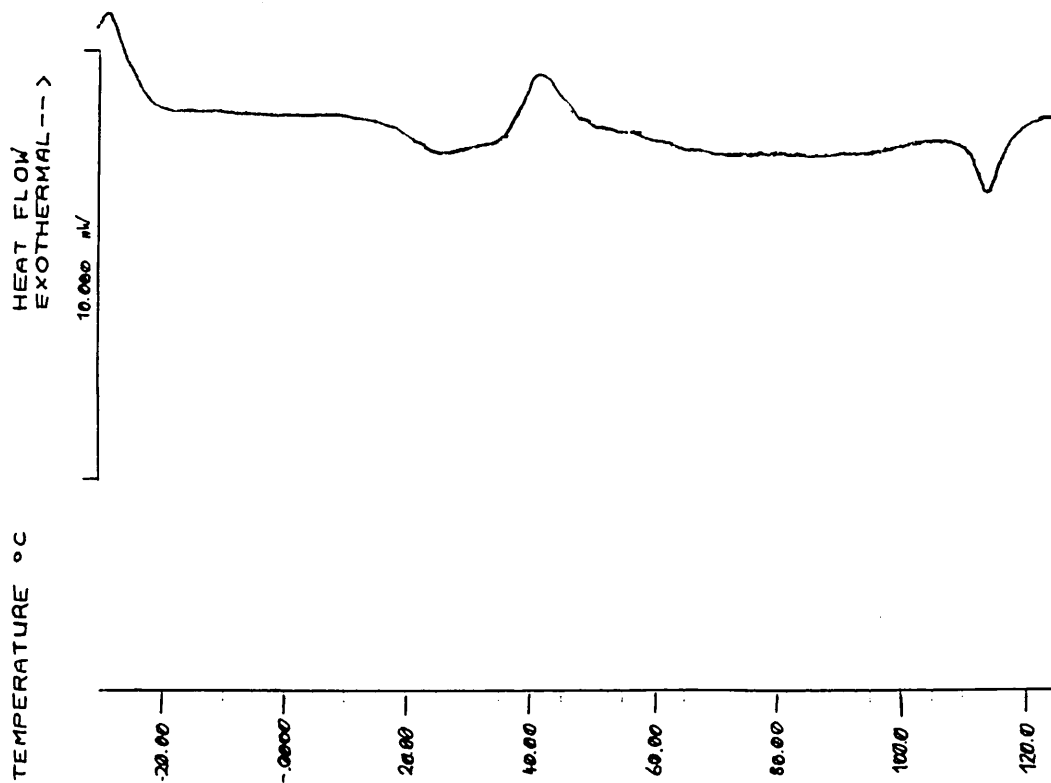


Figure 8.9 Thermogram obtained on heating a sample of  $D_5C_5$  from  $-30$  to  $130^\circ\text{C}$  at rate of  $10^\circ\text{C}\cdot\text{min}^{-1}$

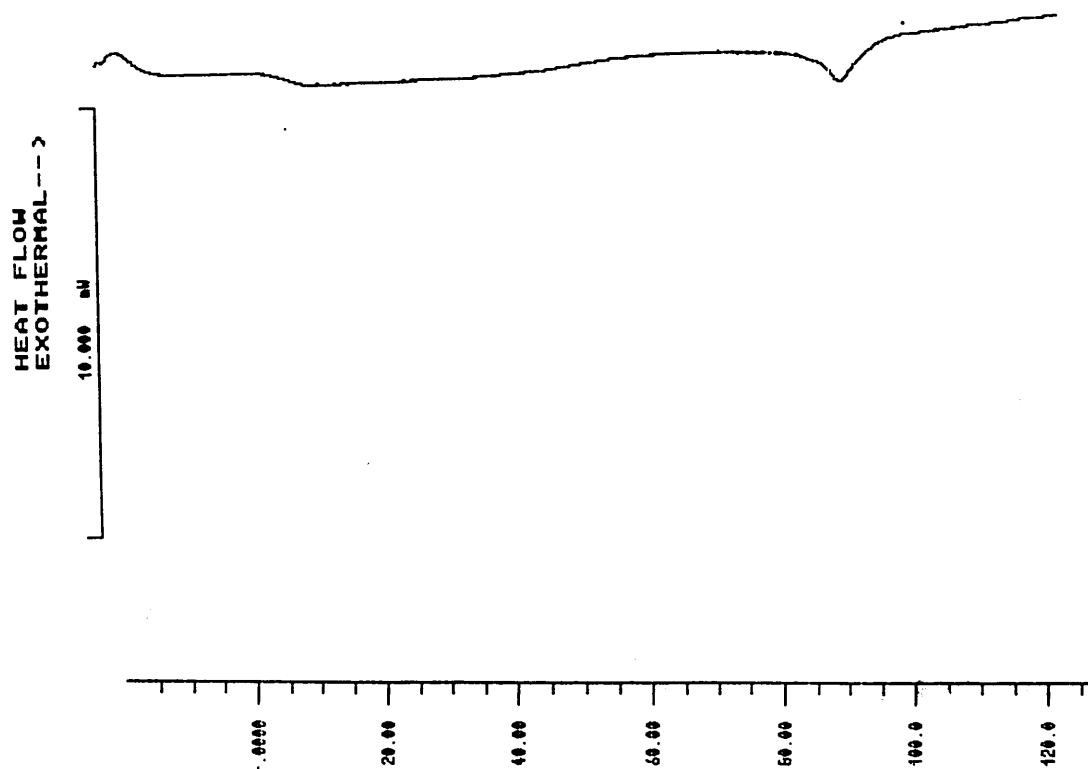


Figure 8.10 Thermogram obtained on heating a sample of  $D_4C_6$  from  $-20$  to  $130^\circ\text{C}$  at rate of  $10^\circ\text{C}\cdot\text{min}^{-1}$

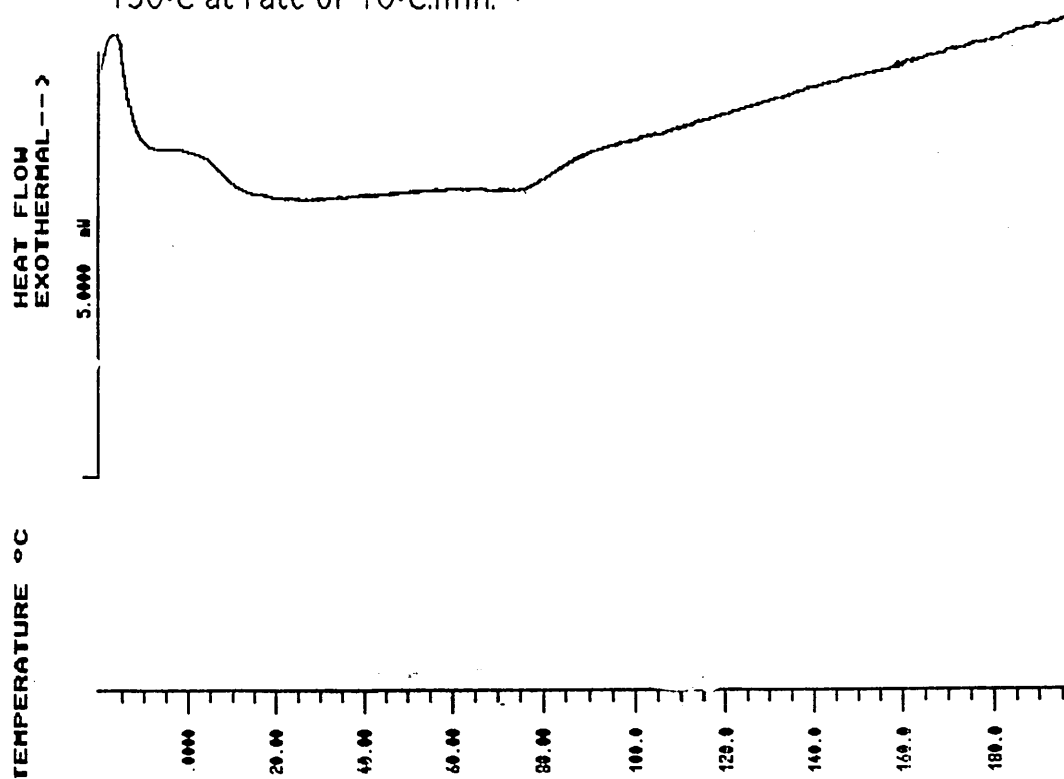


Figure 8.11 Thermogram obtained on heating a sample of  $D_5C_6$  from  $-20$  to  $130^\circ\text{C}$  at rate of  $10^\circ\text{C}\cdot\text{min}^{-1}$

Thermograms were then recorded on cooling the above samples of  $D_4C_5$  and  $D_5C_5$  from 140 to  $-30^\circ\text{C}$  at  $10^\circ\text{C}\cdot\text{min}^{-1}$ . The thermograms were characterised by up to two transitions (hereafter, denoted as  $T_{1c}$  and  $T_{2c}$ , in order of increasing temperature).  $T_{1c}$  was a second order transition, whilst  $T_{2c}$  was a first order endothermic transition. Figure 8.12 shows the thermograms obtained, whilst table 8.3 summarises the results of these analyses.

SAMPLE	TRANSITION TEMPERATURE ( $^\circ\text{C}$ ) AND THE CORRESPONDING CHANGES IN ENTHALPY ( $\text{KJ}\cdot\text{mol}^{-1}$ ) OR SPECIFIC HEAT CAPACITY ( $\text{J}/\text{G}\cdot\text{K}$ )	
	$T_{1c}$ [ $^\circ\text{C} / \text{J}\cdot\text{g}^{-1}\cdot\text{K}^{-1}$ ]	$T_{2c}$ [ $^\circ\text{C}/\text{KJ}\cdot\text{mol}^{-1}$ ]
$D_4C_5$	2/0.35	86/2
$D_5C_5$	1/0.29	111/3

Table 8.3 The transition temperatures and corresponding changes in enthalpy or specific heat capacity observed during the cooling of  $D_4C_5$  and  $D_5C_5$  at a rate  $10^\circ\text{C}\cdot\text{min}^{-1}$ .

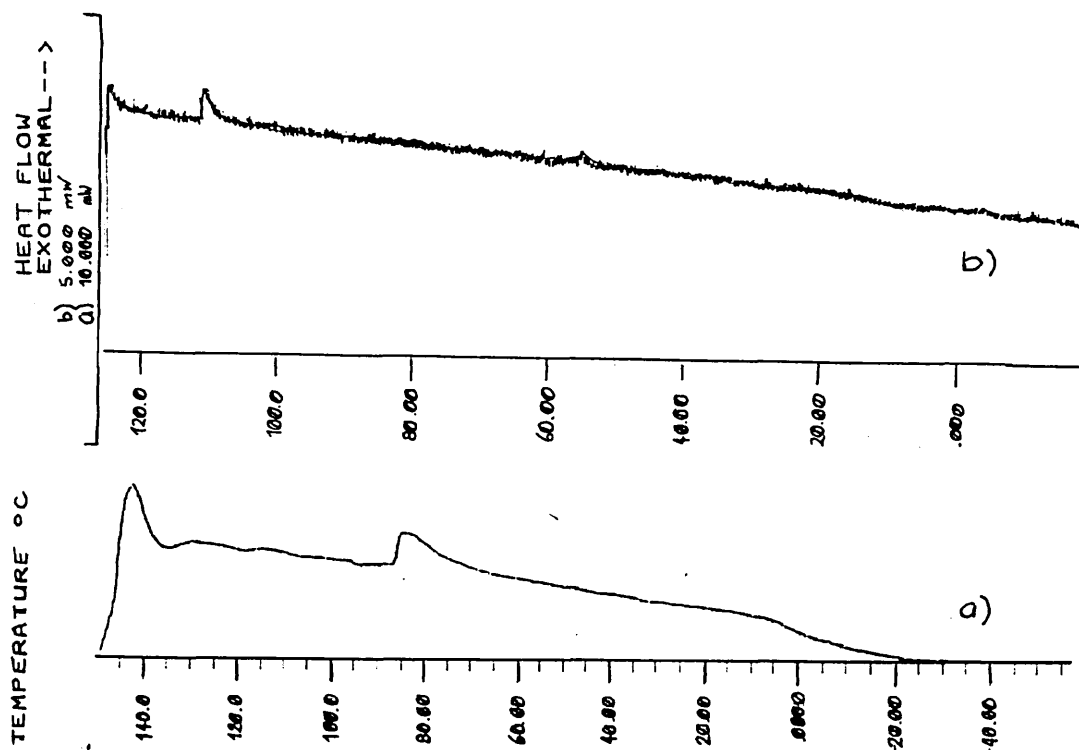


Figure 8.12 Thermograms obtained on cooling a)  $D_4C_5$  and b)  $D_5C_5$ .

### 8.3 Discussion

Optical microscopy indicated that  $D_4C_3$  and  $D_5C_3$  soften from an isotropic solid to a viscous isotropic liquid at 21 and 17°C respectively, and that the viscosity of the isotropic liquid gradually decreased with increasing temperature. The thermograms obtained during the heating of  $D_4C_3$  and  $D_5C_3$  were characterised by one second order transition only (i.e. T1). Bearing in mind the different nature of DSC and optical techniques, the temperature of T1 corresponded to the optical observation of the softening of these samples (see tables 8.1 and 8.2). Thus, the results of the DSC and optical studies of  $D_4C_3$  and  $D_5C_3$  were in general agreement, and it was concluded that both  $D_4C_3$  and  $D_5C_3$  are isotropic in the solid and the liquid states.

Unlike  $D_4C_3$  and  $D_5C_3$ , optical microscopy of  $D_4C_5$ ,  $D_5C_5$ ,  $D_4C_6$  and  $D_5C_6$  indicated the formation of a mesophase prior to the transition to the low viscosity isotropic liquid. The temperature at which these birefringent fluid phases formed depended upon the individual species, but was in the range 7.5 to 21°C (see table 8.1 for transition temperatures). Although the viscosity of these birefringent phases gradually reduced with increasing temperature, no mesophase-mesophase transitions were identified. The schlieren texture, the shimmering birefringence and the low viscosity of these mesophases—at least at temperatures just below the transition to the low viscosity isotropic liquid—were characteristic of nematic mesophases (see figures 8.2-8.5).

The thermograms obtained during the heating of  $D_4C_5$  and  $D_5C_5$  were characterised by three transitions. The transitions observed at the lowest and the highest temperatures (i.e. T1 and T3) corresponded to the optical

observations of the initial softening of the samples and the formation of the isotropic liquid, respectively. However, the remaining DSC transition, T2, did not correspond to any optical event. This, and the low enthalpy change involved, would seem to indicate that T2 corresponds to a relatively minor change in the structural order within the samples. It should also be noted that the exothermic nature of T2 indicates a disorder-order transition. The occurrence of such a transition with increasing temperature suggests that the lower temperature phase may not be the thermodynamically preferred structure, and is metastable.

The thermograms obtained during the cooling of  $D_4C_5$  and  $D_5C_5$  gave only two transitions,  $T1_c$  and  $T2_c$ . As the temperature and nature of T1 and  $T1_c$  were similar, and optical microscopy had demonstrated the reversibility of the solid to mesophase transition, it seems reasonable to suggest that these thermal events correspond to the same solid-mesophase transformations. As the temperature of the  $T2_c$  transition was similar to that of the highest temperature transition observed during the DSC heating (i.e. T3) and the optical observation of the transition to the isotropic liquid, it is reasonable to propose that this transition corresponds to the isotropic liquid-mesophase transition.

Although it should not be considered as conclusive evidence, the fact that no transition corresponding to T2 was observed on cooling, supports the proposition that T2 represented a transition from a metastable phase. Such a phase may have resulted from a cooling of the samples before the molecular segments had time to adopt the thermodynamically preferred spatial arrangement (e.g. the cooling of the samples following the original purification and vacuum drying; see chapter 4). In common with the

reported behaviour of a linear side-chain polysiloxane<sup>344</sup>, T2 may therefore be due to a 'cold crystallisation' occurring during the DSC heating analysis. It is, however, interesting to note that there is little super-cooling of either isotropic-mesophase or mesophase-solid transitions. This would not seem to be in line with the proposal that kinetic effects are important at the heating and cooling rates employed.

The thermograms obtained during the heating of  $D_4C_6$  and  $D_5C_6$  were characterised by two transitions. The low temperature second order transition (T1) corresponds to the optical observation of the initial softening of the samples. The higher temperature transition (T3) was at a lower temperature than the optical observation of the transition to the low viscosity isotropic liquid, particularly so in the case of  $D_5C_6$ . At this stage, no explanation for this discrepancy can be proposed. This, and the observation of a relatively broad transition for T3 of  $D_5C_6$  (~30K peak width) may warrant further investigation.

Unlike  $D_4C_5$  and  $D_5C_5$ , the thermograms of  $D_4C_6$  and  $D_5C_6$  did not exhibit an exothermic transition at temperatures between T1 and T3. At this stage, this different phase behaviour for related molecules with nominally the same thermal history cannot be fully explained. However, if T2 corresponds to a cold crystallisation of  $D_4C_5$  and  $D_5C_5$ , then the increased length of spacer in  $D_4C_6$  and  $D_5C_6$  may result in more flexible segments which are able to adopt the thermodynamically preferred spatial arrangements at higher cooling rates than  $D_4C_5$  or  $D_5C_5$ .

This difference withstanding, the overall behaviour of this series of materials may be summarised as follows:

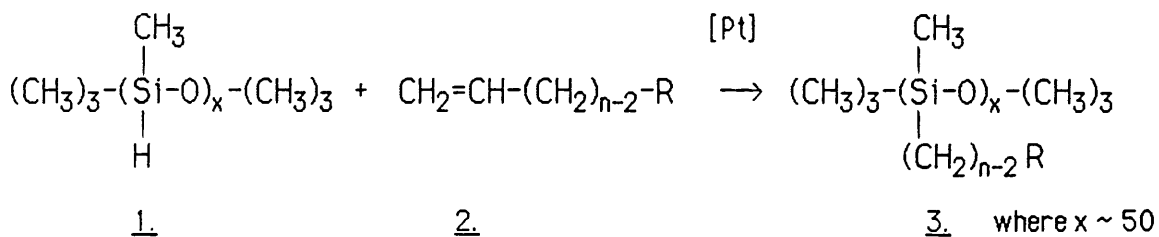
- $D_4C_3$  and  $D_5C_3$  are amorphous solids at low temperature and undergo a glass transition to a viscous isotropic liquid
- $D_4C_5$ ,  $D_5C_5$ ,  $D_4C_6$  and  $D_5C_6$  exist as ordered solids at low temperature and undergo a step-wise melting, via the nematic mesophase, to a low viscosity isotropic liquid.

In attempting to rationalise the behaviour of these novel cyclic systems, it may be useful to briefly review the behaviour of linear non-amphiphilic side-chain systems, in particular the oligomeric and polymeric siloxanes.

The modification of the phase behaviour of monomeric mesogens following fixation to a linear polymeric backbone has been explained by the application of model considerations and with the 'spacer group' concept as originally proposed by Finkelmann *et al.*<sup>64,332,334</sup>. As we have seen in chapter 1, if rod- or disc-type mesogens are attached to a polymer backbone as side-chains, two extreme cases are possible; direct attachment of the mesogen to the backbone or attachment via a long 'spacer' group<sup>64,73</sup> (see figure 1.11, page 25). In the former case, the tendency of the polymer backbone to adopt a statistical distribution of possible chain conformations above the  $T_g$  tends to result, except in a few cases<sup>81,82,84</sup>, in a disruption of any parallel alignment of the mesogen. Thus in most cases, only isotropic polymer melts are observed, or solid polymers with an anisotropic structure which is irreversibly lost if the polymer is heated above its  $T_g$ . Where the mesogen is fixed to the polymer via a long spacer group, the presence of this group decouples the motions of the mesogens and the backbone. Thus, in a manner analogous to that of their small molecule equivalents, a

mesomorphic arrangement of such polymer-bound mesogens is feasible<sup>64</sup>. In line with these model considerations, it also follows that the longer the spacer group, the greater the decoupling of any mesogen-backbone interactions. Consequently, the variation of the length of the spacer group can also influence the type of ordering of the mesogens in side-chain polymers<sup>64</sup>. With short-chain spacers, no positional ordering of the centres of gravity of the mesogens is possible and the nematic and cholesteric phases result. With long-chain spacers, greater positional ordering of the mesogens is possible, and the smectic phases may occur.

With reference to these model considerations, Finkelmann's<sup>99</sup> study of linear side-chain siloxanes which incorporated the same mesogen as that being employed in this research, is of particular relevance. The details of the polymers studied in this work and the corresponding phase transitions have been given in figure 8.13 below.



n	R	Phase transition temperatures(°C)	
		monomer (2.)	polymer (3.)
a 3		k 89 i	g 15 n 61 i
b 4		k 87 i	g 15 n 95 i
c 5		k 90 i	k 87 n 115 i
d 6		k 63 i	g 15 s 46 n 112 i

(where g = glassy; k = crystalline; i = isotropic; n = nematic; s = smectic)

Figure 8.13 The structure and phase behaviour of the non-amphiphilic linear siloxanes studied by Finkelmann *et al.*<sup>99</sup>

From this work, it was concluded that a spacer length of three methylene units (i.e. figure 8.13, structure 3a) was sufficient to decouple the motions of the linear polysiloxane backbone from those of the mesogen. With the degree of orientational and positional freedom afforded by this relatively short spacer group, this polymer formed a nematic mesophase. With spacer groups of four and five methylene units (i.e. figure 8.8, structures 3b and 3c) similar phase behaviour was observed, although the transition temperatures and range of mesophase stabilities were different. With a spacer group of six methylene units (figure 8.8, structure 3d), the efficiency of the spacer group was such that the mesogens attained some degree of both positional and orientational ordering, which resulted in a smectic mesophase.

It is interesting to note that the glass transition of all these side-chain polysiloxanes occur at significantly higher temperatures than the parent linear siloxane backbone (c.f.  $-125^{\circ}\text{C}$  for linear polydimethylsiloxanes<sup>327</sup>). This results from the steric hindrance of the bulky side-chain mesogens which leads to a decrease in the mobility of the polymer segments<sup>64,334</sup>. Conversely, the  $T_g$  of these side-chain mesogenic polymers decreases with increasing length of the spacer group; reflecting a decrease in the interactions between the mesogens and the backbone with increasing length of the spacer group<sup>64,334</sup>.

Unlike the linear side-chain polysiloxane incorporating a spacer group of three methylene units, the cyclic oligomers,  $\text{D}_4\text{C}_3$  and  $\text{D}_5\text{C}_3$ , were not mesomorphic. However, as is the case with linear side-chain polysiloxanes incorporating spacer groups of 5 and 6 methylene units, the corresponding cyclic oligomers,  $\text{D}_4\text{C}_5$ ,  $\text{D}_5\text{C}_5$ ,  $\text{D}_4\text{C}_6$  and  $\text{D}_5\text{C}_6$ , were mesomorphous. These

observations confirm that the use of suitable spacer groups will decouple the motions of the mesogen from those of a cyclic tetrameric and pentameric backbone. Thus, the model considerations applied to linear side-chain polymers are, at least in part, also applicable to these oligomeric cyclic systems. The facts that  $D_4C_3$  and  $D_5C_3$  did not form a mesophase whilst their linear counterparts did, and that  $D_4C_6$  and  $D_5C_6$  formed a less ordered mesophase than the equivalent linear polymer (i.e. nematic as opposed to smectic), indicates that the spacer group has to be more effective to decouple the motions of this mesogen from those of the oligomeric cyclic siloxanes, than is the case with a linear polysiloxane.

To explain the different phase behaviour of these linear and cyclic systems, it is necessary to consider the structural differences between them. As the mesogens and the spacer groups are common to both, the different behaviour must be primarily due to:

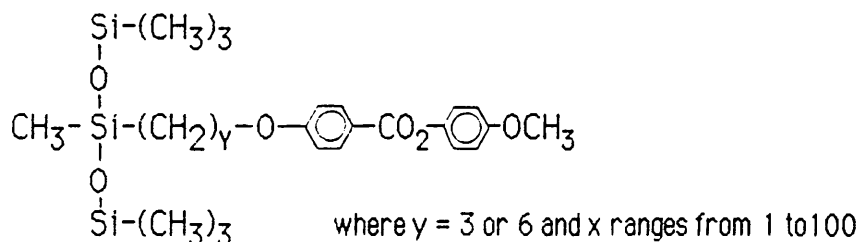
- the cyclic and linear nature of the respective backbones
- their degrees of polymerisation (i.e.  $\overline{DP} = 4$  and  $5$  for the cyclic systems, as opposed to a  $\overline{DP} \sim 50$  for the linear backbone)
- the polydispersity of the respective cyclic and linear backbones.

Considering the possible effects of the cyclic nature of the backbone, we may be guided by our previous study of cyclic amphiphiles (see chapter 6). From this, it was concluded that the relative rigidity of a oligomeric cyclic siloxane may have an adverse effect on the free motions of side-chains attached to it. In linear systems, it is the tendency of the backbone to adopt a statistical distribution of chain conformations that restricts the alignment of mesogens which are attached to it directly, or via a short spacer group<sup>64,332</sup>. In these oligomeric cyclic systems, the backbones are,

due to ring strain, much more rigid than the linear backbones<sup>327</sup>. Hence, although the siloxane ring imposes significant restrictions on the orientational and positional freedom of any mesogens that are attached as side-chains, this is due to the spatial arrangement of the axial bonds around the rigid ring. If we consider this, and the fact that there will be a number of geometric isomers for both the tetrameric and pentameric species (see figure 6.14), it is not surprising that the attachment of a mesogen by a short spacer group of three methylene units, or less, is insufficient to allow the mesogens to orient themselves. The existence of a number of geometric isomers with non-compact structures may also explain the amorphous nature of  $D_4C_3$  and  $D_5C_3$  in the solid phase (i.e. an inability to crystallise).

For  $D_4C_5$ ,  $D_5C_5$ ,  $D_4C_6$  and  $D_5C_6$ , the effect of the longer spacer groups is such that the mesogens can align. Concomitant with an increase in the decoupling of the motions of the bulky side-chains and the backbone, the  $T_g$  of these molecules should be lower than  $D_4C_3$  and  $D_5C_3$ , due to an increase in segmental movement. Disregarding the transition temperatures observed for  $D_5C_5$  which seem anomalously high with respect to those of the other molecules of this series, this appears to be the case (i.e. the  $T_g$  of  $D_4C_5$ ,  $D_4C_6$  and  $D_5C_6$  is indeed lower than that of  $D_4C_3$  and  $D_5C_3$ ; see table 8.2).

As noted earlier, the second major difference between the cyclic systems studied here and the linear polymers studied by Finkelmann is their degree of polymerisation. In a systematic study of the effect of  $\overline{DP}$ , Stevens *et al.*<sup>349</sup> prepared polydisperse samples of the following side-chain linear siloxanes:



These mixtures were separated by gel permeation chromatography into monodisperse oligomers of defined  $\overline{DP}$ . The phase behaviour of these oligomers was then determined. For both systems (i.e.  $y=3$  and  $6$ ) the same characteristic behaviour was observed (see figure 8.14).

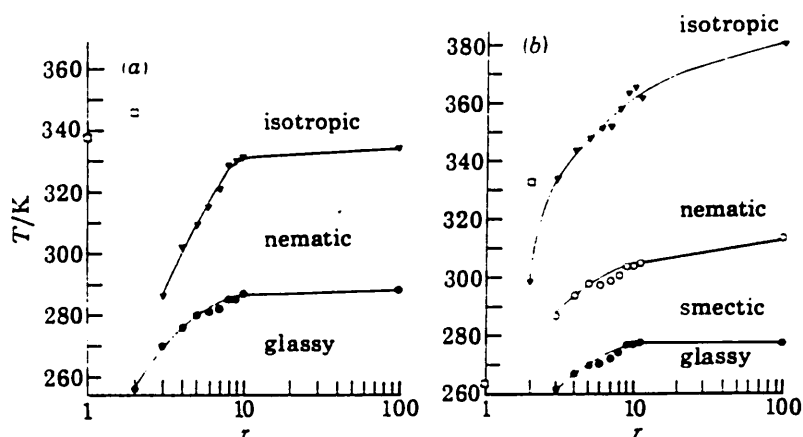


Figure 8.14 The phase behaviour of the monodisperse oligomeric siloxanes as a function of degree of polymerisation.

Derivatives with a  $\overline{DP} = 1$  and  $2$  were non-mesomorphous, whilst derivatives with a  $\overline{DP} \geq 3$  were. Of the latter grouping, the polymers and oligomers with a spacer group of three methylene units ( $y=3$ ) exhibited a nematic mesophase, whilst those with a spacer group of six methylene units ( $y=6$ )

had an additional low temperature smectic phase. For both  $y=3$  and  $6$  all phase transition temperatures increased sharply with an increasing  $\overline{DP}$ , up to a  $\overline{DP}$  of  $10$ . At a still greater  $\overline{DP}$ , the transition temperatures became constant. This behaviour has been observed for a range of linear polymers and has therefore been established as a general principle<sup>334</sup>. Often a change from the nematic to the higher order smectic phases is also observed. This 'stabilisation' of the mesomorphous state following polymerisation, has been explained by the restriction of the translational and rotational motions of the mesogens when they are attached to the polymer backbone<sup>64,334</sup>, and/or a reduction in specific volume following polymer fixation<sup>86</sup> (i.e. an increased packing density).

Applying these considerations to the cyclic oligomers studied here, it would be reasonable to expect that the transition temperatures would increase as a function of  $\overline{DP}$ . From the data presented here for cyclic tetramers and pentamers with  $3$ ,  $5$  and  $6$  methylene spacer groups, it is difficult to propose a relationship between the  $\overline{DP}$  and transition temperatures. Accepting that the results for  $D_5C_5$  are anomalously high, the relationship between  $T_g$  and  $\overline{DP}$  in  $D_4C_3$  and  $D_5C_3$  and in  $D_4C_6$  and  $D_5C_6$  is, if anything, the reverse of that established for linear polymers. There is, however, no pattern for the nematic-isotropic transitions.

Whilst further work would be required to investigate the effect of  $\overline{DP}$ , it is worth noting that increasing the  $\overline{DP}$  of these oligomeric cyclic siloxanes decreases ring strain, which in turn increases the flexibility of the cyclic backbone and would be expected to decrease  $T_g$ <sup>327</sup>. Thus, unlike linear side-chain polymers, this increase in the flexibility of the backbone may give rise to a shift in the transitions of side-chain cyclic oligomers and

polymers to lower temperatures with increasing  $\overline{DP}$ . A similar relationship has been observed in linear side-chain systems, with an increase in the length of the spacer group<sup>89,99,337</sup>, with a more flexible polymer<sup>64,341</sup>, and with the incorporation of non-substituted monomer units<sup>64,334,341</sup>; these all act to increase the flexibility of the chain segments.

#### 8.4 Conclusions

An overview of the thermotropic phase behaviour of these non-amphiphilic side-chain oligomeric cyclic siloxanes has been established. In order to validate the tentative proposals made here, further work is required. None the less, the following general conclusions may be drawn:

1.  $D_4C_3$  and  $D_5C_3$  are amorphous solids at low temperature and undergo a glass transition to a viscous isotropic liquid.
2.  $D_4C_5$ ,  $D_5C_5$ ,  $D_4C_6$  and  $D_5C_6$  exist as ordered solids at low temperature and undergo a step-wise melting, via the nematic mesophase, to a low viscosity isotropic liquid.
3. The use of a suitable flexible spacer group will decouple the motions of mesogenic side-chains from those of the cyclic backbone such that the mesogens may align. Thus, the model considerations applied to linear side-chain polymers may also be generally applicable to these oligomeric cyclic systems.
4. The length of the spacer group required to decouple the motions of the mesogens from those of the cyclic backbone has to be greater than that in the equivalent linear polymers.
5. The variation of the phase behaviour of the cyclic tetramers and pentamers with  $\overline{DP}$  may not follow the relationship established in linear systems. If this is the case, this effect may reflect the increasing flexibility of the cyclic backbone with increasing  $\overline{DP}$ .

## CHAPTER 9. FUTURE WORK

This project has established an overview of the thermotropic and, in selected solvent/amphiphile systems, the lyotropic phase behaviour of a range of novel amphiphilic and non-amphiphilic siloxanes. As a consequence of this work, further research could be directed towards the validation of the proposals made here or the extension of this work.

### 9.1 Validation of Key Areas

A detailed investigation of the structure of the thermotropic mesophases formed by NaD<sub>4</sub> and NaD<sub>5</sub> is required. Further X-ray work and the use of additional spectroscopic techniques such as NMR, may be of assistance in elucidating the structure of these phases.

The proposed absence of ribbon-type phases during the step-wise melting of NaD<sub>4</sub> and NaD<sub>5</sub> may also warrant further work. If this behaviour were to be confirmed, it would be interesting to investigate which structural characteristic(s) of these amphiphilic side-chain oligomers precludes the formation of these phases.

The cyclic and linear amphiphilic siloxanes exhibit different thermal behaviour during initial and subsequent heating cycles. If a quenching of these samples following the initial heating is, as proposed, a contributing factor in this behaviour, then it would be of interest to investigate the effect of utilising slow rates of cooling during further optical and DSC studies of the thermotropic behaviour of these materials.

The intermediate lyotropic mesophase observed at water concentrations between  $H_1$  and  $L_\infty$  during aqueous penetration experiments with  $\text{NaD}_4$  requires further characterisation. The preparation of a range of samples of varying amphiphile concentration, followed by microscopy and X-ray diffraction, may elucidate the structure of this phase.

## 9.2 Extension of this Work

A well-established relationship exists between the thermotropic behaviour of non-amphiphilic side-chain polymers and their  $\overline{DP}$ <sup>64,349</sup>. A similar relationship has been noted for the aqueous lyotropic phase behaviour of some amphiphilic side-chain polymers<sup>67,218</sup>. It would therefore be of great interest to investigate the thermotropic and, where appropriate, the lyotropic phase behaviour of the cyclic amphiphilic and non-amphiphilic oligomers with increasing  $\overline{DP}$ . As the  $\overline{DP}$  of the siloxane ring increases, the behaviour and properties of the resulting 'macro-cyclic' side-chain systems may approach that of the equivalent linear polymer<sup>296</sup>.

The linear  $\alpha$ -functionalised amphiphilic siloxanes form phases in which the siloxane chains constitute the continuous phase and the  $C_{11}$  carboxylate moieties form the micelles cores. At temperatures above the  $T_g$  of the siloxane continuum, these phases are semi-crystalline in nature as the  $C_{11}$  carboxylate groups retain a crystalline arrangement. The polar group and the siloxane chain are linked together via a  $C_{10}$  alkyl chain, which also acts to decouple the steric and kinetic interactions of these two groups. The replacement of this  $C_{10}$  chain with progressively shorter alkyl chains would eventually restrict the ability of the polar groups to crystallise, due to the steric effects of the adjacent bulky PDMS chains. With judicious tailoring

of the polar group region, it may thus be feasible to produce mesophases at temperatures just above the glass transition of the siloxane (i.e.  $>-120^{\circ}\text{C}$ ). Thus, it may be possible to design anionic soaps which are oil-soluble at very low temperatures (i.e. approaching the  $T_g$  of the siloxane backbone).

With this in mind, the lyotropic phase behaviour of the shortest chain length amphiphile of this series ( $\text{Na}_{500}$ ) in non-polar solvents should be studied. As this amphiphile forms a mesophase at temperatures greater than the melting of the polar groups (i.e. at  $T_4$ ), the solubility of this amphiphile in non-polar solvents may increase significantly at this transition.

It would also be of interest to investigate the occurrence and temperature stability of the mesophase formed by amphiphiles similar to  $\text{Na}_{500}$  but with slight variations in the length of the siloxane moiety. It may be reasonable to expect that at lower chain lengths, the mesophase stability would tend towards that of the  $\text{C}_{11}$  sodium soap, with a possible transition to a lamellar mesophase structure due to the corresponding change in the packing constraints. At higher chain lengths, the behaviour would tend towards that of the longer chain length linear amphiphiles,  $\text{Na}_{1000}$ ,  $\text{Na}_{1500}$  and  $\text{Na}_{2000}$  (i.e. decreasing mesophase stability range with increasing chain length).

As a consequence of packing constraints, the  $\alpha$ -functionalised linear amphiphilic siloxanes formed reversed rod micelles and reversed hexagonal phases. The modification of the molecular geometry of these amphiphiles, to give non-reversed micelles in the neat state, may subsequently be expected to result in bilayer or normal rod and disc micelles in aqueous

solution. Such a change in molecular geometry may be achieved with essentially the same non-polar chain, but coupled to a much larger polar group (i.e. a dicarboxylic acid salt, see chapter 7). The potential for the synthesis of water soluble amphiphiles with non-polar chains as long as those synthesised here, would obviously be of interest in studying the effects of variations in both the nature and size of the non-polar chain, and generally, in expanding an understanding of aqueous lyotropic phase behaviour. In particular, the cmc values for such amphiphiles would be expected to be very low; indeed, the measurement of such values may present a challenge.

If the model considerations<sup>64,332,334</sup> previously applied to linear non-amphiphilic side-chain polymers and oligomers also apply to the cyclic non-amphiphilic siloxanes, as proposed here, then increasing the length of the alkyl spacer would eventually be expected to give rise to smectic mesophases (i.e.  $>C_6$ ).

Lastly, this project set out to characterise a diverse range of amphiphilic and non-amphiphilic siloxanes (see figure 1.13). The characterisation of some of the structures which have not been studied here, but for which synthetic routes have been established, would be of interest. In particular, the synthesis of the non-amphiphilic end-functionalised linear siloxanes ( $\alpha$ - and  $\alpha,\omega$ -) and the amphiphilic  $\alpha,\omega$ -functionalised linear siloxanes would be pertinent.

## REFERENCES

1. P. W. Atkins in "Physical Chemistry" (Oxford University Press, Oxford, 1982) 2<sup>nd</sup> Edition, p16-22.
2. G. Friedel, *Annls Phys.*, 18, 273 (1922).
3. R. Virchow, *Archiv.* 6, 502 (1854).
4. F. Reinitzer, *Monatsh. Chem.*, 9, 421 (1888).
5. O. Z. Lehmann, *Phys. Chem.*, 4, 462 (1889).
6. B. Wunderlich, J. Grebowicz, *Adv. Polymer Sci.* 60/61, 1 (1984).
7. G.W. Gray and P.A. Winsor in "Liquid Crystals and Plastic Crystals", Eds. G.W. Gray and P.A. Winsor (Ellis Horwood, Chichester, England 1974) Vol.1, Chapt.1.
8. S. Chandrasekhar in "Liquid crystals" (Cambridge University Press, Cambridge, England, 1977).
9. Sussman in "Liquid Crystals and Plastic Crystals", Eds. G.W. Gray and P.A. Winsor (Ellis Horwood, Chichester, England 1974) Vol.1, Chapt.7.
10. N. H. Hartshorne in "Liquid Crystals and Plastic Crystals", Eds. G.W. Gray and P.A. Winsor (Ellis Horwood, Chichester, England 1974) Vol.2, Chapt.2.
11. G.W. Gray in "Liquid Crystals and Plastic Crystals", Eds. G.W. Gray and P.A. Winsor (Ellis Horwood, Chichester, England 1974) Vol.1, Chapt.7.
12. G. H. Brown and W. G. Shaw, *Chem. Rev.*, 57, 1049 (1957).
13. G. J. T. Tiddy in "Modern Trends of Colloid Science in Chemistry and Biology", Ed. H.-F. Eicke (Birkhauser Verlag, Basel, 1985) p148-183.
14. G. Gray in "Polymer Liquid Crystals", Eds. A. Ciferri, W. R. Krigbaum, and R. B. Meyer (Academic Press, New York, 1982) Chap. 1.
15. J. N. Israelachvili, D. J. Mitchell and B. Ninham, *J. Chem. Soc. Faraday Trans. 2*, 72, 1525 (1976).
16. G. J. T. Tiddy and M. F. Walsh in "Aggregation Processes in Solution",

- Eds. E. Wyn-Jones and J. Gormally (Elsevier Scientific Publishing Company, Amsterdam, Oxford, New York, 1983) Chapt.7.
17. C. Tanford in "The Hydrophobic Effect", 2<sup>nd</sup> Edition (John Wiley and Sons Inc., New York, 1980).
  18. D. G. Hall and B. A. Pethica in "Nonionic Surfactants", Ed. M. Schick (Marcel Dekker Inc, New York, 1967) Chapt.16.
  19. J. M. Corkill, J. F. Goodman, T. Walker and J. Wyer, Proc. Roy. Soc. Ser. A., 312, 243 (1969).
  20. H.-F. Eicke in "Topics in Current Chemistry" (Springer-Verlag, Heidelberg) 87, 85 (1980).
  21. P. A. Winsor in "Solvent Properties of Amphiphilic Compounds", (Butterworths, London, 1954).
  22. P. A. Winsor, Chem. Rev., 68, 1 (1968).
  23. P. Ekwall in "Advances in Liquid Crystals", Ed. G. H. Brown (Academic Press, New York, 1971) Vol. 1, Chapt. 1, p.1.
  24. V. Luzzatti, in "Biological Membranes", Ed. D. Chapman (Academic Press, London, New York, 1968) Chapt. 3.
  25. G. J. T. Tiddy, Physics Reports, 57, 1 (1980).
  26. K. Fontell, L. Mandell and P. Ekwall, Acta Chem. Scand., 22, 3209 (1968).
  27. G. J. T. Tiddy, K. Rendall and C. Adam, unpublished results (1981) (taken from reference 16).
  28. B. L. Forrest and L. W. Reeves, Chem. Rev., 81, 1 (1981).
  29. Y. Hendrix and J. Charvolin, J. Physique, 42, 1427 (1981).
  30. M. C. Holmes and J. Charvolin, J. Phys. Chem, 88, 810 (1984).
  31. M. C. Holmes, N. Boden and K. Radley, Mol. Crystals and Liquid Crystals, 100, 93 (1983).
  32. L. J. Yu and A. Saupe, Phy. Rev. Lett., 45, 1000 (1980).

33. L. Onsager, *Ann. N. Y. Acad. Sci.*, 51, 627 (1949).
34. P. J. Flory, *Proc. R. Soc. London, Ser. A*, 234, 73 (1956).
35. P. J. Flory and G. Ronca, *Mol. Cryst. Liq. Cryst.*, 54, 289 (1979).
36. M. A. Cotter and D. C. Wachter, *Phys. Rev. A*, 18, 2669 (1978).
37. P. J. Flory and G. Ronca, *Mol. Cryst. Liq. Cryst.*, 54, 311 (1979).
38. M. Warner and P. J. Flory, *J. Chem. Phys.*, 73, 6327 (1980).
39. W. Maier and A. Saupe, *Z. Naturforsch.*, 149, 882 (1959)
40. G. R. Luckhurst and G. W. Gray in "The Molecular Physics of Liquid Crystals", Eds. G. R. Luckhurst and G. W. Gray (Academic Press, London, 1979).
41. P. G. de Gennes, in "The Physics of Liquid Crystals" (Oxford Univ. Press, London and New York, 1974).
42. G. W. Gray and J. W. Goodby in "Smectic Liquid Crystals" (Leonard Hill, Glasgow, 1984).
43. J. H. Clint, *Chemistry in Britain*, April, 333 (1990).
44. N. Boden, *Ibid.*, April, 345, (1990).
45. D. Chapman and G. T. Stewart in "Liquid Crystals and Plastic Crystals", Eds. G.W. Gray and P.A. Winsor (Ellis Horwood, Chichester, England 1974) Vol.1, Chapt.6.
46. H. Bader, K. Jorn, B. Hupfer and H. Ringsdorf, *Adv. Polym. Sci.*, 64, 1 (1985).
47. T. Kunitake, N. Nakashima, T. Takarabe, M. Nagai, A. Tsuge and H. Yanaki, *J. Am. Chem. Soc.*, 103, 5945 (1981).
48. G. Bauer in "Polymer Liquid Crystals", Eds. A. Ciferri, W. R. Krigbaum and R. B. Meyer (Academic Press, New York, 1982) Chapt.11.
49. G. F. Weston and R. Bittleston, "Alphanumeric Displays, Devices, Drive Circuits and Applications", Granada, 98 (1982).
50. M. Goscianski, *J. App. Phys.*, 48, 4, 1426 (1977).

51. J. Constant, E. P. Raynes, I. A. Shanks, D. Coates, G. W. Gray and D. G. McDonnell, *J. Phys. D, App. Phys.*, 11, 479 (1978).
52. M. A. Apfel, H. Finkelmann, G. M. Jannini, R. J. Laub, B. H. Luhmann, A. Price, W. L. Roberts, T. J. Shaw and C. A. Smith, *Anal. Chem.* 57, 651 (1985).
53. J. S. Bradshaw, C. Schrengensberger, K. H. C. Chang, K. E. Markides, M. L. Lee, *J. Chromatogr.*, 358, 95 (1986).
54. J. P. Schroeder in "Liquid Crystals and Plastic Crystals", Eds. G.W. Gray and P.A. Winsor (Ellis Horwood, Chichester, England 1974) Vol.1, Chapt.7.
55. R. Templer and G. Attard, *New Scientist*, 4 may, 25 (1991).
56. G. Oster, *J. Gen. Physiol.*, 33, 445 (1950).
57. P. Doty, J. H. Bradbury and A. M. Holtzer, *J. Am. Chem. Soc.*, 78, 947 (1956).
58. G. L. Wilkes, *Mol. Cryst. Liq. Cryst.*, 18, 165 (1972).
59. See for example, S. L. Kowlek (DuPont), U.S. Patent 3,600,350 (1971).
60. P.W. Morgan, *Macromolecules*, 10 1381 (1977).
61. J. W. Hannell, *Polym. News*, 1, 8, (1970).
62. Imperial Chemical Laboratories, *Textile Progress*, U.K., Chapt. 13 (1976).
63. A. Windle, *Proceedings of Adv. Materials '86 Conference*, London, 24-26 June 1986, p1-9, 6128 conference.
64. H. Finkelmann, in "Polymer Liquid Crystals", Eds. A. Ciferri, W. R. Krigbaum and R. B. Meyer (Academic Press, New York, 1982) Chapt.2.
65. R. Thundathil, J. O. Stoffer and S. E. Friberg, *J. Polymer Sci., Polymer Chem.*, 18, 2629 (1980).
66. P. Hall PhD thesis (University College of Wales, 1988).

67. B. Luhmann and H. Finkelmann, *Colloid and Polymer Sci.*, 265, 506 (1987).
68. B. Luhmann, H. Finkelmann and G. Rehage, *Die Angewandte Makromol. Chemie*, 123/124, 217 (2035), (1984).
69. H. Finkelmann and M. A. Schafheutle, *Colloid and Polymer Sci.* 264, 786 (1986).
70. H. Finkelmann, B. Luhmann and G. Rehage, *Colloid and Polymer Sci.* 260, 56 (1982).
71. B. Luhmann, H. Finkelmann and G. Rehage, *Makromol. Chem.*, 186, 1059 (1985).
72. N. Pietschmann, G. Brezesinski, C. Tschierske, H. Zschke and F. Kuschel, *Liquid Crystals*, 5(6), 1697 (1989).
73. S. K. Varshney, *JMS-Rev. Macromol. Chem. Phys.*, C26(4), 551 (1986).
74. G. W. Calundann, in "High Performance Polymers: Their Origin and Development", Eds. R. B. Seymour G. S. Kirshenbaum (Elsevier Science Publishing Co. Inc., 1986) p235.
75. B. Fayolle, C. Noel and J. Billard, *J. Phys.*, C3(4), 485 (1979).
76. S. M. Aharoni, *J. Polym. Sci., Polym. Phys. Ed.*, 18, 1303 (1980).
77. C. Plachetta and R. C. Schulz, *Macromol. Chem. Rapid Commun.*, 3, 815 (1982).
78. W. R. Krigbaum, A. Ciferri, J. Asrar and H. Toriumi, *Mol. Cryst. Liq. Cryst.*, 76, 79 (1981).
79. W. R. Krigbaum, J. Asrar, H. Toriumi, A. Ciferri and J. Preston, *J. Polym. Sci., Polym. Lett., Ed.*, 20, 109 (1982).
80. L. Bosio, B. Fayolle, C. Friedrich, F. Laupretre, P. Meurisse, C. Noel and J. Verlet, in "Liquid Crystals and Ordered Fluids", Eds. A. Griffin and J. Johnson, Vol. 4.
81. V. P. Shibaev, N. A. Plate, *Vysokomol. Soedin., Ser. A*, 19, 923 (1977):

82. P. L. Maganini, A. Marchetti, F. Matera, G. Pizzirani and G. Turchi, *Eur. Polym. J.*, 10, 585 (1974).
83. G. Ceccarelli, V. Frosini, P. L. Maganini, B. A. Newman, *J. Polym. Sci., Polym. Lett. Ed.*, 13, 101 (1975).
84. E. Perplies, H. Ringsdorf, J. H. Wendorff, *Ber. Bunsenges. Phys. Chem.* 78, 921 (1974).
85. W. Bronstow, *Kunststoffe*, 78 (5), 441 (1988).
86. H. Finkelmann, *Angew. Chem. Int. Ed. Engl.*, 26, 816 (1987).
87. A. A. Collyer in "Progress in Rubber and Plastic Technology", Rapra Technology, Shrewsbury, England, 6 (2), 103 (1990).
88. G. S. Attard and G. Williams, *Chem. in Britain*, October, 919 (1986).
89. H. Finkelmann and G. Rehage, *Makromol. Chem. Rapid Commun.*, 1, 31 (1980).
90. H. Kresse and R. V. Talroze, *Makromol. Chem. Rapid Commun.*, 2, 869 (1981).
91. H. Kresse S. Kostromin and V. P. Shibaev, *Makromol. Chem. Rapid Commun.*, 3, 509 (1982).
92. R. Simon and H. J. Coles, *Polymer*, 27, 811 (1986).
93. C. B. McArdle, M. G. Clark, C. M. Haws and M. C. K. Wiltshire, *Liquid Crystals*, 2 (5), 537 (1987).
94. C. S. Hsu and Y. H. Lu, *J. Polym. Sci., Part A, Polym. Chem.*, 29(7), 977 (1991).
95. F. Wu, R. Zhang and Y. Ziang, *Chinese J. Polym. Sci.*, 9(1), 71 (1991).
96. H. J. Coles and R. Simon, *Polymer*, 26, 1801 (1985).
97. R. Simon and H. J. Coles, *Mol. Cryst. Liq. Cryst.*, 102, 43 (1984).
98. H. J. Coles and R. Simon, *Mol. Cryst. Liq. Cryst.*, 102, 75 (1984).
99. H. Finkelmann and G. Rehage, *Makromol. Chem. Rapid Commun.*, 1, 733 (1980).

100. H. Finkelmann and G. Rehage, *Adv. Polym. Sci.*, 60/61, 99 (1984).
101. G. S. Attard and C. Williams, *Polymer*, 27, 2 (1986).
102. N. A. Plate and V. P. Shibaev, *J. Polym. Sci., Polym. Symp.*, 67, 1 (1980).
103. W. Noll in "Chemistry and Technology of Silicones" (Academic Press, New York, 1968).
104. M. G. Voronkov, V. P. Mileshevich and Y. A. Yuzhelevskii in "The Siloxane Bond" (Plenum Press, New York, 1978).
105. R. Perron and C. Madelmont, *Rev. Franc. Corps Gras*, 20(5), 261 (1973).
106. P. A. Winsor, in "Liquid Crystals and Plastic Crystals", Eds. G. W. Gray and P. A. Winsor (Ellis Horwood Ltd., Chichester, England, 1974) Vol. 1, Chapt. 5, p.199-287.
107. D. M. Small, in "Handbook of Lipid Research 4, The Physical Chemistry of Lipids" (Plenum Press, London, 1986) Chapt. 9.
108. B. Gallot and A. Skoulios, *Kolloid-Z. u.Z. Polymere*, 213, 143 (1966).
109. J. J. Duruz, H. J. Michels and P. Franzosini, *Proc. Roy. Soc. Lond.*, A322, 281 (1971).
110. P. Ferloni, M. Sanesi and P. Franzosini, *Z. Naturforsch.*, 30A, 1447 (1975).
111. H. J. Michels and A. R. Ubbelohde, *J. Chem. Soc. Perkin Trans. II*, 1879 (1972).
112. P. Ferloni and P. Franzosini, *Gazz. Chim. Ital.*, 105, 391 (1975).
113. M. Sanesi, P. Ferloni, M. Zangen and P. Franzosini, *Z. Naturforsch.*, 32A, 285 (1977).
114. M. Sanesi, P. Ferloni and P. Franzosini, *Z. Naturforsch.*, 32A, 1173 (1977).
115. B. Gallot and A. Skoulios, *Kolloid-Z. u. Z. Polymere*, 209, 164 (1966).
116. A. R. Ubbelohde, H. J. Michels and J. J. Duruz, *Nature*, 228, 50 (1970).
117. A. R. Ubbelohde, H. J. Michels and J. J. Duruz, *J. Phys. E.*, 5, 283 (1972).

118. J. J. Duruz and A. R. Ubbelohde, Proc. Roy. Soc. Lond., A330, 1 (1972).
119. A. R. Ubbelohde, Nature, 244, 487 (1973).
120. H. J. Michels and A. R. Ubbelohde, Proc. Roy. Soc. Lond., A338, 447 (1974).
121. J. J. Duruz and A. R. Ubbelohde, Proc. Roy. Soc. Lond., A342, 39 (1975).
122. J. J. Duruz and A. R. Ubbelohde, Proc. Roy. Soc. Lond., A347, 301 (1976).
123. A. R. Ubbelohde, in "The Molten State of Matter" (Wiley-Interscience, Chichester, England, 1978).
124. M. Wolfe, J. Bonekamp and J. Jonas, J. Chem. Phys., 70, 3993 (1979).
125. J. Bonekamp, T. Eguchi and J. Jonas, Chem. Phys. Lett., 75, 360 (1980).
126. J. Bonekamp, T. Eguchi, S. Plesko and J. Jonas, J. Chem. Phys., 79, 1203 (1983).
127. J. Bonekamp, I. Artaki, M. L. Phillips, S. Plesko and J. Jonas, J. Chem. Phys., 87, 4991 (1983).
128. S. Plesko, M. L. Phillips, R. Cassell and J. Jonas, J. Chem. Phys., 80, 5806 (1984).
129. J. Bonekamp, B. Hegemann and J. Jonas, Mol. Cryst. Liq. Cryst., 87, 13 (1982).
130. D. Vorlander, Ber. dt. Chem. Gess., 43, 3120 (1910).
131. A. S. C. Lawrence, Trans. Faraday Soc., 34, 660 (1938).
132. J. W. McBain, L. H. Lazarus and A. V. Pitter, Z. Phys. Chem., 147, 87 (1930).
133. R. D. Vold, F. B. Rosevear and R. H. Ferguson, Oil and Soap, 16, 48 (1939).
134. R. D. Vold and M. J. Vold, J. Am. Chem. Soc., 61, 808 (1939).
135. R. D. Vold, J. Phys. Chem., 43, 1213 (1939).
136. J. W. McBain, R. D. Vold and M. Frick, J. Phys. Chem., 44, 1013 (1940).

137. R. D. Vold, R. Reivere and J. W. McBain, *J. Am. Chem. Soc.*, 63, 1293 (1941).
138. J. W. McBain and W. W. Lee, *Oil and Soap*, 20, 17 (1943).
139. J. W. McBain and W. C. Sierichs, *J. Am. Oil Chem. Soc.*, 25, 221 (1948).
140. M. J. Vold, *J. Am. Chem. Soc.*, 65, 465 (1943).
141. A. Skoulios and V. Luzzatti, *Nature*, 183, 1310 (1959).
142. A. Skoulios and V. Luzzatti, *Acta Cryst.*, 14, 278 (1961).
143. B. Gallot and A. E. Skoulios, *Compt. Rend. Acad. Sci*, 260, 3033 (1965).
144. B. Gallot and A. E. Skoulios, *Acta Cryst.*, 15, 826 (1962).
145. A. Skoulios and B. Gallot, *Compt. Rend. Acad. Sci*, 252, 142 (1961).
146. B. Gallot and A. Skoulios, *Kolloid-Z. u. Z. Polymere*, 210, 143 (1966).
147. B. Gallot and A. Skoulios, *Mol. Cryst.*, 1, 263 (1966).
148. W. J. Harrison, Phd Thesis (Sheffield City Polytechnic, England, 1988) Chapt. 1.
149. K. Fontell, in "Liquid Crystals and Plastic Crystals", Eds. G. W. Gray and P. A. Windsor (Ellis Horwood Ltd., Chichester, England, 1974) Vol. 2, Chapt. 4.
150. P. Franzosini, M. Sanesi, A. Cingolani and P. Ferloni, *Z. Naturforsch*, 35A, 98 (1980).
151. R. D. Vold, *J. Am. Chem. Soc.*, 63, 2915 (1941).
152. P. Montmittonet, B. Monasse, J. M. Haudin and F. Delamare, *Materials Letts.*, 3, 98 (1985).
153. R. D. Vold, J. D. Grandine 2nd and M. J. Vold, *J. Colloid Sci.*, 3, 339 (1948).
154. M. J. Vold, G. S. Hattiangdi and R. D. Vold, *J. Colloid Sci.*, 4, 93 (1949).
155. G. S. Hattiangdi, M. J. Vold and R. D. Vold, *Ind. and Eng. Chem.*, 41, 2320 (1949).
156. S. O. Adeosun and S. J. Sime, *Thermochim. Acta*, 17, 351 (1976).

157. S. O. Adeosun, A. O. Kehinde and G. A. Odesola, *Thermochim. Acta*, 28, 133 (1979).
158. H. D. Burrows, H. A. Ellis and M. S. Akanni, *Procs. Eur. Symp. Therm. Anal.*, 1981, 2<sup>nd</sup>, 302.
159. S. Shiba, *Bull. Chem. Soc. Japan*, 34, 804 (1961).
160. S. O. Adeosun, *Can. J. Chem.*, 57, 151 (1979).
161. H. D. Burrows and H. A. Ellis, *Thermochim. Acta*, 52, 121 (1982).
162. I. K-Thege, I. Ruff, S. O. Adeosun and S. J. Sime, *Thermochim. Acta*, 24, 89 (1978).
163. S. O. Adeosun, *J. Therm. Anal*, 14, 235 (1978).
164. P. Spegt and A. Skoulios, *Compt. Rend. Acad. Sci*, 254, 4316 (1962).
165. P. Spegt and A. Skoulios, *Compt. Rend. Acad. Sci*, 251, 2199 (1960).
166. P. A. Spegt and A. E. Skoulios, *Acta Cryst.*, 17, 198 (1964).
167. P. A. Spegt and A. E. Skoulios, *Acta Cryst.*, 21, 892 (1966).
168. P. A. Spegt and A. E. Skoulios, *Acta Cryst.*, 16, 301 (1963).
169. P. Spegt and A. Skoulios, *J. Chim. Phys.*, 62, 418 (1965).
170. V. Luzzatti, A. Tardieu and T. G.-Krzywicki, *Nature*, 217, 1028 (1968).
171. V. Luzzatti and P. A. Spegt, *Nature*, 215, 701 (1967).
172. J. Rogers and P. A. Winsor, 5th Int. Congr. on Surface Active Substances, Barcelona, Vol.2, p.933 Ediciones. Unidas. Barcelona, (1969).
173. R. R. Balmbra, J. S. Clunie and J. F Goodman, *Proc. Roy. Soc. Lond.*, A285, 534 (1965).
174. R. R. Balmbra, J. S. Clunie and J. F Goodman, *Mol. Cryst.*, 3, 281 (1967).
175. P. A. Winsor, in "Solvent Properties of Amphiphilic Compounds" (Butterworth and Co Ltd, London, 1954) pp. 65, 69, 117, 135, and 185.
176. C. Madelmont and R. Perron, *Colloid and Polymer Sci.*, 254, 581 (1976).

177. V. Luzzatti, H. Mustacchi, A. Skoulios and F. Husson, *Acta Cryst.*, 13, 660 (1960).
178. F. Husson, H. Mustacchi and V. Luzzatti, *Acta Cryst.*, 13, 668 (1960).
179. C. Madelmont and R. Perron, *Bull. Soc. Chim. France*, N° 12, 3259 (1973).
180. C. Madelmont and R. Perron, *Bull. Soc. Chim. France*, N° 12, 3263 (1973).
181. C. Madelmont and R. Perron, *Bull. Soc. Chim. France*, N° 3-4, 425 (1974).
182. C. Madelmont and R. Perron, *Bull. Soc. Chim. France*, N° 3-4, 430 (1974).
183. C. Madelmont and R. Perron, *Bull. Soc. Chim. France*, N° 9-10, 1795 (1974).
184. C. Madelmont and R. Perron, *Bull. Soc. Chim. France*, N° 9-10, 1799 (1974).
185. K. Rendall, G. J. T. Tiddy and M. A. Trevethan, *J. Chem. Soc., Faraday Trans. I*, 79, 637 (1983).
186. B. Gallot and A. Skoulios, *Kolloid-Z. u. Z. Polymere*, 208, 37 (1966).
187. A. E. Skoulios, *Advances in Colloid and Int. Sci.*, 1, 79 (1967).
188. J. M. Vincent and A. E. Skoulios, *Acta Cryst.*, 20, 432 (1966).
189. J. M. Vincent and A. E. Skoulios, *Acta Cryst.*, 20, 441 (1966).
190. J. M. Vincent and A. E. Skoulios, *Acta Cryst.*, 20, 447 (1966).
191. B. Mely and J. Charvolin, *Chem Phys. Lipids*, 19, 43 (1977).
192. M. Demarcq and D. Dervichian, *Bull. Soc. Chim. France*, 12, 939 (1945).
193. P. A. Winsor, in "Liquid Crystals and Plastic Crystals", Eds. G. W. Gray and P. A. Winsor (Ellis Horwood Ltd., Chichester, England, 1974) Vol. 1, Chapt. 5, p 252.
194. P. Ekwall, L. Mandell and K. Fontell, *J. Colloid Int. Sci.*, 33, 215 (1970).

195. E. I. Franses and T. J. Hart, *J. Colloid Int. Sci.*, 94, 1 (1983).
196. A. Khan, K. Fontell and B. Lindman, *J. Colloid Int. Sci.*, 101, 193 (1984).
197. H. Wennerstrom, B. Jonsson and P. Linse, *J. Chem Phys.*, 76, 4665 (1982).
198. C. R. Singleterry, *J. Am. Oil Chem. Soc.*, 32, 446 (1955).
199. N. Pilpel, *Chem. Revs.*, 63, 221 (1963).
200. F. M. Fowkes, in "Solvent Properties in Surfactant Solutions", Ed. K. Shinoda (Surfactant Science Series, Marcel Dekker Inc. New York, 1967), Vol. 2, Chapt. 3, p. 65.
201. D. B. Cox and J. F. McGlynn, *Anal. Chem.*, 29, 960 (1957).
202. F. H. Stross and S. T. Abrams, *J. Am. Chem. Soc.*, 73, 2825 (1951).
203. M. J. Vold, G. S. Hattiangdi and R. D. Vold, *Ind. and Eng. Chem.*, 41, 2539 (1949).
204. M. J. Vold and R. D. Vold, *J. Inst. Pet.*, 38, 155 (1952).
205. E. Kissa, *J. Colloid Sci.*, 17, 857 (1962).
206. A. E. Skoulios, *Acta Cryst.*, 14, 419 (1961).
207. P. Spegt and A. Skoulios, *J. Chim. Phys.*, 62, 377 (1965).
208. Y. Uzu, *Yukagaku*, 24, 261 (1975).
209. G. H. Smith and J. W. McBain, *J. Phys. Colloid Chem.*, 51, 1189 (1947).
210. F. H. Stross and S. T. Abrams, *J. Am. Chem. Soc.*, 72, 3309 (1950).
211. T. M. Doscher and R. D. Vold, *J. Phys. Colloid Chem.*, 52, 97 (1948).
212. U. P. Strauss and E. G. Jackson, *J. Polymer Sci.*, 6, 649 (1951).
213. C. M. Paleos, C. I. Stassinopoulou and A. Malliaris, *J. Phys. Chem.*, 87, 251 (1983).
214. C. E. Larrabee Jr. and E. D. Sprague, *J. Polymer Sci., Polymer Lett. Ed.*, 17, 749 (1979).
215. E. Jahns and H. Finkelmann, *Colloid and Polymer Sci.* 265, 304 (1987).
216. M. Tanaka and T. Nakaya, *Makromol. Chem.*, 190, 3067 (1989).

217. D. J. Mitchell, J. G. T. Tiddy, L. Waring, T. Bostock, M. P. McDonald, J. Chem. Soc, Faraday Trans. I, 79, 975 (1983).
218. B. Luhmann, PhD Thesis (Clausthal-Zellerfeld, West Germany, 1985).
219. A.S.C. Lawrence, in Liquid Crystals 2, Ed. G.h. Brown (Gordon and Breach, New York, 1969). Vol.1, p.1.
220. R. Loffler and H. Finkelmann, Makromol. Chem. Rapid Commun., 11, 321, (1990).
221. V. P. Shibaev, S. G. Kostromin and N. A. Plate, Eur. Polym. J., 18, 651 (1982).
222. R. Zentel and H. Ringsdorf, Makromol. Chem. Rapid Commun., 5, 393 (1984).
223. G. Nestor, M. S. White, G. W. Gray, D. Lacey and K. J. Toyne, Makromol. Chem., 188(11), 2759 (1987).
224. I. Yilgor and J. E. McGrath, in "Advances in Organosiloxane Copolymers" (Springer-Verlag, Heidelberg, 1988).
225. P. J. Madec and E. Marechal, J. Polym. Sci., Polym. Chem., 16, 3165 (1978).
226. E. Sh'. Goldberg, I. M. Raigorodskii, G. N. Kovalev, B. S. El'tsefon, V. V. Korshak, A. L. Kuzaev, S. G. Alekseeva, Ya. G. Urman, I. Ya. Slonim, Vysokomol. Soed., 26A, 1369 (1984).
227. B. Hardman and A. Torkelson, in "Encyclopedia of Polymer Science and Engineering", 2<sup>nd</sup> Edition (John Wiley and Sons, New York, 1990) 204-308, V15.
228. H. Jacobson and W. H. Stockmayer, J. Chem. Phy., 18, 1600 (1950).
229. M. G. Voronkov, V. P. Milleshkevich, Y. A. Yushelevskii, in "The Siloxane Bond" (Plenum Press, New York, 1978) Chapt. 3.
230. J. S. Riffle, PhD Thesis, VPI and SU, Blacksburg, Va. (1981).

231. I. Yilgor, J. S. Riffle, G. L. Wilkes and J. E. McGrath, *Polym. Bulletin.*, 8, 535 (1982).
232. J. S. Riffle, R. G. Freelin, A. K. Banthia and J. E. McGrath, *J. Makromol. Sci.-Chem.*, A15 (5), 967 (1981).
233. I. Yilgor, D. Tyagi, G. L. Wilkes and J. E. McGrath, 123 Rubber Div. Mtg., ACS, Toronto, May 10-12<sup>th</sup> (1983), Paper # 47.
234. J. E. McGrath, in "Epoxy Resin Chemistry II", Ed. R. S. Bauer, (ACS Symp. Ser. N<sup>o</sup> 221, 1983) Ch.2.
235. C. Tran, *PMSE Proc.*, 49, 498 (1983).
236. M. G. Voronkov, V. P. Milleshkevich, Y. A. Yushelevskii, in "The Siloxane Bond" (Plenum Press, New York, 1978) Chapt. 4.
237. *Encyclopedia of Polymer Science and Engineering* (John Wiley and Sons, New York) V2, p1-43 and p729-814; V8, 147-220.
238. W. Sundermeyer and W. Noll, in G.B. Patent 922 377.
239. G. G. Cameron and M. S. Chisholm, *Polym.* 26, 437-442 (1985).
240. H. J. Holle and B. R. Lehnen, *Eur. Polym. J.*, 11, 663-667 (1975).
241. *Organic Reactions*, Eds. R. Adams, A. H. Blatt, A. C. Cope, F. C. McGrew, C. Niemann and H. R. Snyder (John Wiley and Sons, New York) VI-VII.
242. *Protective Groups in Organic Chemistry*, Ed. J. F. W. McOmie (Plenum Press, New York, 1973).
243. J. F. W. McOmie, *Chemistry and Industry* 603 (1979).
244. M. Lalonde, T. H. Chan, *Synthesis*, September, 817 (1985).
245. C. S. Cundy, B. M. Kingston and M. F. Lappert, in *Advances in Organometallic Chemistry*, Eds. F. G. A. Stone and R. West (Academic Press, New York, London and Paris, 1973) V11, p253-300.
246. G. W. Gray, D. Lacey, G. Nestor and M. S. White, *Makromol. Chem., Rapid Commun.*, 7, 71 (1986).
247. J. Lipowitz and S. A. Bownan, *J. Org. Chem.*, 38, 162 (1973).

248. I. S. Akhmem, N. M. Christovalova and M. E. Vol'pin, *Russ. Chem. Rev.*, (Eng. Trans.) 52, 542 (1983).
249. P. A. Gemmell, G. W. Gray and D. Lacey, *Mol. Cryst. Liq. Cryst.*, 102, 43 (1984)
250. H. Finkelmann, H. J. Kock and G. Rehage, *Mol. Cryst. Liq. Cryst.*, 89, 23 (1982)
251. H. Benthack-Thoms and H. Finkelmann, *Makromol. Chem.*, 186, 1895 (1985).
252. A. I. Hopwood and H. J. Coles, *Polymer*, 26, 1312 (1985)
253. W. Kreuder and H. Ringsdorf, *Makromol. Chem. Rapid Commun.*, 4, 807 (1983).
254. M. Portugall, H. Finkelmann and H. Ringsdorf, U.S. Patent 4,293,435.
255. A. K. Alimoglu, A. Ledwith, P. A. Gemmell, G. W. Gray and D. Lacey, *Polymer*, 25, 1342 (1984).
256. M. Mauzac, F. Hardouin, H. Richard, M. F. Achard, G. Sigaud and H. Gasparoux, *Eur. Polm. J.*, 22, 137 (1986).
257. H. S. Chen and S. Krishnamurthy, *Polym. Mater. Sci. Eng.*, 60, 801 (1989).
258. S. Krishnamurthy and H. S. Chen, *Makromol. Chem.*, 190(6), 1407 (1989).
259. H. Stevens, G. Rehage and H. Finkelmann, *Makromolekules*, 17 851 (1984).
260. T. R. Formoy, PhD Thesis (York University, England, 1985).
261. J. B. Carmichael and J. Heffel, *J. Phy. Chem.*, 69, 2218 (1965).
262. *Tetrahedron*, No. 3, 43, 451 (1987).
263. E. Baum, D. Demus and H. Sackmann, *Wiss. Z. Univ. Halle*, 19, 37 (1970).

264. N. H. Hartshorne, in "The Microscopy of Liquid Crystals", (Microscope Publications Ltd, London, 1974).
265. F. B. Rosevear, *J. Am. Oil Chem. Soc.*, 31, 682 (1954).
266. F. B. Rosevear, *J. Soc. Cosmetic Chem.*, 19, 581 (1968).
267. L. Mandell and P. Ekwall, *Acta Polytech. Scand.*, Chap. 74, (1968), Part I, p. 1.
268. D. Demus and Richter, in "Textures of Liquid Crystals", Verlag Chemie, Weinheim (1978).
269. A. S. C. Lawrence, in "Surface Activity and Detergency", ed. K. Durham (Macmillan, London, 1961), p.158.
270. R. D. Vold and J. M. Philipson, *J. Phys. Chem.*, 50, 39 (1946).
271. H. Finkelmann, M. Happ, M. Portugal and H.Ringsdorf, *Makromol. Chem.*, 179, 2541 (1978).
272. T. Yamaguchi, T. Hayashi and N. Nakamura, *Mol. Cryst. Liq. Cryst. Letters*, 5(1) 23 (1987).
273. H. Finkelmann, M. J. Kock and G. Rehage, *Makromol. Chem., Rapid Commun.*, 2, 317 (1981).
274. V. Busico, A. Ferraro and M. Vacatello, *J. Phys. Chem.*, 88, 4055 (1984).
275. V. Busico, A. Ferraro and M. Vacatello, *J. Chem. Phys.*, 84, 471 (1986).
276. A. Cingolani, G. Spinolo, M. Sanesi and P. Franzosini, *Z. Naturforsch.*, A35, 757 (1980).
277. J. L. Curat and R. Perron, *Chem. phys. Lipids*, 19, 301 (1977).
278. G. Forster, G. Brezesinski, E. Gerlach, A. Modicke and H. D. Dorfler, *Z. Phys. Chemie, Leipzig*, 6, 1009 (1981).
279. M. J. Vold and R. D. Vold, *J. Colloid Sci.*, 5, 1 (1950).
280. D. B. Cox, *J. Phys. Chem.*, 62, 1254 (1958).
281. M. J. Vold, Y. Uzu and R. F. Bills, *NLGI Spokesman*, 32(10), 362 (1969).
282. R. A. Chivers, J. Blackwell, G. A. Gutierrez, J. B. Stamatoff and H. Yoon,

- in "Polymer Liquid Crystals", ed. A. Bleimstein (Plenum Press, New York and London, 1985) 153-166.
283. J. Blackwell, G. A. Gutierrez and R. A. Chivers, in "Polymer Liquid Crystals", ed. A. Bleimstein (Plenum Press, New York and London, 1985), 167-182.
284. J. Blackwell and A. Biswas, in "Developments in Oriented Polymers - 2", ed. I. M. Ward (Elsevier Applied Science, London and New York, 1988) 153-198.
285. A. Guinier, G. Fournet, C. B. Walker and K. L. Yudowitch, in "Small-Angle Scattering of X-rays", (John Wiley and Sons, Inc, New York, 1955).
286. A. Johansson and B. Lindman, in "Liquid Crystals and Plastic Crystals" ed. G. W. Gray and R. A. Windsor (Ellis Harwood, Chichester, UK, 1974) Vol. 2, p.192.
287. V. Luzzatti and F. Husson, *J. Cell Biol.*, 12, 207 (1962).
288. K. Fontell, *Mol. Crystals Liquid Crystals*, 63, 59 (1981).
289. L. E. Scriven, *Nature*, 263, 123 (1976).
290. T. Bull and B. Lindman, *Mol. Crystals Liquid Crystals*, 28, 155 (1974).
291. G. Lindblom and H. Wennerstrom, *Biophys. Chem.*, 6, 167 (1977).
292. G. Lindblom, K. Larsson, L. B. A. Johansson, K. Fontell and S. Forsen, *J. Amer. Chem. Soc.*, 101, 5465 (1979); K. Larsson, K. Fontell and N. Krog, *Chem. Phys. Lipids*, 27, 321 (1980).
293. G. J. Tiddy, P. Galsworthy and K. Rendall, *Mol. Crystals Liquid Crystals*, 72, 147 (1982).
294. V. Luzzatti, T. Gulik-Krzywicki and A. Tardieu, *Nature*, 218, 1031 (1966).
295. U.K. Patent Application, GB 2039 512A
296. S. J. Mumby and M. S. Beevers, *Polymer*, 29, 14-17 (1988).

297. M. J. Vold, M. Macomber and R. D. Vold, *J. Am. Chem. Soc.*, 63 (1), 168 (1941).
298. P. A. Spegt, A. E. Skoulios and V. Luzzatti, *Acta Cryst.* 14, 866 (1961).
299. P. Pacor and H. L. Spier, *J. Amer. Oil Chem. Soc.*, 45, 338 (1967).
300. J. Roth, T. Meisel, K. Seybold and Z. Halmos, *J. Thermal Anal.*, 10, 223 (1976).
301. D. P. Benton, P. G. Howe, R. Farnand and I. E. Puddington, *Can. J. Chem.*, 33, 1798 (1955).
302. T. Gulik-Krzywicki, E. Shechter, V. Luzzatti and M. Faure, *Nature*, 223, 1116 (1969).
303. M. L. Phillips and J. Jonas, *Liquid Crystals*, 2, №.3, 335 (1987).
304. R. D. Vold and T. D. Smith, *J.A.C.S.*, 73, 2006 (1951).
305. M. J. Vold, H. Funakoshi and R. D. Vold, *J. Phys. Chem.*, 80, 1753 (1976).
306. P. Ekwall, I. Danielsson, and L. Mandell, *Kolloidzeitschrift*, 169, 113 (1960).
307. L. Mandell, K. Fontell and P. Ekwall, *Adv. Chem. Ser. Am. Chem. Soc.*, 63, 89 (1967).
308. P. Ekwall, L. Mandell and K. Fontell, *J. Colloid Interface Sci.*, 31, 508, (1969).
309. L. Fontell, L. Mandell, H. Lehtinen and P. Ekwall, *Acta Polytechn. Scand.*, 78, III (1968).
310. G. J. T. Tiddy, *J. Chem. Soc. Faraday Trans. 1*, 68, 369 (1972).
311. G. Lindblom, B. Lindman and G. J. T. Tiddy, *J. Amer. Chem. Soc.*, 100, 2299 (1978).
312. C. James and J. F. Heathcock, *J. Chem. Soc. Faraday Trans. 1*, 77, 2851 (1981).
313. R. Friman, I. Danielsson and P. Stenius, *J. Colloid Interface Sci.*, 86, 501, 529 (1982).

314. P. G. Neeson and G. J. T. Tiddy, *J. Chem. Soc. Faraday Trans. 1*, 78, 147 (1982).
315. D. W. R. Gruen, *J. Phys. Chem.*, 89 (Nº1) 146-153 (1985).
316. S. J. Clarson, PhD Thesis (University of York, England, 1985).
317. CRC Handbook of Chemistry and Physics, 70<sup>th</sup> Edition, Eds. R. C. Weast and D. R Lide (CRC Press Inc., Boca Raton, Florida, 1989).
318. V. Luzzatti, A. Tardieu, T. Gulik-Krzywicki, E. Rivas and F. Reiss-Husson, *Nature*, 220, 485 (1968).
319. Petrach Systems Catalogue (1985).
320. W. Skoda, *Kolloid-Zeitschrift und Zeitschrift für Polymere*, 234 (2), 1128-1138 (1969).
321. F. W. Southam and I. E. Puddington, *Can. J. Research.*, 25 (2), 121-124 (1947).
322. Petrach Systems Catalogue
323. R. J. Lamb, J. H. Purnell, *J. High Res. Chromatogr. and Chromatogr. Commun.*, 3, 195 (1980).
324. *Polymer Handbook*, 3<sup>rd</sup> Edition, EDs J. Brandrup and E. H. Immergut (John Wiley and Sons, New York).
325. A. E. Skoulios and V. Luzzatti, *Acta Cryst.* 14, 278 (1961).
326. B. Gallot and A. E. Skoulios, *Acta Cryst.*, 15, 826 (1961).
327. S. J. Clarson, K. Dodgson and J. A. Semlynen, *Polymer* 26, 930 (1985).
328. C. Tanford, in "The Hydrophobic Effect", 2<sup>nd</sup> Edition (John Wiley and Sons, New York, 1980) Chapt. 3.
329. C. Tanford, in "The Hydrophobic Effect", 2<sup>nd</sup> Edition (John Wiley and Sons, New York, 1980) Chapt. 8.
330. *Encyclopedia of Polymer Science and Engineering* (John Wiley and Sons, New York) 1, Vol. 10.
331. *Encyclopedia of Polymer Science and Engineering* (John Wiley and

- Sons, New York) 789, Vol. 1.
332. H. Finkelmann, H. Ringsdorf and J. H. Wendorff, *Makromol. Chem.* 179, 273 (1978)
  333. S. M. Nelson and R. C. Pink, *J. Chem. Soc.*, 1744 (1952)
  334. H. Finkelmann, *Phil. Trans. R. Soc. Lond.*, A309, 105 (1983).
  335. *Side-Chain Liquid Crystal Polymers*, Ed. C. B. McArdle (Chapman and Hall, 1989).
  336. V. Percec and D. Tomazos, *Polym. Prepr.* 29, 1, 234 (1988).
  337. H. Finkelmann, H. Ringsdorf, W. Siol and J. H. Wendorff, *Makromol. Chem.*, 179, 829 (1978).
  338. C. B. McArdle, *Liquid Crystals*, 2 (5), 537-584 (1987).
  339. V. P. Shibaev, *Polym. Commun.*, 24, 364 (1983).
  340. V. P. Shibaev, *Polym. Sci. Technol.*, 28, 245 (1985).
  341. S. G. Kostromin, V. P. Shibaev and N. A. Plate, *Liquid Crystals*, 2 (2), 195 (1987).
  342. V. Krone and H. Ringsdorf, *Liquid Crystals*, 2 (4), 411 (1987).
  343. C. S. Hsu, J. M. Rodriguez-Parada and V. Percec, *J. Polym. Sci., Polym. Chem.*, 25 (9), 2425 (1987).
  344. C. S. Hsu and V. Percec, *J. Polym. Sci., Polym. Chem.*, 25 (10), 2909-2923 (1987).
  345. V. Percec and C. S. Wang, *J. Macromol. Sci., Chem.*, A28 (8), 678 (1991).
  346. H. Richard, M. Mauzac, G. Sigaud, M. F. Achard, F. Hardouin, *Liquid Crystals*, 9 (5), 679 (1991).
  347. V. Percec and J. Heck, *Polym. Bull.*, 24 (3), 255 (1990).
  348. G. S. Attard, K. Araki, J. J. Moura-Ramos and G. Williams, *Liquid Crystals*, 3 (6-7), 861 (1988).
  349. H. Stevens, H. Finkelmann, B. Luhmann and G. Rehage, in "*Liquid Crystals and Ordered Fluids*", Eds J. S. Johnson and R. S. Porter, Vol. 4 (1983).